Palaeoenvironmental evolution of SW Iberia during the Holocene based on palynological data

From the Faculty of Georesources and Materials Engineering of the RWTH Aachen University

to obtain the academic degree of

Doctor of Natural Sciences

approved thesis

submitted by

Cristina Val Peón, M.Sc.

Advisors: Herr Univ.-Prof. Dr. rer. nat. Klaus Reicherter
Herr Prof. Dr. José Antonio López Sáez
Herr Prof. Dr. Juan Ignacio Santisteban Navarro

Date of the oral examination: 05.07.2023

"Todo pasa y todo queda,
pero lo nuestro es pasar,
pasar haciendo caminos,
caminos sobre el mar.

(…)

Caminante, son tus huellas
el camino y nada más;
caminante, no hay camino,
se hace camino al andar."

Antonio Machado

Abstract

The Holocene (11.7 ka BP - present) is a period characterized by multiple environmental changes defined by the complex interplay of elements of different nature (climatic, geological, anthropogenic) acting simultaneously at global, regional and local scales. Over these millennia, coastal areas have been perceived as biodiversity hotspots that have acted as poles of attraction for human groups. Their susceptibility to climatic changes and their long history of human settlements turns them into potential areas for the study of long and short-term processes. Thus, their investigation may provide insights into their ecological dynamics, their driving mechanisms, and human-environment relationships. In this work, new data on the environmental evolution of SW Iberia are presented and discussed, with special focus on palynological results.

Considering issues related to the interpretation of fossil pollen records from transitional environments, a study based on modern-pollen samples acquired from the Eurasian Modern Pollen Database was performed. This first approach investigates the role of certain environmental variables in the distribution of vegetation and the existence of possible biases in pollen representativeness. This work successfully assisted on the interpretation of the fossil pollen record, as the variability of specific taxa could be attributed to shifts between arid and humid conditions. Furthermore, it was possible to identify the action of taphonomic elements as causes of certain biases.

For the palaeoenvironmental study, three sedimentary archives were recovered from SW Iberia: two terrestrial cores in La Janda basin (Spain) and one marine core in the Algarve continental shelf (Portugal) were studied. They were analyzed from a sedimentological, geochemical and palynological perspective to reconstruct the palaeoenvironmental evolution of the area and correlate it with the different phases of human occupation during Prehistory.

Results show that La Janda basin evolved from an incised fluvial valley during the Late Pleistocene to a restricted bay connected to the sea between ca. 10-8.7 to 3.5-3.3 ka cal BP, during which the maximum marine flooding was reached at ~7 ka cal BP. After a transitional period, it was transformed into a terrestrial basin ca. 1.3 ka cal BP. The sampling resolution and the preservation of palynomorphs in the S3 core allowed the reconstruction of the vegetation dynamics in the study area, supported by data from the S2 core. The integration of these results into a regional context, including palynological data from the marine sequence drilled in the Algarve, revealed different vegetation trends. These periods can be summarized as an initial episode of forest development with regional nuances (~11.7-7.7 ka cal BP), a gradual forest decrease (~7.7-5.5 ka cal BP), increased arid conditions (~5.5-3.7 ka cal BP), significant anthropogenic impact (~3.7-1.2 ka cal BP), and the development of cultural landscapes (~1.2 ka cal BP onwards).

Although increasing temperatures and moisture characterized the onset of the Holocene, continental conditions were identified in some palynological and hydrological records from the Western Mediterranean. From ca. 10 ka BP onwards, the increase of moisture reflected in the vegetation may be associated to the high summer insolation that may have favoured land-sea temperature contrast and enhanced winter precipitation. Some researchers consider that the progressively decrease in summer insolation and the installation of the present atmosphere circulation in the Northern Hemisphere happened between 7-5.5. ka cal BP. These factors may have led to drier conditions due to the reduced penetration of winter storm tracks, which may have triggered the gradual decline of mesic forests in favour of Mediterranean taxa. From 5 ka cal BP on, enhanced aridity alternating with humid phases has been identified as a consequence of the dipolar North Atlantic Oscillation pattern. Overlapping these long-term trends, the presented records indicates different short-term events of increased aridity at 8.2, 7.7-7.5, 5.9-5.5, and 4.2 ka cal BP. However, the causes of some of these episodes remain unclear and different hypotheses have been suggested.

By correlating the palaeoenvironmental data with the archaeological record of the study area, it was possible to confirm the low impact of hunter-gatherer groups on the landscape during the Upper Palaeolithic and Mesolithic (~20-7.8 ka cal BP). A progressive increase in anthropogenic pressure was identified during the Neolithic, especially from ca. 7 ka cal BP, with markers suggesting herding/livestock activities prior to the punctual presence of cereals, which is only confirmed by the archaeological record from ca. 6 ka cal BP on. Human impact becomes more noticeable during the Chalcolithic and Bronze Age (~5-3 ka cal BP) and it is interrupted by abrupt drops of anthropogenic indicators at different moments until the present time (ca. 3.6-3.2, 2.6-2.2, 1.2-1 ka cal BP). During the last millennia, the transformation of the landscape for agricultural activities is reflected through the local presence of cereals and markers of erosive processes.

The integration of environmental and archaeological data provides long-term perspectives on human responses to environmental change, improving the understanding on the socio-ecological resilience of communities and their adaptive capacity. The current debate on global climate change and biodiversity loss need these interdisciplinary approaches to understand landscape evolution changes and adaptive processes.

Kurzfassung

Die Periode des Holozäns (11,7 ka – heute) zeichnet sich durch zahlreiche Umweltveränderungen aus. Diese Veränderungen weisen auf globaler, regionaler und lokaler Ebene ein komplexes Zusammenspiel von Elementen unterschiedlicher Natur (klimatisch, geologisch, anthropogen) auf. Im Holozän werden Küstengebiete als Biodiversitätshotspots wahrgenommen und stellen ein Anziehungspunkt für menschliche Gruppen dar. Aufgrund ihrer Anfälligkeit für Klimaveränderungen und ihrer langen Geschichte von menschlicher Besiedelung, stellen sie potenzielle Forschungsgebiete von lang- und kurzfristigen Prozessen dar. Ihre Untersuchung ermöglicht Einblicke in ihre ökologische Dynamik, treibende Mechanismen und die Beziehungen zwischen Mensch und Umwelt. Diese Arbeit stellt neue Daten zur Umweltentwicklung von SW-Iberia vor, mit einem Fokus auf palynologischen Ergebnissen.

In Anbetracht der Probleme im Zusammenhang mit der Interpretation fossiler Pollenaufzeichnungen aus Übergangsumgebungen wurde eine Studie auf der Grundlage moderner Pollenproben aus der Eurasian Modern Pollen Database durchgeführt. Der Einfluss von veränderten Umweltbedingungen auf die Vegetationsverteilung und die Repräsentativität der Pollendaten sowie mögliche Störungen dieser wurden untersucht. Diese Arbeit trägt, basierend auf der Variabilität bestimmter Taxa des fossilen Pollenbefundes, auf die klimatischen Wechsel zwischen ariden und feuchten Bedingungen bei. Darüber hinaus konnte der Einfluss von taphonomischen Elementen als Ursache bestimmter Verzerrungen identifiziert werden.

Für die paläoökologische Studie wurden drei geologische Bohrkerne in SW-Iberien untersucht: zwei terrestrische Kerne aus dem La Janda-Becken (Spanien) und ein mariner Kern des Kontinentalschelfs der Algarve (Portugal) untersucht wurde. Die Bohrkerne wurden sedimentologisch, geochemisch und palynologisch analysiert, um die paläoökologische Entwicklung des Untersuchungsgebiets zu rekonstruieren und sie mit den verschiedenen Phasen der menschlichen Besiedlung während der Vorgeschichte in Verbindung zu bringen. Die Ergebnisse der Studie zeigen, dass sich das La Janda-Becken vom späten Pleistozän als eingeschnittenes Flusstal zu einer eingeschnürten marinen Bucht entwickelt hat. Diese Bucht war zwischen ca. 10-8.7 to 3.5-3.3 ka cal BP mit dem Meer verbunden und erreichte bei etwa 7 ka cal BP den Höchststand der marinen Überflutung. Nach einer Übergangsphase wandelte sie sich vor ca. 1,3 cal BP in ein terrestrisches Becken um. Die Probenauflösung und die Erhaltung der Palynomorphe im Kern S3 ermöglichten die Rekonstruktion der Vegetationsdynamik im Untersuchungsgebiet, unterstützt durch die Daten des Kerns S2. Bei der Betrachtung der Ergebnisse im regionalen Kontext, in Verbindung mit den palynologischen Daten des marinen Bohrkerns des Algarve Gebietes, ergeben sich unterschiedliche Vegetationstrends. Diese Perioden lassen sich in eine anfängliche Episode der Waldentwicklung mit regionalen Nuancen (~11.7-7.7 ka cal BP), einen allmählichen Waldrückgang (~7.7-5.5 ka cal BP), darauffolgend zunehmend aride Bedingungen (~5.5-3.7 ka cal BP),

eine Periode mit deutlichem anthropogenen Einfluss (~3.7-1.2 ka cal BP) und die Entwicklung einer Kulturlandschaft (~1.2 ka cal BP bis heute) untergliedern.

Obwohl steigende Temperaturen und Feuchtigkeit den Beginn des Holozäns charakterisieren, wurden in einigen palynologischen und hydrologischen Aufzeichnungen aus dem westlichen Mittelmeer, kontinentale Bedingungen identifiziert. Ab ca. 10 ka BP spiegelt sich der Anstieg der Feuchtigkeit/Niederschläge in der Vegetation wider. Dieses war verbunden mit der hohen Sommerinsolation, die den Land-Meer-Temperaturunterschied begünstigt haben könnte und zu verstärkten Winterniederschlägen führte. Es wird angenommen, dass die allmähliche Abnahme der Sommerinsolation und die Etablierung der derzeitigen atmosphärischen Zirkulation auf der Nordhalbkugel zwischen 7-5.5 ka cal BP stattfanden. Diese Faktoren könnten zu trockeneren Bedingungen geführt haben, aufgrund des geringeren Einflusses von Winterstürmen, was den allmählichen Rückgang der mesophilen Wälder, zugunsten mediterraner Taxa, auslösen könnte. Ein Szenario erhöhter Aridität mit zeitweise abwechselnden feuchten Phasen, wird ab 5 ka cal BP angenommen, als Folge des dipolaren Musters der Nordatlantischen Oszillation. Neben diesen langfristigen Trends zeigen die Pollendaten verschiedene ereignisbezogene Phasen erhöhter Aridität bei 8.2, 7.7-7.5, 5.9-5.5 und 4.2 ka cal BP. Die Ursachen einiger dieser Episoden sind jedoch noch unklar und verschiedene Hypothesen werden diskutiert.

Durch die Korrelation der paläoökologischen Daten mit dem archäologischen Befund des Untersuchungsgebiets konnte der geringere Einfluss von Jäger-Sammler-Gruppen auf die Landschaft während des oberen Paläolithikums und Mesolithikums (~20-7.8 ka cal BP) bestätigt werden. Im Neolithikum wurde eine allmähliche Zunahme des anthropogenen Einfluss, insbesondere ab ca. 7 ka cal BP, nachgewiesen. Marker deuten zunächst auf Hirten-/Viehzuchtaktivitäten hin, bevor der punktuelle Nachweis von Getreide durch den archäologischen Befund ab ca. 6 ka cal BP bestätigt wird. Während des Chalkolithikums und der Bronzezeit (~5-3 ka cal BP) wird der anthropogene Einfluss deutlicher und wird durch einen abrupten Rückgänge dieser anthropogener Indikatoren an verschiedenen Zeitpunkten bis zur Gegenwart unterbrochen (ca. 3.6-3.2, 2.6-2.2, 1.2-1 ka cal BP). Die Transformation der Landschaft spiegelt sich in den letzten Jahrtausenden in der lokalen Präsenz von Getreide und Anzeichen erosiver Prozesse wider. Durch die Integration von Umwelt- und archäologischen Daten ist es möglich, Langzeitperspektiven der menschlichen Reaktionen auf Umweltveränderungen aufzuzeigen und das Verständnis für die sozioökologische Resilienz von Gemeinschaften und ihre Anpassungsfähigkeit zu verbessern. Diese multidisziplinären Ansätze werdenkünftig stärker in den Mittelpunkt der aktuellen Debatten über globale Klimaveränderungen und den Verlust der Biodiversität in den Vordergrund rücken.

Foreword and acknowledgements

I would like to thank my supervisors, Prof. Dr. Klaus Reicherter, Prof. Dr. José Antonio López Sáez and Prof. Dr. Juan Ignacio Santisteban Navarro, because this work would not have been possible without them. I would like to thank Prof. Dr. Reicherter for giving me the opportunity to come to Aachen and develop my research career, supporting me in all the activities that made me gain experience in different fields (conferences, workshops, fieldwork, etc.). I am grateful for the trust placed in me to give me the autonomy to organize the pollen lab and collaborate in different projects.

Quiero agradecer a Antonio todo el conocimiento y experiencia que compartió conmigo, la paciencia en responder a todas mis dudas y, en especial, el cariño y respeto con el que siempre me trató en lo académico y personal. También quiero agradecer a Santi y a Rosa por todo lo aprendido con ellos, por su ayuda y paciencia explicando las cosas, por su cariño en todo momento y por haberme tratado como a una hija cada vez que estuve en Madrid. Sin vosotros tres este trabajo no hubiera podido salir adelante. Deseo muchos años de colaboraciones futuras.

I would like to thank the support of the CRC 806 "Our way to Europe" project and all its members for integrating me into the group, especially to the C1 cluster: Gerd, Trine, Miriam…

También quiero agradecer a los compañeros de la Universidad de Cádiz su colaboración y generosidad cada vez que surge la oportunidad de trabajar en grupo: Pepe Ramos, Eduardo Vijande, Jesús Cantillo, Salvador Domínguez, Serafín Becerra y Diego Fernández.

Aunque como parte de un proyecto paralelo, agradezco la constante motivación y cariño de mis compañeros de Málaga, siempre con una palabra de ánimo: Manolo, Pepe, Curro, Juanma, Caro...

I would like to thank the constant support and affection of my colleagues at the institute and those who were in Aachen at some point, to all of them many thanks for the good moments: Liene, Piero, Vanessa, Farkhod, Xianghe, Simoni, Manu, Gosia…I am really grateful to have had one of the best possible collaborators and a good friend to share good and bad moments in the office, thanks a lot, Lisa. Però no hauria estat possible sobreviure sense una de les persona que més em va ajudar sempre en tot moment, Aachen no seria el mateix sense tu Sara.

Je voudrais remercier Elodie pour son affection, son soutien et pour m'avoir appris qu'il y a différentes façons de travailler.

Me gustaría agradecer a Juan Ochando su ayuda, apoyo y cariño a lo largo de estos años, que espero que se traduzcan en más colaboraciones juntos. Gracias también a Pepe Carrión, por haber sido tan amable siempre conmigo para absolutamente todo.

Gran part del que sé sobre Palinologia ho vaig aprendre en el IPHES, per la qual cosa vull agrair a Quico, Isa, Ethel i a tots els companys de l'institut la possibilitat d'haver après al costat d'ells. Pero especialmente quiero agradecer a las personas que se cruzaron en mi camino, lo hicieron más divertido y aún siguen siendo parte de mi vida de una u otra forma. Gracias a Aitor, Rachel, Cuqui, Andion, Miguel, Mónica, Toni, Edgar, Diego, Josah, Lloyd, Noé…Y a Iván, por haber compartido juntos una parte muy importante de mi vida.

Estou onde es estou e sou o que sou polas persoas que son parte de miña familia, a todas elas quero agradecer que estexan absolutamente sempre ao meu lado, independentemente da distancia.

Mil graciñas a Suso e Clara, por seguir sendo o núcleo duro dende fai tanto tempo, e a Carlos por pasar a formar parte del. Graciñas a Marta, Lidia, Carlos, Ana, Maru e a toda a xente da Coruña por seu cariño e apoio sempre.

Para Tiago as palavras não chegam. Obrigada por estar sempre no pior e ser arquitecto do melhor. Por aparecer e preencher "por descuido um qualquer lugar até então deserto".

Ma, Pin, Repo, gracias por estar siempre, gracias por ser mi hogar, gracias por absolutamente todo.

Ao meu pai, porque algunhas persoas veñen, outras van e outras, como a terra, permanecen.

Contents

List of Figures

List of Tables

1.- Introduction

1.1.- General overview and rationale

Far from being a stable period, the Holocene is characterised by several environmental changes that took place over the last 11.700 years, such as the increase of temperatures, the sea-level rise, a succession of different vegetal dynamics, the existence of abrupt climate events, specific hydrological and geomorphological processes, and the increased impact of human activities (Walker et al., 2012). The echoes of these processes resulted in multiple transformations that affected diverse territories in different ways. Such is the case of the Iberian Peninsula, a territory defined by contrasted climatic, biogeographical and historical conditions that translates in a remarkable environmental heterogeneity (Benayas and Scheiner, 2002; Carrión et al., 2010). These characteristics have made Iberia a reservoir of biodiversity and a wildlife refuge area during the whole Quaternary (Carrión et al., 2010). Moreover, its strategic position between North Africa and Southern Europe has led it to be considered a key area from a geoarchaeological point of view, being a hotspot for the study of hominin population patterns, migratory routes, and cultural exchanges, among other things (Carrión et al., 2010).

Understanding the complex relationships between palaeoecological transformations and human groups, not only affected by environmental changes but as active agents modifying the landscape, requires finding study areas where these elements converge. This is the case of coastal ecosystems and transitional environments, as they are especially sensitive to climate fluctuations and have always acted as poles of attraction for human groups (Basset et al., 2006): the perfect definition for Southwestern Iberia.

Continuous deposits from transitional environments may record ecological changes at global, regional, and local scale, as well as the anthropogenic impact over time. Considering the sensitivity of the vegetation to these elements, its study from a diachronic perspective may provide insights on the environmental evolution of these ecosystems, their dynamics and potential causes (Birks and Birks, 1980; Dincauze, 2000). Thus, palynological analyses are an excellent tool that may contribute with crucial data on long and short-term processes affecting coastal ecosystems (Fægri and Iversen, 1951; Moore et al., 1991). However, the main problem in SW Iberia is the lack of continuous sequences, especially continental, covering the period encompassing from the Early Holocene to the present. Although it cannot be said that there is a lack of palynological studies, it is true that most of them cover short periods of time or lack a good chronological control. Thus, the primary justification for studying the palaeoenvironmental evolution of SW Iberia from a palynological point of view is the need to provide new data from a long-term perspective. This will not only contribute to the knowledge of a

specific area, but will also allow correlating existing studies at a regional scale to understand patterns of natural and anthropogenic origin involved in the transformation of SW Iberian landscapes.

1.2.- Aims and objectives

The main goal of this thesis is to study and present the palaeoenvironmental evolution of SW Iberia during the Holocene from a multidisciplinary approach with focus on palynological data. To accomplish this task, there are specific objectives that serve as structure for the work:

- To understand pollen-vegetation relationships on modern pollen samples in order to establish potential analogues for the study of fossil pollen records.
- To reconstruct the palaeoenvironmental evolution of SW Iberia through the palynological and sedimentological analyses of two cores drilled in La Janda basin (Spain) and one core recovered from the continental shelf of the Algarve (Portugal).
- To identify vegetal dynamics and infer the causes of their changes at different scales (local/regional/global) through the correlation of the presented cores with other palynological records.
- To identify the possible impact of anthropogenic activities through different cultural periods of Prehistory.
- To understand human-environment relationships during the Holocene by correlating the palynological data with the archaeological record.

1.3.- Thesis structure

This thesis is set out in 10 chapters, the first of which presents a general overview that introduces the main objectives and rationale, as well as the structure of the thesis. Chapter 2 presents some important concepts concerning Palaeopalynology as discipline with focus on the methodology, from the sample collection to the data analysis. Chaper 3 outlines a state of the art reviewing the archaeological context, the main climate transformations during the Holocene and the palaeoenvironmental studies based on palynological data carried out in SW Iberia, with a brief explanation of the study sites included in this work. Chapters 4 to 8 present the different case studies that compose the thesis and that are already peer-reviewed published or submitted to be published:

Chapter 4- Representation and biases: pollen-vegetation relationships and their contribution to the study of fossil pollen records in SW Iberia

A multivariate analysis of modern pollen samples collected across different habitats of SW Iberia is presented to explore the relationships between pollen rain and modern vegetation. Some problems affecting the representation of specific taxa are also addressed as possibly caused by different factors that can also be observed in fossil pollen samples.

Chapter 5- 26000 years of environmental evolution of an incised valley in a rocky coast (La Janda wetland, SW Iberia)

A multiproxy analysis (facies, geochemistry, pollen, fossils) were performed on the sediments of 12 cores drilled in La Janda basin. The palaeogeographic evolution is defined and compared with the dynamics of other estuaries in the Gulf of Cádiz to better understand their history during the last fall and rise of the sea level. This chapter gives a general overview that helps to contextualize the results presented in the following chapters.

Chapter 6- Tracing the environmental evolution of coastal ecosystems through Holocene vegetation dynamics in SW Iberia

A multi-proxy approach based on palynological, geochemical and sedimentological analyses carried out in the S3 core drilled in La Janda basin (Cádiz, Spain) is presented in detail to draw the environmental evolution of the study area. Vegetal dynamics and the development of different coastal features are compared between diverse continental cores drilled on the SW Iberian coast in order to define regional patterns.

Chapter 7- Natural and anthropogenic processes in the depression of La Janda (SW Iberia) from the Late Pleistocene to the Mid-Late Holocene

Two sequences retrieved from La Janda basin (Cádiz, Spain), the S3 and S2 cores, are analyzed from a multiproxy approach (palynology, geochemistry, sedimentology) and diachronically correlated with the archaeological record from the eastern part of the Gulf of Cádiz. A selection of specific ecological indicators is used to infer the anthropogenic impact on the landscape between the Late Pleistocene to the Mid-Late Holocene through different cultural periods.

Chapter 8- Environmental changes and cultural transitions in SW Iberia during the Early-Mid Holocene

Palynological and geochemical analyses were carried out in a section from a marine core drilled in the Algarve continental shelf, the GeoB23519-01 core, corresponding to the Early-Mid Holocene. The correlation of these data with the archaeological record of the region allows us to draw a dynamic scenario in which important environmental changes took place during the transition from the Mesolithic to the Neolithic in SW Iberia.

Finally, a general discussion integrating all the data presented in chapters 4 to 8 is developed in chapter 9, culminating in chapter 10, which presents a brief conclusion and outlook that offers some ideas for future studies.

2.- Palaeopalynology as a tool: methodological insights

2.1.-Fundamentals of the discipline

Palynology, as a well-established discipline since the XIX century, studies pollen grains and spores based on the premise that pollen rain represents the vegetation context (Fischer, 1889; Von Post, 1916; Wodehouse, 1935; Traverse, 2007). When applied to fossil records, hence Palaeopalynology, it is assumed that they reflect previously deposited pollen from which the vegetation of the past can be inferred (Fægri and Iversen, 1951; Reille, 1990; Moore et al. 1991; Dincauze, 2000).

Pollen grains are the microgametophyte of seed plants developed from the microspore, while spores are unicellular reproductive units of cryptogams (Fægri and Iversen, 1951; Jackson, 1928). Their outer wall (exine) is composed of an extremely resistant biological material called sporopollenin (Fig. 2.1) that protects the grain and allows its identification due to the specific external morphology of each species and the shared features within genus and family (Fægri and Iversen, 1951; Havinga, 1964; Butzer, 1982; Bradley, 1999).

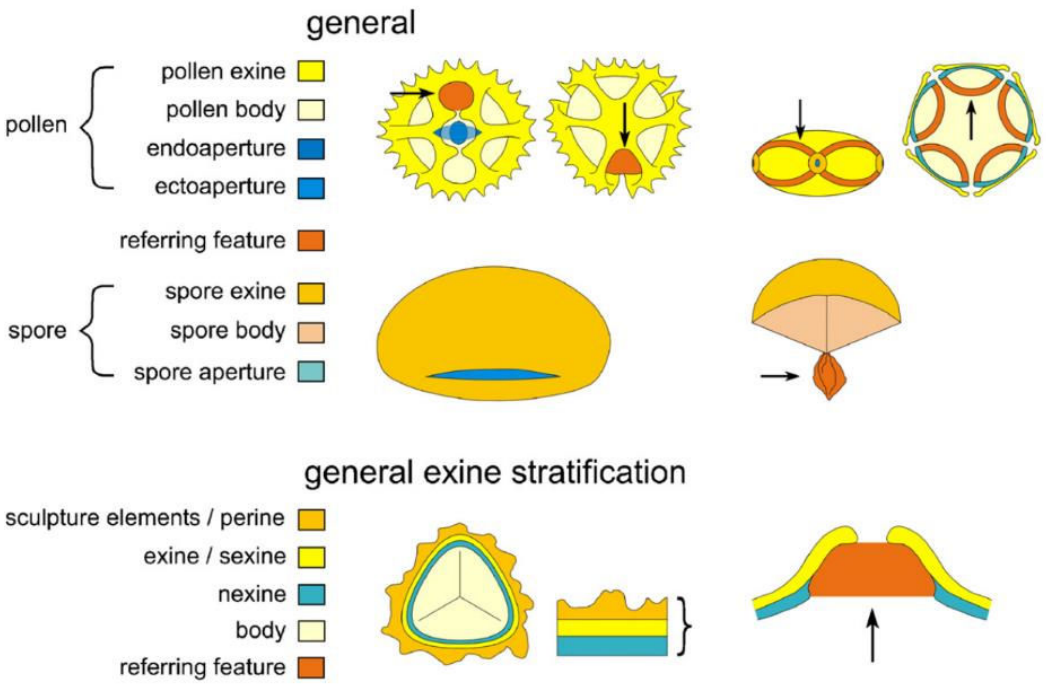

Figure 2.1. Scheme showing the different parts of a pollen grain and a spore, with the exine stratification explained for both of them. Adapted from Punt et al. (2007).

However, palynological analysis often include other palynomorphs, general term for all entities found in palynological preparations (Tschudy, 1961; Punt et al., 2007). When excluding pollen grains and spores of bryophytes and pteridophytes, they are called Non-Pollen Palynomorphs (NPPs) and comprise fungi, micro-algae, dinoflagellates, foraminiferal linings, micro-zoo remains, and micro-charcoal (Van Geel,

2001). They can be composed of sporopollenin, lignin or chitin and their diverse origin and ecological significance may provide key information (Van Geel, 2001; Traverse, 2007; Expósito, 2018). In all cases, the identification of producing plants/organisms is often difficult in fossil records and can usually be traced back to the level of genus or family; only in exceptional cases it is possible to reach the species.

From the moment pollen grains and spores are produced, they are dispersed as part of their reproductive cycle. Dispersal is generally done by wind, animal vectors or water, depending on inherent characteristics of the plant producers, of the grains (size, morphology, weight), and several external factors such as wind speed, atmospheric moisture, etc. (Faegri and Iversen, 1951; Havinga, 1967). Therefore, the palynological residue under study is that which has not reached its target and has become part of the sediment. All the processes that are involved from the moment that grains are generated until they become fossilized are studied by the Taphonomy (Efremov, 1940). Two main phases can be distinguished: biostratinomy, including the production, transport, deposition, and burial; and diagenesis, comprising the processes affecting the material once it is buried (Hunt and Fiacconi, 2018; Expósito, 2018). Considering the differential pollen and spore production of the various species, as well as the vicissitudes arising from the type of dispersal and the elements involved, pollen rain may represent local, regional or extraregional material. In addition, the differences between depositional environments and the potential impact of physical, chemical and biological agents may affect their preservation. Thus, the final representation of vegetation is influenced by several inherent and external factors that come into play throughout the process from pollen/spore production to sediment recovery. In addition to the characteristics and behaviour of the floristic composition, we must consider the potential taphonomic factors that could result into biases of unknown origin. Therefore, taking into account all these elements is essential for interpreting palynological data from sedimentary sequences.

2.2.- Fieldwork and laboratory treatment

The material basis for conducting a palynological study begins with fieldwork, which in this case involved the collection of three sediment cores from marine and continental deposits that are described in detail in chapters 5, 6, 7 and 8.

The cores drilled in La Janda (Cádiz, Spain) were recovered by triple barrel system (Mediavilla et al., 2023). The 27.5 m-long S2 core (36º14'53.88" N, 5º50'21.45" W) was drilled at 4.88 m above sea level (asl), while the 26.78 m-long S3 core (36º15'09.68" N, 5º50'08.52" W) was drilled at 5.59 m asl. Once they were recovered they were encased in PVC pipes and stored at the Geological and Mining Institute of Spain (IGME, CSIC) facilities, to be subsequently opened in two halves, described and photographed. Palynological samples of ca. 10 gr each were collected from the S3 core following a constant interval of ~10 cm to have a good representation of all the sections. These samples were stored in labelled plastic

bags and kept at 4ºC at the Institute of Neotectonics and Natural Hazards (RWTH Aachen University) facilities. In the case of the S2 core, test samples were taken every 40-60 cm by different researchers before the beginning of the present thesis and they were processed after 2 years since their collection. The GeoB23519-01 core (37º00.656, 008º 52.247) was drilled at ~65m water depth in the Algarve continental shelf using a vibracoring system and resulting in a 3.64 m-long sequence (Reicherter et al., 2019; Feist et al., 2023). Once it was recovered, it was encased in PVC pipes and, after the M152 cruise, it was stored at the Institute of Neotectonics and Natural Hazards (RWTH Aachen University) facilities, where it was opened in two halves, described and photographed. Palynological samples of ca. 10 gr each were collected with an interval of 3-7 cm, stored in labelled plastic bags and kept at 4ºC.

The chemical process for isolating palynomorphs from sediment samples at the laboratory can be done in different ways, but there are usually some steps that are common to diverse protocols consisting on the removal of carbonates and humic acids (Faegri and Iversen, 1951; Moore et al., 1991). Although different treatments can be applied depending on the characteristics of the material to be processed, the availability of resources and the characteristics of the facilities may ultimately determine the different steps to follow in many cases. For the present thesis, a protocol for palynological analysis was developed at the Institute of Neotectonics and Natural Hazards (RWTH Aachen University) adapted to the equipment available at the laboratory. This was based on other protocols (Faegri and Iversen, 1951; Goeury and de Beaulieu, 1979; Moore et al., 1991; Burjachs et al., 2003) and it is described in the following steps:

- Determining the sample volume by weighing the sediment on a precision balance.
- Adding two *Lycopodium clavatum* tablets (exotic marker) to each sample to calculate the concentration (grains/gr of dry sediment) following Stockmarr (1971).
- Removing carbonates by adding HCl at 10% to the beaker in which the sediment is placed. This step is followed by different centrifugation and washing cycles with deionized water until a transparent supernatant is obtained. Depending on the sediment, a 0.5 mm sieve could be used to separate macrobotanical remains, archaeological material, etc.
- Removing of humic acids by adding KOH at 10%. Tubes should be placed in a water bath for 10 min at 60°C. Centrifugation and washing cycles should be then performed until a transparent supernatant is obtained. It is important to let the sediment dry by turning the tubes upside down.
- Adding sodium polytungstate - SPT (3NaWO4.9WO3.H2O) at 2.0-2.1 g/cm^3 to the tubes for density separation. Sediment should be mixed until no lumps remain and tubes should be centrifuged for 30 min at 2500 rpm. After this, pollen residue will float in the heavy liquid and the sediment will remain at the bottom. Transfer the pollen residue to new tubes, and perform diverse centrifugation and washing cycles that shall end when the pollen residue remains at the

bottom and the supernatant is transparent. Tubes must be turned upside down to let the residue dry.

- Whether the residue is to be mounted on a slide or stored, a few glycerol drops should be added for preserving the palynological residue in a liquid medium.
- Slides are prepared by mounting a few drops of the residue mixed in glycerol. The slides are sealed by adding Histolaque to the edges of the glass coverlip.

2.3.- Data analysis

For a pollen spectrum to be considered reliable, a minimum number of pollen grains must be reached during the counting process. The behaviour of some taxa in relation to their production and dispersion in Nature is well-know (Fig. 2.2), for which it is recognised that elements such as *Pinus*, aquatic taxa, and NPP may be overrepresented. Because of this, when the percentages of each taxon are calculated from the raw data, some specific sums are made to exclude those elements that may mask the remaining palynomorphs and distort the results (Faegri and Iversen, 1951; Cour, 1974; Moore et al., 1991). Thus, a basis sum/terrestrial pollen sum is calculated including the arboreal pollen (AP) and non-arboreal pollen (NAP) taxa. The excluded taxa are calculated in relation to this sum (and not as part of it), it means, to the total pollen count (López-Sáez et al., 2000). The excluded taxa may vary depending on the characteristics of each deposit: *Pinus* is usually excluded from marine cores (Turon, 1984; Naughton et al., 2007; Gomes et al., 2020), Asteraceae may be excluded from archaeological deposits (Carrión, 1992), aquatic taxa are excluded from lakes (Faegri and Iversen, 1951), etc. Taking this into consideration, the minimum number of pollen grains counted refer to those taxa that will be included in the basis sum/terrestrial pollen sum.

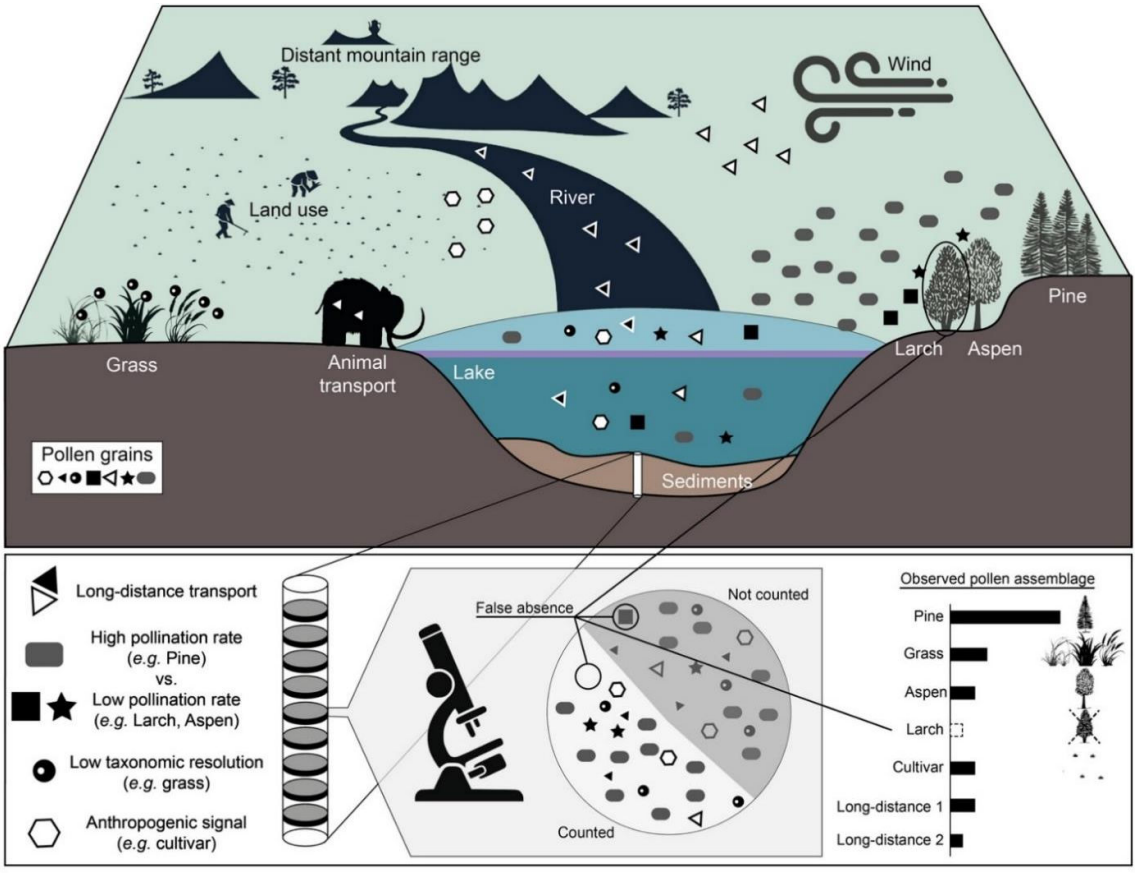

Figure 2.2. Conceptual example explaining different processes involved from pollen production to their recovery in a lake deposit. The squares, stars, rounded rectangles and black circles refer to pollen grains derived from local vegetation around the lake. Black and white triangles indicate regional or extraregional pollen transported over long distances by the river and wind, respectively. Each type of plant produces different quantities of pollen (trees on the right shore of the lake), some of them indistinguishable at the level of species or even genus (grasses on the left shore of the lake). The white hexagons represent cultivated plants (e.g., maize or rice fields) and anthropogenic activity. Animals on the landscape (e.g., mammoth) can also transport pollen that is deposited in the sediments. All these pollen grains accumulate at the bottom of the lake from where sediments are collected using coring equipment (white cylinder). After the lab treatment, the pollen residue under the microscope is composed of a pollen assemblage that represents a combination of all the processes in action in this landscape and in the lab. Adapted from Chevalier et al. (2020).

Statistical treatment of the significant minimum pollen count (MPC) dates back to the 30s, when the comparison of samples from diverse environments from temperate humid regions of North America and Europe were done using different correlation coefficients and suggesting a MPC of 150-200 pollen grains (Erdtman, 1932; Barkley, 1934; Lytle and Wahl, 2005). Different approaches have been carried out in successive decades, concluding that the distinct sedimentary nature of samples may result determinant: in altered contexts, such as archaeological deposits, a minimum of 150 pollen grains was determined as reliable (Burjachs, 1990; Sánchez-Góñi, 1993), while in sediments in which there is a good preservation and high concentration of pollen grains, such as in peat bogs, counts can reach 500 grains (Moore et al., 1991). Based on different statistical techniques and considering that fossil sequences may represent a succession of diverse sedimentary environments, a minimum of 300 pollen grains has been established as reliable for natural deposits (e.g., Reille, 1990; Moore et al., 1991; Lau et al., 2018; Djamali and Cilleros, 2020).

Furthermore, a certain taxonomic diversity must be achieved to be sure that results are realistic and not biased. Several authors established that a minimum of 20 taxa that can coexist in the same vegetal formation should be identified in order to be ecologically coherent (Pons and Reille, 1986; Sánchez-Goñi, 1993).

For the present thesis, palynomorphs were counted using a Leica ICC50 HD optical microscope at 400x and 1000x to a minimum terrestrial pollen sum of 300 pollen grains with the help of published keys and atlases to assist in their identification (van Geel, 1978, 2001; van Geel et al., 1980, 1986, 1989, 2003; Moore et al., 1991; Reille, 1992, 1995). Some species such as those corresponding to the genera *Pinus* and *Quercus* were discriminated based on morphometric studies following Carrión et al. (2000a, 2000b). Poaceae ≥45μm was classified as Cerealia type according to López-Sáez and López-Merino (2005). Pollen concentrations (grains/gr) were estimated by adding two *Lycopodium clavatum* tablets to each sample (Stockmarr, 1971), allowing us to know the richness/poverty of pollen grains per sample as well as to test the validity of the laboratory treatment. Terrestrial pollen sum (TPS) excluded aquatic pollen types, which were included in the total sum (TS) together with Non-Pollen Palynomorphs. Palynological diagrams were plotted against age and depth using TiliaIT software (version 2.1.1, Illinois State Museum, Research and Collection Center, Springfield USA).

2.4.- Multi-proxy approach

Apart from the palynological analyses on which this thesis is based, other destructive and non-destructive analyses have been performed on La Janda cores at the Geological and Mining Institute of Spain (IGME, CSIC) facilities.

Non-destructive-analyses include:

- Core colour scan (high resolution images with a down core resolution of 50 μm) with a Geoscan IV coupled to the MSCL GEOTEK.
- Colour (RGB) analyses were performed with 1 mm down core resolution using a Konica Minolta 700-d spectrophotometer integrated in the GEOTEK XRF core scanner. Each channel had values ranging from 0 up to 255 and a R/(G+B) colour index was used to represent the dominant tones (red/brownish against green/greyish) and a (R+G+B)/3 index represents the grey scale range.
- Geophysical properties (P-wave velocity, gamma density, non-contact resistivity and magnetic susceptibility) were analysed with 1 cm down core resolution with a GEOTEK Multi-Sensor Core Logger (MSCL-GEOTEK).
- XRF scanning with a GEOTEK XRF core scanner in a He purged atmosphere with an illumination window of 15 mm (cross-core slit width) x 10 mm (down-core resolution). Two runs, with 30 seconds count time exposure, were performed for 10 kV and 40 kV (detecting from Mg to U). XRF spectra were processed with bAxil. Element intensities are represented in counts per second (cps).

Destructive sampling analyses:

- Mineralogical analysis by X-ray diffractometry (PTE-RX-04) for bulk sample and <2μm fraction. These analyses were used to check the sources of the chemical elements obtained from geochemical analyses.
- Geochemical analysis of major oxides and trace elements by X-ray fluorescence and atomic absorption spectroscopy (XRF and AAS). The results were used to check the validity of the non-destructive high-resolution XRF scanning.
- C (organic, inorganic and total) and S by elemental analyser (ELTRA). S data was used to check the results of XRF core scanning. C values gave an estimate of organic matter and carbonate content, and they can be compared to other results from non-destructive techniques (XRF core scanning and colour).

XRF scanning with an ITRAX core scanner (resolution 2 mm, 20 s exposure time, 30 kV, 55 mA) was performed on the GeoB23519-01 core at the Köln University (Germany) facilities.

3.- State of the art

3.1.- Archaeological context

SW Iberia has a long history of human occupation and it has also been regarded as a reservoir of biodiversity during the Late Pleistocene and the Holocene, reinforcing its role as a favorable settlement area throughout Prehistory (Carrión et al., 2008). Indeed, the archaeological record in the study region indicates that, during the Holocene, human groups adapted to various and dynamic environments through a diversity of strategies and choices during the Mesolithic, Neolithic, Chalcolithic, and Bronze Age periods (Giles Pacheco and Sáez, 1978; Sanchidrián, 1992; Domínguez-Bella, 1995; Ramos Muñoz et al., 1998, 2004-2005, 2006b, 2010b, 2011; Ramos Muñoz, 2004a, 2006b, 2008; Domínguez-Bella et al., 2015; Becerra et al., 2019).

The period between the Late Pleistocene-Holocene transition until ca. 7.8 ka cal BP witnessed the last hunter-gatherer groups in the Peninsula. In SW Iberia, most of the Mesolithic sites concentrate in the Western area, near Cape São Vicente, while a low number of sites are preserved in the eastern part of the Gulf of Cádiz (Uzquiano et al., 2000; Ramos et al., 2005). In all cases, they are located along the coast, close to marine environments or transitional areas between fluvial and marine influences (Carvalho et al., 2007). It is possible to characterize those sites as shell-middens of different sizes or open air camps, in both cases interpreted as seasonal occupations for the exploitation of natural resources (Valente et al., 2009). By the end of this period, important cultural transformations are identified in the material record reflecting a change from the socio-economic organization of the last hunter-gatherer groups to a new life based on food production of the first agropastoral communities.

Although analyzing diverse Neolithic trajectories and cultural dynamics within this period is beyond the reach of this thesis, it is important to mention that the process of neolithization in Southwestern Iberia is controversially disputed and different theories attempt to explain its origin. Some authors interpret it as a maritime pioneer colonisation of depopulated regions by Neolithic groups from the Western Mediterranean (Zilhão, 2001), while others propose indigenous origins defined by the continuity of local Mesolithic groups in certain regions, suggesting that the beginnings of agriculture could have had an autochthonous nature (Massieu and Socas, 2013). Many authors consider that the area of Andalusia, the Algarve, and the Moroccan Atlantic fringe have shared similar traits during this process (Manen et al., 2004), which would explain the existence of Neolithic "enclaves" with specific regional features (Carvalho, 2010) or a southern neolithization route along the North African coast (Borja et al., 2010; Linstädter, et al., 2012). Recent palaeogenetic studies have shed light on this complicated situation, confirming that Southern Iberian Neolithic humans share the same genetic composition as the Cardial Mediterranean culture that reached Iberia ca. 7.5 ka BP (Fregel et al., 2018). This may support the notion

that Neolithic migrants from the Eastern Mediterranean mixed with resident hunter gatherers, although the pace of this process and the implications in cultural and socio-economic terms is something that need further research. However, the inherently intricate interpretation of such complex processes is weighed down by the lack of absolute datings in clear stratigraphic sequences and the absence of information regarding the Mesolithic period at a regional scale, as well as the transition to the Neolithic in SW Iberia (Martín- Socas et al., 2018).

The Neolithic period in SW Iberia is reflected in a diversity of settlement typologies. In the Western area, some temporary open-air sites and shell-middens based on the seasonal exploitation of marine resources are still present (Carvalho, 2007). Exceptionally, some Mesolithic sites revealed Early Neolithic layers (Carvalho, 2007; Valente and Carvalho, 2009; Peyroteo-Sterna, 2020). The use of caves in mountain areas become relatively generalized across the Gulf of Cádiz, in some cases used as necropolis, and several open-air sites were identified and interpreted as residential basecamps and sedentary occupations. These new Neolithic sites are located in coastal zones, river valleys, plains and the inland countryside (Martín-Socas et al., 2018). Transformation processes probably involved diverse social, political and economic changes, which were reflected in the concentration and sedentarisation of the population from ca. 6 ka cal BP, especially in areas of great farming potential (Thomas, 2009). According to some researchers, the differences in the material culture between sites should be understood in the context of their geographical location and different rhythms of implantation of the new farming societies (Martin-Socas et al., 2018). Nevertheless, certain environmental changes impacting the coastline may have not only influenced settlement patterns but also affected the preservation of archaeological sites. Therefore, it is advisable to exercise caution to avoid potential interpretative biases (Val-Peón et al., 2021).

The Chalcolithic in SW Iberia is, according to the synthesis provided by García-Rivero and Escacena-Carrasco (2015), defined by the existence of populations that vary in size, with a dense occupation of the territory preferring fertile areas (*campiñas*, river valleys). The economy of these groups was based on livestock and agricultural activities with exploitation of their by-products, and a rich symbolic world dominated by funerary structures with multiple burials, rock art and figurines (*ídolos*). However, the Early Bronze Age is defined by smaller and scattered settlements distributed through heterogeneous ecosystems (mountain areas, littoral, *campiña*…) (García-Rivero and Escacena-Carrasco, 2015). In some cases, it seems that the economy was less extensive than that of the Chalcolithic and had a marked pastoral aspect (Lull et al., 2010). During this period some artistic representations, such as idols, disappeared and new funerary rites characterized by individual burials in pits or cists forming necropolises emerged (Carrasco and Reyes, 1986). Interestingly, there are just a few continuous stratigraphies with Early Bronze Age levels directly above those of the Chalcolithic (Belén et al., 2000).

Some authors consider the climatic conditions as main drivers of a "population decrease", arguing that the trend towards a drier climate would have been more marked in SW Iberia and might have led to agricultural and social problems (Martín- Puertas et al., 2008). However, other authors prefer to approach this idea with caution, as divergent levels of resolution and different timing in changes are identified in palaeoenvironmental records from Southern Iberia (Lillios et al., 2016). Some historical hypotheses aim to explain these changes through two ideas that are not mutually exclusive: a) there was a process of change within the same population; b) there was a substitution of human groups with different cultural backgrounds (García-Rivero and Escacena-Carrasco, 2015). Some recent approaches interpret that the general scenario suggests the presence of distinct human communities which, with their natural internal diversity throughout their populations, coexisted, came into contact (generating a spatially and chronologically variable archaeological record) and eventually replaced each other (García-Rivero and Escacena-Carrasco, 2015).

3.2.- Holocene climate: the Iberian Peninsula in a global context

The Holocene is the most recent stratigraphic unit and interglacial period covering the time interval from 11.7 ka BP until the present day (Walker et al., 2012). Although it has been traditionally considered a rather uniform period by some authors, especially when compared to other climatic epochs (e.g., Dansgaard et al., 1993), investigations performed during the last decades revealed major climate transformations at different time scales (e.g., Bond et al., 2001; Borzenkova et al., 2015; Bini et al., 2019). Orbital-scale variations in the Earth´s position relative to the Sun resulted in alterations in seasonal insolation, which implied a series of gradual changes in the seasonal energy input from the Sun (Mayewski et al., 2004). On a millennial-scale, a number of climatic events associated with ice- bearing, freshwater inputs into the North Atlantic Ocean that would have provoked changes in the thermohaline and atmospheric circulations have also been identified (Fig. 3.1) (Bond et al., 1997, 2001; Grootes et al., 1999). As a result of these long and short-term processes, atmospheric and oceanic circulation patterns have been continuously adjusting and changing, thus affecting the temperature and precipitation distribution, as well as vegetation patterns (Dallmeyer et al., 2021). However, the consequences of these changes have been strongly determined by the heterogeneous orographic characteristics in areas from Southern Europe, such as the Iberian Peninsula, resulting in large spatial variability and the existence of many subregional features (Lionello, 2006; Jalut et al., 2009).

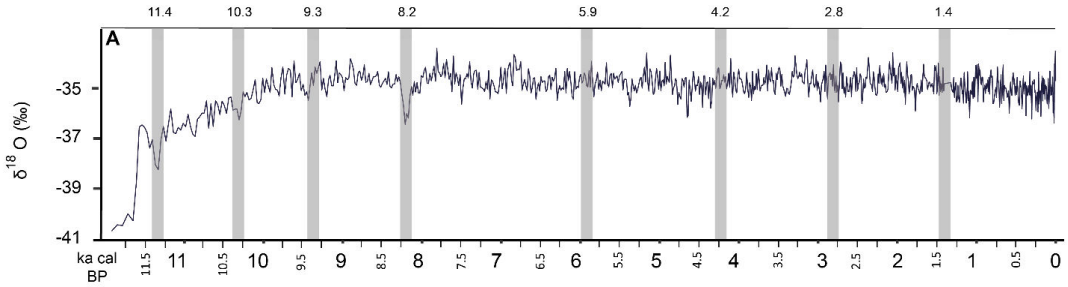

Figure 3.1. GISP2 oxygen isotope curve for the Holocene adapted from Grootes et al. (1999) where light grey lines and their chronologies correspond to ice-rafted debris events in the North Atlantic Ocean based on Bond et al. (1997, 2001).

The Iberian Peninsula is located in a transition zone between temperate central Europe and arid North Africa, subjected to the North Atlantic Oscillation (NAO) and influenced by both Atlantic and Mediterranean atmospheric regimes (Trigo et al., 2006; Lionello, 2012). Most of the precipitation in the Iberian Peninsula occurs during winter season and are strongly influenced by the NAO, the main pattern of atmospheric variability affecting the Northern Hemisphere, calculated as the pressure differences between the Icelandic Low and the Azores High (Hurrell, 1995). As a synthesis, during positive phases of the NAO the large pressure difference between the Icelandic Low and the Azores High results in cooler and drier conditions over Southern Europe and Northern Africa, with below-average precipitation rates over large parts of the Western and Northern Mediterranean (Ulbrich et al., 1999; Trigo et al., 2002, 2004). During negative phases of the NAO (small pressure difference), storm tracks are directed towards the Iberian Peninsula, which experiences wetter winters (Trigo et al., 2006; Schirrmacher et al., 2019). The pronounced difference in precipitation is not only evident on a large scale, but also within the Iberian Peninsula with a clear seasonal variability between the Atlantic and Mediterranean areas. Areas with Atlantic climate are defined by relatively cool temperatures and evenly distributed precipitation throughout the year, while those affected by Mediterranean climate are characterized by pronounced seasonal contrasts and a marked hot summer season (Lionello, 2012). Two main regions are also identified from a biogeographical/climatic point of view (Fig. 3.2), the Eurosiberian and the Mediterranean, that are home to a wide range of ecosystems derived from multiple environmental nuances (De la Serna et al., 2016; Rivas-Martínez et al., 2017).

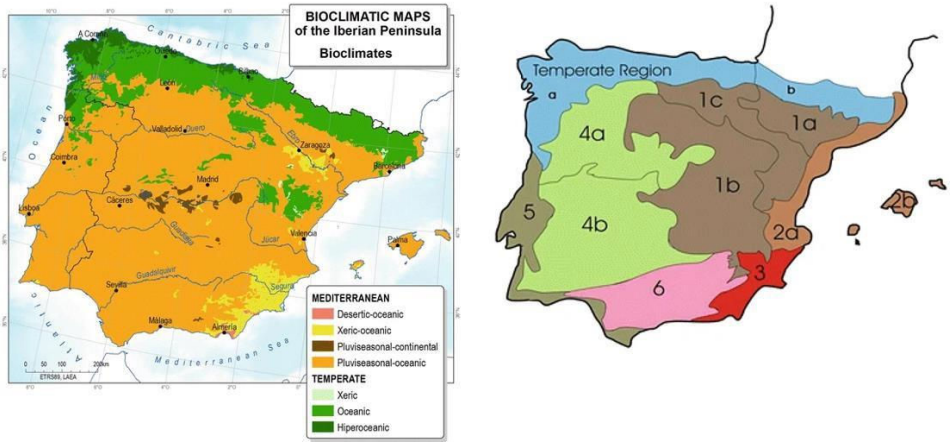

Figure 3.2. A) Bioclimatic map of the Iberian Peninsula with it associated legend adapted from Rivas-Martínez et al. (2017); B) Iberian biogeographic regions adapted by De la Serna et al. (2016) from Rivas-Martínez et al. (2011): Temperate region: (a) Atlantic-European Province, (b) Cévennean-Pyrenean Province; Mediterranean region: (1) Mediterranean Central Iberian Province (Subprovinces: a. Low Aragonese, b. Castilian, c. Oro- Iberian), (2) Balearic-Catalan-Provençal Province (Subprovinces: a. Catalan-Valencian, b. Balearic), (3) Murcian Almeriensian, (4) Mediterranean West-Iberian Province (Subprovinces: a. Carpetan-Leonese, b. Lusitanan- Extremadurean), (5) Coastal-Lusitanian-Andalusian Province, (6) Betic Province.

Considering this general scenario, the heterogeneity and multiplicity of factors involved in present and past climate variability must be taken into account when studying them from a diachronic perspective. Although local and regional diversity are significant, several palaeoenvironmental studies carried out in the Iberian Peninsula revealed the existence of some general trends. With the post-glacial warming, a rapid sea-level rise took place changing the morphology of coastal areas and flooding river valleys (e.g., Frigola et al., 2007; Zazo et al., 2008; Vacchi et al., 2016, 2021; Mediavilla et al., 2023). The increased temperatures and moisture also resulted in the expansion of temperate and Mediterranean forests to the detriment of steppe vegetation across Southern Europe (e.g., Desprat et al., 2007; Carrión et al., 2010; Camuera et al., 2019; Gomes et al., 2020). A period of maximum forest expansion was recorded during part of the Early-Mid Holocene, with a duration and temporal extension that differs among regions (e.g., Pérez-Obiol and Julià, 1994; Carrión and Van Geel, 1999; Martrat et al., 2004; Fletcher et al., 2007). A general aridification trend was identified in several sequences from ca. 5 ka cal BP, attributed by some authors to a decrease in the insolation and the installation of the present atmosphere circulation in the Northern Hemisphere (Bond et al., 2001; Jalut et al., 2009; Fletcher et al., 2013). Parallel to this, the impact of anthropogenic activities was becoming increasingly evident up to the present (e.g., Carrión et al., 2010; Revelles et al., 2016).

3.3.- Palaeoenvironmental research in SW Iberia

Although the study of palynological sequences in the Iberian Peninsula has considerable increased over the last years (e.g., synthesis from Carrión et al., 2010), there are still some gaps to be filled in areas such as SW Iberia. As already mentioned, one of the main problems is the scarcity of continuous continental sequences, partly related to the geological characteristics of the territory, the inherent dynamism of transitional environments and the hazardous nature of the SW Iberian Atlantic Margin (Zazo et al., 2008; Newton et al., 2014; Mediavilla et al., 2023). On a recurring basis, preservation problems are also common and may result in a lack of palynological material in entire sequences or sections (Fletcher, 2005; Schröder et al., 2018). In other cases, a lack of a good chronological control and an accurate age-depth model, especially in the older cores, makes interpretations more complicated. However, there are well-dated continental deposits with a good resolution that fall within the Holocene and allow to reconstruct the environmental evolution of the study area from a diachronic perspective. These are located in: the Guadiana estuary (Fletcher, 2005; Fletcher et al, 2007), Las Madres (Yll et al., 2003), Doñana (Jiménez-Moreno et al., 2015; López-Sáez et al., 2018; Manzano et al., 2018), Laguna de Medina (Reed et al., 2001; Schröder et al., 2018, 2020) and the cores drilled in La Janda presented in this thesis. Other palynological studies have been carried out on natural deposits from SW Iberia providing important data, although they do not rely on any age-depth model: Las Madres (Stevenson, 1985; Stevenson and Harris, 1992), Mari López (Zazo et al., 1999; Yll et al., 2003), Marismillas (Yll et al., 2003), El Asperillo (Stevenson, 1984), El Acebrón (Stevenson and Moore, 1988; Stevenson and Harris, 1992), Doñana (Stevenson, 1985), and Los Alcornocales (Gutiérrez et al., 1996). In many cases, the influence that local factors such as tides, subsidence, the development of spit barriers, etc., has in these transitional environments resulted in great landscape transformations over time, e.g., the transition from a coastal lake to a wetland, the closure of an estuary, etc. (Yll et al., 2003; López-Sáez et al., 2018; Mediavilla et al., 2023). This inevitably affected the development of some vegetal communities dependent on specific soil conditions that may be constantly changing. While an important part of the pollen signature has a local character, being sometimes overrepresented, these continental sequences share some general trends that allow to define regional patterns that will be further explored in other chapters of this work.

In contrast, palynological sequences corresponding to marine cores may likely reflect a regional-extraregional pollen signature due to their wider catchment areas. Several marine sequences were drilled in Southern Iberia: near the NW coast of Africa (Hooghiemstra et al., 1992), in the Southern Portuguese Atlantic Margin (Hooghiemstra et al., 1992; Lèzine and Denèfle, 1997; Turon et al., 2003; Chabaud et al., 2014) and in the Alborán Sea (Fletcher and Sánchez-Goñi, 2008; Combourieu-Nebout et al., 2009). However, only two were recovered from the Gulf of Cádiz: the SU-8118 core (Parra, 1994; Carrión et al., 2000) and the GeoB23519-01 core presented in this thesis (Val-Peón et al., 2021). Therefore, land-

sea pollen correlations should be done with caution, as Southern Iberia shows a strong spatial and temporal variability and some global-regional trends from distant areas may not be easily extrapolated to the Gulf of Cádiz.

3.4.- Selection of study sites and related projects

3.4.1.- La Janda basin

The study of different cores drilled from La Janda basin (Fig. 3.3) was framed within two projects: the CRC 806 "Our way to Europe" project (no.57444011–SFB806) funded by the Deutsche Forschungsgemeinschaft (DFG) and the associated "Climatic and environmental changes in the Upper Pleistocene – Middle Holocene of the Iberian Peninsula" project (GESTEC2686) funded by the Spanish Ministry of Science and Innovation (MCIN). In addition, some analyses were funded by a "Severo Ochoa" extraordinary grant for excellence IGME-CSIC (AECEX2021). The main objective of both projects was to study palaeoenvironmental changes and their impact in human groups, with the *Homo sapiens sapiens* expansion across Europe as a backdrop (Richter, 1996). Therefore, the study of La Janda aims to provide new data on the environmental evolution of Southwestern Iberia as a key location for archaeological investigations over the Late Pleistocene and the Holocene. However, due to the results obtained (explained in the following chapters), the present work focuses on the Holocene.

La Janda basin (Fig. 3.3) is located in a tectonic graben of about 35 km^2 in the Southwestern Atlantic margin of the Iberian Peninsula, near the Strait of Gibraltar (Mediavilla et al., 2023). It is placed in the convergence area of the Eurasian-African plates, being a NW-SE fault-controlled depression in which the lowest point is about 3 m asl and the highest surrounding areas are higher than 400 m asl (Goy et al., 1995; Zazo et al., 1999; Luque et al., 2001). The basin develops on the allochthonous units of Campo de Gibraltar and the detrital post-orogenic materials from the upper Miocene to the Quaternary (Gutiérrez-Mas et al., 1991; Luque et al., 2001). Present day basin is drained by the Barbate River and its tributaries, Almodóvar and Celemín rivers, which are heavily disturbed by farming activities (Mediavilla et al., 2023). The Barbate River crosses the basin and runs to the sea through a narrow gorge flowing into a marsh complex with a tidal range of near 2 m (Instituto Hidrográfico de la Marina, 2019).

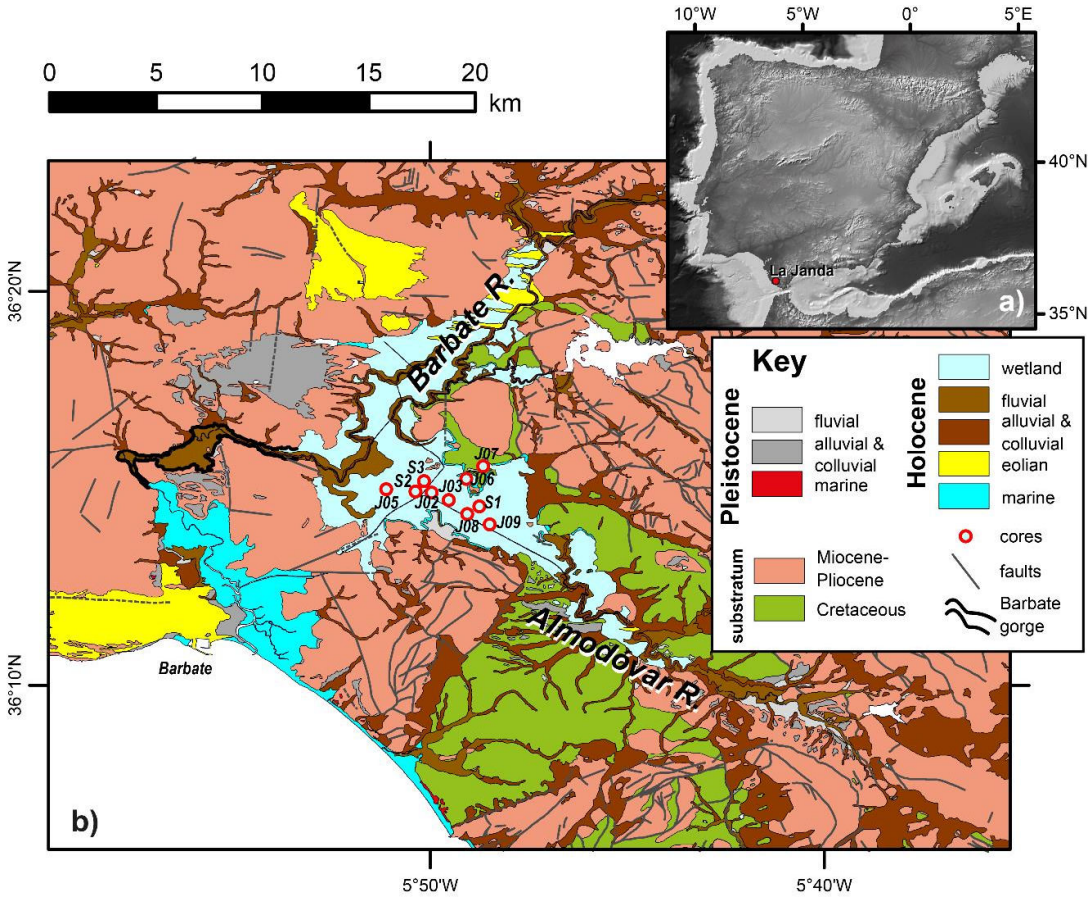

Figure 3.3. A) La Janda basin marked with a red square in the Iberian Peninsula; B) Geological map of La Janda basin and borders, simplified from the Continuous Geological Map of Spain 1:50.000 (GEODE). Red and orange dots indicate all the cores drilled in the basin and their names. Geographical data provided by the Spanish Geographical Institute (IGN) and the geological map by the Instituto Geológico y Minero de España, CSIC (Roldán et al., 2021). Adapted from Mediavilla et al. (2023).

The Mediterranean climate of the region is classified as Csa type, characterized by mild winters and hot and dry summers (Kottek et al., 2006). Mean annual temperature is 20ºC, with average minimum temperatures of 5.3ºC in January and average maximum temperatures of 33.1ºC in July and August (period 1971-2000; AEMET, 2011). Mean annual precipitation averages between 600-800 mm, concentrated in autumn and winter (period 1971-2000; AEMET, 2011). Prevailing winds are followed by W and SW winds in frequency (Dueñas López and Recio Espejo, 2000). From a biogeographical point of view, La Janda is framed in the Gaditano-Onubense Littoral and the Aljibe sectors (Junta de Andalucía, 2004; Rivas-Martínez et al., 2014). The first is included within the humid to sub-humid thermomediterranean ombrotypes, and the second is categorized as thermomediterranean with dry to humid ombrotypes with a marked oceanic influence due to the proximity of the Gibraltar Strait (Rivas-Martínez et al., 2014).

La Janda basin is nowadays composed of different land units such as wetlands, farmlands and the

mountains surrounding the area. This natural setting is composed of diverse environments and their vegetal communities: fir forests in the high-mountains and oakwoods in medium-high areas at the Alcornocales Park; Mediterranean formations at lower altitudes; riparian forests running from the mountains to the sea; and heathland communities growing in different soils (Rivas-Martínez et al. 1990; Domínguez et al., 1993; Loidi et al., 2007; Espírito-Santo et al., 2017). Transitional environments play a major role in biodiversity, not only in La Janda basin but in nearby areas such as La Breña y Marismas del Barbate and El Estrecho parks. There, vegetation is mostly defined by the substrate and drying cycle, with temporary ponds of saline, brackish or freshwater, more or less opened coastal marshes, dunes, lakes, etc. (Rivas-Martínez et al., 1990; Latorre et al., 1996; Espírito-Santo et al., 2017; Marcenò et al., 2018). A significant part of the surface in La Janda and its surroundings is dedicated to livestock and agricultural activities, with irrigated crops in flat areas, dry grasses on gentle slopes, and pastures on lands that are less suitable for agricultural purposes (Junta de Andalucía, 2014a, 2014b). The vegetation is described in more detail in chapters 4, 6 and 7.

3.4.2.- The Algarve continental shelf

The study of different cores drilled in the Algarve continental shelf are part of a wider research focused on the characterization of tsunami events through diverse sedimentary parameters (Reicherter et al., 2019). This investigation was supported by the Fundação para a Ciência e Tecnologia (FCT, Portugal) through the "OnOff" project and by the Deutsche Forschungsgemeinschaft (DFG) through the METEOR Cruise M152/1 and the "Holocene offshore tsunami archive – Tsunami deposits on the Algarve shelf (Portugal)" project (Feist et al., 2023). Nineteen cores were drilled in 2018 in the Algarve continental shelf for this purpose (Fig. 3.4). Although palynological analysis was not within the objectives of this research, one core was sampled with the secondary goal of characterizing the environment as a general scenario for the occurrence of specific tsunami events. Therefore, the lower part of the GeoB23519-01 core is presented in this thesis in order to discuss some issues on direct land-sea pollen correlations in SW Iberia.

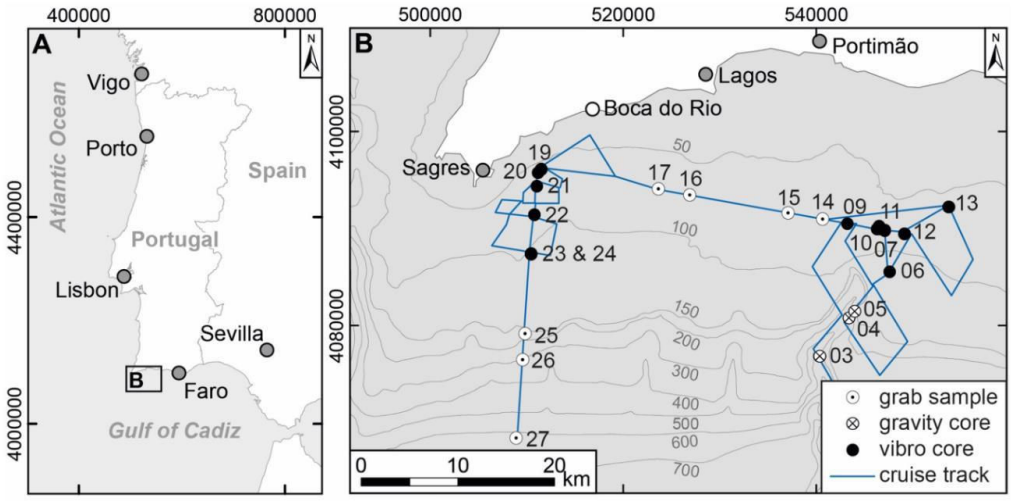

Figure 3.4. A) The western Iberian Peninsula with the major cities and the study area (B) marked; B) Transects and drilling points corresponding to the expedition M152/1 in the Algarve continental shelf. Adapted from Reicherter et al. (2019).

The Algarve continental shelf stretches from cape São Vicente to the Guadalquivir alloctonous unit in SW Iberia, with a mean width of ca. 17 km (Feist et al., 2023). The westernmost part is a Meso- Cenozoic sedimentary basin overlying Carboniferous basement, which extends offshore as far as 100 km south until ca. 100-150 m water depth (Ramos et al., 2016). However, most of the coast is dominated by Neogene basins defined by the presence of several estuaries conforming littoral lowlands, some of them sheltered by sand spits (Dabrio et al., 2000; Hernández-Molina et al., 2006). The Western Algarve is affected by the Mediterranean Outflow Water (MOW), a complex system of currents flowing from the Mediterranean Sea into the Gulf of Cádiz (Baringer and Price, 1999) as well as for storm waves with west to southwest direction (Feist et al. 2023).

The vast area encompassing the Algarve region in SW Iberia may vary in terms of climate: temperate climate with dry/hot summers (Csa type), mostly at high altitudes and inland; and dry/temperate summers (Csb type) with oceanic influence, mostly in the littoral (Rivas-Martínez et al., 1990; Kottek et al., 2006). Temperatures and precipitation differ considerably between zones, with annual average minimum temperatures that range between 10-15 ºC on the coast and 5-10 ºC in the uplands, while average maximum temperatures vary between 22-20 ºC on the coast and 20-15 ºC in the uplands (period 1971-2000; AEMET, 2011). Precipitation concentrates during the winter season with mean annual values that range between 400-1000 mm, reaching 1400 mm in high altitudes (period 1971- 2000; AEMET, 2011). Vegetal communities are common to those already described for La Janda basin, and are explained in detail in chapter 7.

4.- Representation and biases: Pollen-vegetation relationships and their contribution to the study of fossil pollen records in SW Iberia

This chapter is a slightly modified version of an article published in Review of Palaeobotany and Palynology:

Val-Peón, C., Maié, T., López-Sáez, J.A., Santisteban, J.I., Mediavilla, R., Reicherter, K. (2023). Representation and biases: Pollen-vegetation relationships and their contribution to the study of fossil pollen records in SW Iberia. https://doi.org/10.1016/j.revpalbo.2023.104919

Abstract

In order to provide a better framework for the interpretation of fossil pollen records, a set of 49 modern pollen samples collected across different habitats of SW Iberia, categorised by context and sample type (soil vs moss), were selected to explore pollen-vegetation relationships by multivariate analysis and identify possible biases in pollen representativeness. The distribution of both samples and pollen taxa in the plots is successfully explained according to specific environmental variables in some clusters (A, B and E) in which plant communities depend on certain environmental conditions. On the other hand, other clusters (C, D and F) are better explained by opposition to some variables and suggest a wider range of adaptability of their floristic communities. The classification of samples by context consistently explains their differences in vegetal and environmental terms. However, some discrepancies seem to be better explained by sample type (soil vs moss), which raises some questions on how taphonomic factors may cause biases in both modern and fossil pollen samples.

Keywords: Modern pollen samples, SW Iberia, Environmental variables, Taphonomy, Fossil records, Open databases

4.1.- Introduction

Palynological analyses of sedimentary archives are a powerful tool to understand vegetation changes and reconstruct past environments (e.g. Sánchez-Goñi et al., 2006; Jalut et al., 2009; Fletcher et al., 2010; Oliveira et al., 2018; Camuera et al., 2019). Based on the uniformitarian premise that pollen rain represents the vegetation context, it is assumed that fossil pollen records reflect previously deposited pollen from which the vegetation of the past can be inferred (Fægri and Iversen, 1989; Reille, 1990; Moore et al. 1991; Dincauze, 2000). However, pollen representation may vary depending on differential processes such as pollen production, transport and preservation (Birks and Birks, 1989; Campbell, 1999; Lebreton, 2010).

One of the pillars upon which the interpretation of fossil pollen records is based is the study of modern pollen samples from present environments that can be described in terms of vegetation, climate or edaphology, among other aspects (Barboni, 2004; López-Sáez et al., 2010). In this sense, the study of the modern pollen rain in pollen traps or surface samples may help to define present-day vegetation zones, disentangle issues affecting representation biases and, in summary, provide a better dataset for understanding pollen-vegetation relationships (Iglesias et al., 2017).

Few studies on modern pollen samples have been developed in the Iberian Peninsula, and although their number is quite low compared to those on fossil pollen records, they have been steadily increasing in recent years. Some of them are focused on the NW (González Porto et al., 1993, 1997; García-Moreiras et al., 2015), NE (Burjachs, 1990), Central Iberia (López-Sáez et al., 2018, 2019, 2020; Morales-Molino et al., 2020), Sierra Morena (Díaz-Fernández, 1993), the Pyrenees (Cañellas-Boltà et al., 2009), the Canary Islands (de Nascimento et al., 2014) and SW Iberia (Stevenson, 1985; Stevenson and Moore, 1988; Fletcher, 2005; Gutiérrez González, 2008). In most cases, these studies are focused on the study of specific plant communities in mountain regions (Gutiérrez González, 2008; López-Sáez et al., 2010a, 2010b, 2013, 2015, 2020), and only a few were carried out in coastal ecosystems (Stevenson, 1985; Stevenson and Moore, 1988; Fletcher, 2005; García-Moreiras et al., 2015) or showed a wider geographical distribution (de Nascimento et al., 2014; Morales-Molino et al., 2020).

In SW Iberia, the study area, research on modern pollen rain was undertaken in the Doñana National Park (Stevenson, 1985; Stevenson and Moore, 1988), Los Alcornocales Natural Park (Gutiérrez González, 2008) and the Guadiana Valley (Fletcher, 2005), providing information not only on their main plant communities, but also on key questions concerning the differential representation of certain taxa in relation to their productivity and dispersal. Addressing these problems might be especially complicated in fossil pollen records from dynamic areas that have undergone significant changes over time, such as lakes, wetlands, marshes, etc (Carrión et al., 2009). Therefore, exploring pollen-vegetation relationships

from a wider geographical perspective that encompasses diverse environments with different dominant plant communities could help to unravel these issues.

With the aim of assisting the interpretation of future palaeoenvironmental research in the area, we present a selection of different modern pollen samples from the Eurasian Modern Pollen Database – EMPD (Davis et al., 2020) that were collected from diverse areas of Southwestern Iberia, representing diverse environmental gradients. The main objectives of our study are: i) to understand how vegetation is featured in modern pollen samples; ii) to establish the relationships between pollen rain and modern vegetation through multivariate analysis; iii) to identify possible biases in the representation of some taxa and their causes for possible extrapolation to the interpretation of fossil records, considering their contexts and sample type.

4.2.- Study area

Southwestern Iberia is a broad geographical area with climatic conditions that may vary in terms of rainfall, temperatures and seasonality depending on the location. Following Köppen-Geiger (Kottek et al., 2006), the region is defined by a temperate climate with dry/hot summers in southern and central areas (Csa type) and dry/temperate summers in the northwestern coast (Csb type). Most of the study area is categorized as thermomediterranean with oceanic influence and mild winters, but higher altitudes in inland areas are defined as mesomediterranean with continental influence and cold winters (Rivas-Martínez et al., 1990). This region is defined by pronounced seasonal contrasts that are sometimes attenuated by the oceanic influence that penetrates up river valleys (Lionello, 2012). Thus, temperatures and precipitation differ considerably between regional zones, especially from the coast to the uplands. Annual average minimum temperatures range between 10-15 ºC on the coast and 5-10 ºC in the uplands, while average maximum temperatures vary between 22-20 ºC on the coast and 20-15 ºC in the uplands (period 1971-2000; AEMET, 2011). Precipitation concentrates during the winter season with mean annual values that range between 400-1000 mm, reaching 1400 mm in high altitudes (period 1971-2000; AEMET, 2011).

Southwestern Iberia encompasses a wide variety of vegetal associations linked to different environmental conditions, such as altitude, temperature, soil, winds, etc. In upper mesomediterranean and supramediterranean areas, such as Sierra de Grazalema (Cádiz), relict populations of *Abies pinsapo* can be found (Alba-Sánchez et al., 2010). This taxon develops in a humid-hyperhumid ombrotype and it does not usually reach the high summits, where it is replaced by creeping shrubs (Guzmán Álvarez et al., 2012). Some versatile *Pinus* species also develop in medium-high mountain areas: *Pinus sylvestris* mainly grows in cool shady hillsides and *Pinus nigra* is adapted to rocky soils, being able to tolerate strong xeric conditions (López-Tirado and Hidalgo, 2014).

Some other characteristic wood formations in medium-high areas are oak forests. Although different taxa may be locally dominant depending on the geographical zone, some of the most common are *Quercus pyrenaica*, *Q. faginea, Q. canariensis, Q. estremadurensis, Q. suber* and *Q. rotundifolia*. Some of them may be mixed with *Abies* and *Pinus* and be accompanied by an understorey consisting of *Arbutus unedo*, *Smilax aspera* and *Rosa sempervirens*, among other taxa (Domínguez et al., 1993; Rivas-Martinez et al., 1997; Latorre and Cabezudo, 2003). At lower altitudes, sclerophyllous grooves of *Quercus ilex* and thermophilous forest of *Olea europaea* grow accompanied by thickets such as *Quercus coccifera, Pistacia lentiscus, Phillyrea angustifolia, Myrtus communis, Rhamnus oleoides, Asparagus albus* and *Chamaerops humilis* (Domínguez et al., 1993; Gutiérrez et al., 1996; Rivas-Martinez et al., 1997; Latorre et al., 1996). Riparian elements such as *Salix* grow in high, middle or low watercourses, although they may also appear as a stage of degradation replacing other riparian forests (Domínguez et al., 1993; Latorre et al., 1996). *Fraxinus angustifolia* prefers the banks of lowflow streams and *Fraxinus excelsior* may accompany *Alnus,* this one as the main component of dense alluvial forests that needs high edaphic and atmospheric humidity. These riparian formations may be accompanied by *Nerium oleander* and *Tamarix* spp. (Rivas-Martínez, 1988; Domínguez et al., 1993; Rivas-Martínez et al., 1990, 2001).

At the slopes of the mountains or in depressions with groundwater permanence, hygrophilous shrubby heaths (*Erica ciliaris, Erica erigena, Calluna vulgaris, Ulex minor, Cistus psilosepalus, Genista ancistrocarpa*, and *Genista triacanthos*) develop in cool and humid areas with oligotrophic soils (Domínguez et al., 1993; Espírito-Santo et al., 2017). Heathlands may represent advanced stages in the regression of humid to sub-humid forests, but they can also expand in areas under natural or anthropogenic disturbance (Loidi et al., 2007). Scrub communities adapted to dryer conditions may include different species of *Cistus*, *Lavandula*, and *Halimium*, while in incipient eroded soils dominate the genera *Ulex, Thymus, Rosmarinus*, and *Helianthemum* (Domínguez et al., 1993; Espírito-Santo et al., 2017; Rivas-Martínez et al. 1990).

In stabilised dunes and sandbanks, the vegetation is dominated by *Pinus pinea*, but also *P. pinaster* and *P. halepensis*. These pinewoods may be accompanied by xerophytic shrubby communities of *Juniperus phoenicea, J. oxycedrus, Halimium, Rosmarinum,* and *Genista*, while at lower altitudes vegetation thickens and *Pistacia lentiscus, Daphne gnidium, Myrtus communis, Phillyrea angustifolia*, and *Calluna* appear. A rich mosaic of herbs adapted to coastal dune environments can be also identified: *Anthemis maritima, Cyperus capitatus, Eryngium maritimum, Polygonum maritimum, Artemisia crithmifolia*, and different species of *Euphorbia and Silene*, among others (Rivas-Martínez et al., 1990; Latorre et al., 1996; Espírito-Santo et al., 2017; Marcenò et al., 2018).

Typical vegetation of lagoons, coastal wetlands and marshes is present along the SW Iberian coast. Temporary pools and ponds are usually flooded during the winter and spring, with waters of low to

moderate nutrient content and important inputs of freshwater. Plant communities vary according to the substrate and the drying cycle, but some of the most representative are macrophyte groups of *Myriophyllum, Ranunculus, Potamogeton, Callitriche* and *Isoetes* (Domínguez et al., 1993; Cirujano et al., 2014). Water channels within the marshes are usually covered by Cyperaceae (*Scirpus maritimus, S. lacustris, S. littoralis, Eleocharis multicaulis*). Annual pioneer plants, mainly Chenopodiaceae, dominate on the open spaces of coastal marshes, the edges of lagoons, and temporary pools of saline or brackish water. These formations may suffer slight flooding at high tide, living on wet or very wet and markedly saline soils. Some of the most representative genera are *Salicornia, Sarcocornia, Suaeda, Spergularia, Frankenia, Halimione* and *Limonium*. In the intertidal zone, vegetation can be submerged or emerged depending on the tides. Pioneer formations of *Spartina* colonise these saline sediments stabilising coastal sediments (Domínguez et al., 1993; Latorre et al., 1996; Galán de Mera et al., 1997: Rivas-Martinez et al., 1997).

4.3.- Material and methods

4.3.1.- Data acquisition

A total of 49 modern pollen samples were selected from the Eurasian Modern Pollen Database (Davis et al., 2020; see also Davis et al., 2013; Chevalier et al, 2019). These samples were collected at various locations in SW Iberia (Fig. 1) by different researchers who provided the palynological data as raw numbers and percentage values. For the purpose of this research, samples were classified by number, site, reference, sample type, altitude (meters above sea level - m asl-), and context (Table 1).

Bioclimatic variables were taken from the WorldClim database in a 30-sec resolution (~1 km2) (Fick and Hijmans, 2017) (supplementary material: Table 1). In addition, the altitude of the sampling sites provided at the EMPD was also included as a quantitative variable.

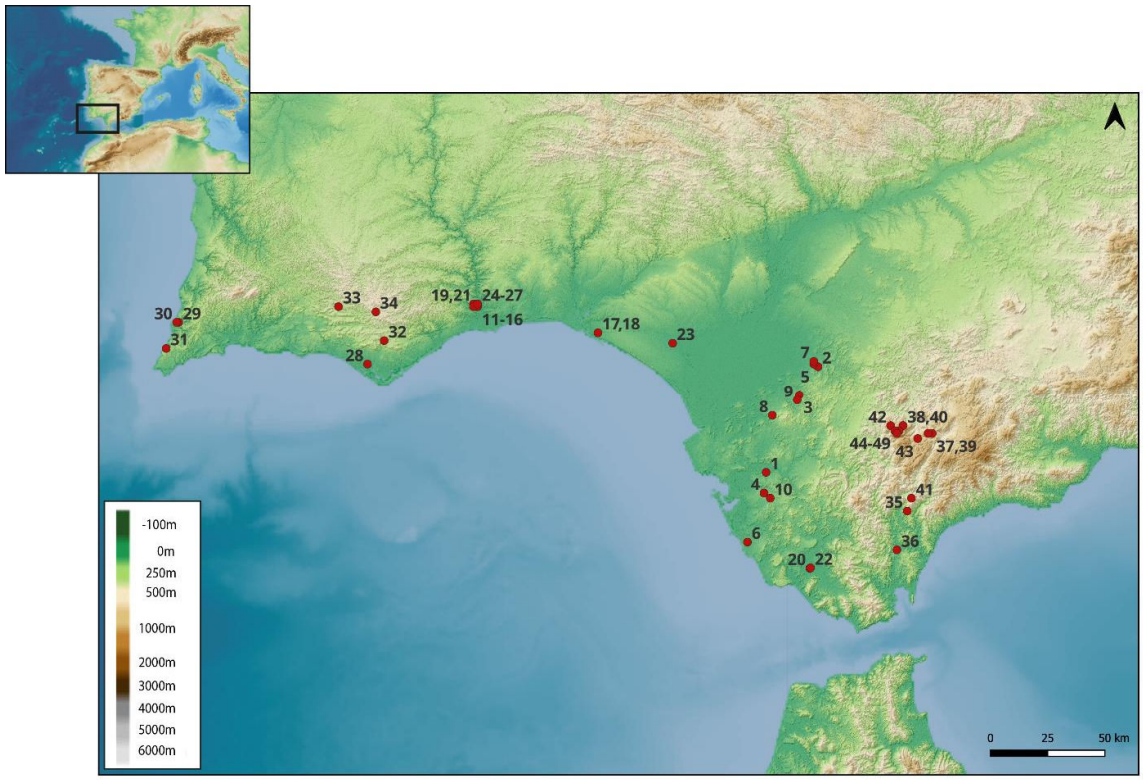

Figure 4.1. Location of the selected modern pollen samples from SW Iberia (red dots). Their associated data are described in Table 4.1 and it can be consulted, together with their coordinates, in the Supplementary Material or at the Eurasian Modern Pollen Database (https://empd2.github.io/).

Table 4.1. Selection of modern pollen samples from the EMPD with their reference code (Ref.) and site of collection (Site). They are organized by number (Number), sample type (soil, moss), altitude (m asl), and context (semi-permanent lake, seasonal lake, estuarine, wetland, pasture, orchard, scattered trees/shrubs, forest and closed forest). Samples from La Janda S2 and S3 are not yet referenced in the EMPD. Publications in which some of the samples appear are listed in the last column (Associated reference). EMPD is listed as reference for those that are not published elsewhere and are only available in the database.

Number	Site	Ref.	Sample type	Context	m asl	Associated references
1	Laguna Medina	Barboni_a891	soil	semi-permanent lake	15	EMPD
2	Laguna Zarracatín	Barboni_a919	soil	semi-permanent lake	23	EMPD
3	Laguna Taraje	Barboni_a913	soil	semi-permanent lake	68	EMPD
4	Laguna Tarage	Barboni_a912	soil	semi-permanent lake	70	EMPD
5	Laguna Arjona	Barboni_a859	soil	seasonal lake	28	EMPD
6	Laguna Campano	Barboni_a862	soil	seasonal lake	30	EMPD
7	Laguna Alcaparrosa	Barboni_a853	soil	seasonal lake	30	EMPD
8	Laguna Tollos	Barboni_a916	soil	seasonal lake	55	EMPD
9	Laguna Pilón	Barboni_a897	soil	seasonal lake	75	EMPD
10	Laguna Comisario	Barboni_a871	soil	seasonal lake	78	EMPD
11	Guadiana-Beliche	Fletcher_a7	soil	estuarine	2	Fletcher (2005)
12	Guadiana-Beliche	Fletcher_a1	soil	estuarine	3	Fletcher (2005)
13	Guadiana-Beliche	Fletcher_a6	soil	estuarine	3	Fletcher (2005)
14	Guadiana-Beliche	Fletcher_a9	soil	estuarine	3	Fletcher (2005)
15	Guadiana-Beliche	Fletcher_a8	soil	estuarine	4	Fletcher (2005)
16	Guadiana-Beliche	Fletcher_a2	soil	estuarine	9	Fletcher (2005)
17	Laguna Las Madres I	Barboni_a971	soil	wetland	3	topsoil sample included in: Stevenson (1985)
18	Laguna Las Madres II	Barboni_a349	soil	wetland	3	topsoil sample included in: Stevenson (1985)
19	Guadiana-Beliche	Fletcher_a10	soil	wetland	4	Fletcher (2005)
20	La Janda S2	-	soil	wetland	4,88	this paper
21	Guadiana-Beliche	Fletcher_a11	soil	wetland	5	Fletcher (2005)
22	La Janda S3	-	soil	wetland	5,5	this paper
23	El Acebrón	Barboni_a374	soil	wetland	25	topsoil sample included in: Stevenson and Moore (1988)
24	Guadiana-Beliche	Fletcher_a3	soil	pasture	9	Fletcher (2005)
25	Guadiana-Beliche	Fletcher_a4	soil	orchard	9	Fletcher (2005)

Number	Site	Ref.	Sample type	Context	m asl	Associated references
26	Guadiana-Beliche	Fletcher_a12	soil	scattered trees/shrubs	7	Fletcher (2005)
27	Guadiana-Beliche	Fletcher_a5	soil	scattered trees/shrubs	9	Fletcher (2005)
28	Gambelas	Connor_b1	moss	scattered trees/shrubs	25	Araújo et al. (2011)
29	Carrapateira 1	Connor_b7	moss	scattered trees/shrubs	25	Araújo et al. (2011)
30	Carrapateira 2	Connor_b8	moss	scattered trees/shrubs	25	Araújo et al. (2011)
31	Castelejo	Connor_b6	moss	scattered trees/shrubs	60	Araújo et al. (2011)
32	Machados	Connor_b2	moss	scattered trees/shrubs	150	Araújo et al. (2011)
33	Rocha da pena	Connor_b5	moss	scattered trees/shrubs	440	Araújo et al. (2011)
34	Barranco do Velho	Connor_b3	moss	scattered trees/shrubs	490	Araújo et al. (2011)
35	S.Pablo Buceite	Barboni_a385	moss	forest	100	EMPD
36	Castillo Castellar	Barboni_a386	moss	forest	100	EMPD
37	Grazalema / Montejaque	Barboni_a505	moss	forest	660	EMPD
38	Sierra Pinar Grazalema	Lopez_a193	moss	closed forest	704	EMPD
39	Grazalema / Montejaque	Barboni_a504	moss	closed forest	740	EMPD
40	Sierra Pinar Grazalema	Lopez_a192	moss	closed forest	745	EMPD
41	Gaucín	Barboni_a384	moss	closed forest	750	EMPD
42	Sierra Pinar Grazalema	Lopez_a194	moss	closed forest	765	EMPD
43	Grazalema	Barboni_a503	moss	closed forest	770	EMPD
44	Sierra Pinar Grazalema	Lopez_a195	moss	closed forest	797	EMPD
45	Sierra Pinar Grazalema	Lopez_a200	moss	closed forest	1029	EMPD
46	Sierra Pinar Grazalema	Lopez_a197	moss	closed forest	1100	EMPD
47	Sierra Pinar Grazalema	Lopez_a198	moss	closed forest	1100	EMPD
48	Sierra Pinar Grazalema	Lopez_a199	moss	closed forest	1100	EMPD
49	Sierra Pinar Grazalema	Lopez_a196	moss	closed forest	1146	EMPD

4.3.2.- Data analysis

The acquired raw pollen count data was normalized as percentages and filtered to ensure that taxa with low representation (defined as ≤3% presence across all samples) or uncommon (defined as taxa present in less than 3 samples) were excluded. Percentages were calculated using a terrestrial pollen sum (TPS)

that excluded aquatic pollen types. Aquatic pollen types were still included in the total sum (TS). After filtering, percentages were recalculated. For the visualization of palynological results per sample, a pollen diagram was plotted using TiliaIT software (version 2.1.1, Illinois State Museum, Research and Collection Center, Springfield USA) (Fig. 2).

A Detrended Correspondence Analysis (DCA) was run to determine whether the data was homogeneous and therefore more suitable for linear methods, or inversely for unimodal ordination methods (Oksanen et al., 2022). The DCA's first axis length was larger than 2.5 standard deviation units, thus, the Canonical Correspondence Analysis (CCA), a unimodal ordination method, was chosen (ter Braak and Prentice, 1988).

To assert, which environmental variables were relevant and suitable to include in the final CCA, the Pearson correlation coefficient, as well as the variance inflation factors (VIFs) were computed. Then, independently, for each environmental variable, a CCA and an ANOVA like permutation test were performed. We should note that to compute the VIFs and the CCA's, a square-root transformation was applied to the percentage data (Legendre and Birks, 2012).

4.4.- Results

4.4.1. Pollen diagram

After the statistical analyses, a total of 45 taxa were recorded and the most significant vegetal trends were synthesised in Table 2. A palynological diagram illustrates pollen relative frequencies in percentages (Fig. 2), which are arranged according to the context and sample type provided by the EMPD (Davis et al., 2020).

Abies is the dominant taxa in samples from closed forests above 800 m asl, while deciduous and evergreen *Quercus* prevail in samples from this same context between 800-700 m asl. Samples collected from forests display slight differences according to the altitude: above 600 m asl the most significant taxa are both deciduous and evergreen *Quercus*; below 150 m asl deciduous *Quercus* and *Olea* are the best represented. Moss samples from the scattered trees/shrubs context display heterogeneous results, with evergreen *Quercus* dominating the pollen spectra in those between 490-150 m asl, and high values of high-mountain and Mediterranean pines in samples between 60-25 m asl. However, soil samples below 25 m asl from this same context reflect a predominance of herbs, mainly Chenopodiaceae. This similar trend is followed by soil samples collected from pasture and orchard contexts. The vegetal composition within wetland samples is diverse and differs between them, with Chenopodiaceae, Poaceae, Cyperaceae, Asteraceae Cichorioideae, A. Asteroideae and A. Carduoideae as predominant taxa; some of them also display high values of *Erica*, Mediterranean pines, *Quercus* undiff.*, Phillyrea, Salix*, monolete fern spores and *Isoetes*.

Estuarine contexts show an important contribution of Chenopodiaceae, Asteraceae Cichorioideae and Poaceae with different values depending on the sample. These taxa are also well represented in seasonal lakes, together with high-mountain pines, *Olea*, evergreen *Quercus*, Asteraceae Asteroideae and Cyperaceae. Semi-permanent lakes show a predominance of *Olea,* evergreen *Quercus* and herbs such as Poaceae, Asteraceae Cichorioideae, A. Asteroideae and Chenopodiaceae.

Table 4.2. Synthesis of the most representative taxa in each sample according to their number, context, altitude (m asl), type, and vegetation belt.

Sample Nr.	Context	m asl	Sample type	Vegetation belt	Pollen signature	NAP / AP % (max.- min. / min.- max.)
1-4	Semi-permanent lake	15-70	soil	Thermomediterranean	*Olea,* evergreen and undiff. *Quercus.* Variable values of *Phillyrea,* Poaceae, Chenopodiaceae, A.Asteroideaea and A.Cichorioidea. Some samples display high values of Cyperaceae and *Ruppia* .	60.3 - 40.7 / 39.7 - 59.3
5-10	Seasonal lake	28-78			High-mountain pines, *Olea,* evergreen and undiff. *Quercus.* Poaceae, Chenopodiaceae, A.Asteroideae, A.Cichorioideae and Cyperaceae.	68.8 - 46.3 / 31.3 - 53.7
11-16	Estuarine	<10	soil	Thermomediterranean	A.Cichorioideae, Chenopodiaceae, Poaceae and A.Asteroideae. Some samples display high values of *Olea* and *Cistus* .	97.5 - 63.6 / 2.5 - 36.4
17-23	Wetland	3-25	soil	Thermomediterranean	Variable values of Chenopodiaceae, Poaceae, Cyperaceae, Asteraceae, *Erica* , Mediterranean pines, *Quercus* undiff., *Phillyrea* , *Salix* , monolete spores and *Isoetes* .	94.3 - 44 / 5.7 - 56
24-25	Pasture/Orchard	9	soil	Thermomediterranean	Chenopodiaceae, A.Cichorioideae, A.Asteroideae and Poaceae.	96.7 - 92.9 / 3.3 - 7.1
26-27	Scattered trees/shrubs	7-9	soil	Thermomediterranean	Chenopodiaceae. Low percentages of Poaceae and A. Asteroideae. Some samples display high values of *Tamarix.*	96.5 - 91.8 / 3.5 - 8.2
28-31		25-60	moss		Variable values of high-mountain pines, Mediterranean pines, A.Asteroideae, *Plantago coronopus* and *P. lanceolata* .	83.6 - 13.5 / 16.4 - 86.5
32-34		150-490	moss		High-mountain pines and *Olea.* Variable values of evergreen, deciduous and undiff. *Quercus* between samples. Some samples display high values of *Isoetes* , *Calluna, Erica* and *Olea* .	30.2 - 9 / 69.8 - 91
35-36	Forest	100	moss	Thermomediterranean	Deciduous *Quercus* and *Olea.*	32.7 - 6.7 / 67.3 - 93.3
37		660	moss	Thermomediterranean	Evergreeen and deciduous *Quercus* .	8.7 / 91.3
38-44	Close forest	700-800	moss	Mesomediterranean	Evergreeen and deciduous *Quercus.* Variable values of Mediterranean pines, *Phillyrea, Pistacia* and *Genista* between samples. Some display high values of *Ceratonia* and *Prunus.*	14.3 - 4.1 / 85.7 - 95.9
45-49		>1000	moss	Mesomediterranean	*Abies, Daphne,* deciduous *Quercus, Prunus* and high-mountain pines.	23.7 - 12.3/76.3 - 87.7

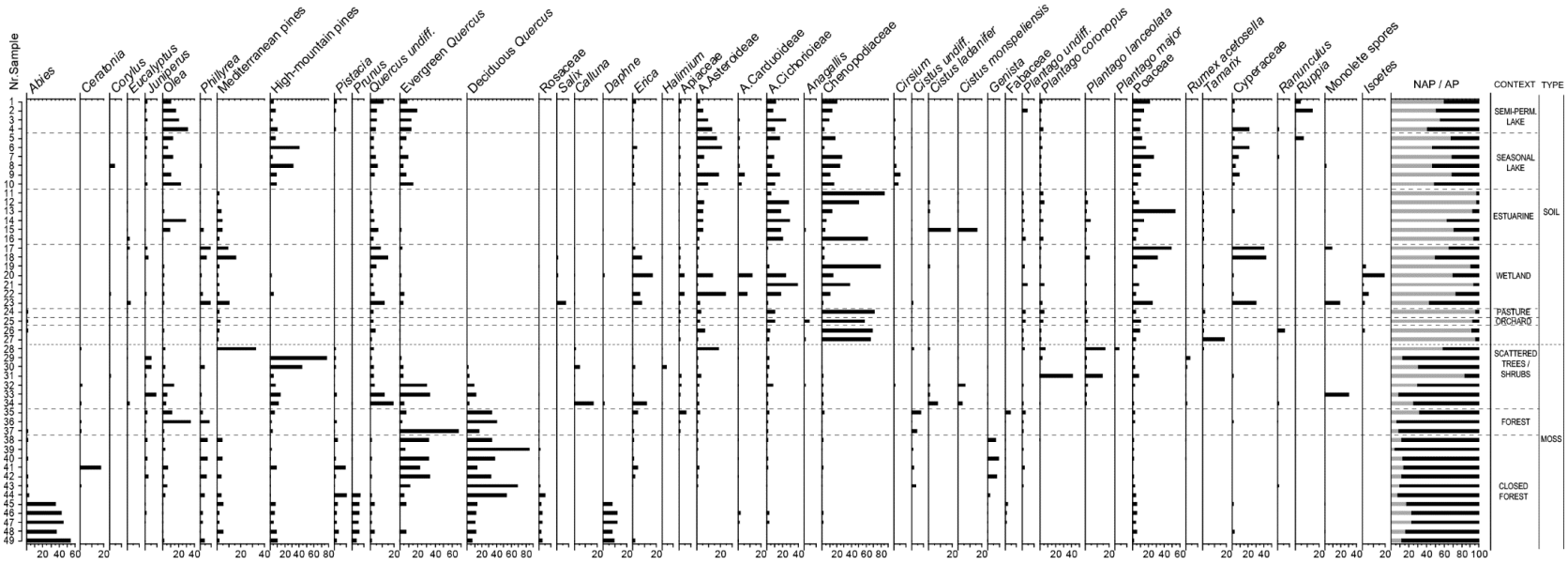

Figure 4.2. Pollen diagram of the most representative taxa from the 49 selected samples (%). The sum of the Non-Arboreal and Arboreal pollen (NAP/AP) expressed in percentages is depicted on the right side. Columns on the right indicate the context and sample type, which are separated by dashed lines.

4.4.2.- Ordination and clustering

All environmental variables revealed high variance inflation factor (VIFs > 20). Notably, the variables with the lowest VIFs were, bio14, bio15, bio17, bio18 and m asl (supplementary material: Figure 4.1). When evaluated with the permutation test under independent CCAs, all environmental variables reported an adjusted p-value below 0.05, with a variance explained varying from 4 (bio15) to 18% (m asl) (Table 4.3).

Table 4.3. Percentage variance explained for each environmental variable after permutation test (*p < 0.05; **p ≤ 0.01).

Environmental variables	Variance explained	P.value	Adjusted P.value	Significance
m asl	18.0080081	0.001	0.0011765	**
bio1	17.9843575	0.001	0.0011765	**
bio11	17.1143512	0.001	0.0011765	**
bio8	17.0691717	0.001	0.0011765	**
bio12	16.2804992	0.001	0.0011765	**
bio19	15.9697039	0.001	0.0011765	**
bio6	15.1485157	0.001	0.0011765	**
bio16	15.1105457	0.001	0.0011765	**
bio3	15.1078902	0.001	0.0011765	**
bio10	14.8664226	0.001	0.0011765	**
bio9	14.5988266	0.001	0.0011765	**
bio18	14.1882852	0.001	0.0011765	**
bio13	12.6475498	0.001	0.0011765	**
bio17	12.1865631	0.001	0.0011765	**
bio5	8.88274703	0.001	0.0011765	**
bio4	7.60941901	0.001	0.0011765	**
bio14	7.52859419	0.001	0.0011765	**
bio7	5.08148377	0.007	0.0073684	**
bio2	4.38211509	0.006	0.0066667	**
bio15	4.19182164	0.014	0.014	*

The selection of environmental variables was then based on those variables with a low correlation coefficient between them in order to better capture the complex relationships between environmental variables and pollen taxa (supplementary material: Figure 4.2). The selected variables were: Bio8 (mean temperature of the wettest quarter), Bio9 (mean temperature of the driest quarter), Bio14 (precipitation of the driest month), Bio15 (precipitation seasonality), Bio17 (precipitation of the driest quarter), Bio18 (precipitation of the warmest quarter), and meters above sea level (m asl) (Table 4.4).

Table 4.4. Eigenvalues, environmental variables and canonical coefficients of the first four CCA axes.

ID	CCA1	CCA2	CCA3	CCA4
Eigenvalue	0.411387	0.147377	0.123055	0.107295
bio8	-0.94636	0.00817	0.148012	-0.20123
bio9	-0.84284	-0.24595	-0.06779	0.425297
bio14	0.406208	0.588016	-0.54326	0.134351
bio15	-0.20451	-0.39808	-0.14254	-0.41948
bio17	0.736651	0.33347	0.069794	0.450752
bio18	0.835459	0.297032	0.094349	0.179797
m asl	0.98028	0.041666	-0.07104	0.114259

Considering that each arrow points in the direction of maximum change in the value of the associated variable and their length is proportional to this maximum rate of change (ter Braak and Verdonschot, 1995), examining the final CCA we observe that axis 1 best explains the distribution of the samples depending on altitude in opposition to temperature. Following the gradient of altitude represented by the m asl arrow, sampling sites reflect the succession from low (clusters F, D and E) to high elevations (clusters B and A) (Fig4). CCA axis 2 is mainly defined by the precipitation of the driest month in quasi-opposition to the precipitation seasonality. Following the gradient of precipitation of the driest month represented by the Bio14 arrow, sampling sites reflect the succession from high (A, D and E) to low (F, C, and part of the B and G) precipitation (Fig. 4.4).

4.5.- Discussion

4.5.1.- Environmental variables and modern pollen samples in relation to their context

CCA axis 1 shows a positive correlation with altitude and the precipitation of the driest and wettest quarters of the year (Bio17 and Bio18, respectively). These environmental variables successfully explain the sample distribution and the pollen taxa associated with cluster A (Figs. 4.3 and 4.4), as they correspond to moss samples collected from closed fir forests above 1000 m in Sierra de Grazalema, an area characterized by its high rainfall with mean annual precipitations of ca. 2000 mm (Arista and Talavera, 1994). In the highest areas of these mountains, *Abies pinsapo* forms dense forests with a limited distribution, but at lower altitudes it forms mixed oak-fir forests with species such as *Quercus rotundifolia, Quercus faginea* and a dense shrub layer composed of *Daphne laureola, Prunus spinosa* together with Leguminoseae, Anacardiaceae and Oleaceae (Arista et al., 1997). As altitude decreases in Sierra de Grazalema and the surrounding area, the landscape is dominated by forests and thicket formations composed of thermo-Mediterranean taxa such as *Olea*, *Quercus ilex, Ceratonia siliqua, Phillyrea angustifolia, Pistacia lentiscus,* etc. This stage is well represented by samples from closed forests and forests located below 800 m asl (cluster B), which are arranged in a space influenced by the altitude and projected in the same direction as precipitation seasonality (Bio15) (Figs. 4.3 and 4.4). Some taxa within these forest

communities, such as *Olea* and *Quercus ilex*, have proven to have physiological mechanisms to tolerate water and drought-stress, being resistant to seasonal aridity through different water-saving strategies (Ozturk et al., 2010). The vegetal composition of most samples within cluster B is strongly defined by the presence of these thermo-Mediterranean taxa, explaining the ordination of the sampling sites along these two environmental gradients (m asl and Bio15) (Figs. 4.3 and 4.4).

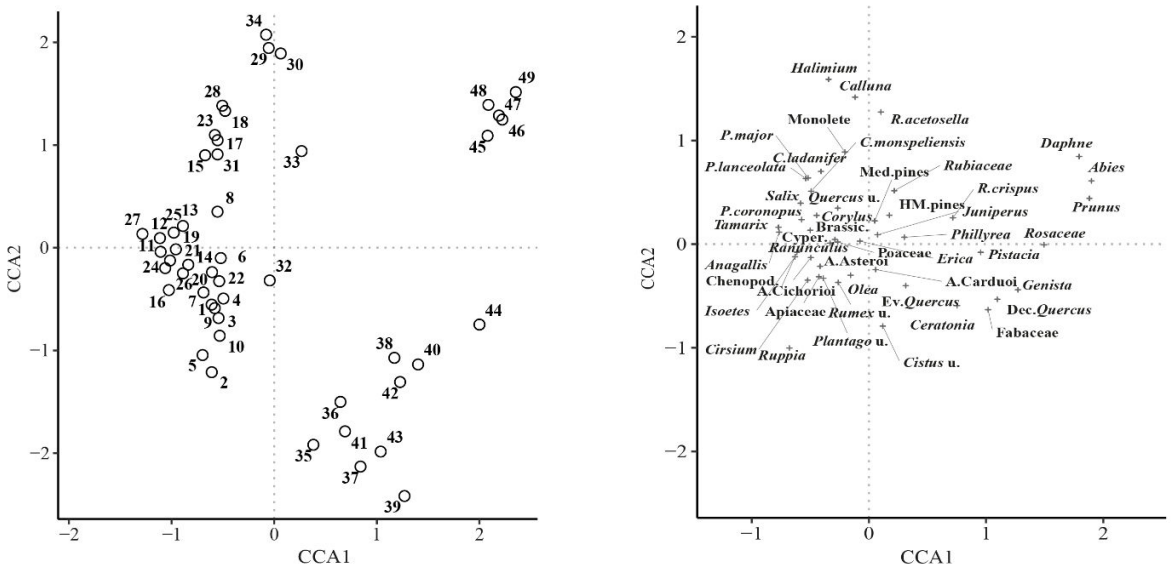

Figure 4.3. Canonical Correspondence Analysis (CCA) ordination biplots of the 49 samples studied where A) dots and numbers indicate the dispersion of sampling sites (Table 4.1); and B) crosses show the dominant pollen taxa and their dispersion along axes 1 and 2.

The opposite trend is displayed by a small cluster of samples (C) that is arranged relatively close to the arrowhead representing the precipitations of the driest month of the year (Bio14) (Figs. 4.3 and 4.4). These samples were collected at 25 m asl on the slopes of Serra de Monchique (30 and 29) and between 500-400 m asl in Serra do Caldeirão (34 and 33); therefore, altitude is not a factor affecting their clustering. Both mountainous areas record mean annual precipitation values between 600-1000 mm and above 1200 mm at the highest points (Espírito-Santo et al., 2017). As stated by Araújo et al. (2011), an important component of these samples are *Pinus*. Indeed, they display the highest percentages of high-mountain pines within the context of scattered trees/shrubs, which in this case includes *Pinus sylvestris*. This is a versatile species well adapted to continental climates that may grow in areas with a thermal amplitude of 50ºC but avoids harsh xeric conditions (López-Tirado and Hidalgo, 2014). The main interpretive problem relies in the fact that *Pinus sylvestris* is absent from this region and appear in native condition near the Minho and Central Portugal, where it reaches the south-western boundary of its geographic distribution (Tavares, 1959). Therefore, its presence may reflect a distant transport from mountain regions in the

centre of Portugal (Mateus, 1992) or, considering the high percentages in the samples, it may result from the presence of pine monocultures. Given this context, the projection of cluster C near the arrow representing the precipitation of the driest month (Bio14) may result coherent attending to the environmental variables of the region. But attention should be drawn to the possible interpretative distortion derived from the presence of high-mountain pines.

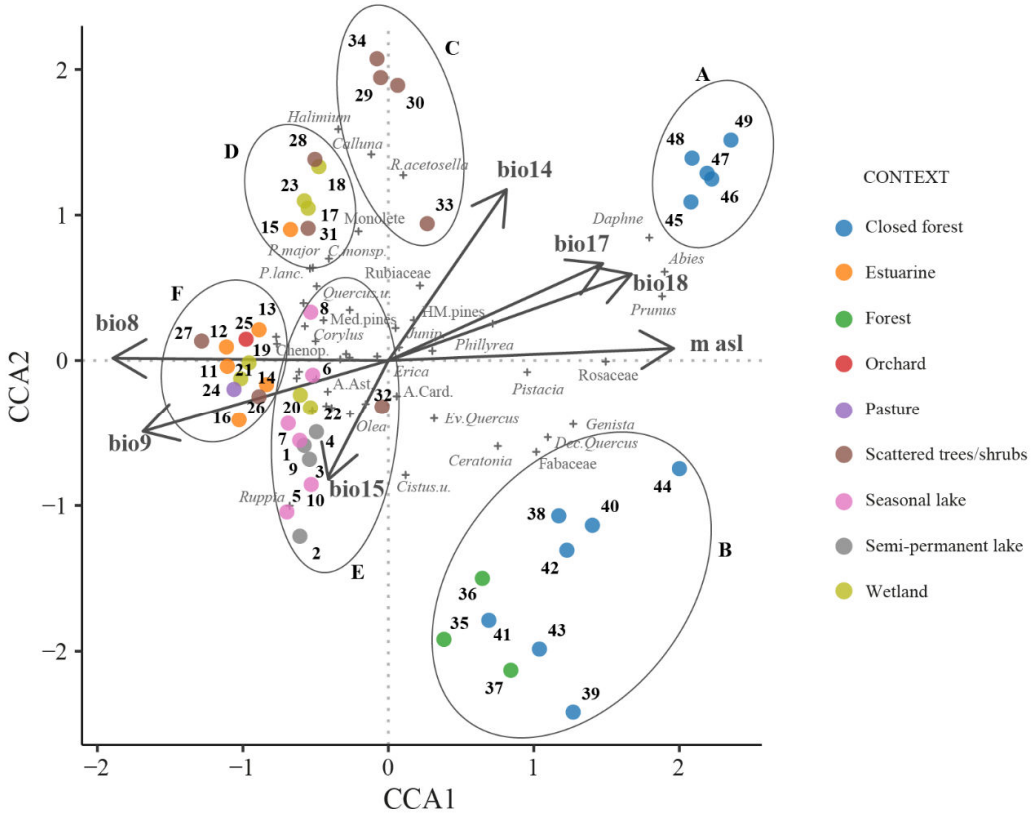

Figure 4.4. Canonical Correspondence Analysis (CCA) ordination biplot of the 49 samples studied categorized by their context (coloured circles according to the legend). Dots indicate the sampling sites, crosses show the dominant pollen taxa and arrows represent the selected environmental variables. Capital letters correspond to the clusters defined by axes 1 and 2.

The space between the precipitation of the driest month (Bio14) and the mean temperature of the wettest quarter of the year (Bio8) is occupied by a diverse group of samples (D) from different contexts (Figs. 4.3 and 4.4): seasonal lake (8: Laguna de los Tollos), estuarine (15: Guadiana-Beliche), wetlands (23, 18 and 17: El Acebrón and Laguna de las Madres) and scattered trees/shrubs (31 and 28: Castelejo and Gambelas). Their content is heterogeneous in terms of vegetation (Fig. 4.2, Table 4.2), but there are some common features that contribute to their clustering. One is the low presence of *Olea* recorded in all the samples, especially if compared to the higher percentages of this taxon in other samples from the same contexts. The other, is that most of them display high values of aquatic taxa. However, the pollen taxa dispersion does not contribute to a coherent ordination of the samples along any specific environmental

gradient. Rather, it seems that sampling site distribution is better explained by opposition to certain variables, in this case to the precipitation seasonality (Bio15).

Cluster E (Figs. 4.3 and 4.4) is projected in the same direction as the arrow representing the precipitation seasonality (Bio15) and it is composed of samples from seasonal lakes (9, and 7-5), semi-permanent lakes (4-1), wetlands (22 and 20) and scattered trees/shrubs (32) contexts (Fig. 4.2). With exception of one sample collected from a context of scattered trees and shrubs in Machados (32), all the sampled areas correspond to environments that are strongly affected by seasonal changes in water levels. Samples 22 and 20 were collected from La Janda wetlands, a depression that is periodically and partially flooded during periods of heavy rainfall (Mediavilla et al., 2023). Most of the semi-permanent and seasonal lakes sampled correspond to endorheic complexes such as those of Utrera (Zarracatín, Arjona, Alcaparrosa), Puerto Real (Taraje) and Lebrija-Las Cabezas (Pilón). These basins, due to their nature, are more sensitive to experiencing water losses through water percolation and evapotranspiration, being more dependent on the precipitation regime than other lakes and lagoons (Yapiyev et al., 2017). The presence of thermo-Mediterranean taxa adapted to water stress, such as *Olea* and some evergreen *Quercus* species, is common to most of the samples (Fig. 4.2, Table 4.2). In addition to these taxa, samples show important values of Chenopodiaceae and other herbs that may be adapted to saline conditions, sometimes relatable to periods of drought-stress and changes in the water level (Mediato et al., 2020). Thus, the determining water stress during periods of low precipitations and the presence of vegetation adapted to these environments is well reproduced by the correlation with Bio15.

The last cluster (F) is arranged following the gradient of increasing temperatures represented by the Bio8 and Bio9 arrows, associated with both the wettest and driest quarters of the year, respectively (Figs. 4.3 and 4.4). All these samples were collected from diverse contexts in the Guadiana Valley: estuarine (16 and 14-11), wetlands (21 and 19), orchard and pasture (25 and 24), and scattered trees/shrubs (27) (Fletcher, 2005). It is possible to infer the diversity of habitats by identifying some of the major communities on the basis of their associated pollen rain (Fig. 4.2, Table 4.2): saltmarshes dominated by Chenopodiaceae, transitional saline-freshwater zones affected by grazing composed of Asteraceae and *Plantago*, scrubs formed by *Cistus* in the drier ombrotypes and *Erica* under a wetter regime, xerophytic forest margins of *Olea* and *Phillyrea*, and pinewoods from the coastal zone or plantations, among others (Fletcher, 2005). Furthermore, all of the samples are located at lower altitudes (below 10 m asl), which in turn explains their negative correlation with the altitude (m asl). Rather than being determined by temperature, the distribution of pollen taxa in this part of the plot seems to respond to the greater range of adaptability of some taxa to certain conditions, as opposed to others with better-defined specificities such as those dependent on rainfall and altitude (e.g., *Abies*).

4.5.2.- Sample types and pollen spectra: implications for fossil pollen records

It must be taken into account that pollen-vegetation relationships are not linear, just as pollen percentages are not linear with plant abundance. Distortions have been observed between pollen rain and vegetation, mainly related to processes such as differences in pollen production among species, pollen dispersal, deposition and differential preservation (Coles et al., 1989; Holloway, 1989; Campbell, 1999; Lebreton et al., 2010; Hunt and Fiacconi, 2018). Indeed, variations in pollen preservation (and thus representation) were recognized to derive from differences between deposition environments and pollen types (Xu et al., 2016). In modern pollen studies, these environments may translate into diverse sample types that typically include moss pollsters, surficial soils of distinct origins, and pollen traps located in diverse places (Tauber, 1967). However, potential differences in pollen content between these media have received little attention (Lisitsyna et al., 2012).

Some studies comparing the pollen assemblages recorded in moss and soil samples from nearby sites with similar vegetation show that they do differ, being that soils contain fewer arboreal and more herb taxa than adjacent moss samples (Fang et al., 2022). In other cases, some taxa, such as *Pinus, Quercus* and *Alnus*, appear strongly over-represented, while others (*Urtica*, Poaceae, *Populus*) were under-represented in moss pollsters (Spieksma et al., 1994). Generally, it seems that higher percentages of some anemophilous taxa such as *Pinus* and other bisaccate grains may be over-represented in moss samples compared to other pollen traps and lake sediments (Pardoe et al., 2010; Lisitsyna et al., 2012).

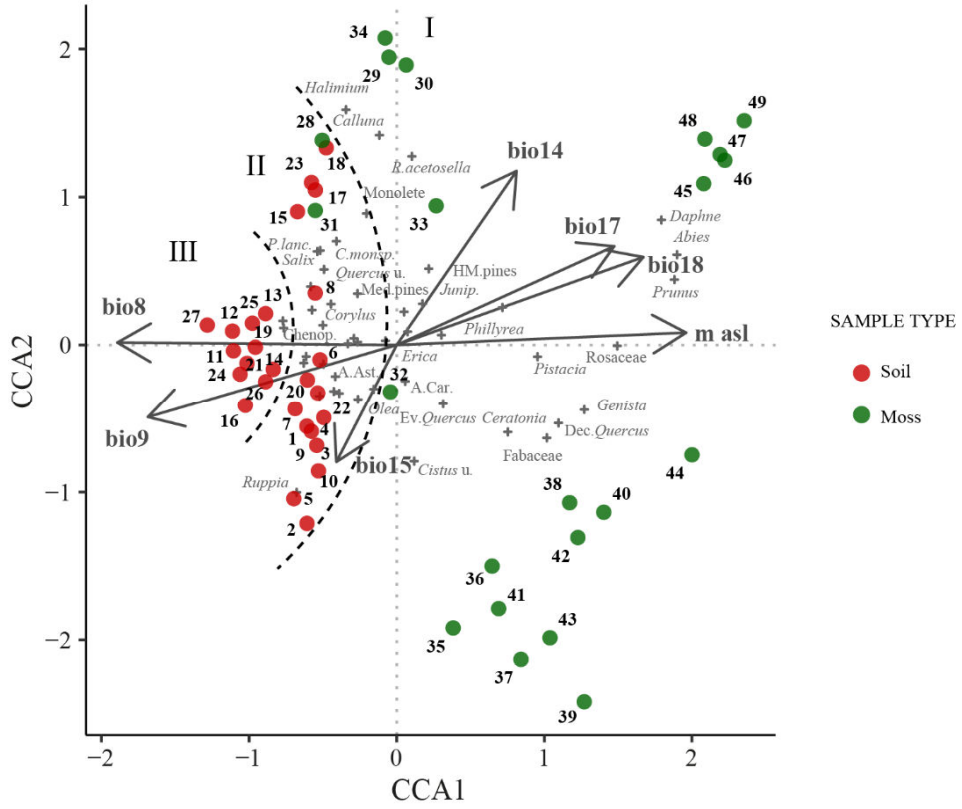

Figure 4.5. Canonical Correspondence Analysis (CCA) ordination biplot of the 49 samples studied categorized by their type (soil or moss). Dots indicate the sampling sites, crosses show the dominant pollen taxa and arrows represent the selected environmental variables. Roman numbers correspond to the areas separated by dashed lines that show a potential clustering depending on the sample type.

In the present work, moss samples were collected between 25 and 1146 m asl from closed forests, forests and scattered trees/shrubs contexts (Figs 4 and 5). All of them, except one, are dominated by arboreal taxa with values above 60%, and above 80% in more than half of the samples (Fig. 4.2; Table 4.2). Although vegetal composition reflects changes related to altitudinal gradients in all contexts, arboreal input is not affected by this variable, as some samples display similar percentages of arboreal and non-arboreal pollen both at 440 m asl (33) and at 25 m asl (29). The context category, which in this case is partly determined by the forest cover density, seems to have a stronger influence in relation to the arboreal input, as expected. *Abies, Quercus* and high-mountain pines are the main represented arboreal taxa in moss samples from all three contexts. Some studies indicate that the low air pollen level found in open *Abies pinsapo* forests could denote short-distance pollen dispersal (Arista and Talavera, 1994), which may lead to its under-representation in the pollen record in favour of other species. This will explain its extremely low values in mixed oak-fir forests below 800 m asl with higher percentages of *Quercus*. On the other hand, the presence of high-mountain pines corresponds to their natural habitat in medium to high

altitudes (López-Tirado and Hidalgo, 2014), except for the samples collected from Southern Portugal in which their values may be explained as being of regional origin (or local if they involve contemporary pine monocultures). With this exception, it can be inferred that pollen grains in moss samples originate from local sources.

However, the pollen composition greatly differs between samples collected in the context of scattered trees/shrubs, with soils containing more herbaceous and less arboreal taxa than mosses (Fig. 4.5; Table 4.2). Diverse studies indicate that pollen assemblages in soil samples can represent regional vegetation moderately, while local taxa may be over-represented (Li et al., 2005). In other cases, high amounts of non-local pollen taxa entering the local pollen spectrum were identified in open environments in which the pollen productivity of local plant population was low (Stevenson, 1985). It is difficult to estimate which of these options could better explain the differences between these samples, as some of them were collected relatively close to each other, on the southern coast of Portugal between 7 and 25 m asl in a similar environment (e.g., samples 26-30). It is possible that different situations may have occurred between samples, but what seems more plausible is to consider that these significant changes in the floristic composition may be due to the type of sample rather than other factors.

The significance of herbaceous taxa in the vegetation is a common trend observed in the remaining soil samples collected at different altitudes from different contexts, with non-arboreal taxa above 60% in 17 of the 25 samples (Fig. 4.2, Table 4.2). The predominance of Chenopodiaceae, Asteraceae, Poaceae and Cyperaceae in most of the samples from pasture, orchard, wetland, estuarine and lake contexts is, in these cases, a mirror image of the local vegetation associated to the several habitats identified on the coastal area (Stevenson, 1985; Fletcher, 2005). However, within this set of samples, both semi-permanent and seasonal lakes display higher percentages of arboreal pollen, suggesting an under-representation of arboreal taxa in the non-lake samples (Fig. 4.5, Table 4.2). Although the context is a determining factor influencing floristic composition, these differences in lake samples may be strongly biased by pollen transport.

It is assumed that the most likely routes for pollen to enter a lake is by aerial or water transport (Havinga 1964; Xu et al., 2012). In the case of lakes with inflowing rivers, it is believed that most of the palynomorphs are fluvially transported from river catchments (Cross et al., 1966; Peck, 1973; Bonny, 1976, 1978; DeBusk, 1997; Brown et al., 2007), but in arid areas, it has been suggested that pollen transported by inflow streams make little contribution (Zhao et al., 2021). Higher values of arboreal taxa in soil samples collected from seasonal and semi-permanent lakes may be therefore caused by their role as "forestry drains" (Pittam et al., 2006) for arboreal pollen grains carried by wind, rivers and surface wash. The presence of high-mountain pines, growing at higher altitudes, in all these samples may

corroborate this idea. In addition, slightly higher values of arboreal taxa are found in those lakes located near mountains or elevated areas, which may be acting as important pollen sources; such is the case of Medina, Zarracatín, Tarage, Campano, Tollos and Comisario lakes. Whether arboreal pollen was airborne or water transported cannot be deduced, but the local and regional character of the floristic assemblage recorded in lake basins is evident.

An important aspect to be considered is that of taphonomic factors, as pollen assemblages in soils are often biased by physical, chemical and biological agents (Val-Peón et al., 2019; Fang et al., 2022). This is of special importance in the case of environments affected by fluctuations in the water level, as several processes such as oxidation (Lebreton et al., 2010), moisture fluctuations related to evaporative processes (Holloway, 1989), repeated wetting and drying (Twiddle and Bunting, 2010), alkaline/oxidative environmental alternation (Tian et al., 2009), and mechanical damages related to transport in water (Twiddle and Bunting, 2010) may lead to the degradation of pollen grains. Indeed, these processes may occur at different stages in pre-depositional (e.g., soil inwash in lakes and peatbogs) and post-depositional environments (e.g., lake fluctuations) (Carrión et al., 2009). Some other factors to be considered when interpreting pollen assemblages in lake contexts are secondary transport and re-sedimentation processes that may be caused by lake water circulation and the temperature difference between water layers (Davis, 1968; Davis and Brubaker, 1973; Davis et al., 1984). For these reasons, coarse-grained sediments and lower pollen concentrations tend to be found in shallower, near-shore areas, whereas higher pollen concentrations and smaller grain size can be found in central areas (Tian et al., 2008). Therefore, the sampling location can greatly influence the palynological content. Susceptibility to these disturbance factors depends on the inherent characteristics of each taxon, whereby sporopollenin content and exine thickness may be critical for the preservation of pollen grains (Elsik, 1971; Havinga, 1971; Brooks and Shaw, 1972). For example, it has been suggested that the exine thickness and high sporopollenin content of some species within *Pinus* and Asteraceae, endows them with good preservation potential and resistance to decay (Sangster and Dale, 1961; Campbell and Campbell, 1994; Tomescu, 2005; Lebreton et al., 2010; Val-Peón, et al., 2019). This may influence pollen representativeness in both modern and fossil soil samples, leading to over/under-representations of some taxa.

4.6.- Conclusions

The inherent characteristics of each pollen grain (size, shape, weight, etc.), differences in pollen production among species, means of pollen dispersal, the type of deposit into which the pollen is incorporated and the role of taphonomic factors in pollen preservation are forces affecting the representativeness of pollen grains and the way they reflect the vegetation in both modern and fossil samples (Coles et al., 1989; Holloway, 1989; Campbell, 1999; Lebreton et al., 2010; Hunt and Fiacconi,

2018). Disentangling all these variables so that they can be identified and understood in order to carry out an interpretative exercise on vegetation is difficult in modern samples, but specially in fossil records as they can reflect very distinct environments in a rapid diachronic succession.

The analysis of modern pollen samples from diverse environments of SW Iberia allowed us to identify the vegetal composition of each specific habitat and the main environmental variables influencing their development. In addition, it has been proposed the impact of taphonomic factors as active agents affecting the representativeness of pollen taxa, which may distort results depending on the context but also the sample type. The main conclusions are:

- There are three clusters (A, B and E) that successfully explain the distribution of the samples according to specific environmental variables related to altitude, precipitation, and precipitation seasonality. The other clusters (C, D and F) seem to be better explained by opposition to them (Fig. 4.4).
- The distribution of pollen taxa shows two scenarios: one in which their dispersion reflects the dependence of some taxa to specific conditions, mainly altitude and precipitations; another in which their distribution reflects the wide range of adaptability of some taxa to certain variables, sometimes grouped in opposition rather than in agreement to them (Fig. 4.3).
- Both context and sample type categories coherently explain the dispersion of the samples (Figs.4 and 5). In the first case, most of the categories are well defined by the floristic vegetation they represent; in the second, some differences between moss and soil samples seem to explain certain variations in the pollen content that may be related to the incidence of taphonomic factors.
- Altitude and precipitation successfully explain the sample and pollen taxa distribution corresponding to samples collected from closed fir forest in Sierra de Grazalema (cluster A).
- As the altitude decreases mixed oak-fir forests give space to oak formations with increased thermo-Mediterranean elements, which is reflected in the ordination of samples in the same direction as precipitation seasonality (cluster B).
- Samples collected from open formations of scattered trees and shrubs at the slopes of Serra de Monchique and in Serra do Caldeirão reflect a preference for low precipitation seasonality. High percentages of *Pinus sylvestris*, which is absent from this area, may be an artefact derived from the presence of pine monocultures (cluster C).
- A group of samples of diverse origin (cluster D) and heterogeneous vegetal composition is grouped in opposition to the precipitation seasonality too.
- The periods of water stress to which seasonal and semi-permanent lakes are subjected during periods of low rainfall are faithfully reflected in their correlation with high precipitation seasonality (cluster E).

- The heterogeneous group of samples conforming cluster F is successfully explained by its negative correlation with high altitudes, which is in turn related to higher temperatures.
- Moss samples from closed forests, forests and areas with scattered trees and shrubs reflect dominant arboreal vegetation of local origin. However, discrepancies between moss and soil samples from scattered trees/shrubs contexts were observed, with sample type being the most plausible factor explaining these changes in floristic composition.
- Soil samples from the remaining contexts are dominated by herbaceous taxa, providing a consistent picture of the local vegetation adapted to these coastal environments.
- Within the soil samples, those from semi-permanent and seasonal lakes account for higher percentages of arboreal taxa, suggesting that may be indeed an under-representation of arboreal pollen in the non-lake soil samples.
- The transport of pollen grains to lakes by wind, rivers and surface wash may result in these basins acting as forestry drains reflecting floristic assemblages of both local and regional character.
- Taphonomic factors must be taken into account as agents affecting pollen preservation and representation, especially in soil samples that are easily biased by physical, chemical and biological elements. This is especially important in environments affected by fluctuations in the water level as several processes related with the oxidation, evaporation, repeated wetting and drying cycles, secondary transport and re-sedimentation can provoke biases in the palynological content of both modern and fossil samples.
- The impact that these processes may have on pollen grains may also depend on taxon-specific factors such as sporopollenin content or the exine thickness. This can lead to over or under-representation of some taxa in both modern and fossil samples.

As a final remark, it is important to stress the need to compare different sample types from the same context and altitude in order to better understand pollen-vegetation relationships and identify possible biases more accurately.

4.7.- Acknowledgements

This research was funded by the Deutsche Forschungsgemeinschaft-DFG (project no.57444011 – SFB 806) and a "Severo Ochoa" extraordinary grant for excellence IGME-CSIC (AECEX2021). The authors would also like to thank all the authors who have contributed in any way to the EMPD, as well as to Doris Barboni and Michel Leydet, for their help in resolving some queries, and specially to Basil Davis, for kindly providing specific information on some samples.

4.8.- Supplementary material

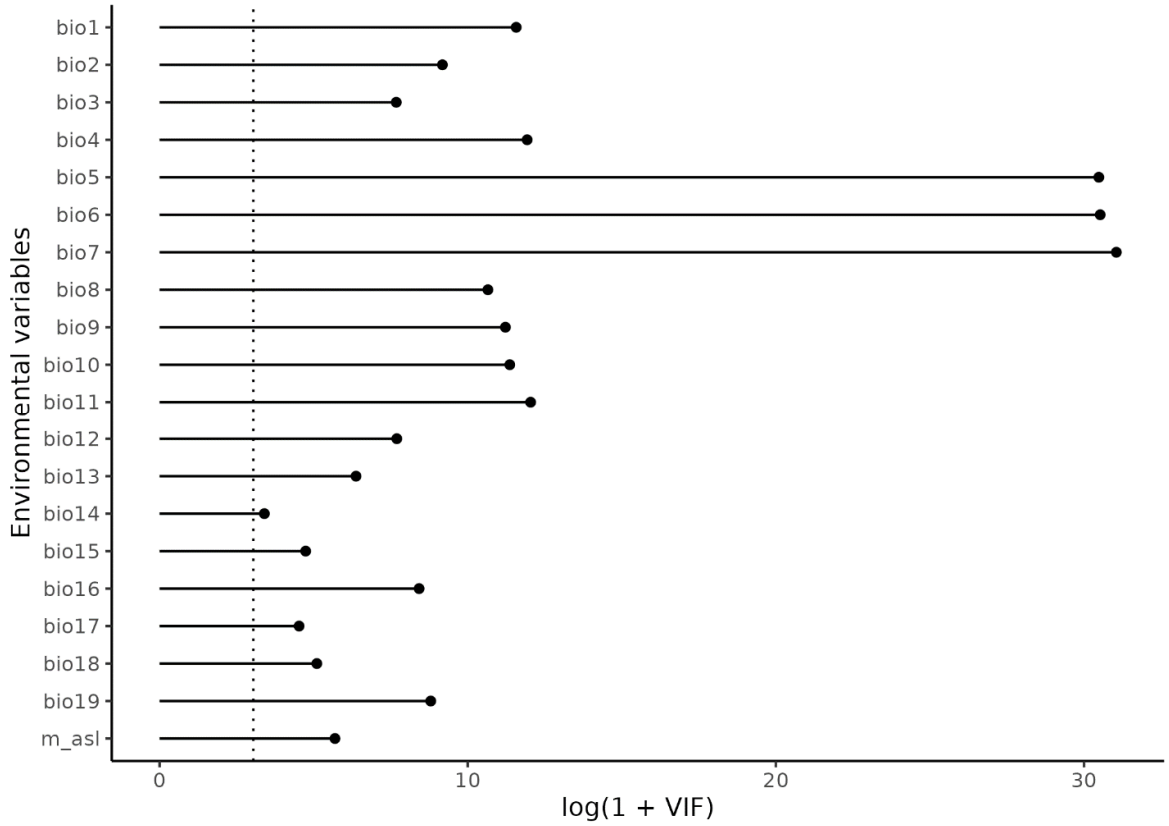

Appendix 4.Sup1. Variance Inflation Factors (VIFs).

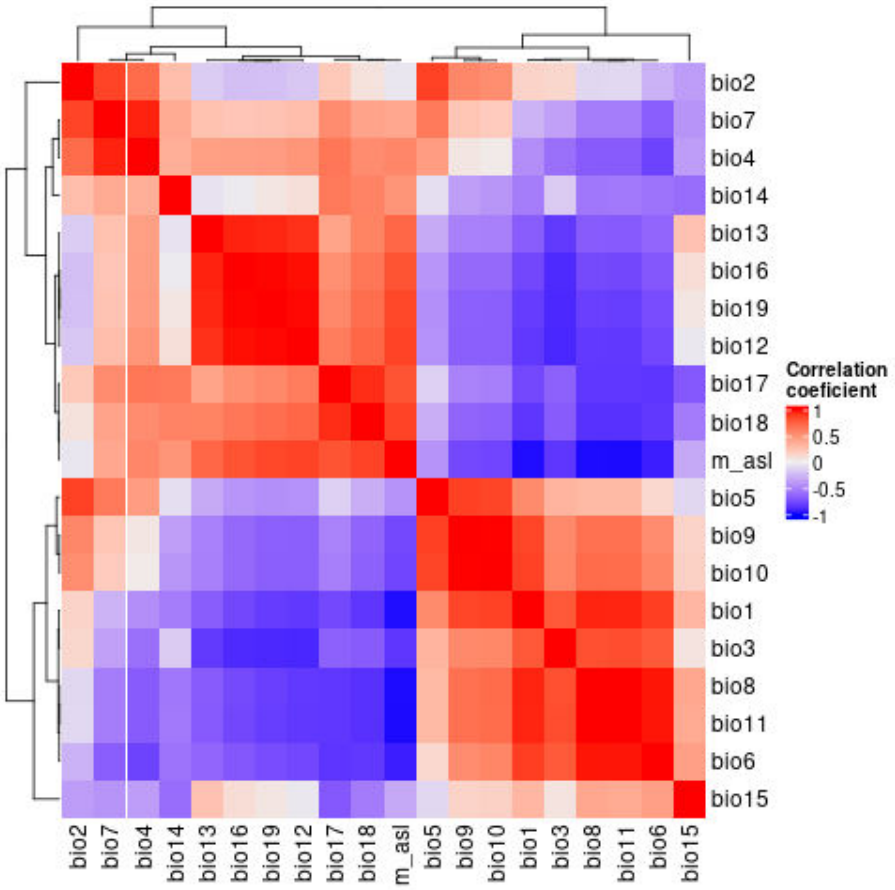

Appendix 4.Sup2. Correlation between environmental variables.

id	m asl	Sample type	Context	X	Y	bio1	bio2	bio3	bio4	bio5	bio6	bio7	bio8	bio9	bio10	bio11	bio12	bio13	bio14	bio15	bio16	bio17	bio18	bio19
sample_1	15	soil	semi-permanent lake	-6.05	36.62	17.8125	9.8083334	41.737591	492.00943	30.7	7.2	23.5	13.083334	23.816668	24.266666	12.133333	577	104	1	71.354691	283	19	23	257
sample_2	23	soil	semi-permanent lake	-5.8	37.03	17.904167	11.691667	43.625622	534.97858	33	6.2	26.8	12.683333	24.5	24.983334	11.783334	580	101	1	69.228958	272	18	23	247
sample_3	68	soil	semi-permanent lake	-5.89	36.92	17.766666	11.316667	42.866161	532.65771	32.7	6.3	26.4	12.6	24.383333	24.783333	11.7	591	105	1	69.193428	282	21	25	256
sample_4	70	soil	semi-permanent lake	-6.06	36.54	17.691666	9.5	40.254238	499.94016	30.8	7.2	23.6	12.95	23.833334	24.299999	12	607	105	1	70.386925	291	19	24	266
sample_5	28	soil	seasonal lake	-5.82	37.04	17.883333	11.733334	43.781094	533.10553	32.9	6.1	26.8	12.650001	24.450001	24.916668	11.766666	574	101	1	69.442734	271	18	23	246
sample_6	30	soil	seasonal lake	-6.14	36.35	17.625	7.9333334	38.511326	455.88324	28.5	7.9	20.6	13.333333	23.116667	23.583334	12.35	608	106	0	72.824028	295	16	19	270
sample_7	30	soil	seasonal lake	-5.82	37.05	17.875	11.75	44.007492	532.39807	32.8	6.1	26.7	12.633333	24.416666	24.883333	11.75	574	101	1	69.442734	271	18	23	246
sample_8	55	soil	seasonal lake	-6.02	36.84	17.770834	10.808333	42.220051	521.58612	32.2	6.6	25.6	12.733334	24.233334	24.65	11.816667	591	106	1	69.302605	285	22	26	258
sample_9	75	soil	seasonal lake	-5.9	36.9	17.783333	11.15	42.557255	531.38898	32.6	6.4	26.2	12.650001	24.383333	24.783333	11.733334	594	106	1	69.018303	283	21	26	258
sample_10	78	soil	seasonal lake	-6.03	36.52	17.733334	9.5666666	40.365681	500.90524	31	7.3	23.7	13.033333	23.9	24.366667	12.049999	615	106	1	70.806931	295	18	23	270
sample_11	2	soil	estuarine	-7.44	37.26	17.775	10.900001	43.600002	504.76593	31.9	6.9	25	12.95	24.1	24.4	12.066667	492	93	2	70.768959	239	17	22	216
sample_12	3	soil	estuarine	-7.44	37.27	17.6625	10.858334	43.433334	506.33765	31.8	6.8	25	12.816667	24	24.316666	11.933333	498	94	2	70.491913	241	18	22	218
sample_13	3	soil	estuarine	-7.44	37.26	17.775	10.900001	43.600002	504.76593	31.9	6.9	25	12.95	24.1	24.4	12.066667	492	93	2	70.768959	239	17	22	216
sample_14	3	soil	estuarine	-7.45	37.26	17.775	10.900001	43.600002	504.76593	31.9	6.9	25	12.95	24.1	24.4	12.066667	492	93	2	70.768959	239	17	22	216
sample_15	4	soil	estuarine	-7.44	37.26	17.775	10.900001	43.600002	504.76593	31.9	6.9	25	12.95	24.1	24.4	12.066667	492	93	2	70.768959	239	17	22	216
sample_16	9	soil	estuarine	-7.44	37.27	17.6625	10.858334	43.433334	506.33765	31.8	6.8	25	12.816667	24	24.316666	11.933333	498	94	2	70.491913	241	18	22	218
sample_17	3	soil	wetland	-6.86	37.16	18.033333	10.583333	42.164677	517.49103	31.8	6.7	25.1	12.9	24.4	24.716667	12	481	83	2	69.099564	232	20	22	204
sample_18	3	soil	wetland	-6.86	37.16	18.033333	10.583333	42.164677	517.49103	31.8	6.7	25.1	12.9	24.4	24.716667	12	481	83	2	69.099564	232	20	22	204
sample_19	4	soil	wetland	-7.45	37.27	17.704166	10.891667	43.393097	506.26733	31.9	6.8	25.1	12.883333	24.049999	24.35	11.983334	497	94	2	70.651566	241	18	22	218
sample_20	4.88	soil	wetland	-5.83929	36.2483	17.9375	8.5749998	41.22596	444.79376	29	8.2	20.8	13.766666	23.283333	23.716667	12.766666	755	126	0	74.339714	358	16	22	332
sample_21	5	soil	wetland	-7.46	37.27	17.729166	10.925	43.353176	505.98447	32	6.8	25.2	12.9	24.083334	24.383333	12.016666	499	94	2	70.046585	241	18	23	218
sample_22	5.5	soil	wetland	-5.8357	36.25019	17.950001	8.666667	41.467304	444.97192	29.1	8.2	20.9	13.766666	23.283333	23.733334	12.783333	749	125	0	74.219559	355	16	22	329
sample_23	25	soil	wetland	-6.5	37.12	18.091667	11.516666	42.812889	538.16534	33.1	6.2	26.9	12.666667	24.783333	25.033333	11.816667	505	88	2	68.171471	241	21	24	214
sample_24	9	soil	pasture	-7.44	37.27	17.6625	10.858334	43.433334	506.33765	31.8	6.8	25	12.816667	24	24.316666	11.933333	498	94	2	70.491913	241	18	22	218
sample_25	9	soil	orchard	-7.44	37.27	17.6625	10.858334	43.433334	506.33765	31.8	6.8	25	12.816667	24	24.316666	11.933333	498	94	2	70.491913	241	18	22	218
sample_26	7	soil	scattered trees/shrubs	-7.46	37.26	17.741667	10.933333	43.559097	505.39737	32	6.9	25.1	12.933333	24.083334	24.4	12.05	499	94	2	70.046585	241	18	23	218
sample_27	9	soil	scattered trees/shrubs	-7.44	37.27	17.6625	10.858334	43.433334	506.33765	31.8	6.8	25	12.816667	24	24.316666	11.933333	498	94	2	70.491913	241	18	22	218
sample_28	25	moss	scattered trees/shrubs	-7.97	37.04	17.508333	9.4333334	42.492493	445.18042	29.5	7.3	22.2	13.35	23.049999	23.333334	12.416667	522	113	2	77.516983	268	15	22	247
sample_29	25	moss	scattered trees/shrubs	-8.88	37.2	16.341667	7.2333331	45.208332	310.24063	24.7	8.7	16	13.566667	19.933334	20.35	12.75	508	85	2	69.762527	241	17	23	222
sample_30	25	moss	scattered trees/shrubs	-8.89	37.2	16.387501	7.125	45.094936	303.69785	24.6	8.8	15.8	13.666667	19.883333	20.316666	12.866667	503	84	2	69.736488	238	17	23	220
sample_31	60	moss	scattered trees/shrubs	-8.94	37.1	16.420834	6.9416666	44.784946	302.01941	24.6	9.1	15.5	13.75	19.883333	20.35	12.95	502	84	1	70.453903	238	16	22	220
sample_32	150	moss	scattered trees/shrubs	-7.89	37.13	17.0875	10.308333	42.59642	487.24234	30.8	6.6	24.2	12.566667	23.25	23.533333	11.616667	555	112	2	73.031204	272	17	24	253
sample_33	440	moss	scattered trees/shrubs	-8.11	37.26	16.066668	9.9666672	41.876751	480.90509	29.8	6	23.8	11.633333	22.166666	22.416666	10.683333	592	112	2	70.162315	282	20	26	265
sample_34	490	moss	scattered trees/shrubs	-7.93	37.24	15.420834	10.158333	41.462582	502.78976	29.7	5.2	24.5	10.816667	21.833334	22.1	9.833333	630	116	3	68.252808	296	24	30	279
sample_35	100	moss	forest	-5.37	36.47	17.220833	9.0583334	40.987934	465.40527	29.7	7.6	22.1	13	23.016666	23.450001	12.066667	690	129	0	76.312866	345	14	21	318
sample_36	100	moss	forest	-5.42	36.32	17.279167	8.3249998	39.832535	447.12442	29	8.1	20.9	13.216667	22.783333	23.25	12.283334	741	138	0	76.999794	370	15	22	345
sample_37	660	moss	forest	-5.25	36.77	14.5125	11.108334	40.39394	571.39832	30.4	2.9	27.5	9.1499996	21.816666	22.1	8.1166668	746	121	2	70.933487	345	20	25	333
sample_38	704	moss	closed forest	-5.39	36.8	14.0125	10.141666	38.270439	572.25677	29.4	2.9	26.5	8.666667	21.333334	21.6	7.5999999	785	123	2	69.800529	356	22	27	346
sample_39	740	moss	closed forest	-5.27	36.77	14.233334	10.966667	40.02433	573.34479	30.1	2.7	27.4	8.8666668	21.566668	21.85	7.8166666	763	122	2	70.522987	350	21	25	339
sample_40	745	moss	closed forest	-5.39	36.8	14.0125	10.141666	38.270439	572.25677	29.4	2.9	26.5	8.666667	21.333334	21.6	7.5999999	785	123	2	69.800529	356	22	27	346
sample_41	750	moss	closed forest	-5.35	36.52	14.741667	9.7333336	39.089691	533.6275	29.1	4.2	24.9	9.8833332	21.533333	21.866667	8.8000002	802	128	1	73.578171	371	18	24	365
sample_42	765	moss	closed forest	-5.45	36.8	13.708333	10	38.022812	571.07086	29	2.7	26.3	8.3833332	21.016666	21.283333	7.3166666	815	126	2	69.098785	365	24	28	356
sample_43	770	moss	closed forest	-5.32	36.75	13.975	10.4	38.805969	568.80054	29.5	2.7	26.8	8.666667	21.25	21.533333	7.5833335	778	123	2	70.497536	355	21	26	344
sample_44	797	moss	closed forest	-5.41	36.78	13.8375	9.8249998	38.081394	560.70215	28.7	2.9	25.8	8.583333	20.983334	21.25	7.5166669	793	124	2	69.833839	359	22	27	349
sample_45	1029	moss	closed forest	-5.43	36.78	13.2625	9.9250002	37.737644	572.72125	28.5	2.2	26.3	7.9333334	20.6	20.85	6.8333335	836	127	2	69.062965	372	24	29	364
sample_46	1100	moss	closed forest	-5.42	36.77	12.525	9.8999996	37.218044	583.8606	28.1	1.5	26.6	7.1166668	20.049999	20.266666	6.0166664	877	130	3	68.139946	384	27	32	379
sample_47	1100	moss	closed forest	-5.42	36.77	12.525	9.8999996	37.218044	583.8606	28.1	1.5	26.6	7.1166668	20.049999	20.266666	6.0166664	877	130	3	68.139946	384	27	32	379
sample_48	1100	moss	closed forest	-5.42	36.77	12.525	9.8999996	37.218044	583.8606	28.1	1.5	26.6	7.1166668	20.049999	20.266666	6.0166664	877	130	3	68.139946	384	27	32	379
sample_49	1146	moss	closed forest	-5.42	36.77	12.525	9.8999996	37.218044	583.8606	28.1	1.5	26.6	7.1166668	20.049999	20.266666	6.0166664	877	130	3	68.139946	384	27	32	379

Appendix 4.Sup3. Study samples (sample_1 to sample_49) and their characteristics: m asl, type, contexts and coordinates. Environmental variables from the WorldClim database coded as follows: bio1= annual mean temperature (°C); bio2 = annual mean diurnal range (°C); bio3 = isothermality (%); bio4 = temperature seasonality (standard deviation, °C × 100); bio5 = max temperature of warmest month (°C); bio6 = min temperature of coldest month (°C); bio7 = annual temperature range (°C); bio8 = mean temperature of wettest quarter (°C); bio9 = mean temperature of driest quarter (°C); bio10 = mean temperature of warmest quarter (°C); bio11 = mean temperature of coldest quarter (°C); bio12 = annual precipitation (mm); bio13 = precipitation of wettest month (mm); bio14 = precipitation of driest month (mm); bio15 = precipitation seasonality (coefficient of variation, %); bio16 = precipitation of wettest quarter (mm); bio17 = precipitation of driest quarter (mm); bio18 = precipitation of warmest quarter (mm); bio19 = precipitation of coldest quarter (mm).

5.- 26,000 years of environmental evolution of an incised valley in a rocky coast (La Janda wetland, SW Iberia)

This chapter is a slightly modified version of an article published in Continental Shelf Research:

Mediavilla, R., Santisteban, J.I., Val-Peón, C., Galán de Frutos, L., Mathes-Schmidt, M., López-Sáez, J.A., Gracia, F.J., Reicherter, K. (2023). 26000 years of environmental evolution of an incised valley in a rocky coast (La Janda wetland, SW Iberia). https://doi.org/10.1016/j.csr.2023.105028

Abstract

The La Janda wetland record allows to expand the knowledge of the evolution of a restricted estuary since the Last Glacial Maximum. Multiproxy analysis of the sediments (facies, geochemistry, pollen, fossils) reveals that this system exhibits a classic incised valley sequence but differences with the adjacent estuaries can be established. The La Janda sedimentary infill can be split in four(?) main sequences: (1) the Falling Stage Systems Tract (> 20.6 ka BP) and (2) the Lowstand Systems Tract (16.7-20.6 ka BP) deposits record fluvial sedimentation in a narrow and incised valley, here seminally identified in the Gulf of Cadiz estuarine system; and (3) the Transgressive Systems Tract (7-16.7 ka BP), ending with the Holocene marine flooding surface at 7 ka BP, is composed of estuarine and marine basin deposits infilling a still steep and narrow topography coupled with the fast retreat of the river mouths. The (4) Highstand Systems Tract (0-7 ka BP) is composed of estuarine basin deposits with fluvial and tidal currents deposits in a wide a gentle sloped estuarine valley and it records the transformation of the basin into a terrestrial one. Comparison to other areas in the Gulf of Cádiz allows to correlate the different estuaries and to distinguish between open and restricted ones by the development of spit systems during the Highstand Systems Tract. But further work is needed to clarify the stratigraphy of the present eustatic cycle in the Gulf of Cádiz as the scarcity of data does not allow to determine the evolution of its estuaries during the last fall and rise of sea level. Such knowledge is crucial to disentangle the role of climate and tectonics in the future evolution of our coasts and design measures to adapt to sea level rise.

Keywords: MIS 1/3, Open and restricted estuaries, Gulf of Cádiz, Sea level, Tectonics, Stratigraphic and sedimentary architecture.

5.1.- Introduction

Marine flooding of coastal areas due to increasing rate of sea level rise is one of the main risks linked to present climate change (Haasnoot et al., 2021; Nicholls et al., 2021; Strauss et al., 2021). This is one of the reasons why the analysis and comparison of recent examples of evolution of coasts is necessary. However, coastal systems are so complex and diverse that there is still a need to increase the knowledge on their dynamics and evolution.

Incised valleys and their sedimentary records are systems that supply valuable information about the environmental evolution of many coastal areas as a result of their main dependence on sea level changes (Zaitlin et al., 1994; Dalrymple et al., 1994; Allen & Posamentier, 1994) and, to a lesser extent, to direct climate change (Billeaud et al., 2009; Poirier et al., 2017) and recent human action (Cearreta et al; 2004, 2013; Evans, 2008). Beyond these allocyclic factors, autocyclic factors such as estuarine hydrodynamics (waves, tidal currents and fluvial supply), marine and terrestrial sediment availability and bed morphology (Chaumillon et al., 2008) play a fundamental role in their infill.

Of these autocyclic controls, hydrodynamics is the most influential and, consequently, wave or tide dominated estuaries are considered endmembers (Zaitlin et al., 1994; Boyd et al., 2006). However, there are many examples on which bed morphology play a key role on their hydrodynamics and sediment transport during the rise of sea level and their infill as the Bay of Biscay (Chaumillon et al., 2008; Allard et al., 2010) and the Gulf of Cádiz (de Castro & Lobo, 2018). So, the infill of incised valleys in the same region or geological context, and under comparable sea level and climate conditions, can show a great variability (Menier et al., 2010).

The coastline of the SW Iberian Peninsula (between the Gibraltar Strait and Saint Vincent Cape) contains some well-studied records of incised valleys as the estuaries of the Guadalete (Dabrio et al., 2000; Lario et al., 2002), Tinto-Odiel (Borrego et al., 1999; Dabrio et al., 2000), Piedras (Borrego et al., 1993), Boca do Rio (Hindson et al., 1998), Quarteira (Schneider et al., 2010) and Guadiana (Morales, 1997; Lobo et al., 2003; Boski et al., 2008; Mendes et al., 2020) rivers. The common feature of these records is the prevalence of the hydrodynamics upon the bed morphology. However, La Janda lake is an incised valley resulting from the confluence of the Almodóvar and Barbate rivers in the Campo de Gibraltar region. This valley preserves the complete record of the complete last 26,000 years of an estuary controlled by the bed morphology, today transformed into a wide wetland area.

The aim of this paper is to describe and interpret the sedimentology and stratigraphy of the La Janda wetland using a sequential stratigraphy model (Catuneanu et al., 2011; Catuneanu, 2019) and the influence of the local and global factors in the sedimentation as well as the differences with the nearby coetaneous systems.

5.1.1.- Geographic and geological setting

La Janda Basin (Hernández-Pacheco & Cabré, 1913) is located at the south of the Iberian Peninsula, near Vejer de la Frontera, 10 km away from the Atlantic coast (Gulf of Cádiz) and near 30 km from the Gibraltar Strait (Fig. 5.1a). It is a NW-SE fault-controlled depression (Goy et al., 1995; Zazo et al., 1999; Luque et al., 2001) almost 25 km in length and contains the wetlands and former lakes. Its lowest point is about 3 m a.s.l. (meters above sea level), while the highest surrounding areas are higher than 400 m a.s.l. Present-day basin is crossed and drained by the Barbate River along the western limits of the lake basin, and also by other tributaries, Almodóvar and Celemín rivers, being heavily disturbed by farming activities. After crossing the basin, the Barbate River flows to the west and then dramatically changes its trace to the SE (Fig. 5.1b), running to the sea through a narrow gorge and flowing into a marsh complex with a tidal range of c. 2 m (Instituto Hidrográfico de la Marina, 2019).

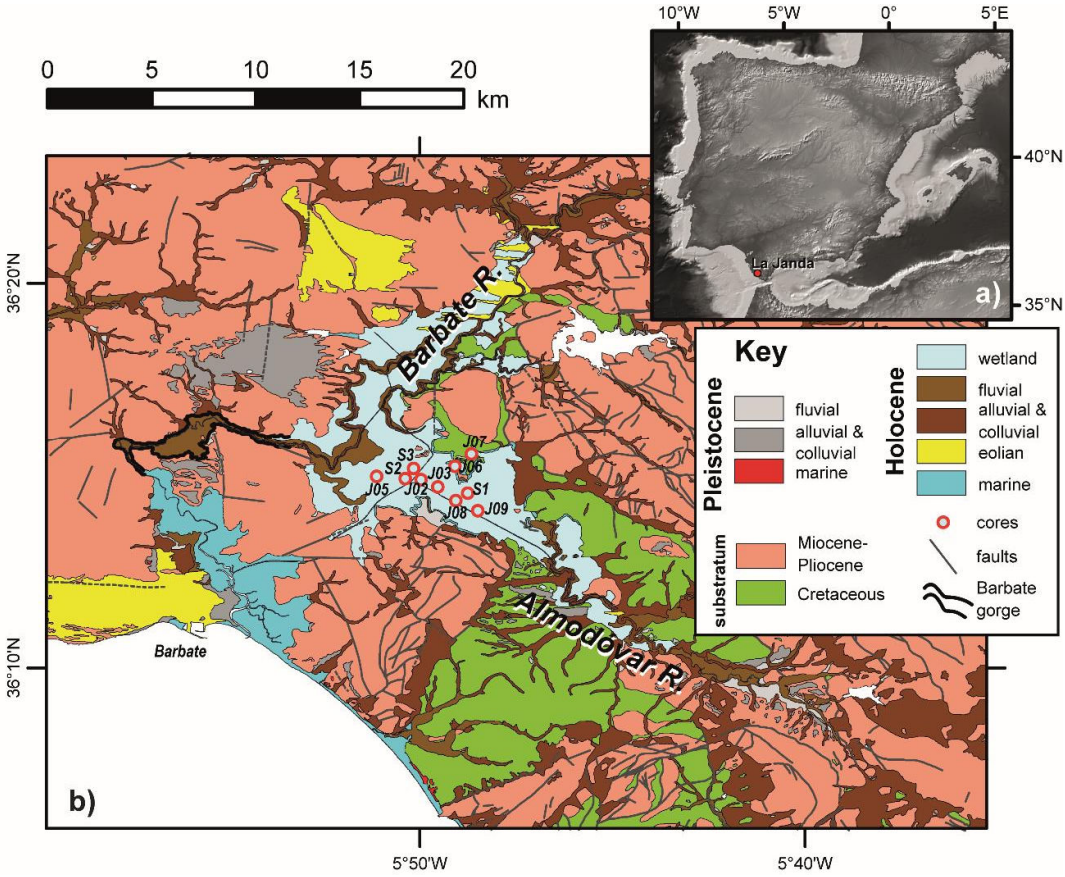

Figure 5.1. (a) Location of the studied area. (b): Geological map of La Janda basin and borders, simplified from the Continuous Geological Map of Spain 1:50.000 (GEODE). Geographical data provided by the Spanish Geographical Institute (IGN) and the geological map by the Instituto Geológico y Minero de España, CSIC (Roldán et al., 2021).

The Mediterranean-Atlantic climate of the region is characterized by an annual average rainfall of c. 850 mm, mostly during winter months, and mean annual temperatures from 16ºC to 19ºC and a thermal

range between 10-16ºC. Easterly prevailing winds are frequently followed by W and SW winds (Dueñas López & Recio Espejo, 2000).

La Janda is placed in the convergence area of the Eurasian-African plates, at the westernmost sector of the Betic Cordileras and in the Gibraltar Arc structure, being subjected to an intense tectonic activity during Cenozoic times (Benkhelil, 1976; Sanz de Galdeano, 1990; Azañón et al., 2002). From Burdigalian until Tortonian, the Gibraltar Arc uplifted under a WNW-ESE compressive stress field (Balnayá & García Dueñas, 1987; Leblanc, 1990; Sanz de Galdeano, 1990; Vergés & Fernández, 2012; González-Castillo et al., 2015). Since then, and until recent times, the stress field has rotated to NW-SE to NNW-SSE direction (Benkhelil, 1976; Sanz de Galdeano, 1990; Goy et al., 1995; Zazo et al., 1999; Gracia et al., 1999; Reicherter & Peters, 2005). The geology of the Gibraltar Arc in the studied area is composed by siliciclastic and carbonated pre- and synorogenic turbiditic deposits (Almarchal, Algeciras and Aljibe Series of the Gibraltar Flysch), spanning from Late Cretaceous to Middle Miocene times, affected by thrusts, backthrusts and dextral strike-slip faults (Hernaiz Huerta et al., 1991). Upper Miocene-Pliocene postorogenic sediments consist of breccias, calcarenites and siliciclastic marine deposits filling subsiding troughs affected by Plio-Pleistocene compressive tectonics (García de Domingo et al., 1991; Goy et al., 1995). The distribution of Quaternary deposits is controlled by neotectonics, being preferential along the present coastline of the Gibraltar Strait (Rodríguez Vidal et al., 2004), fluvial valleys and the La Janda basin (Fig. 5.1b). Luque et al. (1999) found estuarine siliciclastic deposits, dated as 3810 cal. BP, at -5 m a.s.l. revealing that the basin was below sea level. Later basin infill led to the isolation from the sea and the beginning of alluvial and, afterwards, lacustrine sedimentation (Luque et al., 1999, 2001; Dueñas López & Recio Espejo, 2000).

5.2.- Methods

In 2016 and 2017 twelve cores were recovered in two coring campaigns by triple barrel system (cores S1, S2 and S3) and a portable Atlas Copco vibracoring system (cores named JAN), all of them encased in PVC or methacrylate pipes (Table 1). The cores were split in two in the laboratories of the Spanish Geological Survey (IGME, CSIC), and one half was stored as an archive, whilst the other half was used for description, analyses and sampling. All of them were photographed, their sedimentary features were described and stratigraphic logs (scale 1:20) were elaborated correcting the depths to remove the effect of compaction due to drilling.

Table 5.1. Location of cores. Bold: cores presented in this paper (see location in Fig. 5.1b).

Core	Latitude	Longitude	Height (m.a.s.l.)	Length (m)
S1	36º14'29.62" N	5º48'44.33" W	4.11	10.00
S2	**36º14'53.88" N**	**5º50'21.45" W**	**4.88**	**27.50**
S3	**36º15'09.68" N**	**5º50'08.52" W**	**5.50**	**26.78**
JAN-02	36º14'53.63" N	5º49'57.24" W	4.81	3.00
JAN-03	**36º14'40.76" N**	**5º49'31.26" W**	**3.65**	**13.50**
JAN-05	**36º14'57.61" N**	**5º51'06.16" W**	**4.80**	**13.00**
JAN-06	36º15'13.62" N	5º49'04.22" W	5.28	2.00
JAN-07	36º15'31.68" N	5º48'38.85" W	8.23	3.00
JAN-08	36º14'19.82" N	5º49'03.65" W	3.67	3.00
JAN-09	**36º14'03.80" N**	**5º48'28.39" W**	**4.28**	**13.00**

5.2.1.- Physical properties, mineralogical and geochemical composition of the sediments

Non-destructive analyses were run on the cores, at the laboratories of the Spanish Geological Survey (IGME, CSIC), including:

- Core colour scan (high resolution images with a down core resolution of 50 □ m) with a Geoscan IV coupled to the MSCL GEOTEK.
- Colour (RGB) analyses were performed with 1 mm down core resolution using a Konica Minolta 700-d spectrophotometer integrated in the GEOTEK XRF core scanner. Each channel had values ranging from 0 up to 255 and a R/(G+B) colour index was used to represent the dominant tones (red/brownish against green/greyish) and a (R+G+B)/3 index represents the grey scale range.
- Geophysical properties (P-wave velocity, gamma density, non-contact resistivity and magnetic susceptibility) were analysed with 1 cm down core resolution with a GEOTEK Multi-Sensor Core Logger (MSCL-GEOTEK).
- XRF scanning with a GEOTEK XRF core scanner in a He purged atmosphere with an illumination window of 15 mm (cross-core slit width) x 10 mm (down-core resolution). Two runs, with 30 seconds count time exposure, were performed for 10 kV and 40 kV (detecting from Mg to U). XRF spectra were processed with bAxil. Element intensities are represented in counts per second (cps).

Sampling was carried out in cores S2 and S3 to characterize the sedimentary facies at the IGME laboratories:

- Mineralogical analysis by X-ray diffractometry (PTE-RX-04) for bulk sample and <2μm fraction. These analyses were used to check the sources of the chemical elements obtained from geochemical analyses.
- Geochemical analysis of major oxides and trace elements by X-ray fluorescence and atomic absorption spectroscopy (XRF and AAS). The results were used to check the validity of the non-destructive high-resolution XRF scanning.
- C (organic, inorganic and total) and S by elemental analyser (ELTRA). S data was used to check the results of XRF core scanning. C values gave an estimate of organic matter and carbonate content, and they can be compared to other results from non-destructive techniques (XRF core scanning and colour).

5.2.2.- Dating and age-depth model

A total of 25 samples (cores JAN05A, S2, S3, JAN09A) were 14C-dated (Beta Analytic Inc., USA and Keck Carbon Cycle AMS Facility at UC Irvine, USA). Calibration was performed with CALIB 8.2 (Stuiver et al., 2021) using the IntCal20 and Marine20 calibration datasets (Reimer et al., 2020; Heaton et al., 2020) and different reservoir effect values (Table 1). These reservoir effects/values have been recalculated based on the literature (Soares and Dias, 2006; Soares and Martins, 2010; Martins and Soares, 2013) and using the web application of Reimer and Reimer (2017) following the methodology of Soulet (2015).
Due to the peculiar setting of the sediments (in a restricted and shallow environment) several calibration sets were developed to check which calibration curve and reservoir effect values (if applied) were the best. Bchron (Haslett & Parnell, 2008), clam (Blaauw, 2022), rbacon (Blaauw & Christen, 2011), rcarbon (Crema & Bevan, 2021) and a simple lineal interpolation were used to build a reliable age-model.

5.2.3.- Pollen analysis

Sampling for palynological analyses was undertaken as follows: 52 test-samples were collected from core S2 at different intervals and 160 samples were collected from core S3 maintaining a regular interval of 10 cm. All samples were chemically treated with HCl (10%) to remove carbonates, KOH (10%) to remove humic acids, and Sodium Polytungstate (SPT: 3Na2WO4·9WO3·H2O) at 2.0-2.1 gr/cm^3 for densimetric separation. The final residue was mounted on slides with the use of glycerol. Pollen concentrations (grains/gr of dry sediment) were estimated by adding two *Lycopodium clavatum* tablets to each sample (Stockmarr, 1971). Palynomorphs were counted using an optical microscope at 400x and 1000x up to a minimum pollen sum of 300 terrestrial pollen grains. Palynomorphs were identified using published keys (Moore et al., 1991; Reille, 1992, 1995; Van Geel, 1978, 2001; Van Geel et al., 1980, 1986, 1989, 2003).

For the purpose of this paper, three well-represented palynomorphs were selected as good ecological indicators of specific environments related to the study area (Figs. 2a, 3a, 3b). Species from the Chenopodiaceae family grow in temporary pools of brackish or saline water, the edges of lagoons, the open spaces of coastal marshes, and areas affected by tides (Domínguez et al., 1993; Galán de Mera et al., 1997; Latorre et al., 1996; Rivas-Martinez et al., 1997); hence, it is used here as a good marker of marine influence. *Isoetes* typically grows in shallow waterlogged environments associated to fresh water marsh communities, usually with oligotrophic waters (Cirujano et al., 2014); thus, it is used as an indicator of environments with a progressive loss of marine influence. *Glomus* (HdV-207) is associated to processes related to the development of new soils, soil erosion from watersheds, dry or desiccated areas, and farming activities (Anderson et al., 2011; López-Sáez et al., 2000; van Geel et al., 1989); therefore, it is considered a marker of erosive processes of different nature.

Concentrations and percentages were calculated using TiliaIT software (version 2.1.1, Illinois State Museum, Research and Collection Center, Springfield USA). Percentages were calculated considering a terrestrial pollen sum (TPS) that excluded aquatic pollen types, which were included in the total sum (TS) together with Non-Pollen Palynomorphs.

5.3.- La Janda record

5.3.1.- Age-depth model

Before applying the different age models to the dated samples, four samples were rejected as, presumably, they contain reworked carbon (Table 5.2). Several age-depth models were discarded based on inconsistencies (age reversals, unreasonable sedimentation rates, etc.) and, for the remaining ones, the simplest one, a simple lineal model (Fig. 5.2a), was applied to the cores for further checking by comparison of different proxies among cores (Fig. 5.2b). Despite their similarity, age-depth models for the different cores cannot be combined in a single one as differences in sedimentation rates caused artifacts that result in unrealistic correlations.Cores S2 and S3 show the longest records, ca. 20 ka BP for core S2 and ca. 27 ka BP for core S3. They begin with low sedimentation rates during the late Pleistocene. For core S3 this is interrupted by a discontinuity while core S2 record is continuous and it shows a gradual increase in sedimentation rate at the end of the Pleistocene.

Table 5.2. Radiocarbon data and calibration results for cores JAN-5A, JAN-S2, JAN-S3 and JAN-9A. The rejected samples correspond to possibly reworked material.

Lab code	Number in figures	Sample	Depth in core (m)	^{14}C	error	$\delta^{13}C$	ΔR	error	Cal. BP 2σ median [range]	Material	Curve
Beta-635182	**1**	JAN5-1	-2.7	1410	30	-24.5	-	-	1319 [1287, 1352]	Organic matter	IntCal20
Beta-635183	**2**	JAN5-2	-3.9	2010	30	-25.8	-	-	1947 [1869, 2002]	Organic matter	IntCal20
Beta-635184	**rejected**	JAN5-3	-7.7	5840	30	-20.1	-	-	6658 [6596, 6739]	Organic matter	IntCal20
Beta-635185	**rejected**	JAN5-4	-9.7	6520	30	-25.9	-	-	7430 [7418, 7505]	Organic matter	IntCal20
UCIAMS-231721	**3**	JAN-5A	11.5	6625	20		301	201	6580 [6126, 7068]	Shell	Marine 20
UCIAMS-236153	**rejected**	JAN-S2-0	0.46	1100	15		-	-	997 [957, 1007]	Charcoal	IntCal20
Beta-618143	**4**	JAN-S2-1	2.78	1440	30	-20.9	-	-	1331 [1297, 1373]	Organic matter	IntCal20
Beta-459036	**5**	JAN-S2-2	5.16	2480	30	-9.9	-315	220	2353 [1775, 2889]	Shell	Marine 20
Beta-459037	**6**	JAN-S2-4	11.55	6660	30	-2.6	301	201	6618 [6178, 7115]	Shell	Marine 20
Beta 459038	**7**	JAN-S2-5	14.6	7680	30	2	301	201	7670 [7260, 8093]	Shell	Marine 20
Beta-459039	**8**	JAN-S2-6	20.44	8220	40	-27.7	-	-	9185 [9024, 9302]	Charcoal	IntCal20
Beta-557793	**9**	JAN-S2-16	23.46	10440	30	-25	-	-	12.341 [12537, 12607]	Charcoal	IntCal20
Beta-635181	**10**	JANS2-17	26.67	16340	60	-25	-	-	19.723 [19552, 19882]	Organic matter	IntCal20

Beta-526017	**11**	JAN-S3-2	1.46	400	30	-25.8	-	-	471 [428,512]	Charcoal	IntCal20
Beta-618144	**12**	JAN-S3-3	4.04	1620	30	-23.2	-	-	1481 [1409, 1544]	Organic matter	IntCal20
Beta-618145	**rejected**	JAN-S3-4	5.75	2880	30	-26.1	-	-	3008 [2921, 3078]	Organic matter	IntCal20
Beta-526108	**13**	JAN-S3-5	6.33	2810	30	-25.9	-	-	2912 [2846, 2998]	Charcoal	IntCal20
UCIAMS-259331	**14**	JAN-S3-6	7.81	4115	15	-5.5	200	426	3744 [2702, 4833]	Shell	Marine 20
Beta-526109	**15**	JAN-S3-7	8.94	4570	30	-1.6	50	152	4516 [4076, 4925]	Shell	Marine 20
Beta-526110	**16**	JAN-S3-8	11.23	6760	30	-22.9	-	-	7615 [7574, 7668]	Organic matter	IntCal20
UCIAMS-259332	**17**	JAN-S3-9	15.51	8040	20	-2.1	17	183	8327 [7911, 8816]	Shell	Marine 20
Beta-526111	**18**	JAN-S3-10	18.3	7890	30	-26.4	-	-	8668 [8593, 8779]	Vegetal remain	IntCal20
Beta-540083	**19**	JAN-S3-11	22.64	22400	90	-26.5	-	-	26.728 [26405, 27006]	Organic matter	IntCal20
UCIAMS-231722	**20**	JAN-9A 1	5.9	4275	15		-251	169	4523 [4044, 4975]	Shell	Marine 20
UCIAMS-231723	**21**	JAN-9A 2	11.54	6450	20		301	201	6390 [5920, 6853]	Shell	Marine 20

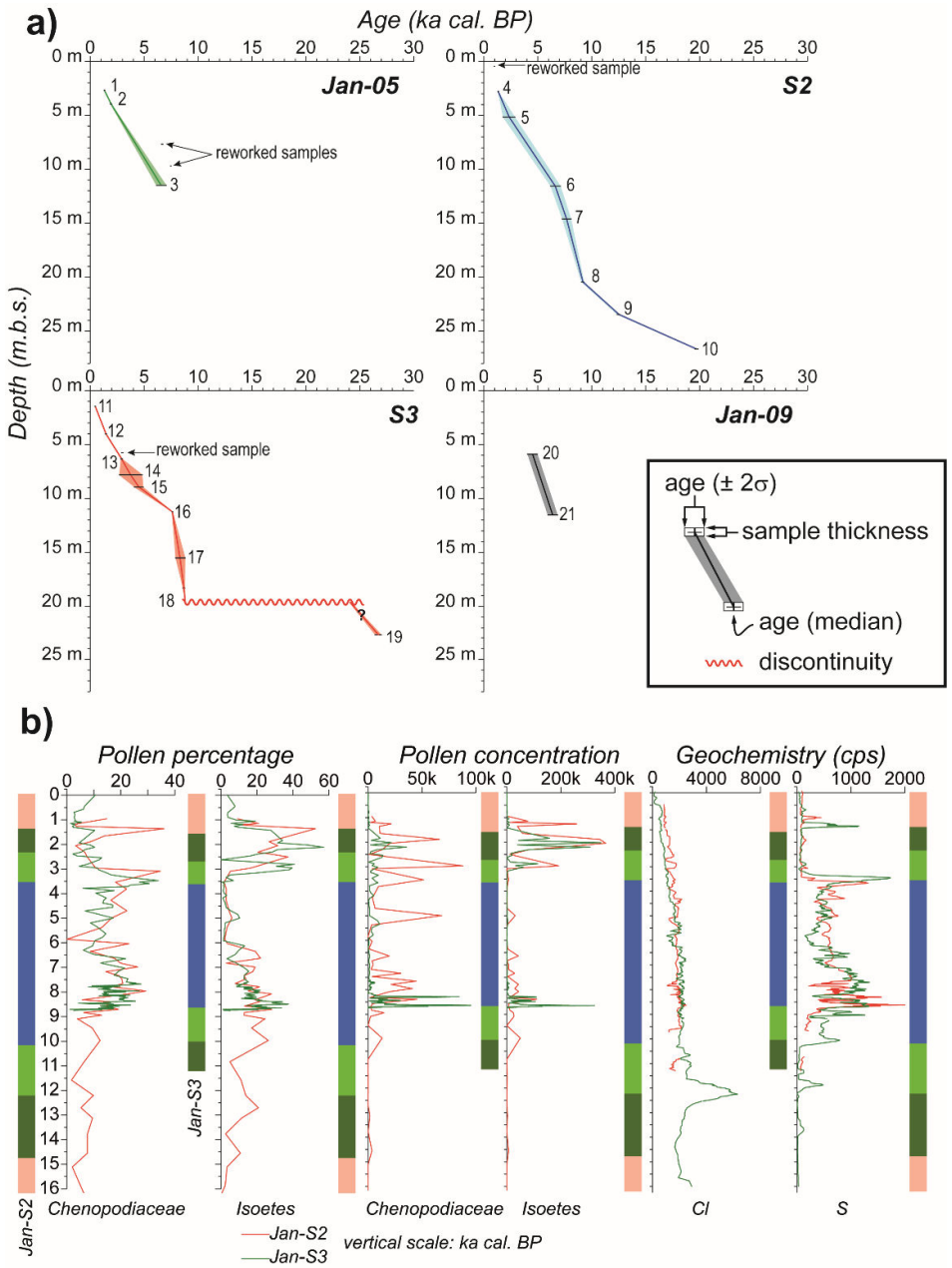

Figure 5.2. Age models for (a) cores S2, S3, JAN-05A and JAN-09A. The numbers for reference are those of Table 5.2. (b) Comparison of age-depth models for cores S2 and S3 based on pollen and geochemistry. Vertical colour bars: see Fig. 5.3 key.

The Holocene record starts with high sedimentation rates for cores S2 and S3 until ca. 7 ka BP, when the sedimentation rate for all cores, except JAN-09, decreases. The greater rates for core JAN-09 can be due to its proximity to a river mouth, which increased the supply of sediment at this location. Despite the noticeable decrease in sedimentation rate for the last 7 ka, in comparison to the 7 to 9 ka BP period, it is worth to notice that sedimentation rates increased slowly until present.

5.3.2.- Facies analysis

Facies have been characterized by visual inspection as well as by their geophysical properties, geochemical and mineralogical composition. Such parameters show both gradual and abrupt changes and, therefore, we describe the logs and then the Facies Groups (which are composed of different facies but grouped in a larger set). These groups are the basis for the environmental interpretation.

5.3.2.1.- Geophysical logs

Due to the homogeneity of the sediments, the more distinctive logs are those of colour that can be linked to their oxidation or reduction degree and composition.

The lowermost materials show higher values of the R/(G+B) and Grey indexes, indicative of warm pale tones. Similar R/(G+B) values can be observed at the top of the sections, but, in this case, the Grey index points to darker tones. Between these levels, the R/(G+B) and Grey indexes fall except for some intercalations that show paler tones, and sometimes more ochre, coincidental with coarser siliciclastic levels. The colour of the sediments is indicative of their oxidation level (Lyle, 1983; Nagao & Nakashima, 1992). Thus, brown and ochre colours are indicative of oxidizing conditions typical of emerged setting. The appearance of green to grey colours implies reductive processes by consumption of the bottom oxygen (submerged conditions) while the mixture of colours (mottling) indicate alternating conditions.

The remaining parameters (gamma ray density, magnetic susceptibility and resistivity) are dependent on the mineralogical composition and grain size of the sediment. Due to the dominance of clay minerals, the profiles are very homogeneous and they only show changes where coarser grain siliciclastic or mixed siliciclastic-bioclastic levels appear. In such cases, the three parameters increase their values for siliciclastic coarser grain size levels but not for bioclastic levels.

The geophysical proxies are indicative of the grain size and composition of the sediments and, thus, they provide information about the energy of the environment. In this case, the general sedimentation is fine-grained, pointing to a sedimentation from suspension, with some coarser-grained deposits, more energetic, intercalated among them. The composition of these more energetic levels can be siliciclastic, bioclastic and mixed, indicating a mixture of provenances that are exogenous (siliciclastics) and endogenous (bioclastic). Such episodes can be then linked to external inputs to the basin (from rivers) and the reworking of the bottom of the basin by waves or currents.

5.3.2.2.- Geochemistry and mineralogy

The studied sediments are composed by siliciclastics (mostly mud with some levels of sands and gravels) with contributions of carbonates (nodules and shells, sparse or in levels) and sparse organic matter,

gypsum, pyrite and halite sparse inside them (Fig. 5.3). Thus, the geochemical composition of these materials is controlled by this mineralogical composition. Some elements are shared between minerals, but major components represent most of the content of the main ions. As an example, Calcium (Ca, CaO) can be present in carbonates, gypsum and some silicates. However, the good correlation with inorganic Carbon (TIC) indicates that most of it is linked to the carbonates. However, Sulphur (S) is mainly linked to the presence of gypsum and/or pyrite, pointing to the minor contribution of these minerals to the bulk composition of the sediments. Another question is the difference in techniques. As pointed by several authors, the XRF scanning is usually applied on wet sediments and the water content can affect the results, which can be different to those obtained by classical "destructive" techniques in which the sample is grounded, desiccated and homogenized (Tjallingii et al., 2007; Dunlea et al., 2020). For this reason, in addition to the XRF scanning a selection of samples from cores S2 and S3 (the longest ones) were analysed by ICP spectrometry and AAS.

The results of these mineralogical and geochemical analyses are shown in Figure 5.4 and reveal the good agreement among the mineralogical, "classical" geochemical analysis and XRF scanning. Sometimes, the Facies Groups show clear changes in the composition, but also there are gradual changes that can be better explained as an evolution. The siliciclastic components (exogenous component) are best described by the content in silicon (Si), aluminum (Al), zirconium (Zr) and titanium (Ti). Si is shared by all of them, but it increases with the amount of quartz, as well as Zr, being noticeable at coarser levels. Al is shared by clay minerals and feldspars, but being the latter less present, its content can be ascribed to the clay content. Thus, volume changes of these elements reflect changes in the ratio exogenous/endogenous minerals and in grain size (energy). The composition in the cores is very homogeneous except where gravel and sandy layers appear and the relative Al content decreases. Due to the highest intensity of Al peaks, the sandy levels rich in matrix are masked. The endogenous components are carbonates, gypsum, halite and pyrite/haematite. These are of terrestrial or marine origin. The carbonates are recorded by TIC, which correlates to Ca and CaO. They are present in two components: nodules and forming part of the matrix (edaphic) and shells (entire or broken, marine and transition). The edaphic carbonate is recorded by a background Ca content without noticeable peaks. The marine carbonate content is larger on the average and conspicuous peaks corresponding to shells (isolated or in levels) are observed. The content in sulphur varies with gypsum and pyrite content, but also with organic carbon (TOC). The upper and lower portions of the cores are poor in S and a sharp boundary can be traced with the S-rich levels. In the S-poor sections, some S peaks correlate with bromine (Br) and chlorine (Cl). It must be noticed that, on the overall, decreases in S are correlative to increases in Si or Ca. Cl and Br (halides) variations follow the natrium (Na) and TOC changes, as well as the presence of halite. The lower part of cores S2 and S3 show low contents of Cl and Br, both of which increase somehow abruptly above the transition from the lowermost sands and gravels to the dark muds. This increment is also noticed in Na- and TOC-

excursions in cores S2 and S3. Upon this, they show an increasing trend that changes around the middle of the cores S2 and S3 to a decreasing one at the top of the cores. These trends are punctuated by lower content levels that coincide with siliciclastic-rich coarser grain levels. Br is associated to saline minerals and organic matter (Ziegler et al., 2008) and some authors link the Cl content to pore sea water content (Tjallingii et al., 2007). However, the good correlation to Na data, obtained from dry samples (classical XRF analysis), and to Br and TOC leads us to consider that this content is related to the halite identified by DRX analysis and to the organic matter content. S correlates to pyrite (Chéron et al., 2016). Na and Cl can be absorbed by clay in marine sediments (Charlet and Tournassat, 2005). The fact that Cl and Br do not show a correlation to grain size and that the lower values correspond to the more permeable facies indicates that this is not linked to a present saline aquifer as proposed by Luque et al. (1999). The correlation of S, Br and Cl with TOC can be indicative of an origin linked to the organic matter, which is common in the case of S. It means that these ions are trapped by the clays and organic matter as the parent minerals are degraded. Thus, we can interpret S as a proxy of reductive conditions (which is also correlated to the preservation of organic matter) while Br and Cl are proxies of sea water influence, as well as of organic content.

5.3.2.3.- Pollen record

The bottom sediments of both cores are characterized by poor preservation of palynomorphs, resulting in low concentrations of all taxa. Samples from core S3 are palynologically sterile for this period and core S2 shows alternating percentages of Chenopodiaceae and *Isoetes*. Thereafter, between ca. 7-10 ka BP in core S2 and ca. 7.5-8.7 ka BP in core S3, the percentages and concentration values of *Isoetes* increase. In both cores, ca. 8-9 ka BP, Chenopodiaceae and *Isoetes* display raised values. Between ca. 3-9 ka BP, Chenopodiaceae progressively increase to the detriment of freshwater vegetation, although displaying variable values and concentration peaks within this period. From ca. 1-3 ka BP, there is an increase in the percentages and concentration values of *Isoetes*, especially remarkable in core S3. There is a peak of Chenopodiaceae ca. 1 ka BP in both cores, which culminates in the decline of both salt marsh and freshwater taxa from this date onwards. On the other hand, *Glomus* concentrations and percentages are rather low in both cores until they undergo a significant rise from ca 1.5 ka to the top of both sections.

5.3.2.4.- Other fossil content

The fossil content is low in all the cores. According to Luque et al. (1999), at the top of the section, there are some ostracods (*Ilyiocypris gibba*, *Candona neglecta* and *Candona sp.*) and few charophyte remains, while below 4.5 m in depth occasionally some foraminifera (*Haynesina*, *Ammonia*, *Elphidium*), ostracods (*Cyprideis torosa* and *Loxoconcha elliptica*), bivalves (*Cerastoderma edule*, *Scrobicularia scrobicularia*, and *Ostrea sp.*) and gastropods (*Hydrobia sp.*) are encountered. We have studied additional samples that allow to include *Retusa*

sp., gastropod, few broken remains of bryozoa, fish remains, siliceous spicules of sponges, arthropod remains, and to improve the foraminifera record (*Ammonia tepida*, *A. beccarii*, *Haynesina germanica*, *H. depressula*), as well as a fragment of *Cassidulina*, few small miliolids (*Triloculina*) and possible Nonionidae. The microfaunal remains are indicative of freshwater or brackish water (*Ilyocypris gibba*, *Candona neglecta*, *Candona sp.*, charophytes) or brackish water (*Cyprideis torosa*, *Loxoconcha elliptica*, charophytes, bivalves and gastropods), however a certain marine influence can be deduced from the presence of foraminifera.

5.3.2.5.- Facies and sedimentary model

Four facies groups can be described according to the composition and properties of the sediments and their position in the cores (Fig. 5.3).

Fluvial Facies

Channel subfacies

Ochre to orange siliciclastic sediments located at the bottom of cores S2 and S3. Poorly to moderately sorted subrounded gravels, sands, and sometimes laminated muds, are arranged in fining upward sequences with concave upwards erosive base. The coarsest sediments show internal erosive surfaces. Towards the top of this facies, root traces, mottling and nodules increase typical for a hydromorphic soil. Sediments show brighter colours and greater density and magnetic susceptibility than the surrounding sediments. The low calcite content (Ca and inorganic C) is linked to carbonate clasts derived from the substratum or carbonate nodules. The S content is very low, which correlates with the absence of gypsum and pyrite. Cl and Br content are also low and increase towards the boundary with the supratidal facies. Sediments are azoic or barren and the pollen content is very low and poorly preserved.

Interpretation: The grain size and erosive base of these deposits are indicative of channelled facies of a certain energy. The presence of internal erosive surfaces reveals that their infill was episodic. The fining upwards sequence, ending with paleosols, indicates filling of these channels sometimes clearly above the ground water table (calcic soils) and others with the ground water table near or at the surface (hydromorphic soils).

Floodplain/fluvial wetland subfacies

Brown to ochre muds with some sandy layers (in the eastern cores, JAN-03A and JAN-09A) found topsection. They show mottling, some charred particles, carbonate nodules and root traces as well as sparse clasts, but with planar boundaries. They have finer grain sizes and darker tones than their channel equivalents. The coarser levels owe larger magnetic susceptibility and density values than the finer facies. Their S content is very low and this is linked to the absence of gypsum and pyrite. The calcite, Ca and TIC content is linked to the presence of carbonate nodules and the Br and Cl content is also low but

increasing towards the supratidal facies. The most diagnostic feature is the presence of Glomus chlamydospores and the decrease in Chenopodiaceae pollen and *Isoetes* spores, as compared to the underlying levels, as well the presence of Characeae. According to Luque et al. (1999), these sediments can contain ostracods (Ilyiocypris gibba, Candona neglecta and *Candona* sp.) and few charophyte remains.

Interpretation: The colour, finer grain size, planar boundaries and the presence of mottles, nodules and root traces reveal subaerial sedimentation linked to overbanks of the fluvial system. The geochemical features, similar to those of the fluvial channel facies are indicative of clastic supply in a low salinity environment dominated by oxidizing conditions. The abundance of *Glomus*, in comparison of other facies, points to subaerial erosion in a vegetated plain. In addition, the presence of Characeae and freshwater ostracods reveal the development of shallow ephemeral (seasonal?) ponded areas.

Supratidal Facies

Brown to green muds showing abundant hydromorphic features (mottling), carbonate nodules, organic matter mottles and root traces. A distinctive feature is the presence of some broken shells (bivalves). The hydromorphic features, broken shells and burrowing are more common towards the contact with the intertidal facies and the colour is also usually green. In the proximity of the fluvial facies, root traces and carbonate nodules are more frequent, and the colour is dominantly brown. S, Cl and Br content is low, but larger as the fluvial facies. No gypsum, pyrite or halite have been detected. Ca and TIC are low and related to the presence of carbonate nodules and few shell fragments. At the base of cores S2 and S3, low concentration and percentages of Chenopodiaceae and *Isoetes* was observed. But towards the top, the percentages and concentration values of all the palynomorphs increase, and few charophytes can be present (Luque et al., 1999). It is remarkable that, at that position, Chenopodiaceae and *Isoetes* show a relative maximum in their percentages.

Interpretation: The fine grain size of these deposits and abundance of edaphic features is interpreted as an area where sedimentation was episodic, probably linked to extreme flood events (marine and fluvial) at the boundary of coastal and fluvial domains. On these mudflats, some stable ponds filled with freshwater (vegetated by *Isoetes*) or brackish waters (surrounded by Chenopodiaceae) developed. The landscape resembles very much present marshes.

Intertidal s.l. Facies

Mainly green muds changing to ochre towards the boundary with supratidal facies are partly laminated without edaphic features. The muds usually contain shells (broken or unarticulated) and mottles of iron oxides or organic matter, and are bioturbated. Their content in S is low and no gypsum or pyrite have been detected. Cl and Br content is slightly larger than for fluvial and supratidal facies. Some halite is

present, but the higher values coincide with organic matter mottles. TIC and Ca (calcite and aragonite) content is low. Chenopodiaceae pollen show a relative maximum and *Isoetes* an increasing upwards trend while *Glomus* spores percentages are very low.

Interpretation: The dominance of green muds is interpreted as periodic submergence and water saturated pores that sporadically dry (ochre mottles: oxidizing conditions). The abundance of Chenopodiaceae and *Isoetes* are indicative of the presence or proximity to brackish and freshwater ponds. Adding the presence of marine shell fragments and halite, this allows interpreting these deposits as a mudflat in the intertidal area.

Subtidal s.l. Facies

Dark grey to black muds and clay characterized by the relative abundance of entire unarticulated and broken shells (bivalves and gastropods) in living position. They can show parallel lamination, burrowing, organic matter mottles and carbonized vegetal remains, mostly near the boundary with the intertidal facies, where they form conspicuous levels. In addition to these features, the geochemical and mineralogical composition is more diagnostic. This subfacies is characterized by the presence of gypsum, pyrite, haematite and halite, and, consequently, the highest content in S, Cl and Br. On the average, these sediments show the highest content in TOC. While the transition to the surrounding intertidal facies is gradual for Br, Cl and TOC, the change in content for S is abrupt, providing a sharp boundary. It is remarkable that this is the only subfacies in which molluscs in living position have been found, as well as foraminifera, and ostracods change to assemblages with *Cyprideis torosa* and *Loxoconcha elliptica* (Luque et al., 1999). The preservation of pollen and non-palynomorphs is better at the base and decreases to very low values towards the top. *Glomus* is almost absent, Chenopodiaceae is relatively high and *Isoetes* is present at the bottom but nearly disappears towards the top.

Interpretation: The colour, mineralogical, geochemical and fossil composition of this facies point to deposition on a submerged environment and in oxygen-depleted marine waters (hypoxic conditions). The dominance of muddy sediments is typical of an area only sporadically affected by currents. The presence of charcoal-rich levels near the boundary with the intertidal facies are indicative of episodes of riverine input. These conditions correspond to an environment below the fair-weather wave base level and below the low spring tidal level. Thus, this facies can be interpreted as representative of a fair-weather subtidal environment.

Estuarine-tidal channel Facies

This sequence is composed of layers with an erosive base (concave upwards), interbedded with supratidal and intertidal facies, filled by gravels to sands forming fining-upwards sequences. Mainly siliciclastic

clasts, prevailing on supratidal facies, and bioclastic components that are more frequent on intertidal facies, with increasing matrix content and green tones are found towards the western parts of the basin. Like the fluvial channel facies, these can present internal erosive boundaries, but the sediment sorting and roundness increase towards the intertidal facies. They contain occasionally muddy clasts from the marsh facies and dewatering structures.

Interpretation: Their similarity to the fluvial channel subfacies, position, and increase in hydromorphic features suggest the extension of the fluvial channels into the supratidal and intertidal areas without discarding a tidal origin for some channels filled with finer-grained sediments.

Mixed (fluvial and tidal) current Facies

Centimeter to decimeter thick clastic intervals with erosive base ranging from gravel to fine sand have been encountered embedded in intertidal and subtidal facies. The layers are composed by a mixture of siliciclastic fragments decreasing content from E to W and bioclastic fragments increasing content from E to W. Both facies show decreasing grain size and increasing matrix content from E to W. The siliciclastic grains are rounded to subangular, they are moderate to well-sorted while the bioclastic fraction is poorly to moderately sorted and scarcely rounded (from entire unarticulated shells to broken fragments). The siliciclastic-dominated layers show lower contents in S, Cl, and Br compared with the muddy facies in which they are included or the bioclastic-dominated levels, and pollen grains are poorly preserved.

Interpretation: The clastic nature of the sediments and the flat erosive base relate them to unconfined currents. The reverse relation between the siliciclastic and S, Br and Cl contents are indicative of an origin linked to freshwater inputs from rivers for this sequence, while the invariance of the geochemical marine proxies for the levels dominated by bioclasts points to marine currents as their transport agent. Wave-related currents are discarded as the dimensions of the basin prevent the formation of waves able to have a noticeable action on the bottom and, thus, tidal currents are invoked for their origin. Despite fluvial and tidal currents coincide in time, their record at precise times and the wider extension of the bioclastic fraction point to extraordinary tides (astronomical and storm) and not to ordinary ones. The westward (seaward) fining of the grain size of both fractions reveals the vanishing of the currents in this sense, and the dominance of ebb vs. flood currents.

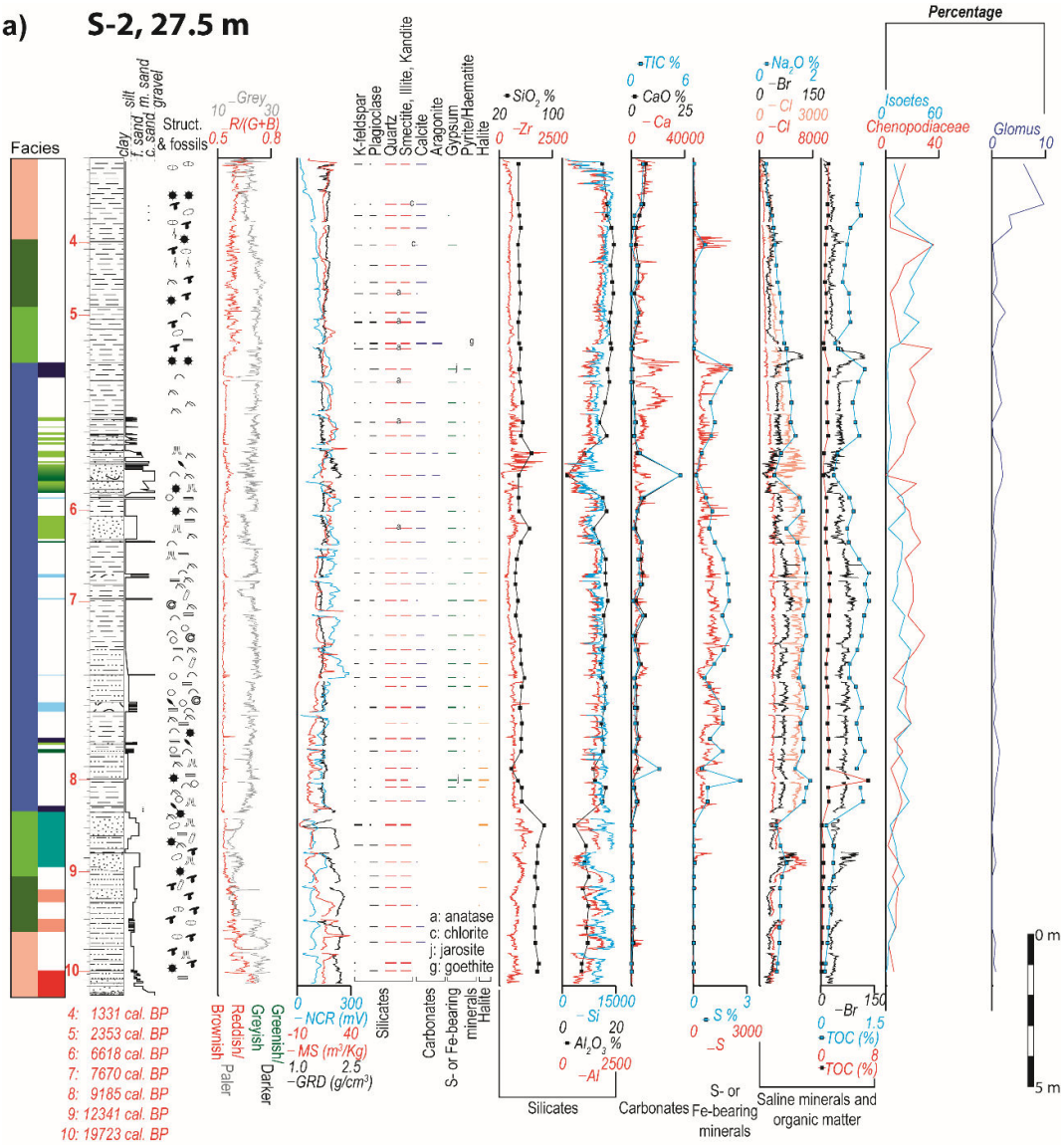
a) S-2, 27.5 m
Facies
clay
silt
f. sand
m. sand
c. sand
gravel
Struct.
& fossils
Grey
R/(G+B)
K-feldspar
Plagioclase
Quartz
Smectite, Illite, Kandite
Calcite
Aragonite
Gypsum
Pyrite/Haematite
Halite
SiO2 %
Zr
TIC %
CaO %
Ca
Na2O %
Br
Cl
Percentage
Isoetes
Chenopodiaceae
Glomus
4: 1331 cal. BP
5: 2353 cal. BP
6: 6618 cal. BP
7: 7670 cal. BP
8: 9185 cal. BP
9: 12341 cal. BP
10: 19723 cal. BP
Brownish
Reddish/
Greyish
Greenish/
Paler
Darker
NCR (mV)
MS (m3/Kg)
GRD (g/cm3)
Silicates
Carbonates
S- or Fe-bearing minerals
Halite
a: anatase
c: chlorite
j: jarosite
g: goethite
Si
Al2O3 %
Al
S %
S
TOC (%)
Silicates
Carbonates
S- or Fe-bearing minerals
Saline minerals and organic matter
0 m
5 m

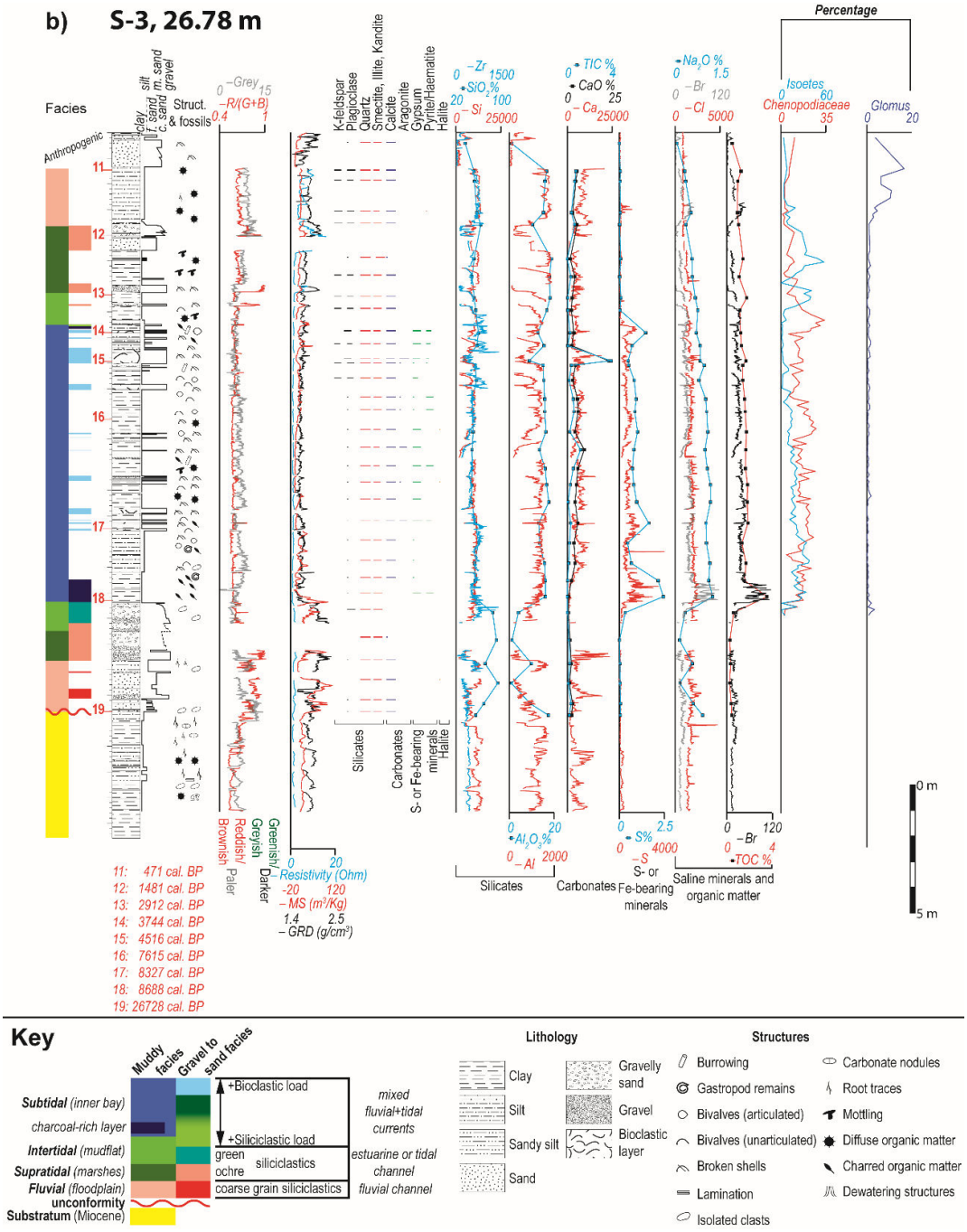
b) S-3, 26.78 m
Facies
Anthropogenic
Struct. & fossils
Grey
R/(G+B)
Reddish/ Brownish
Paler
Greyish/ Greenish
Darker
Resistivity (Ohm)
MS (m³/Kg)
GRD (g/cm²)
K-feldspar
Plagioclase
Quartz
Smectite, Illite, Kandite
Calcite
Aragonite
Gypsum
Pyrite/Haematite
Halite
Silicates
Carbonates
S- or Fe-bearing minerals
Zr
SiO₂ %
Si
Al₂O₃ %
Al
TIC %
CaO %
Ca
S %
S
Na₂O %
Br
Cl
TOC %
Percentage
Isoetes
Chenopodiaceae
Glumus
Saline minerals and organic matter
0 m
5 m
11: 471 cal. BP
12: 1481 cal. BP
13: 2912 cal. BP
14: 3744 cal. BP
15: 4516 cal. BP
16: 7615 cal. BP
17: 8327 cal. BP
18: 8688 cal. BP
19: 26728 cal. BP
Key
Muddy facies
Gravel to sand facies
Subtidal (inner bay)
charcoal-rich layer
Intertidal (mudflat)
Supratidal (marshes)
Fluvial (floodplain)
unconformity
Substratum (Miocene)
+Bioclastic load
+Siliciclastic load
green siliciclastics
ochre siliciclastics
coarse grain siliciclastics
mixed fluvial+tidal currents
estuarine or tidal channel
fluvial channel
Lithology
Clay
Silt
Sandy silt
Sand
Gravelly sand
Gravel
Bioclastic layer
Structures
Burrowing
Gastropod remains
Bivalves (articulated)
Bivalves (unarticulated)
Broken shells
Lamination
Isolated clasts
Carbonate nodules
Root traces
Mottling
Diffuse organic matter
Charred organic matter
Dewatering structures

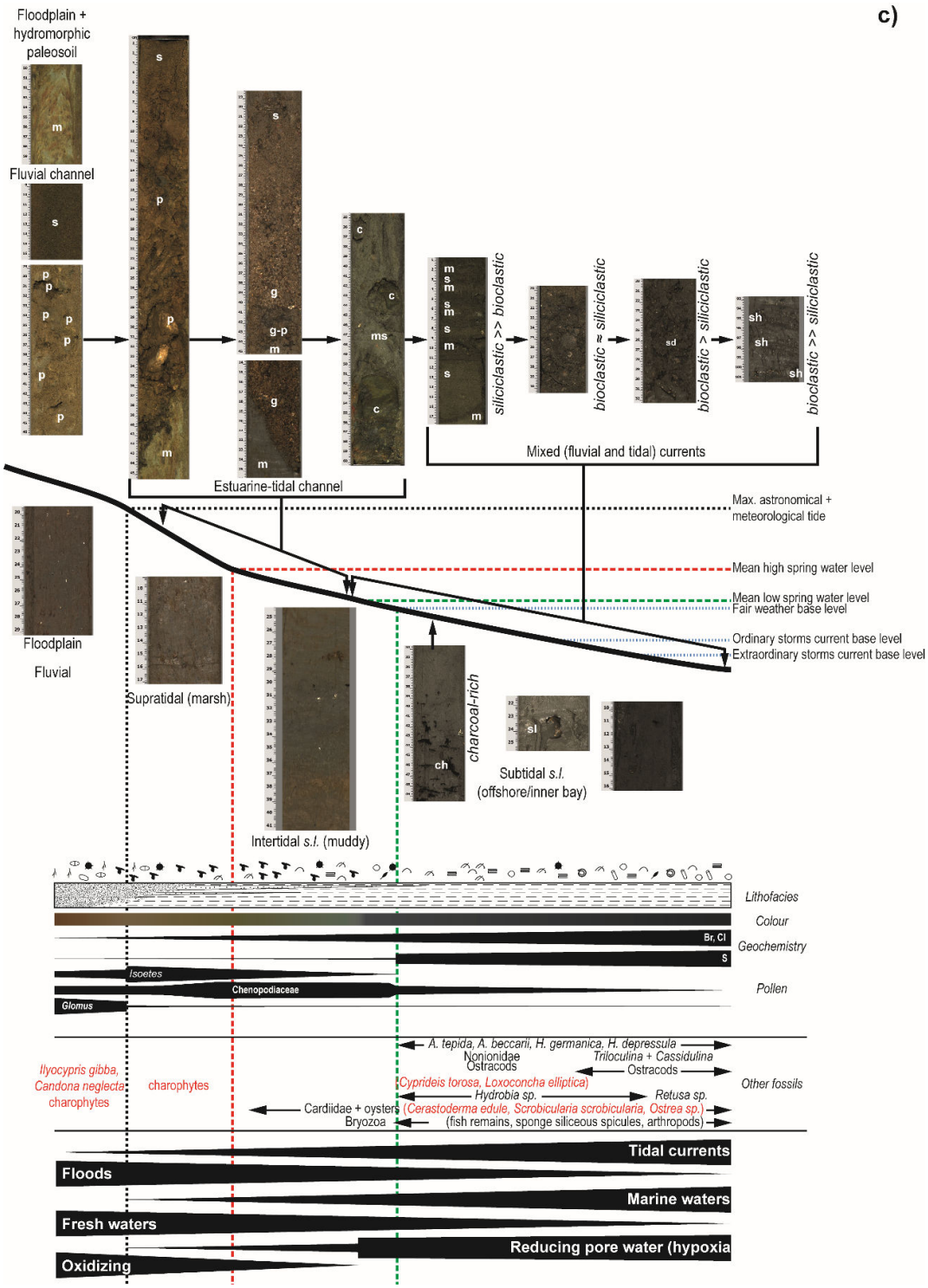

Figure 5.3. Sections for cores (a) S2 and (b) S3 showing selected parameters: facies and subfacies, dated samples (numbers from Table 5.2), lithology, grain size, structures and fossil content, color and geophysical logs (resistivity, magnetic susceptibility [MS], gamma ray density [GRD], non-contact resistivity [NCR]), mineralogy [relative abundance: width of the bars, thickness of the sample: height of the bars], selected oxides and inorganic (TIC) and organic (TOC) carbon (in percentage) and geochemical XRF scan (in counts per second) and selected pollen and non-palynomorph taxa as percentages and concentrations. (c) Sedimentary model and identified subfacies. m: mud,

s: sand, p: pebble, g: granule, c: cobble, sd: shell debris, sh: shells, ch: charcoal, sl: shell in living position.

5.3.3.- Stratigraphic architecture and palaeogeographic evolution

The spatial arrangement and stacking of facies allows to analyse the evolution of the sedimentary system and its main trends in relation with sea level changes (Figs. 4, 5). The oldest deposits are fluvial facies, mainly channelized subfacies indicative of a certain slope, lying on an erosive surface carved in the underlying Miocene deposits of the substratum. These deposits are dated around 27 ka BP in core S3 and ca. 20 ka BP in core S2, where they are encountered around three meters deeper than in core S3. This arrangement points to a staircase disposition of the fluvial facies that is compatible with a sea level drop of near 11 meters in ca. 4 ka, according to the sea level model of Lambeck et al. (2014). These features, coherent with a forced regression, along with the development of a hydromorphic soil on top of the deposits, indicative of later rising sea level conditions, allow us to place allows to interpret the S3 deposits as deposited during a sea level fall in the falling stage systems tract (FSST after Catuneanu et al., 2011; Catuneanu, 2019). While those of core S2 have been accumulated during the beginning of the rise in the lowstand systems tract (LST) (after Catuneanu et al., 2011; Catuneanu, 2019). For this period sedimentation rates were below 1 mm/yr.

The beginning of the transgression (transgressive systems tract, TST) is evidenced by the above mentioned paleosol, marking the transgressive surface (ts), and the development of supratidal facies, ca. 12-17 ka BP in core S2 and ca. 10-11 ka BP in core S3, and intertidal, ca. 10-12 ka BP in core S2 and ca. 8.7-10 ka BP in core S3. The marine water incursion reached the location of core S2 around 10 ka BP, causing the development of hypoxic conditions. The continued sea level rise caused the marine flooding of higher areas (core S3) around 8.7 ka BP. During this transgressive period, in the inner bay areas, only bioclastic ebb current-related deposits are found in cores S2 and S3, but no siliciclastic or mixed deposits (fluvial or tidal current), probably recording the fast landward shifting of the river mouths.

In the meantime, coarse grain deposits accumulated in the supra- and intertidal areas. This can be explained due to a fast sea level rise upon a steep slope of a narrow paleovalley, so channelized facies prevail, and ancient/older fluvial sediments were easily reworked in the coastal areas as the coastline retreated landwards. This is confirmed by the sudden change to fine grain subtidal deposits and low sedimentation rates (≈ 1 mm/yr), implying a fast transgression. During the last stage of the TST to ca. 9 ka BP, sedimentation rates showed a noticeable increase up to 8 mm/yr for core S3, and, 4 mm/yr for core S2, that could be related to more sediment availability and increased accommodation space.

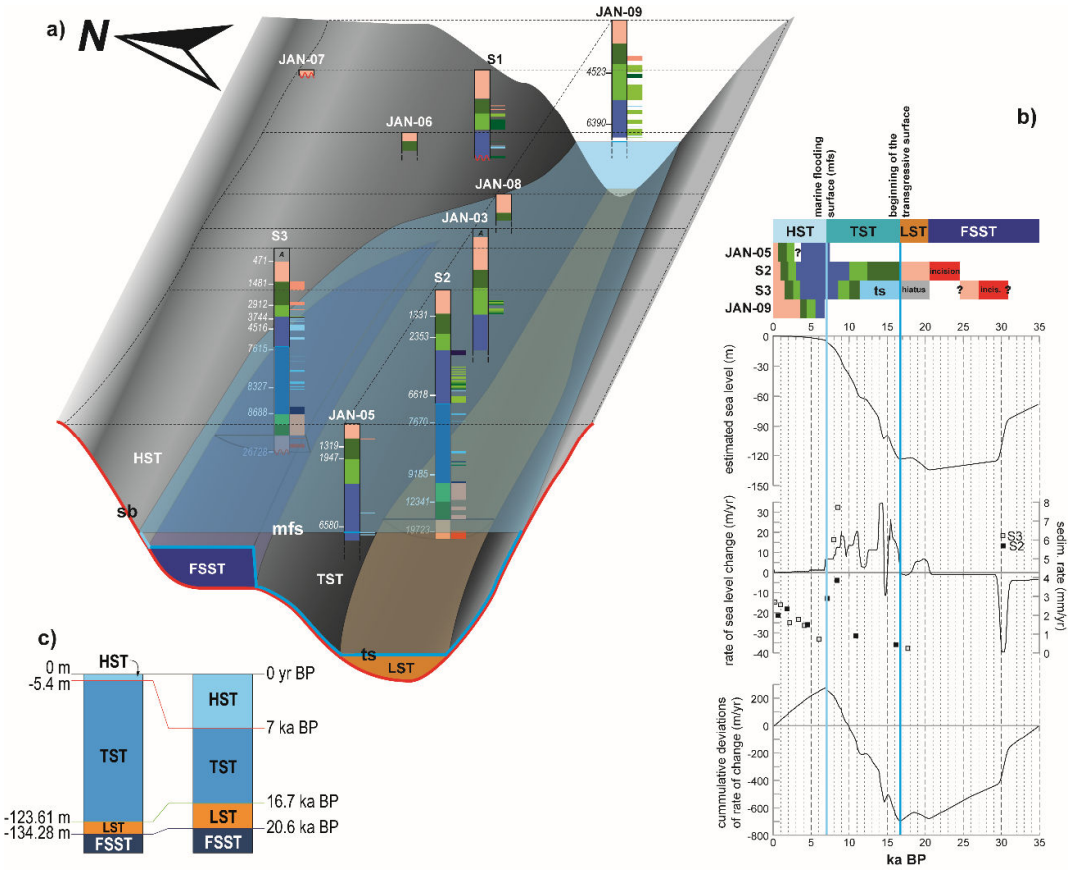

Figure 5.4. (a) 3D correlation panel for the studied cores. Numbers at the right side of the sections are calibrated ages BP. A: anthropogenic deposits, FSST: falling-stage systems tract, LST: lowstand systems tract, TST: transgressive systems tract, HST: highstand systems tract, sb: sequence boundary, ts: transgressive surface, mfs: maximum flooding surface. Facies and subfacies color code like Fig. 5.3 (b) Chronostratigraphic diagram for studied sections and comparison against changes in sea level (after Lambeck et al., 2014) and vertical sedimentation rate; (c) Systems tract boundaries: position relative to present sea level (left) and in time (right).

The marine maximum flooding surface (mfs) is marked by a fall in the sedimentation rate down to c. 1 mm/yr and a change in the stacking pattern from aggradation with retrogradation to progradation that took place around 7 ka BP. After 7 ka BP, sea level rise began to slow down and changes in sedimentation took place. Fluvial or tidal current deposits were more abundant in time and space, except for core S3 where they are absent and ebb current deposits are more frequent. In addition, sedimentation rates increased to 2-3 mm/yr. The change in stacking to a progradational normal regression and the increase of sedimentation rate imply a change in the sedimentation/accommodation rate, in favour of the first, and the beginning of the highstand systems tract (HST).

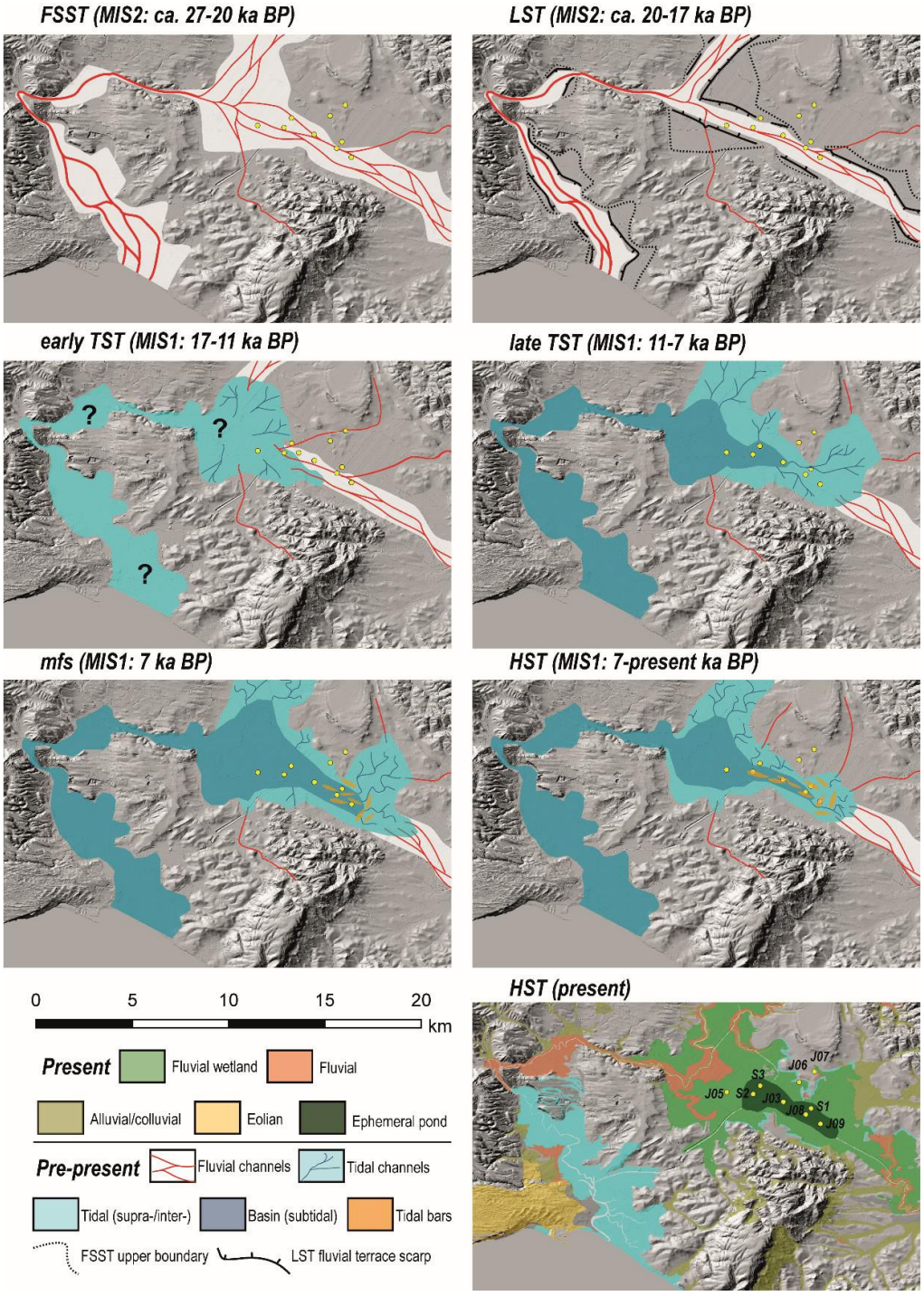

Figure 5.5. Paleogeographic reconstruction for the last 27 ka BP.

The increase in sedimentation rate and decrease of sea level rise caused the advance of coastal and terrestrial systems, near river mouth areas, fluvial or tidal current structures advanced into the estuary of the Almodóvar River (cores JAN-09, S1, JAN-03, S2). On the other hand, the decrease of slope/gradient due to the basin infill promoted the accumulation of finer sediments in comparison to channelized facies and increased the surface affected by tidal currents that were recorded in those areas far from river

mouths (core S3). At the present stage of the HST, the progradation of the terrestrial systems has transformed the area in an episodically ponded fluvial plain (Fig. 5.5).

5.4.- Discussion

In the Gulf of Cádiz, several sedimentological, paleontological and geochemical studies focused on the recent dynamics of its estuaries and their facies (Dabrio, 1982; Borrego et al., 1995, 2004; Ruiz et al., 2004; Morales et al., 2006). However, few of these records are long enough and well-dated as to obtain a reliable correlation among them. In this section, the records of the La Janda wetland of the Almodóvar estuary (this study), the Guadalete and Odiel-Tinto (Dabrio et al., 1999, 2000), the Guadiana (Boski et al., 2008) and the Quarteira (Schneider et al., 2010) estuaries are compared (Fig. 5.6). All the records are found in incised valleys, carved into a Neogene (La Janda, below -23 m.a.s.l., and Odiel-Tinto, -35 m.a.s.l.) or Paleozoic (Guadiana, -51 m.a.s.l.) substratum, and start with a basal fluvial unit.

In the Odiel-Tinto area, this fluvial unit has only been dated in core SN11 as 25-30 ka BP (Dabrio et al., 1999), and this age was assumed for the whole unit for the Guadalete and Guadiana areas (Dabrio et al., 2000; Boski et al., 2008). This single dated interval prevented the identification of any stratigraphic architecture for this unit and, using previous time scales, placed it on Isotopic Stage 3, during a previous highstand (HST) that did not reach present sea level. Consequently, the erosive surface at top of this unit recorded the LST of the last stratigraphic sequence, and it was its boundary (Dabrio et al., 1999, 2000). There are no reliable dates for the fluvial unit at the base of the Quarteira record, but they have been attributed to 7.5-8 ka BP, a pre-transgressive period as they assume that the transgression started at about 7.5 ka BP (Schneider et al., 2010).

In La Janda area, the fluvial unit has provided ages of 27 ka BP (core S3) and 20 ka BP (core S2) and shows a staircase disposition in a riverine environment. New time scales and sea level reconstructions and models (Lisiecki & Raymo, 2005; Lambeck et al., 2014; Spratt & Lisiecki, 2016; Past Interglacials WG PAGES, 2016) place the MIS 3/2 boundary at 29 ka BP and consider that the MIS 3 was not a true highstand (Fig. 5.6a). Recalibrated dates of Odiel-Tinto area are between 29-30 ka BP, and these and La Janda dates encompass the end of a sea level fall period, according to the sea level reconstruction of Lambeck et al. (2014) (Fig. 5.6). Consequently, the fluvial sediments dated between 27 and 30 ka BP and the erosive surface below and the following fluvial deposits accumulated during the FSST (sensu Catuneanu et al., 2011; Catuneanu, 2019) (Fig. 5.6b, c). The La Janda fluvial sediments dated as c. 20 ka BP are affected by a hydromorphic paleosol, piled up at lower topographic positions during the beginning of the last sea level rise, and, therefore represent the LST (sensu Catuneanu et al., 2011; Catuneanu, 2019) (Fig. 5.6b, c). We cannot rule out that part of the undated sediments of the Guadalete, Odiel-Tinto, Guadiana and Quarteira areas could be included in any of these system tracts.

Marine flooding was diachronous and its beginning was recorded at different moments in each estuary. Thus, in the Almodovar estuary (La Janda) the first record is c. 16.7 ka BP, in the Guadalete before 10.5 ka BP, in the Odiel-Tinto around 10 ka BP, in the Quarteira estuary c. 7.5 ka BP and in the Guadiana River around 13 ka BP. From this time on until the maximum marine flooding, ca. 7 ka BP, the sediments show a transgressive pattern that in the open Almodóvar, Quarteira and Guadiana estuaries is recorded by a supratidal, intertidal to estuarine basin or salt marsh to mud flat. The Guadalete estuary was protected by the rocky substratum that bounds the Cádiz Bay and the TST record is composed by fluvio-marine (head bay delta) to estuarine basin, with flood delta deposits (Dabrio et al., 2000) what supports the hypothesis of a confined estuary. The position of the MFS in time and depth is variable among estuaries (La Janda: 7 ka BP, 10.8 to 12.7 m b.s.; Guadalete: 6.5 ka BP, 10.5 m b.s.; Odiel-Tinto: 6.5 ka BP, 14.3 m b.s.; Guadiana: 7.5 ka BP, 9.4 m b.s.; Quarteira: 6.7 ka BP, 6.0 m.b.s.) accordingly to the different studies. And the position of the arbitrary 7 ka BP reference level, at 10.8-12.7 m b.s. (La Janda), 13.3 m b.s. (Guadalete), 17.0 m b.s. (Odiel-Tinto), 9.0 m b.s. (Guadiana), and 6.9 m b.s. (Quarteira), point to tectonic activity modifying these records.

After 7 ka BP, the rate of sea level rise slows down (HST) and this is invoked as the trigger of the development of barrier islands (Freitas et al., 2003). The barrier island systems developed in the Guadalete estuary until ca. 3 ka BP, when they change to spit systems and the intertidal and supratidal deposits that appear in the record around 4 ka BP. In the Guadiana estuary, the barrier island systems established at marine positions (5640-6250 yrs BP, Boski et al., 2002) while upstream intertidal systems evolving to salt marshes filled the valley. In the Odiel-Tinto estuary, the HST was composed of central basin and sand shoals evolving to tidal flats. This was an open estuary that began to close around 3 ka BP as the present spit systems started to grow.

The HST of the open estuaries of Quarteira and Almodóvar (La Janda) are very similar, and they record the infill of the estuarine basin. In Quarteira, tidal channels and tidal flats developed until ca. 4.1 ka BP, when the sea influence clearly vanished and salt marshes changed into fluvial floodplains prevailed. In the Almodóvar estuary (La Janda), the inner bay and mixed current deposits were gradually substituted by intertidal, supratidal and fluvial floodplain that were episodically ponded. The clogging of the estuaries can be better explained by the destruction of accommodation space by infilling, whereas the formation of the spit systems played a minor control. In all examples the fluvial systems advance on the estuarine areas, but the present stage of this displacement is variable.

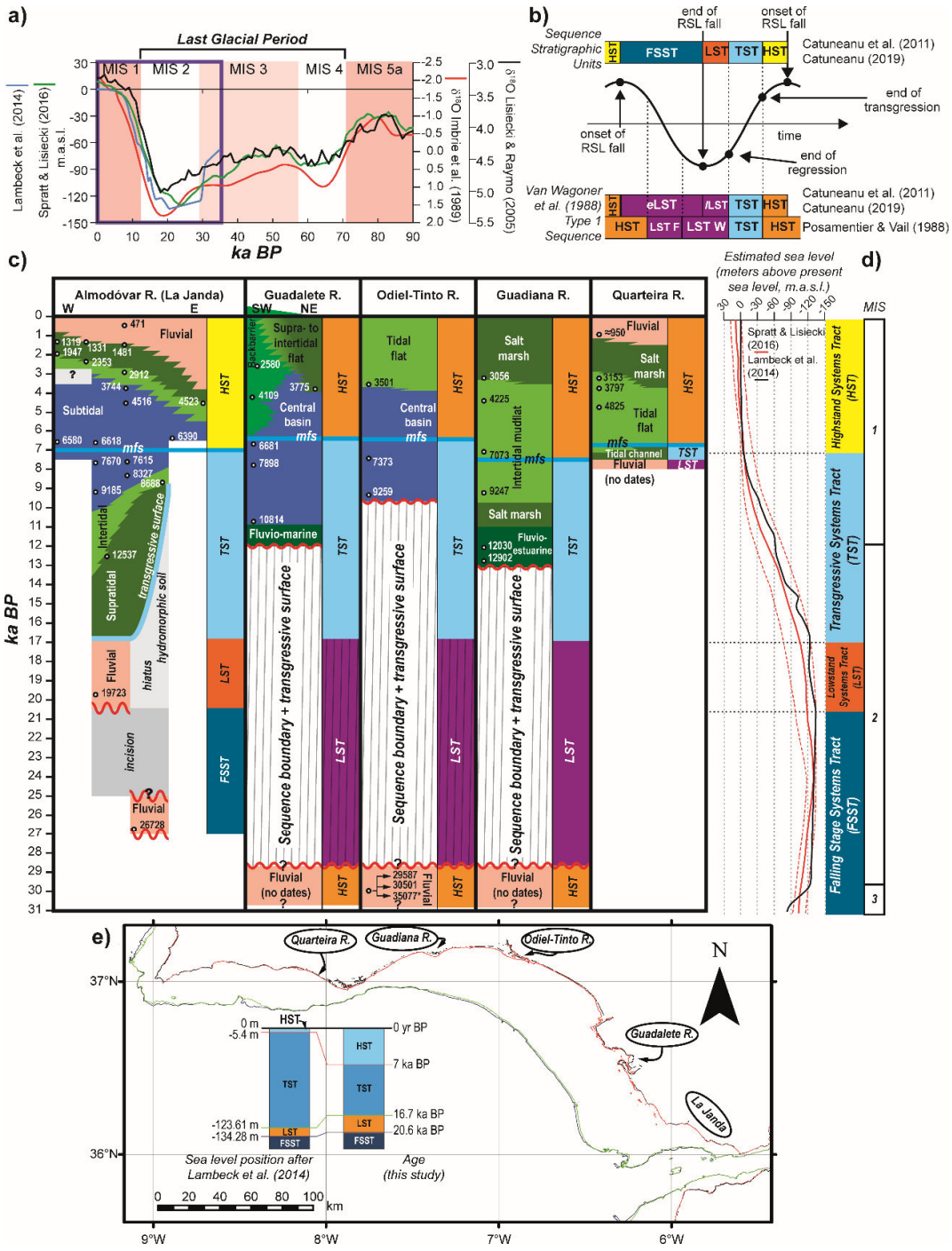

Figure 5.6. (a) Chronological placement of the studied period (purple square), sea level curves (Lambeck et al., 2014; Spratt & Lisiecki, 2016) and oxygen isotope reference curves (SPECMAP: Imbrie et al., 1989; LR04: Lisiecki & Raymo (2005). Marine Isotope Stages (MIS) after Lisiecki & Raymo (2005) except for the MIS 2/1 boundary that has been placed in the more accepted value of 11.7 ka BP. (b) Conceptual model relating Van Wagoner et al. (1988) type 1 sequence systems tracts (after Posamentier & Vail, 1988, and Catuneanu et al., 2011, 2019) and Catuneanu et al. (2011) systems tracts. FSST: falling stage systems tract, LST: lowstand systems tract, eLST: early LST, LST F: LST fan, lLST: late LST, LST W: LST wedge, TST: transgressive systems tract, HST: highstand systems tract. (c) Comparison of the Late Pleistocene-Holocene record of five estuarine areas in SW Iberian

Peninsula: La Janda (this work), Guadalete River (Dabrio et al., 2000), Odiel-Tinto rivers (Dabrio et al., 2000), Guadiana River (Boski et al., 2008), Quarteira River (Schneider et al., 2010). All the dates have been recalibrated by using IntCal20 and Marine20 curves (the date marked with an * should be discarded as it can be reworked, but it has been included because the original authors did it). (d) Proposal of stratigraphic architecture for the Gulf of Cádiz: sea level data from Lambeck et al. (2014) model and Spratt & Lisiecki (2016) reconstruction, systems tracts, and MIS. (e) Location of the compared estuaries and the inferred position of the coastline for the end of each systems tract. Bathymetric data from EMODNET (EMODNET, 2020).

5.5.- Conclusion

The use of a multiproxy approach combining sedimentological, geochemical, palynological and paleontological data to the sedimentary record of the last 26,000 years of La Janda wetland enables a detailed characterization of facies by the interpretation of the complementary proxies. Using a robust age-depth model and a 3D reconstruction of the stratigraphic architecture of the deposits, we conclude that these sediments record the infill of an incised valley carved during the last sea level fall. As a peculiarity, the location of the system inside a restricted valley, bounded by rocky hills, and with a narrow connection to the open sea caused that the dynamics of the environment was conditioned by the topography, slope gradient, erosion rates and by the basin infill.

The sediments correspond to the FSST (older than 20.6 ka BP) and LST (16.7 to 20.6 ka BP), and are identified for the first time in this area of the Gulf of Cádiz, correspond to encased high gradient fluvial systems flowing through narrow valleys carved during this lapse. The scarcity of dates for these sediments in other areas around the Gulf of Cádiz prevents the clear identification of the system tracts in a sequence stratigraphic interpretation as previous studies placed them in the MIS 3, and assumed a highstand, which led to the interpretation as belonging to an older sequence (Fig. 5.6).

Around the Gulf of Cádiz, the evolution of the TST and HST was controlled by the morphology of the estuaries (open, Odiel-Tinto, narrow at its mouth, Guadiana, narrow during the whole valley, Quarteira), the rocky substratum that protects the estuaries from the sea action (Guadalete and Almodóvar), and tectonic activity, as the main reference levels (i.e., maximum marine flooding surface) are found today at different depths among estuaries. These differences can be observed in the regressive and transgressive stages, but they are more noticeable in the latter.

During the TST (16.7 to 7 ka BP), all estuaries experienced a fast deepening from supratidal to estuarine basin environments and the widening of the valleys. The maximum extent of the marine flooding was reached around the Gulf of Cádiz at c. 7 ka BP. After that, the sea level rise rate slowed down in addition to a widening of the paleovalleys and decreasing slopes by erosion and infilling of the basin, which promoted the normal regression of the HST sediments (7 ka BP to present). The period is characterized

by a marine basin and estuarine conditions dominated by tides. During final stages of the HST, the basin was occupied by a ponded fluvial floodplain that constitutes present landscape for the Quarteira and Almodóvar estuaries while tidal flats and salt marshes developed in the Guadalete, Odiel-Tinto and Guadiana estuaries.

As a conclusion, the analysed incised valleys of the Campo de Gibraltar region developed under the identical climate and sea level conditions. Therefore, their differences must be linked to allocyclic controls, mainly basin morphology and composition that, in turn, control the estuarine hydrodynamics (waves, tidal currents and fluvial supplies) and the amount of sediment available from marine sources, and active tectonics. A better knowledge of the reaction of these systems under such climatic and tectonic variability is a key to evaluate their future evolution under the changing climate scenarios.

5.6.- Acknowledgements

The authors are grateful to the "Centro Nacional IGME, CSIC" for the analytical facilities provided for this study. We are also in debt to the colleagues from the U. Köln and RWTH-Aachen for all the support in the field. This research was funded by the Deutsche Forschungsgemeinschaft (DFG project no.57444011 – SFB 806) and a "Severo Ochoa" extraordinary grant for excellence IGME-CSIC (AECEX2021). The authors are grateful to the CEOs, managers and personnel of "Las Lomas" farm for all their help during the drilling and in the accurate positioning of the drilling points.

6.- Tracing the environmental evolution of coastal ecosystems through Holocene vegetation dynamics in SW Iberia

This chapter is a slightly modified version of a manuscript that will be submitted to Quaternary Science Reviews:

Val-Peón, C., López-Sáez, J.A., Santisteban, J.I., Mediavilla, R., Reicherter, K. Tracing the environmental evolution of coastal ecosystems through Holocene vegetation dynamics in SW Iberia.

Abstract

A new palynological record obtained from La Janda basin (SW Iberia) is presented together with other sedimentological, chronological and geochemical data. This sequence provides new insights into the palaeoenvironmental evolution of the study area throughout the Holocene. Its correlation with other continental cores from SW Iberia allowed to define diverse phases attending to vegetal dynamics: a period of forest development with regional peculiarities between ~11.7-7.7 ka cal BP; a gradual decrease of regional forests ~7.7-5.5 ka cal BP; a shift towards a drier climatic regime in a context of increased anthropogenic pressure ~5.5-3.7 ka cal BP; a combination of arid conditions and anthropogenic impact between ~3.7-1.2 ka cal BP; and the development of cultural landscapes from ~1.2 ka cal BP on. The effects of millennial-scale climate variability in the vegetation allowed to define phases of increased aridity at 8.2, 7.7-7.5, 5.9-5.5, and 4.2 ka cal BP, some of them recorded in other continental sequences of SW Iberia. Deciphering the interplay of diverse factors (climatic, geological, human, etc.) at different scales (global, regional, local) is key to understanding the complexity of transitional environments and their evolution over time, but also to protect them as biodiversity hotspots.

Keywords: Transitional environments, SW Iberia, Long-term trends, Abrupt climate events, Anthropogenic impact, Palaeoenvironmental evolution

6.1.- Introduction

Coastal areas include a heterogeneity of ecotones between terrestrial, freshwater, and marine ecosystems that fall under the definition of transitional waters systems, e.g., lagoons, marshes, coastal ponds, wetlands, etc. (Basset et al., 2006). These habitats have always been poles of attraction for human populations, providing natural resources and recreational areas; but they not only have substantial socioeconomic and historical value, as they are also important hotspots for vegetal diversity (Newton et al., 2013). In the last decades, the study of coastal ecosystems has demonstrated their importance as blue carbon sinks (Lovelock and Duarte, 2019). Thus, their conservation may contribute, among other things, to mitigate and adapt to climate change (Serrano et al., 2019).

In this sense, the coastline of the Gulf of Cádiz (SW Iberia) is considered an area of great ecological value as reservoir of biodiversity, including diverse sedimentary environments and geomorphological features (Dabrio et al., 2000; Zazo et al., 2008; Carrión et al., 2010; López-Sáez et al., 2018). The evolution of their coastal ecosystems throughout the Holocene has been, and it is, linked to a number of global, regional and local drivers. The post-glacial marine transgression during the Late Pleistocene-Early Holocene transition was one of the main controlling factors that shaped littoral landscapes, resulting in the development of estuaries, lagoons, coastal wetlands, etc. (Dabrio et al., 2000; Teixeira et al., 2005; Boski et al., 2008; Zazo et al., 2008; Schneider et al., 2010; Delgado et al., 2012; Trog et al., 2013; Rodríguez-Ramírez et al., 2014). Regional and local elements affecting depositional processes (e.g., marine currents or river streams) have also contributed to the displacement of sediment, leading to the formation of closed or semi-enclosed coastal systems (Dabrio et al., 2000; Lario et al., 2002). Additionally, regional and local tectonic movements have been an important element modulating the effect of relative sea level and the sediment supply during uplift or subsidence periods (Mediavilla et al., 2023). Environmental disturbances derived from human activities, such as changes in the land-use, soil erosion, etc., have also had an increasing impact over time (Newton et al., 2020).

The complex interplay of climatic, marine, tectonic and anthropogenic elements contributes to the characterisation of coastal ecosystems as complex areas with a high temporal variability and spatial heterogeneity (Basset et al., 2006). Considering the sensitivity of the vegetation to these same factors, its study from a long-term perspective may provide insights on the environmental evolution of these ecosystems, its driving mechanisms, and dynamics (Birks and Birks, 1980; Dincauze, 2000). Thus, palynological analyses are an excellent tool that may contribute with crucial data on long and short-term processes affecting coastal ecosystems in the past, but may also lay the foundations for future ecological research and models (Fægri and Iversen, 1951; Moore et al., 1991; Cheng et al., 2021). But tracing the history of transitional environments through their vegetation from a diachronic perspective requires continuous stratigraphic sequences. Although there are very well studied deposits that have reported

high-resolution information of past environments in SW Iberia, such as the Doñana marshlands (Jiménez-Moreno et al., 2015; López-Sáez et al., 2018; Manzano et al., 2018), sedimentological discontinuities resulting in the lack of a good chronological frame are a problem to deal with. In some instances, problems are related to bad palynological preservation, as in the hypersaline lake of Laguna Salada (Schröder et al., 2018) or in some cores from the Guadiana estuary (Fletcher, 2005).

As a means to contribute to this discussion with new data, we present the palaeoenvironmental results (palynological, sedimentological, geochemical) of a sediment sequence drilled in La Janda basin, an area that has undergone multiple environmental changes by cause of both natural and anthropogenic factors over the Holocene. The main objectives of this research are: i) to reconstruct the vegetation history of La Janda basin during the Holocene; ii) to infer the environmental evolution based on the presence of diverse vegetal communities; iii) to understand the vegetation dynamics in the area and deduce the causes of their changes; iv) to correlate our results with other continental sequences of SW Iberia for better defining palaeoenvironmental transformations at a regional level.

6.2.- Regional setting

La Janda basin is located at the southwestern Atlantic margin of the Iberian Peninsula, in the eastern part of the Gulf of Cádiz and near the Strait of Gibraltar (Fig 6.1). It is placed in a tectonic graben of about 35 km^2 and 10 km from the current coastline, with its lowest point at 3 m asl and the highest in surrounding areas above 400 m asl (Mediavilla et al., 2023). The origin of the depression relates to the two faults (NW-SE and NE-SW direction) that release the efforts of N-S tectonic compression produced by the Iberian and African plates movement (Goy et al., 1995; Luque et al., 2001). Present day basin is drained by the Barbate River and its tributaries, Almodóvar and Celemín rivers, being heavily disturbed by farming activities (Mediavilla et al., 2023). The Barbate River crosses the basin and runs to the sea through a narrow gorge flowing into a marsh complex with a tidal range of near 2 m (Instituto Hidrográfico de la Marina, 2019). During the last centuries, La Janda lagoon was desiccated for agricultural purposes and only during periods of heavy rainfall it is flooded by the water from the Barbate and Almodóvar rivers (Castro Román et al., 2000; Dueñas and Recio Espejo, 2000; Castro Román and Recio Espejo, 2007).

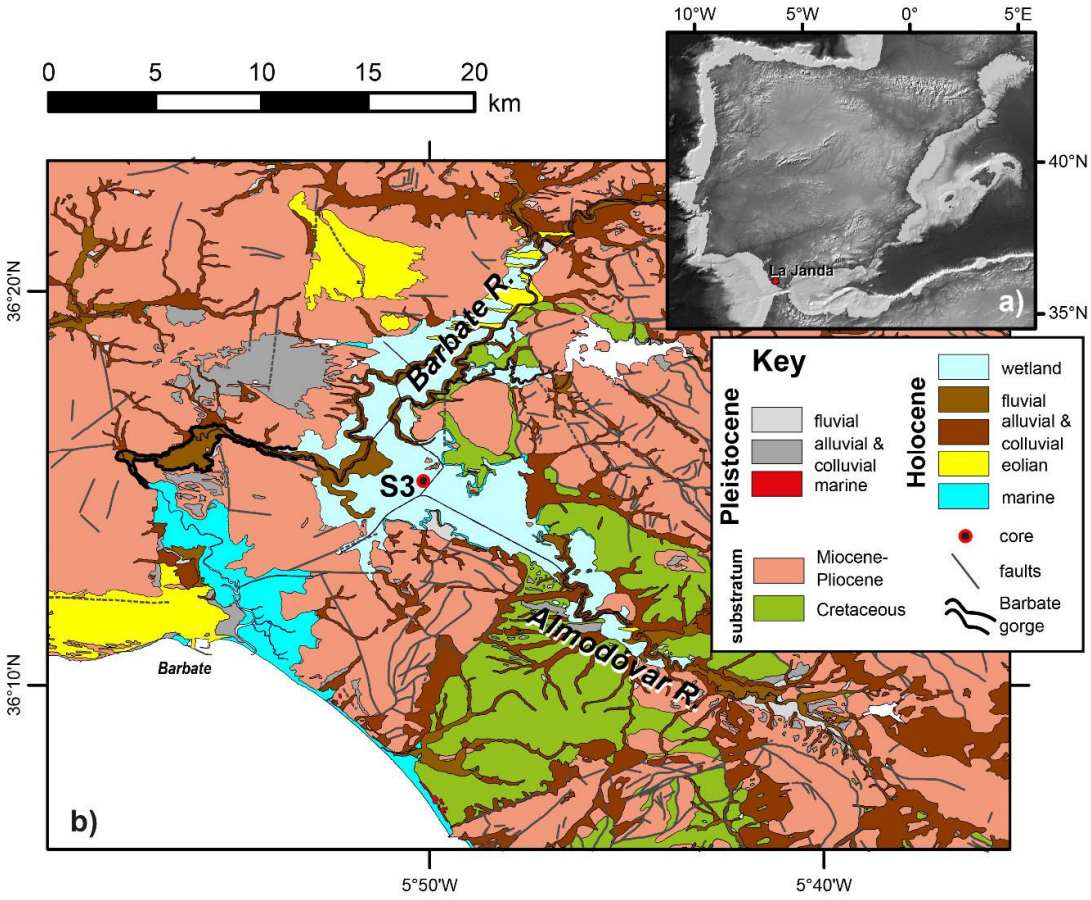

Figure 6.1. (a) Location of the study area in the Iberian Peninsula; (b) Geological map of La Janda basin and borders, simplified from the Continuous Geological Map of Spain 1:50.000 (GEODE). Geographical data provided by the Spanish Geographical Institute (IGN) and the geological map by the Instituto Geológico y Minero de España, CSIC (Roldán et al., 2021). Adapted from Mediavilla et al. (2023).

La Janda is located in a region with Mediterranean climate type Csa, defined by mild winters and hot and dry summers (Kottek et al, 2006). Mean annual temperature is 20ºC, with average minimum temperatures of 5.3ºC in January and average maximum temperatures of 33.1ºC in July and August (period 1971-2000; AEMET, 2011). Mean annual precipitation averages between 600-800 mm and concentrates in autumn and winter (period 1971-2000; AEMET, 2011). A diversity of plant communities can be found in the study area (chapter 4), with rich oak formations of *Quercus suber, Q. faginea,* and *Q. rotundifolia* at different altitudes of the natural park of Los Alcornocales (Latorre et al., 1996). They may be accompanied by other trees such as *Sorbus torminalis* or *Acer monspessulanum* with an understorey composed of *Arbutus unedo, Calluna, Viburnum, or Rhamnus* among others (Domínguez et al., 1993; Latorre et al., 1996; Rivas-Martínez et al., 1997; Latorre and Cabezudo, 2003). Thermo-Mediterranean communities of *Olea europaea* and *Quercus ilex* grow in lower areas together with tickets such as *Q. coccifera, Pistacia lentiscus, Myrtus communis, Rhamnus oleoides, Asparagus albus* and *Chamaerops umilis* (Domínguez et al., 1993; Gutiérrez et al., 1996;

Latorre et al., 1996; Rivas-Martinez et al., 1997). At the slopes of the mountains or in depressions with groundwater permanence, hygrophilous shrubby heaths (*Erica ciliaris*, *Calluna vulgaris*, *Ulex minor*, etc.) develop in humid areas (Espírito-Santo et al., 2017). However, heathlands may also thrive in zones under natural or anthropogenic disturbance (Loidi et al., 2007). Riparian elements such as *Salix* grow in high, middle or low watercourses, although they may also appear as a stage of degradation replacing other riparian forests. *Fraxinus angustifolia* prefers the banks of low flow streams, and *Alnus* is the main component of dense alluvial forests that needs high edaphic and atmospheric humidity (Domínguez et al., 1993; Latorre et al., 1996). In stabilised dunes and sandbanks the vegetation is dominated by *Pinus pinea*, but also *P. pinaster* and *P. halepensis*, that may be accompanied by xerophytic shrubby communities (*Juniperus phoenicea, J. oxycedrus, Pistacia lentiscus, Daphne gnidium,* etc.). Typical vegetation of lakes, coastal wetlands, and marshes are present in the natural parks of La Breña y Marismas del Barbate and El Estrecho. Some of these vegetal communities are still identifiable in certain zones of La Janda during its periodic floodings. Temporary pools and ponds are usually flooded during the winter and spring. Plant communities vary according to the substrate and the drying cycle, but some of the most representative are macrophyte groups of *Myriophyllum*, *Ranunculus*, *Potamogeton*, *Callitriche* and *Isoetes* (Domínguez et al., 1993; Cirujano et al., 2014). Water channels within the marshes are usually covered by Cyperaceae (*Scirpus maritimus*, *S. lacustris*) and annual pioneer plants, mainly Chenopodiaceae (*Salicornia*, *Sarcocornia*, *Frankenia*, etc.), that dominate in temporary pools of brackish or saline water, the edges of lagoons, the open spaces of coastal marshes, and areas affected by tides (Domínguez et al., 1993; Latorre et al., 1996; Galán de Mera et al., 1997; Rivas-Martinez et al., 1997).

6.3.- Methods

In 2016 and 2017 twelve cores were drilled in two coring campaigns by triple barrel system (cores S1, S2 and S3) and a portable Ejkelkamp vibracoring system (cores named JAN) (Mediavilla et al., 2023). The following methods were applied to all the cores in order to reconstruct the evolution of La Janda basin within a chronological framework provided by an age-depth model, in which the core S3 is included together with the other sequences. Mediavilla et al. (2023) provides a more detailed data on the methods and results for all cores, while the present work focuses on the S3 core.

6.3.1.- Sediment coring

In 2017 the S3 core (36º15'09.68" N, 5º50'08.52" W) of 26.78 m-long was recovered from La Janda basin by triple barrel system. It was drilled at 5.59 m asl and encased in PVC pipes and stored at the Geological and Mining Institute of Spain (IGME) facilities, where it was later divided in two halves (one for study, one as archive), described and photographed.

6.3.2.- Mineralogical and geochemincal analysis

Several non-destructive analyses were run on all the cores using a GEOTEK Multi-Sensor Core Logger (MSCL-GEOTEK) to track their semi-quantitative chemical element variations and geophysical properties: core colour scan, P-wave velocity, gamma density, non-contact resistivity, magnetic susceptibility and X-Ray. XRF spectra were processed with bAxil and element intensities are represented in counts per second (cps). Destructive samples were carried out in cores S2 and S3 to characterize and correlate their sedimentary facies: major oxides and trace elements by X-ray fluorescence and atomic absorption spectroscopy (XRF and AAS), C (organic, inorganic and total) and S by elemental analyser (ELTRA) and mineralogical analysis by X-ray diffractometry (PTE-RX-04).

6.3.3.- Dating and age model

An age-depth model in which the core S3 is included was calculated based on a total of 25 samples collected from four cores that were 14C-dated (Beta Analytic Inc., USA and Keck Carbon Cycle AMS Facility at UC Irvine, USA) (Mediavilla et al., 2023). Ten of these 25 samples were collected from core S3 (Table 6.1). Calibration was performed with CALIB 8.2 (Stuiver et al., 2021) using the IntCal20 and Marine20 calibration datasets (Reimer et al., 2020; Heaton et al., 2020) and different reservoir effect values (Table 6.1). These reservoir effects/values have been recalculated based on the literature (Soares and Dias, 2006; Soares and Martins, 2010; Martins and Soares, 2013) and using the web application of Reimer and Reimer (2017) following the methodology of Soulet (2015). Due to the peculiar setting of the sediments (in a restricted and shallow environment) several calibration sets were developed to check which calibration curve and reservoir effect values (if applied) were the best. Bchron (Haslett and Parnell, 2008), clam (Blaauw, 2022), rbacon (Blaauw and Christen, 2011), rcarbon (Crema and Bevan, 2021) and a simple lineal interpolation were used to build a reliable age-model.

Table 6.1. Radiocarbon data and calibration results for core S3 samples, following the correlative numbers of the complete set of dates from all the cores that can be consulted in Mediavilla et al. (2023). The reworked material from one sample led us to reject it for the age-depth model.

Lab code	Number	Sample	Depth in core (m)	^{14}C	error	$\delta^{13}C$	ΔR	error	Cal. BP 2σ median [range]	Material	Curve
Beta-526017	**8**	JAN-S3-2	1.46	400	30	-25.8	-	-	471 [428,512]	Charcoal	IntCal20
Beta-618144	**9**	JAN-S3-3	4.04	1620	30	-23.2	-	-	1481 [1409, 1544]	Organic matter	IntCal20
Beta-618145	**rejected**	JAN-S3-4	5.75	2880	30	-26.1	-	-	3008 [2921, 3078]	Organic matter	IntCal20
Beta-526108	**10**	JAN-S3-5	6.33	2810	30	-25.9	-	-	2912 [2846, 2998]	Charcoal	IntCal20
UCIAMS-259331	**11**	JAN-S3-6	7.81	4115	15	-5.5	200	426	3744 [2702, 4833]	Shell	Marine 20
Beta-526109	**12**	JAN-S3-7	8.94	4570	30	-1.6	50	152	4516 [4076, 4925]	Shell	Marine 20
Beta-526110	**13**	JAN-S3-8	11.23	6760	30	-22.9	-	-	7615 [7574, 7668]	Organic matter	IntCal20
UCIAMS-259332	**14**	JAN-S3-9	15.51	8040	20	-2.1	17	183	8327 [7911, 8816]	Shell	Marine 20
Beta-526111	**15**	JAN-S3-10	18.3	7890	30	-26.4	-	-	8668 [8593, 8779]	Vegetal remain	IntCal20
Beta-540083	**16**	JAN-S3-11	22.64	22400	90	-26.5	-	-	26.728 [26405, 27006]	Organic matter	IntCal20

6.3.4.- Palynology

With the aim of obtaining a representative sampling of all the sections, 160 samples were collected from the core S3 maintaining a regular interval of 10 cm. Sediment samples, of about 10gr each, were kept in plastic bags and stored in a fridge at 4ºC. All samples were processed at the Institute of Neotectonics and Natural Hazards – RWTH Aachen University (Aachen, Germany). They were chemically treated with HCl (10%) to remove carbonates, KOH (10%) to remove humic acids, and Sodium Polytungstate (SPT: 3Na2WO4·9WO3·H2O) at 2.0-2.1 gr/cm^3 for densimetric separation. The final residue was mounted on slides with the use of glycerol. Pollen concentrations (grains/gr) were estimated by adding two *Lycopodium clavatum* tablets to each sample (Stockmarr, 1971). Palynomorphs were counted using an optical microscope at 400x and 1000x to a minimum pollen sum of 300 terrestrial pollen grains and they were identified using published keys (van Geel, 1978, 2001; van Geel et al., 1980, 1986, 1986, 2003; Moore et al., 1991; Reille, 1992, 1995). Some species such as those corresponding to the genera *Pinus* and *Quercus* were discriminated based on morphometric studies following Carrión et al. (2000a, 2000b). Poaceae ≥45µm was classified as Cerealia type according to López-Sáez and López-Merino (2005). Terrestrial pollen sum (TPS) excluded aquatic pollen types, which were included in the total sum (TS) together with Non-Pollen Palynomorphs. Palynological diagrams were plotted against age and depth using TiliaIT software (version 2.1.1, Illinois State Museum, Research and Collection Center, Springfield USA).

6.4.- Results

6.4.1.- Age-depth model

One sample was discarded due to possible reworked material and, after it, a simple lineal model was applied and used to correlate different proxies among cores (Fig 6.2). Despite their similarity, age-depth models for the different cores cannot be combined in a single one as differences in sedimentation rates caused artefacts that result in unrealistic correlations. However, cores S2 and S3 could be well correlated (Mediavilla et al., 2023). The S3 core begins with low sedimentation rates during the Late Pleistocene, followed by an interruption and a posterior gradual increase in sedimentation rate at the end of this period. The Holocene record starts with high sedimentation rates until ca. 7 ka cal BP, when the sedimentation rate decreases. Despite the noticeable decrease in sedimentation rate for the last 7 ka, in comparison to the 9 to 7 ka cal BP period, is worth to notice that sedimentation rates increased slowly until present.

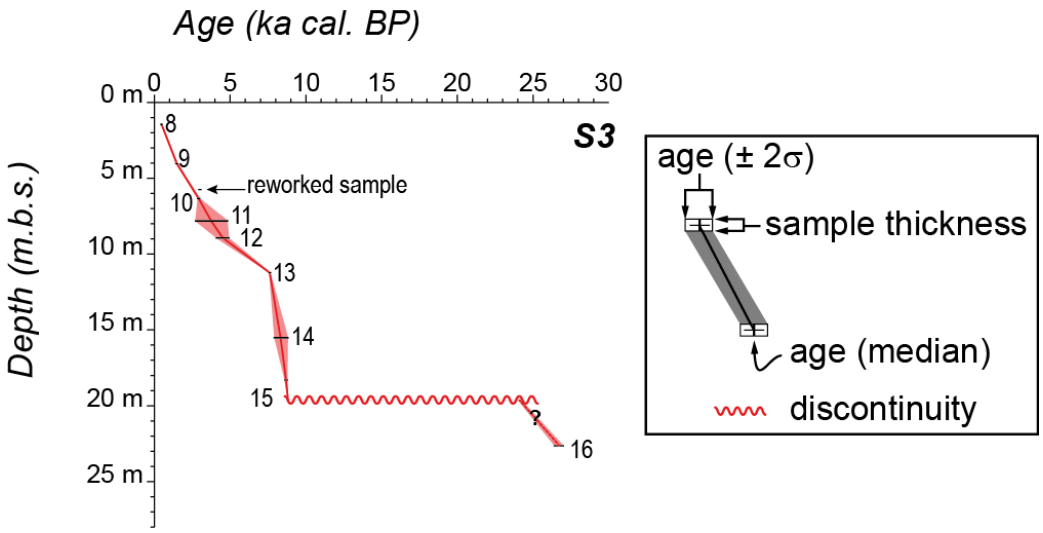

Figure 6.2. Age-depth model for core S3. Sample numbers correspond to those of Table 6.1.

6.4.2.- Facies analysis

Facies have been characterized by visual description as well as by their geophysical properties, geochemical and mineralogical composition, and microfossil analyses. Based on that, five facies have been identified:

- Fluvial wetland facies: brown to ochre muds with some sand layers. They show mottling, traces of roots, nodules and carbonaceous remains, as well as some scattered clasts. They contain freshwater ostracods and Characeae.

- Supratidal facies: brown to green muds with some levels of yellow sands and grey gravels forming grain-decreasing sequences. Traces of roots, hydromorphic features and flecks of organic matter are frequent. There are fragments of bivalves.

- Intertidal facies: green muds, sometimes laminated, with some levels of sands or gravels (siliciclastic or mixed with bioclasts). Broken or disarticulated bivalves are frequent, as well as mottled sediment due to iron oxides or organic matter. Bioturbation and fluid leakage may be present. These facies show a slight increase in Cl and Br content and evidence of halite.

- Subtidal facies: dark grey to black muds with bivalves in living position and disarticulated or broken shells. Sediments are laminated, bioturbated and have coarse-grained intercalations (mainly bioclastic). Gypsum-pyrite, hematite and halite are present. There are high contents of S, Cl, Br, and organic C. These facies contain marine foraminifera and marine ostracods.

6.4.3.- Palynology

Of the 160 samples collected from the core S3, those from ca. 23 m to the bottom belong to pre-Quaternary chronologies, while those between ca. 19 and 23 m were found to be palynologicaly sterile. Therefore, a total of 132 samples resulted valid to include in the present study. Twelve pollen zones were identified in core S3, which showed a diverse and taxonomically rich palynological content, although with poor preservation of pollen grains in most of the samples (Fig. 6.3). Results are synthesised in Table 6.2.

Table 6.2. Pollen zone description for the S3 core with their associated depths and chronologies.

Zone	Depth range (cm)	Age range (cal yr BP)	Pollen signature
JAN-S3-A1	1886-1840	8761-8701	Dominance of A. Cichorioideae (50-66,8%), Poaceae (13,5-26,9%) and A. Asteroideae (4-17,5%). Chenopodium (1,1-12,9%) and *Isoetes* (1-21,3%) display irregular values. Filicales triletes undiff.(6,3-17,7%) and *Phaeoceros* (3,1-10,1%) mark their maximumm. Peak of *Glomus* (0,5-3,4%).
JAN-S3-B1	1840-1454	8701-8166	Drop of A. Cichorioideae (0,3-10,3%) and Poaceae (3,3-17,9%). Increase of *Erica* type (13,5-34,3%) and oak forest development: deciduous *Quercus* (3,3-16,5%); *Quercus suber* (0,9-5,7%); evergreen *Quercus* (2,6-9,3%). Increment of *Olea* (0,3-5,6%), *Alnus* (0,3-5%), *Arbutus unedo* (0,6-3,4%) and Fabaceae undiff (0,9-3,3%). Rise of Chenopodiaceae (4,3-25,4%) and *Isoetes* (11,8-38%) with irregular values.
JAN-S3-B2	1454-1355	8166-8000	Abrupt drop of *Erica* type (4,5-20,2%), deciduous and evergreen *Quercus* (1,3-5,7% and 2,5-8%), *Q. suber* (0-2,8%), and Chenopodiaceae (11,9-23,3%). Rise of Poaceae (8,5-26,5%) and A. Cichorioideae (2,8-26,6%).
JAN-S3-B3	1355-1133	8000-7631	Increase of deciduous and evergreen *Quercus* (3,4-9% and 0,6-6,1%) and *Q. suber* (1-4,7%). Rise of *Erica* type (9,4-25,6%) and Chenopodiaceace (8-27,4%) with irregular values. Peak of *Artemisia* (0-9,3%). Progressive decrease of *Isoetes* (8,8-22,2%) . Slight increase of Sordariaceae (0,4-3,2%). Presence of foraminiferal linings and dinoflagellates.
JAN-S3-C1	1133-986	7631-5772	Slight decrease of deciduous *Quercus* (0,3-7,3%) . Decerase o *Erica* type (6,3-19%) with a peak at the end of the zone. Increase of Poaceae (5,7-31,4%), A.Asteroideae (9,6-21,7%), and A. Cichorioideae (6,9-21,4%) with irregular values. Variable values of Chenopodium (6,1-22,6%) and *Isoetes* (1,3-16,1%). Progressive decrease of Filicales trilete undiff (0-2,3%). Peaks of Sordariaceae (0,8-3,5%), *Sporomiella* (0-4%) and *Chaetomium* (0-4,4%).
JAN-S3-C2	986-786	5772-3778	Irregular values of *Erica* type (5,1-20,5%) and decrease of Poaceae (3,1-13,9%). Higher and irregular values of A. Asteroideae (14,6-30,3%) and A. Cichorioideae (5,7-25,3%). Lower values of *Isoetes* (1-10,7%) and presence of foraminiferal linings.
JAN-S3-C3	786-677	3778-3164	Abrupt increase of *Erica* type (9,3-34,9%). Progressive decrease of Poaceae (0-7,4%) and A. Cichorioideae (5,1-20,1%). irregular values of A. Asteroideae (11,5-26,7%). Maximum values of Chenopodiaceae (14,9-33,9%) and Cyperaceae (0,8-3,2%). Slight increase of Pseudoschizaeae (0-2,1%). Abrupt decrease of *Sporomiella* (0-1,2%) and Sordariaceae (0-3,1%). Maximum values of *Gloeotrichia* (0-1,4%). Presence of foraminiferal linings.
JAN-S3-D1	677-616	3164-2812	Brusque peaks of *Erica* type (5,1-43,9%) and A. Cichorioideae (2-31,2%). Abrupt decrease of Chenopodiaceae (4,6-11,7%) and rise of *Isoetes* (31,1-41,3%). Maximum values of *Typha angustifolia* type (0,7-4,7%). Slight increase of *Coniochaeta* (0,7-1,5%) and Sordariaceae (0,8-2,9%).
JAN-S3-D2	616-389	2812-1425	Maximum values of *Erica* type (14,8-53%) followed by and abrupt decrease at the end of the zone. Progressive decrease of *Q. suber* (0-1,9%). Slight increase of *Alnus* (0-2,3%) and progressive rise of A. Carduoideae (1,2-7,1%). Irregular values of A.Cichorioidea (0-24,1%) and Chenopodiaceae (2,2-12,9%). Minimum and maximum values of *Isoetes* (0-48,9%). Maximum percentage of *Botryococcus* (0-2,7%).
JAN-S3-D3	389-226	1425-786	Slight peaks of *Pinus nigra-sylvestris* (0,3-1,7%). Progressive decrease of deciduous and evergreen *Quercus* (0,6-2,8% and 0-1,2%); also *Alnus* (0,3-1,2%). Irregular values of *Erica* type (7,9-25,4%), A. Asteroideae (10,2-65,5%) and A. Cichorioideae (2,4-25,5%). Maximum peak of A. Carduoideae (10,5-27,7%). Decrease of Chenopodiaceae (2,7-5,5%) and *Isoetes* (3,5-19,9%), this with variable percentages. Maximum values of *Pseudoschizaeae* (2,8%).
JAN-S3-D4	226-140	786-452	Low percentages of deciduous and evergreen *Quercus* (0,5-1% and 0-1%). Maximum values of A. Asteroideae (48-55,3%). Slight drop of *Erica* type (7,5-8,5%) and *Glomus* (6,6%). Progressive decrease of Sordariaceae (3,4-1,7%).
JAN-S3-D5	140- surface	452-present	Slight increase of *Pinus nigra-sylvestris* (1,4-4%), *P. Pinaster* (0,3-1%), deciduous and evergreen *Quercus* (1,9-3,3% and 1,9-4%) and *Olea* (1,9-2,3%). Progressive decrease of *Erica* type (14,1-6,3%) and A.Asteroideae (33,3-23,9%). Maximum values of *Glomus* (17,2-4,1%) and Poaceae ≥ 45µm (0,3-2,3%). Presence of *Coniochaeta* (1-2%), *Sporomiella* (1%), Sordariaceae (1,6-2%) and *Chaetomium* (1,4-1%).

The earliest record of the vegetation in the S3 core corresponds to intertidal facies (JAN-S3-A1: 8.8-8.7 ka cal BP) in which the vegetation is mostly composed by Asteraceae Cichorioideae and filicales trilete spores (undifferentiated and *Phaeoceros*). Immediately afterwards, an increase of shrubs and maximum values of mesophilous, riparian and Mediterranean arboreal taxa occur between ~8.7-7.7 ka cal BP (zones A2 to B3), corresponding to subtidal facies. A progressive decrease of freshwater vegetation parallels a gradual rise of saltmarsh taxa within these zones, coincident with the presence of foraminiferal linings and dinocysts. These trends are briefly interrupted ca. 8.2-8 ka cal BP by an abrupt rise of Poaceae and Asteraceae Cichorioideae (JAN-S3-B2).

A

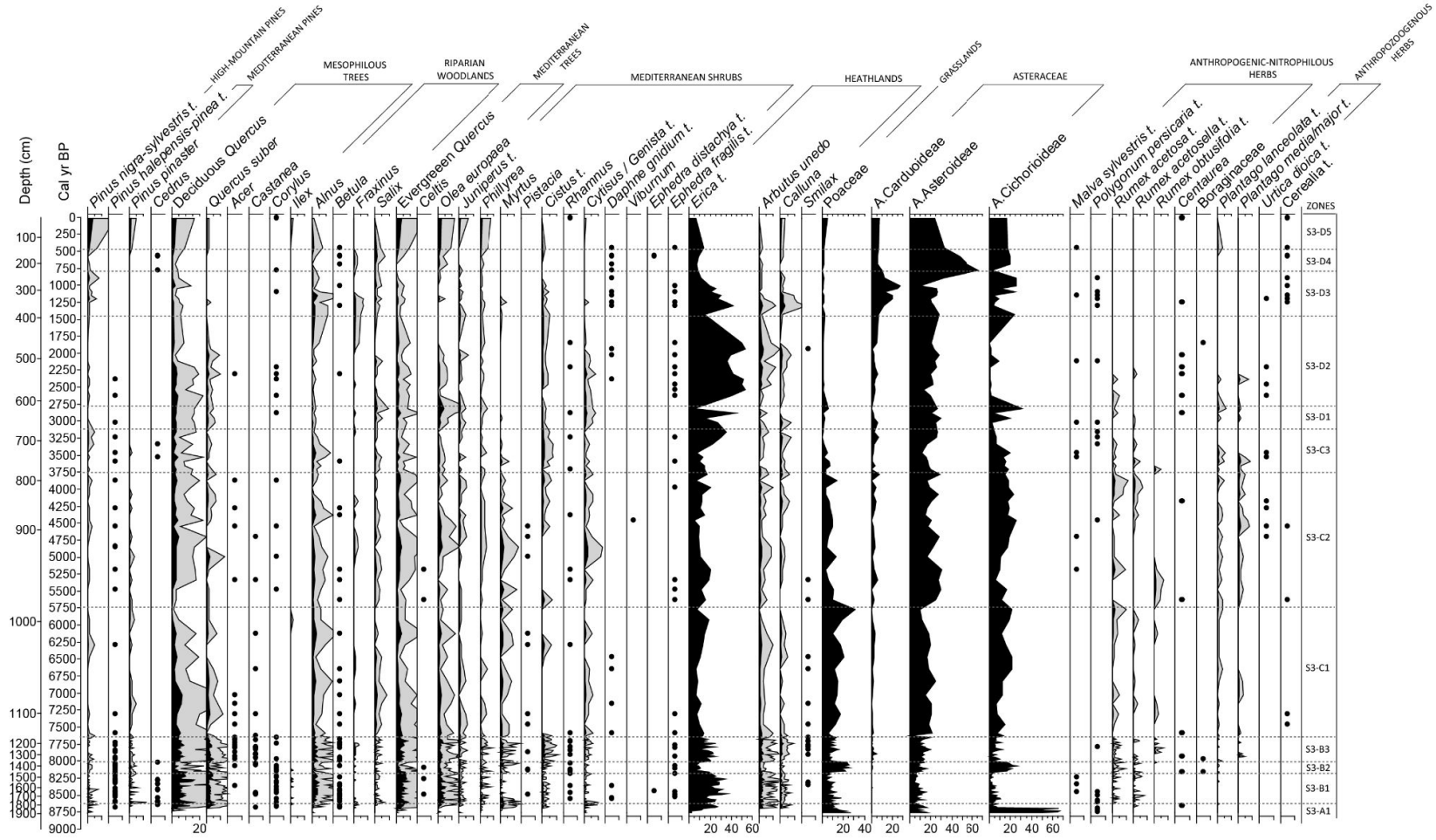
Depth (cm)
Cal yr BP
HIGH-MOUNTAIN PINES
MEDITERRANEAN PINES
MESOPHILOUS TREES
RIPARIAN WOODLANDS
MEDITERRANEAN TREES
MEDITERRANEAN SHRUBS
HEATHLANDS
GRASSLANDS
ASTERACEAE
ANTHROPOGENIC-NITROPHILOUS HERBS
ANTHROPOZOOGENOUS HERBS
Pinus nigra-sylvestris t.
Pinus halepensis-pinea t.
Pinus pinaster
Cedrus
Deciduous Quercus
Quercus suber
Acer
Castanea
Corylus
Ilex
Alnus
Betula
Fraxinus
Salix
Evergreen Quercus
Celtis
Olea europaea
Juniperus t.
Phillyrea
Myrtus
Pistacia
Cistus t.
Rhamnus
Cytisus / Genista t.
Daphne gnidium t.
Viburnum
Ephedra distachya t.
Ephedra fragilis t.
Erica t.
Arbutus unedo
Calluna
Smilax
Poaceae
A.Carduoideae
A.Asteroideae
A.Cichorioideae
Malva sylvestris t.
Polygonum persicaria t.
Rumex acetosa t.
Rumex acetosella t.
Rumex obtusifolia t.
Centaurea
Boraginaceae
Plantago lanceolata t.
Plantago media/major t.
Urtica dioica t.
Cerealia t.
ZONES
S3-D5
S3-D4
S3-D3
S3-D2
S3-D1
S3-C3
S3-C2
S3-C1
S3-B3
S3-B2
S3-B1
S3-A1

B

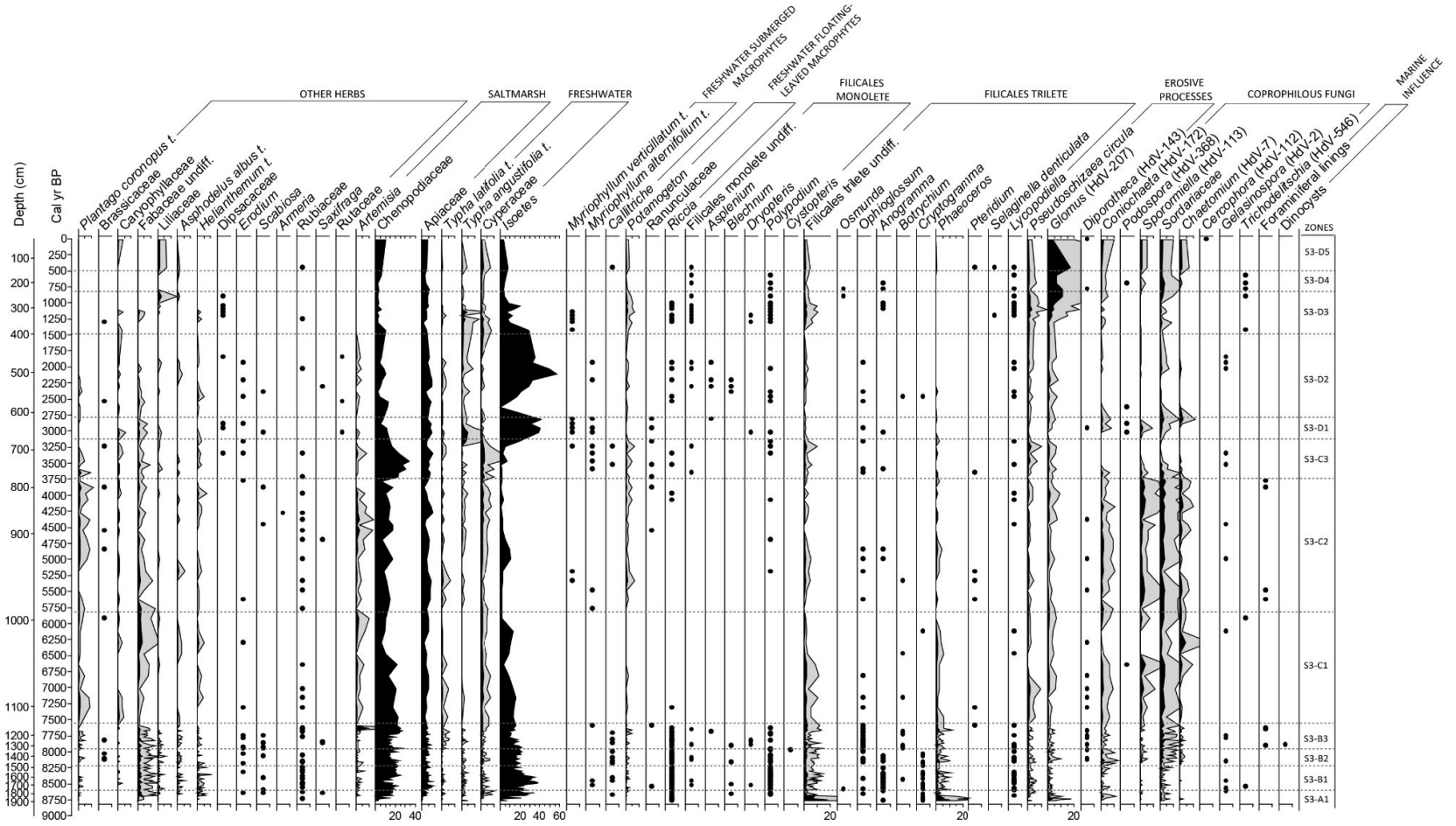

Figure 6.3. Percentage palynological diagrams (A and B) of the S3 core, plotted against age and depth. Grey silhouettes indicate the x5 exaggeration curve, black dots the values below 3%, and dashed lines the different pollen zones calculated after using CONISS. Groups of palynomorphs were assigned based on taxonomy and/or ecological affinities.

Another fast contraction of mesophilous and riparian forest taxa is visible ca 7.5 ka cal BP together with a peak of *Artemisia* (corresponding to zone JAN-S3-C1: 7.6-5.7 ka cal BP). Although with variable values, this period is defined by an escalation of herbaceous taxa, especially Poaceae, paralleling a progressive decline of arboreal percentages that culminates between ~5.9-5.5 ka cal BP. From this point onwards it is also noticeable the continuous expansion of *Erica* type and coprophilous fungi. From ca 5.5 ka cal BP on (JAN-S3-C2: 5.7-3.7 ka cal BP) there is a progressive decrease of arboreal taxa with some fast contractions between ~ 4.5-4 ka cal BP. Asteraceae Cichorioideae and A. Asteroideae continue to show high percentages, while grasslands progressively decrease. Freshwater vegetation displays their lowest percentages and dinoflagellates appear at 5.6 and 3.8 ka cal BP. Maximum values of coprophilous fungi were identified within this phase, followed by a sudden drop during the transition between zones C3 and D1. These period (JAN-S3-C3 and D1:3.7-2.8 ka cal BP) corresponds to intertidal sediments characterised by an abrupt rise of saltmarsh vegetation followed by a decline at ~ 3 ka cal BP, which is coincident with high percentages of freshwater vegetation. There are brusque peaks of *Erica* type and freshwater taxa that reach maximum values between ~2.8-1.4 ka cal BP (JAN-S3-D2), mostly coinciding with supratidal facies. A decrease of coprophilous fungi is identified between ~ 2.5-2.2 ka cal BP. Both mesophilous and Mediterranean forests decrease during this phase, while riparian woodlands exhibit a slight rise at the end of the zone. Zones D3 and D4 (1.4 ka cal BP – 452 cal BP) represent the transition from supratidal to fluvial facies and they are characterised by low values of arboreal and shrubby taxa, a decrease of saltmarsh and freshwater communities and the highest values of Asteraceae Asteroideae. A progressive increase of *Glomus* sp. is also observed, together with the continuous presence of Cerealia type. The last zone (D5: 452 cal BP to the present) is composed of anthropogenic facies defined by maximum values of *Glomus* sp., the dominance of herbs and the presence of Cerealia type.

6.5.- Interpretation and discussion

This section presents a chronological division of the different environmental phases and vegetation dynamics identified in the S3 core with the aim of discussing major environmental changes in La Janda basin and correlate them to other palynological continental sequences from SW Iberia (Fig. 6.4).

6.5.1.- Marine transgression and regional forest development (~11.7-7.7 ka cal BP)

According to Mediavilla et al. (2023), the marine transgression began to inundate La Janda basin between 14-12 ka cal BP, being recorded at different depths and chronologies in each drilling due to the geometry of the depression. Something similar happened along the Gulf of Cádiz, where the sea level rise is identified at different moments and with different results depending on the architecture of each estuary and the depth of the incised valleys (Boski et al., 2008; Dabrio et al., 2010; Schneider et al., 2010; Lambeck et al., 2014; Mediavilla et al., 2023).

The first millennia of the Early Holocene cannot be depicted in terms of palaeovegetation in La Janda due to poor pollen preservation in samples from this period. The only continental sequence covering these chronologies in SW Iberia is located in the Guadiana estuary, indicating the development of a local saltmarsh as consequence of the marine transgression and rapid oscillations in regional *Quercus* forests reflecting an early increased precipitation followed by relatively dry conditions (Fletcher et al., 2007). The expansion of the regional forest with thermo-Mediterranean, riparian and mesophilous taxa takes place in this area between ca.10-8 ka cal BP (Fig. 6.4), suggesting a warm, moist and oceanic climate (Fletcher et al., 2007). A dense forest cover surrounding a semi closed-estuary is also identified in Doñana for this time frame (Manzano et al., 2018). However, the palynological record from Laguna de Medina indicates episodes of certain continentality with a dominance of high-mountain pines in concordance with evergreen *Quercus* between ca 9.5-7.8 ka cal BP, although the constant presence of mesothermophilous trees allows discarding arid conditions (Schroder et al., 2018, 2020).

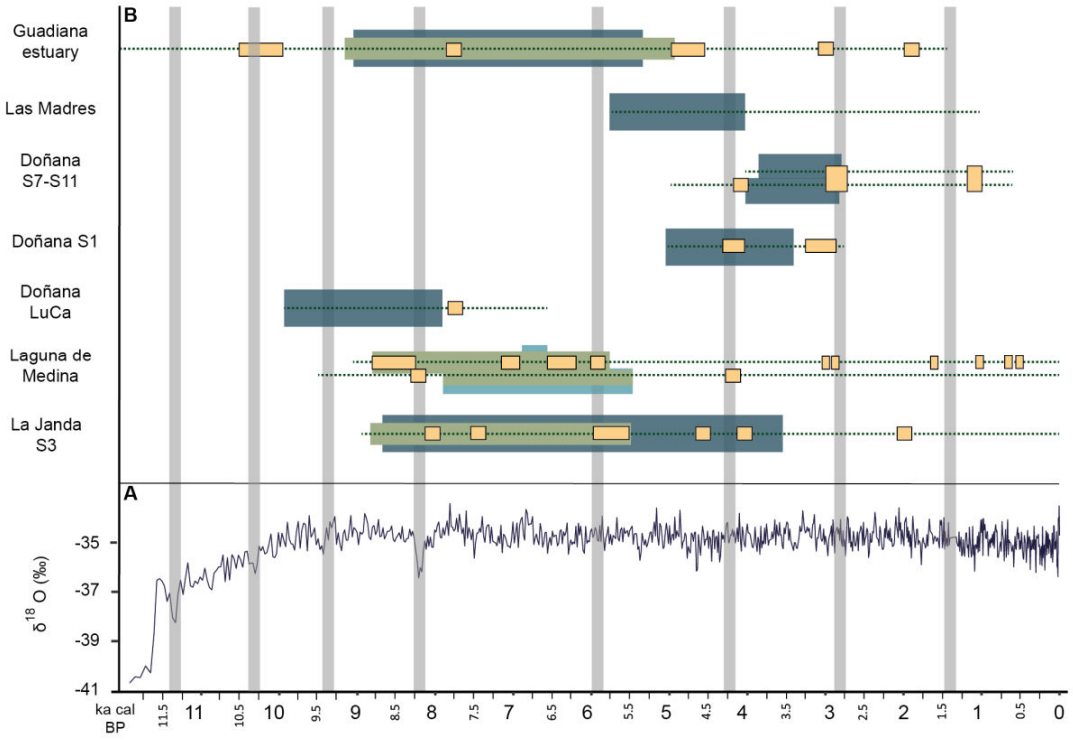

Figure 6.4. Composite figure showing: A) GISP2 oxygen isotope curve for the Holocene based on Grootes et al. (1999) where light grey lines correspond to ice-rafted debris (IRD) events in the North Atlantic Ocean based on Bond et al. (1997, 2001); B) Continental sequences from SW Iberia in which dark blue areas indicate periods of maximum marine influence in La Janda (Mediavilla et al., 2023), Doñana (Jiménez-Moreno et al., 2015; López-Sáez et al., 2018; Manzano et al., 2018), Las Madres (Yll et al., 2003), and the Guadiana estuary (Fletcher et al., 2007; Boski et al., 2008) and light blue areas correspond to maximum lake levels for Laguna de Medina (Reed et

al., 2001; Schröder et al., 2018). Green areas indicate periods of maximum forest development and yellow polygons show aridification phases with associated forest setbacks.

The earliest palynological record in the S3 core corresponds to intertidal facies (~ 8.8-8.7 ka cal BP) typical from terrestrial-marine environments with a vegetation composed of Asteraceae Cichorioideae and trilete fern spores, being poor in taxonomic diversity (Fig. 6.5). Rather than representing an open landscape, this bias may be explained by the fact that intertidal soils are constantly subjected to alternating emersion and submersion, leading to diverse processes that may destroy pollen grains (Havinga, 1967; Holloway, 1989; Hoffmann, 2002; Carrión et al., 2009; Lebreton et al., 2010; Twiddle and Bunting, 2010; Val-Peón et al., 2019, 2023b). Certain taxa may be more resistant to these processes due to inherent characteristics, this would have been the case of some species of Asteraceae and trilete fern spores, this latter sometimes indicative of reworked sediment input (Sangster and Dale, 1961; Campbell and Campbell, 1994; Fletcher et al., 2005; Tomescu, 2005; Lebreton et al., 2010; Val-Peón, et a., 2019, 2023b). The presence of temperate and Mediterranean forest taxa in other deposits of SW Iberia for these chronologies (Fletcher et al., 2007; Manzano et al., 2018; Schröder et al., 2018, 2020) may confirm this hypothesis.

The influx of oceanic waters and the flooding of the basin are recorded in La Janda at ca. 8.7 ka cal BP coinciding with a progressive predominance of saltmarsh vegetation growing on saline shore soils. Although the input of local taxa is predominant, the regional pollen signature is well reflected during this phase corresponding to the development of a restricted bay connected to the sea. The period between ca 8.7-7.7 ka cal BP is defined by the expansion of mesophilous and Mediterranean trees, with special prominence of deciduous and evergreen *Quercus* that would form dense forests in the nearby mountains, nowadays corresponding to the Alcornocales natural park (Fig. 6.5). The presence of these taxa suggest the existence of moist and temperate conditions that allow the development of a subhumid forest. Riparian woodlands spread, with *Alnus* as main component, illustrating the proximity of the main rivers draining into the basin. The existence of an important mass of heaths, mainly composed of *Erica* type, with a curve that follows a fairly similar evolution to that of mesophilous taxa, suggests their development as oakwoods understorey or in humid environments on mountain slopes (Gutiérrez et al., 1996; Loidi et al., 2007).

Within this phase of arboreal advance, an important forest setback took place between ca. 8.1-8 ka cal BP. Greenland ice cores reflect well-defined anomalies in the period between 8.4–8 ka cal BP with very low values of $\delta^{18}O$ around 8.2 ka cal BP (Rasmussen et al., 2007). The 8.2 ka cal BP event has been linked to a fresh water influx into the North Atlantic Ocean that would have provoked changes in temperatures and thermohaline circulation, and thus in moisture availability (Bond et al., 1997, 2001; Renssen et al., 2001). The contraction of mesophilous and thermophilous elements in La Janda (*Quercus*, *Alnus* and *Olea*

europaea) accompanied by a peak of open-ground taxa (mainly Poaceae and A. Cichorioideae) may indicate an abrupt decrease in moisture availability, but also a cooling of temperatures between ca. 8.1-8 ka cal BP. The decline of heaths, saltmarsh and freshwater vegetation also point to arid conditions. In other continental deposits from SW Iberia (Fig. 6.4), such as the Laguna de Medina, an increase of herbaceous taxa was identified at around 8.2 ka cal BP (Schröder et al., 2018). Indeed, there is a lake-level decrease ca. 8 ka cal BP concluding in a desiccation phase that has been related to global climatic instability centred on this event (Reed et al., 2001). In other cases, as in Doñana, vegetation remains practically unaltered during this episode, but some inputs of coarse material were detected between 8.2-8 ka cal BP together with a turbidite event (E9) of unknown origin at 8.2 ka cal BP (Manzano et al., 2018).

6.5.2.- Maximum marine flooding and regional forests decrease (~7.7-5.5 ka cal BP)

After a rapid recovery of arboreal taxa and heaths, a turning point in the vegetation is identified in La Janda from ~7.7 ka cal BP with a progressive increase of some herbaceous elements (Poaceae, Asteraceae Cichorioidea and A. Asteroidea). From this point onwards, saltmarsh vegetation spread in detriment of freshwater communities corroborating the marine influence in the landscape (Fig. 6.5). The punctual presence of foraminiferal linings and dynocists suggest periodic increments of salinity, but their low percentages and irregular appearance through the sequence may also reflect preservation problems. Some peaks of saltmarsh taxa accompanied by marine elements, such as the one at ~7.6 ka cal BP, point to periodic episodes of decreased moisture/freshwater inputs related to arid conditions rather than marine influence. Its coincidence with a peak of *Artemisia* ca 7.6 ka cal BP and the gradual contraction of deciduous *Quercus, Quercus suber* and *Alnus* culminating at ~7.5 ka cal BP seems to corroborate the existence of dry conditions within this time frame. Other continental sequences in SW Iberia mirror diverse episodes of forest setbacks for these chronologies (Fig. 6.4). An increase of herbaceous taxa and shrubs was recorded between 7.9-7.1 ka cal BP in Doñana, and diverse episodes suggesting dune development periods under arid and wind-enhanced conditions were identified from ~7.8 ka cal BP (Manzano et al., 2018). A peak of xerophytic taxa was observed at ~7.8 ka cal BP in the Guadiana estuary, interpreted as an arid interval that lasted until 7.3 ka cal BP and resulted in a *Quercus* forest decline and the expansion of shrublands (Fletcher et al., 2007).

From ca 7.3 ka cal BP on, a steadily rise of coprophilous fungi values is observed in the S3 core (Fig. 6.5). The ascospores of coprophilous fungi occur on the dung of wild herbivores as well as domestic livestock, being a good indicator of their presence (Van Geel et al., 2003; Cugny et al., 2010; Lee et al., 2022). Interestingly, pollen of Cerealia type is identified ca 7.3 ka cal BP (see also chapter 6), although a single grain cannot be considered an indicator of agricultural activities. The archaeological record suggests that animal domestication took place before the development of agricultural activities, which are only confirmed around 6 ka BP, for now (López-Sáez et al., 2011). Thus, increased values of coprophilous

fungi would indicate the presence of herbivores congregating near the depression and in the surrounding freshwater ponds, probably due to animal herding activities.

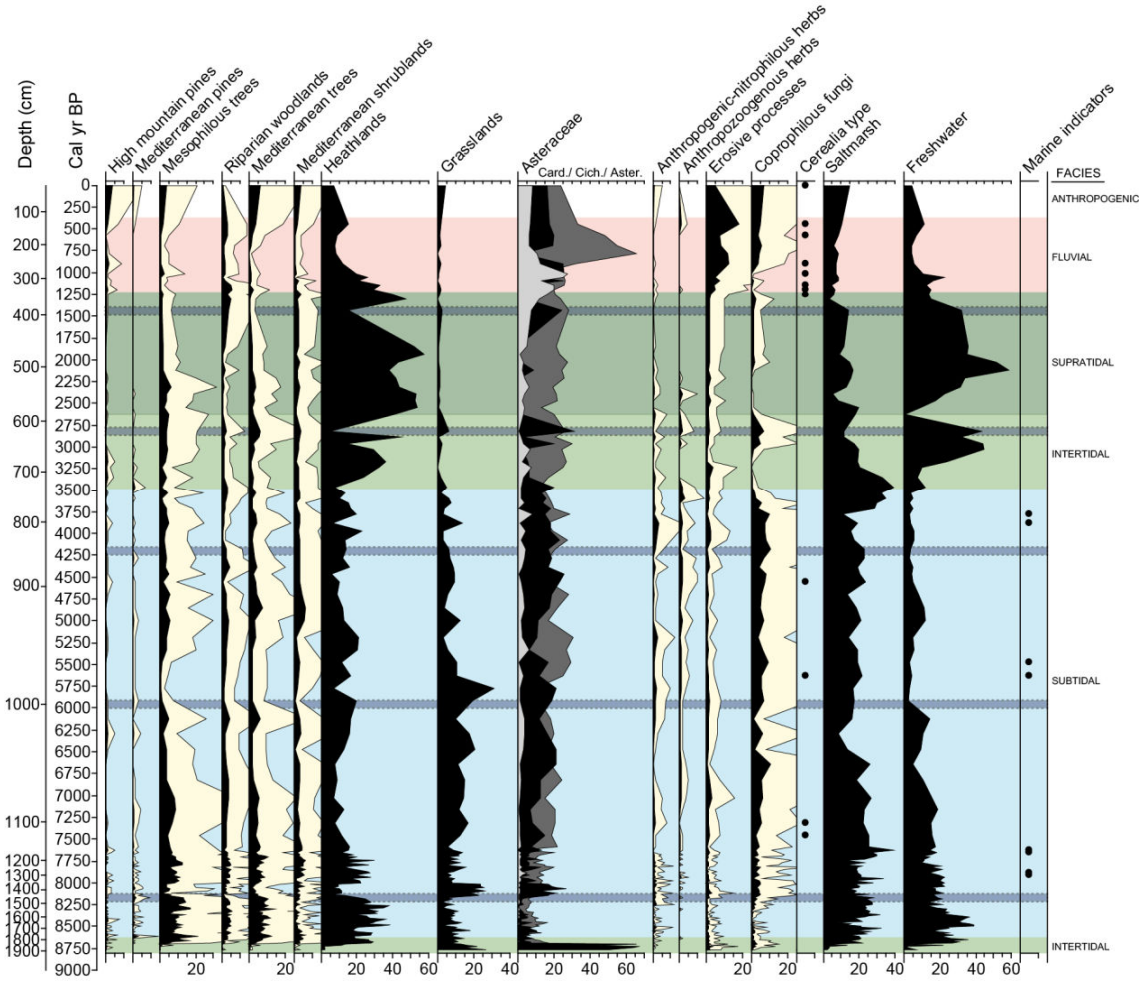

Figure 6.5. Synthetic diagram with a selected ecological groups of palynomorphs from the S3 core, plotted against age and depth. Different colours correspond to the identified sedimentological facies, explained on the right side of the plot. Dark lines correspond to the 8.2, 5.9, 4.2, 2.8 and 1.4 ka BP events (Bond et al., 1997).

The maximum marine inundation is recorded in diverse estuaries of the Gulf of Cádiz ca. 7 ka cal BP (Mediavilla et al., 2023), resulting in the development of an intertidal mudflat environment in the Guadiana estuary (Fletcher et al., 2007; Boski et al., 2008), different closed basin episodes in Doñana (Manzano et al., 2018), the development of a marine embayment in Las Madres (Yll et al., 2003) and the maximum flooding surface of the restricted bay in La Janda basin. However, this event is not reflected in the vegetation of these sequences, as their aquatic habitats were already depending on marine influence and they were also strongly influenced by local factors such as subsidence, spit barriers development, tides, etc. (López-Sáez et al., 2018; Mediavilla et al., 2023).

The dynamic of forest retreat immediately followed by a sharp increase in their values that was observed in La Janda for earlier chronologies is repeated with a drop of mesophilous, Mediterranean and riparian trees ca. 6.3 ka cal BP followed by their rise ca. 6.1 ka cal BP (Fig. 6.5). However, the background scenario is dominated by a gradual forest decline and a progressive spread of herbaceous taxa that culminates ca. 5.9-5.5 ka cal BP with an increase of *Artemisia* and Poaceae and an important drop of deciduous and evergreen *Quercus*, *Quercus suber*, *Alnus*, *Salix* and *Olea europaea*, suggesting a shift towards a less humid climate. Local vegetation adapted to freshwater conditions shows minimal values during this time frame, which may be indicative of a decrease in precipitation. At 5.9 ka cal BP, an abrupt ice-rafted debris (IRD) event occurred in the North Atlantic Ocean, similar in nature to the one linked to the 8.2 event (Bond et al., 1997, 2001). However, this episode is not mirrored in other continental sequences from the study area, but Reed et al. (2001) identified a lake level decrease phase marked by an increase of salinity ca. 5.9 ka cal BP (Fig. 6.4).

6.5.3.- Mediterranean conditions and anthropogenic influence (~5.5-3.7 ka cal BP)

From ca 5.5 ka cal BP onwards, regional forests composed of mesophilous and Mediterranean taxa display low but stabilized values in La Janda, while Mediterranean shrubs slightly increase and show rather balanced percentages (Fig. 6.5). The significant presence of Mediterranean elements, both arboreal and arbustive, corroborates a gradual shift to a more arid climate. Although grasslands progressively decrease, Asteraceae Cichorioideae and A. Asteroideae continue to show high values, indicating an increasing prominence of local herbaceous vegetation as marine waters retreat from the depression. In fact, these changes in the sea level are considered to be the trigger for the development of new geomorphological features on the Gulf of Cádiz coast, such as barrier island systems and the closure of some estuaries (Mediavilla et al., 2023). One example is the transformation of Las Madres in a coastal lake due to the development of a beach barrier that isolated it from the sea, resulting in the replacement of the halophytic vegetal association by a freshwater one (Stevenson et al., 1985; Yll et al., 2003).

The phase ca 5.5-5 ka cal BP reflects a shift towards a drier climatic regime in all continental sequences. This trend is identified all over the Western Mediterranean and some studies consider it may have been caused by a reduced summer insolation and the installation of the present atmosphere circulation in the northern hemisphere, coinciding with the end of the humid period in Northern Africa (Jalut et al., 2009). In addition, some studies attributed the onset of Mediterranean climate at 5.3 ka BP for Southern Iberia (Walczak et al., 2015). Within this context, different aridification phases affecting vegetation were identified in Las Madres with an abrupt drop of deciduous *Quercus* ca. 5.2-4.5 ka cal BP (Stevenson et al., 1985; Yll et al., 2003), in the Guadiana estuary between ~4.9-4 ka cal BP with a peak of xerophytes at 4.8 ka cal BP (Fletcher et al., 2007), in Doñana with a progressive decrease of Montenegro woodland between 4.5-4 ka cal BP (Jiménez-Moreno et al., 2015; López-Sáez et al., 2018) and in La Janda with a decline of deciduous and evergreen *Quercus*, *Quercus suber* and *Alnus* ca. 4.6-4.5 ka cal BP (Fig. 6.4). The same taxa show a drop in the S3 core at ca. 4.1 ka cal BP, although in this case riparian woodlands, especially *Alnus*, are more affected. The ice-rafted debris event occurred at 4.2 in the Northern Atlantic Ocean (Bond et al., 1997, 2001) is reflected as an abrupt aridity phase in some Western Mediterranean records, although the regional heterogeneity in the area does not allow confirming clear patterns (Bini et al., 2019). The effects of this episode in other continental sequences from SW Iberia is echoed in a pollen gap related to low preservation of organic matter in Laguna de Medina ca. 4.25 ka cal BP (Schröder et al., 2018, 2020) and an increase of xerophytic taxa in Doñana between ~4.2-4 ka, coincident with an extreme wave event (López-Sáez et al., 2018).

The presence of coprophilous fungi is slightly higher during this period in La Janda, when anthropogenic-nitrophilous herbs and anthropozoogenous taxa slightly increase (Fig. 6.5). Some species of these two categories may naturally occur in transitional systems, but their correlation with other markers, such as coprophilous fungi and the appearance of Cerealia type at 5.6 and 4.5 ka cal BP, suggest a stronger anthropogenic footprint related to livestock and agricultural activities. A rise of these elements is also recorded in Doñana, confirming the evidence of anthropization during these chronologies (López-Sáez et al., 2018). In the Guadiana estuary, a decline of *Pinus,* which cannot be explained by the shift to a drier climate, has been interpreted as the result from the clearance of pinewoods by human groups during this period (Fletcher et al., 2007). The role of human activities and their impact on ecosystems is still subject to debate regarding the chronology from which they are visible (Oldfield and Dearing, 2003; Beaulieu et al., 2005; Jalut et al., 2009; Anderson et al., 2011). It is considered that human impact on ecosystems has occurred since ca. 7.5 ca kal BP in Western Mediterranean but the role of climatic changes was somehow notorious until more or less 5.5 ka cal BP (Fletcher et al., 2007; Jalut et al., 2009). From this point onwards, the effects of anthropogenic activities added to the aridification trend, with the development of sclerophyllous formations and the decrease of some forest taxa (Stevenson et al., 1985; Fletcher et al., 2007; Schröder et al., 2020). However, it should be taken into account that sequences from transitional

ecosystems are subjected to several factors and they may alternatively reflect local and regional pollen signatures, overlapping human impact or showing other prominent vegetal trends.

6.5.4.- Transitional environments within an aridification trend (~3.7-1.2 ka cal BP)

Before the transition to the intertidal zone ca 3.5 ka BP in La Janda basin, the punctual appearance of marine elements is followed by an abrupt increase of saltmarsh vegetation between ~3.7-3.3 ka cal BP (Fig. 6.5). This might be related to the new edaphic conditions from a subtidal to an intertidal environment, as Chenopodiaceae species would propagate in saline soils slightly inundated during high tide. Immediately afterwards (~3.2-2.8 ka cal BP), the gradual decline of marine influence may have led to the development of temporary ponds colonized by freshwater communities, as reflected by a peak of *Isoetes*. The abrupt changes in the values of saltmarsh and freshwater vegetation seem to reflect important local-scale alterations related to the progressive disappearance of the bay. The gradual desalinization and development of new soils (ca. 2.6-1.2 ka cal BP) that would have been seasonally flooded led to an expansion of freshwater plant communities. The brusque increase of heaths may indicate their local character, spreading through these new soils with groundwater permanence in the depression. However, their presence could also answer to their preference for local areas under natural or anthropogenic disturbance, and may also be part of a regional component indicating an advanced stage of the subhumid forest regression (Loidi et al., 2007). The overrepresentation of *Erica* type and Asteraceae Asteroideae, besides being due to their local character, may also suggest the action of taphonomic agents generating a possible bias of the results in this transitional environment.

It is noteworthy to mention that during this transitional period an abrupt drop of coprophilous fungi is observable for the first time ca. 3.5-3.2 ka cal BP. The absence of anthopozoogenous herbs may corroborate the hypothesis of a reduced anthropogenic impact in the landscape during these centuries. Interestingly, an almost non-existent evidence of anthropization was also observed in Doñana during these same chronologies, interpreted as a cessation of arable and livestock husbandry activities (López-Sáez et al., 2018). The existence of two energy wave events in Doñana within this time frame was considered the possible cause affecting settlements in the area and their economic activities, but the contemporaneity of these palynological results with those of La Janda record could suggest the existence of an episode with a larger scale impact, perhaps with a cultural rather than a natural cause.

From a regional perspective, riparian woodlands exhibit their lowest values in La Janda while mesophilous and Mediterranean forest show low but relatively stable percentages until ca. 2 ka cal BP, when they suffer an important decrease and *Quecurs suber* almost disappear (Fig. 6.5). A major decline of oakwoods and riparian forests was also identified in the Guadiana valley accompanied by the expansion of lowland scrub vegetation between ~ 4-2.8 ka cal BP (Fletcher et al., 2007) and the development of a saltmarsh ca 3.2 ka

cal BP (Fletcher et al. 2007; Boski et al., 2008). In Laguna de Medina, the anthropogenic impact is especially clear from 3.4 ka cal BP on coinciding with the accelerated infilling of the lake, the existence of abrupt desiccation events and a marked decline of arboreal pollen (Reed et al., 2001; Schröder et al., 2020). The increased anthropogenic influence in the landscape is also notable in Doñana, especially after 3.1 ka cal BP, with traces of human subsistence practices on vegetation formations (López-Sáez et al., 2018) in a context of progressive closure of the estuary (Jiménez-Moreno et al., 2015).

6.5.5.- Cultural landscapes (~1.2 ka cal BP-present)

The gradual infilling of La Janda depression accelerates from ca. 1500 cal BP with an increase in sedimentation rates that can be related to an increment in anthropogenic activity. From ca. 1.2 ka cal BP, a totally emerged environment typical from flood plain deposits is fully developed. The local vegetation is dominated by Asteraceae (A. Carduoideae and A. Cichorioideae reach their maximum percentages) (Fig. 6.5). Forest and shrublands show low values, and local freshwater and saltmarsh communities suddenly suffer an important drop. NPP indicative of erosive processes grow during this period, especially *Glomus* sp. (HdV-207), associated to the development of new soils, soil erosion from watersheds, the existence of dry or desiccated areas and/or farming activities (Anderson et al., 1984; van Geel et al., 1989; López-Sáez et al., 2000). The decrease of arboreal and shrubby vegetation is a general trend but it is especially marked between ~1.1- 0.6 ka cal BP, fitting with a peak of Asteraceae Asteroideae ca. 0.9-0.7 ka cal BP. Similarly, the palynological record of Laguna de Medina shows increased anthropogenic influence, erosive phenomena and dry climate conditions for this period coinciding with the Mediaeval Climate Anomaly (ca. 1.15–0.65 cal. ka BP, Martín-Puertas et al., 2008; Schröder et al., 2020).

The impact of human activities shaping the landscape is extremely visible in all continental sequences. A strong taphonomic influence of anthropogenic origins is observed in La Janda, with exaggerated values of Asteraceae, the increased presence of *Glomus* sp. and the rise of trilete fern spores that may be indicative of reworked sediment input (Fletcher, 2005). Indeed, during the last centuries, the sequence indicates the presence of an artificial infilling in the depression for agricultural purposes, which explains high values of erosive markers. A slight increase of the arboreal and shrubby vegetation is observed during the last centuries, with maximum values of *Pinus sylvestris-nigra* and *P. halepensis*, increased coprophilous fungi, Cerealia type and a drop of *Glomus* sp., although it does not disappear (Fig. 6.5). This may be due to the development of new soils that, although constantly subjected to agricultural and livestock pressure, are relatively more stable than the previous ones affected by both anthropogenic and natural processes. On the other hand, although the presence of pines may indicate dry conditions, their behaviour throughout the sequence suggest the presence of monoculture plantations in nearby areas during this period, a dynamic that was also identified in Laguna de Medina (Schröder et al., 2020). The existence of a long-

term aridification trend during the Late Holocene is well identified in SW Iberia together with the anthropogenic pressure that may have even increased their effects on the vegetation and resulted in the development of cultural landscapes.

6.6.- Conclusions

A new continental sequence drilled in La Janda basin (SW Iberia) was studied from a multiproxy perspective with focus on palynological analysis, revealing diverse vegetation trends throughout the Holocene. Sedimentological analyses allowed to identify different environmental phases in the basin. Following the sea-level rise that progressively flooded the fluvial valley existing in the study area during the Late Pleistocene (Mediavilla et al., 2023), the S3 core indicate intertidal facies between ca. 8.8-8.7 ka cal BP. The development of a restricted bay connected to the sea was defined through the identification of subtidal deposits between ca. 8.7- 3.5 ka cal BP, which are followed by a transitional period of intertidal (ca 3.5-2.6 ka cal BP) and supratidal facies (ca. 2.6-1.3 ka cal BP) that culminates in a fluvial environment between ca. 1.3 ka cal BP to the present. During the last centuries, an artificial infilling for agricultural purposes was recorded in the upper section of the core.

Different vegetation dynamics were identified through the sequence, which were correlated with other continental cores and allowed to define regional trends in SW Iberia that are summarized as follows:

- ~11.7-7.7 ka cal BP: phase of forest development and period of maximum forest extension ca. 10-7 ka cal BP, with regional differences.
- ~7.7-5.5 ka cal BP: gradual forest decrease in most of que sequences, with regional peculiarities in some cores.
- ~5.5-3.7 ka cal BP: decrease of mesophilous taxa in favour of Mediterranean formations that parallels a shift towards a drier climatic regime. The anthropogenic pressure is notorious.
- ~3.7-1.2 ka cal BP: the effects of anthropogenic activities are added to the aridification trend with an opening of the landscape.
- ~1.2 ka cal BP-present: landscapes are strongly modified by humans.

La Janda record also show millennial-scale climate variations representing events of increased aridity at 8.2, 7.7-7.5, 5.9-5.5, and 4.2 ka cal BP, some of them identified in other continental sequences from SW Iberia. Some of these episodes are associated to Atlantic coolings linked to meltwater discharges, but others have less clear origins.

By combining different proxies it was possible to establish different phases of the palaeoenvironmental evolution, not only in the study area but also on a regional scale, integrating our data in a broader context. This allowed us to identify, define and better understand the connection between the diverse geological,

climatic and anthropogenic factors involved, a multifactorial perspective to be adopted in order to develop more accurate policies for the protection of transitional environments.

6.7.- Acknowledgements

This research was funded by the Deutsche Forschungsgemeinschaft-DFG (project no.57444011 – SFB 806) and a "Severo Ochoa" extraordinary grant for excellence IGME-CSIC (AECEX2021). The authors would also like to thank the direction and management of the "Las Lomas" farm for their assistance both in the precise positioning of the drilling points and during the drilling process.

7.- Natural and anthropogenic processes in the depression of La Janda (SW Iberia) from the Late Pleistocene to the Mid-Late Holocene

This chapter is a slightly modified version of an article published in Continental Shelf Research:

Val-Peón, C., López-Sáez, J.A., Santisteban, J.I., Mediavilla, R., Becerra, S., Domínguez-Bella, S., Fernández-Sánchez, D.S., Ramos Muñoz, J., Vijande Vila, E., Cantillo Duarte, J.J., Reicherter, K. (2023). Natural and anthropogenic processes in the depression of La Janda (SW Iberia) from the Late Pleistocene to the Mid-Late Holocene. https://doi.org/10.1016/j.csr.2023.105067

Abstract

A multiproxy study (pollen, non-pollen palynomorphs, sedimentology, and geochemistry) was carried out in two cores drilled in La Janda basin (SW Iberia) to trace the environmental evolution and human impact on the landscape. An incised fluvial valley existed in the basin during the Late Pleistocene, followed by a transitional environment characterized by the development of saltmarsh vegetation affected by the increased marine influ- ence ca. 10/8.7 ka cal BP. During this period comprising the Upper Palaeolithic and Mesolithic (>~7.8 ka cal BP), the impact of hunter-gatherer groups on the landscape was rather low according to palynological and geochemical records. A restricted estuary connected to the sea was identified in La Janda between ca. 10/8.7- 3.5/3.3 ka cal BP, coinciding with a predominance of saltmarsh vegetation developing on saline shore soils and the punctual presence of foraminifera and dynoflagellate cysts. The anthropogenic pressure was progres- sively increasing during the Neolithic, especially from ca. 7 ka cal BP, with markers suggesting herding/livestock activities prior to the punctual presence of cereals, which is only confirmed by the archaeological record ca. 6 ka cal BP. Human pressure become more noticeable throughout the Chalcolithic and Bronze Age (~5-3 ka cal BP), period during which a new transitional phase is recorded in La Janda (ca. 3.5/3.3-1.3 ka cal BP), culminating in the terrestrialization of the area. The predominance of freshwater taxa and decrease of saltmarsh vegetation is observed during this period, and the transformation of the landscape for agricultural activities over the last centuries is reflected in the local presence of cereals and markers of erosive processes.

Keywords: Palaeoenvironmental evolution, Multiproxy approach, Palynology, Prehistory, Archaeological record, SW Iberia

7.1.- Introduction

The last twenty thousand years encompass multiple environmental changes that have had a deep impact on the Iberian Atlantic Margin, such as the postglacial marine transgression, climatic events, tectonics, etc. Sea-level changes caused important alterations in coastal landscapes of SW Iberia, resulting in the inundation of fluvial valleys and the development of new features such as estuaries, lagoons, tidal flats, etc. (Rodríguez-Ramírez et al., 1996, 2005; Dabrio et al., 2000; Teixeira et al., 2005; Boski et al., 2008; Zazo et al., 2008; Schneider et al., 2010; Delgado et al., 2012; Trog et al., 2013). Palynological studies from terrestrial and marine sedimentary records show that the vegetation adapted to new edaphic conditions, but also responded to the increase of temperatures and moisture with a progressive expansion of forests during the Early Holocene (Fletcher et al., 2007, 2010; Combourieu Nebout et al., 2009; Chabaud et al., 2014; Camuera et al., 2019; Gomes et al., 2020; Val-Peón et al., 2021). Such dynamics led to major landscape modifications that may have affected human groups and their settlement patterns in some way.

SW Iberia has a long history of human occupation and it is considered a key territory from a geoarchaeological point of view, in part due to its geographic position between Eurasia and Africa (Pérez-Díaz et al., 2017). It has also been a reservoir of biodiversity and a wildlife refuge area during the Late Pleistocene and the Holocene (Carrión et al., 2008). Indeed, the archaeological record in the region indicates that human groups adapted to different environments through a diversity of strategies and choices during the Upper Palaeolithic, Mesolithic, Neolithic, Chalcolithic and Bronze Age (Giles Pacheco and Sáez, 1978; Sanchidrián, 1992; Domínguez-Bella, 1995; Ramos Muñoz et al., 1998, 2004-2005, 2006b, 2010b, 2011; Ramos Muñoz, 2004a, 2006b, 2008; Domínguez-Bella et al., 2015; Becerra et al., 2019).

Coastal areas are extremely sensitive to environmental factors, which makes them highly dynamic zones that are prone to experience and record significant changes over time. Moreover, the increasing human impact throughout the Holocene may be also reflected in environmental disturbances derived from anthropogenic activities and changes in the land use. Thus, combined archaeological and palaeoenvironmental studies can provide a long-term perspective to unravel landscape change from both a natural and anthropogenic perspective.

The present research focuses on the study of the depression of La Janda (SW Iberia), an area that has undergone a complex evolution in which both natural and anthropogenic processes have intervened. A multidisciplinary research based on palynological data, sedimentology and geochemistry was performed in two sedimentological cores drilled in the basin. Furthermore, these data were correlated with the archaeological record. Thus, our aims are: i) to reconstruct the environmental evolution of La Janda depression; ii) to identify the possible impact of anthropogenic activities on the landscape; iii) to better

understand the relationship between human groups and environmental changes throughout the different cultural periods of Prehistory.

7.2.- Study area

7.2.1.- Biogeographical and geological setting

La Janda basin is located in a tectonic graben of about 35 km2 in the southwestern Atlantic margin of the Iberian Peninsula, near the Strait of Gibraltar (Fig. 7.1). The origin of the depression is related with the two faults that, with NW-SE and NE-SW direction, release the efforts of N-S tectonic compression produced by the Iberian and African plates movement (Goy et al., 1995; Luque et al., 2001).

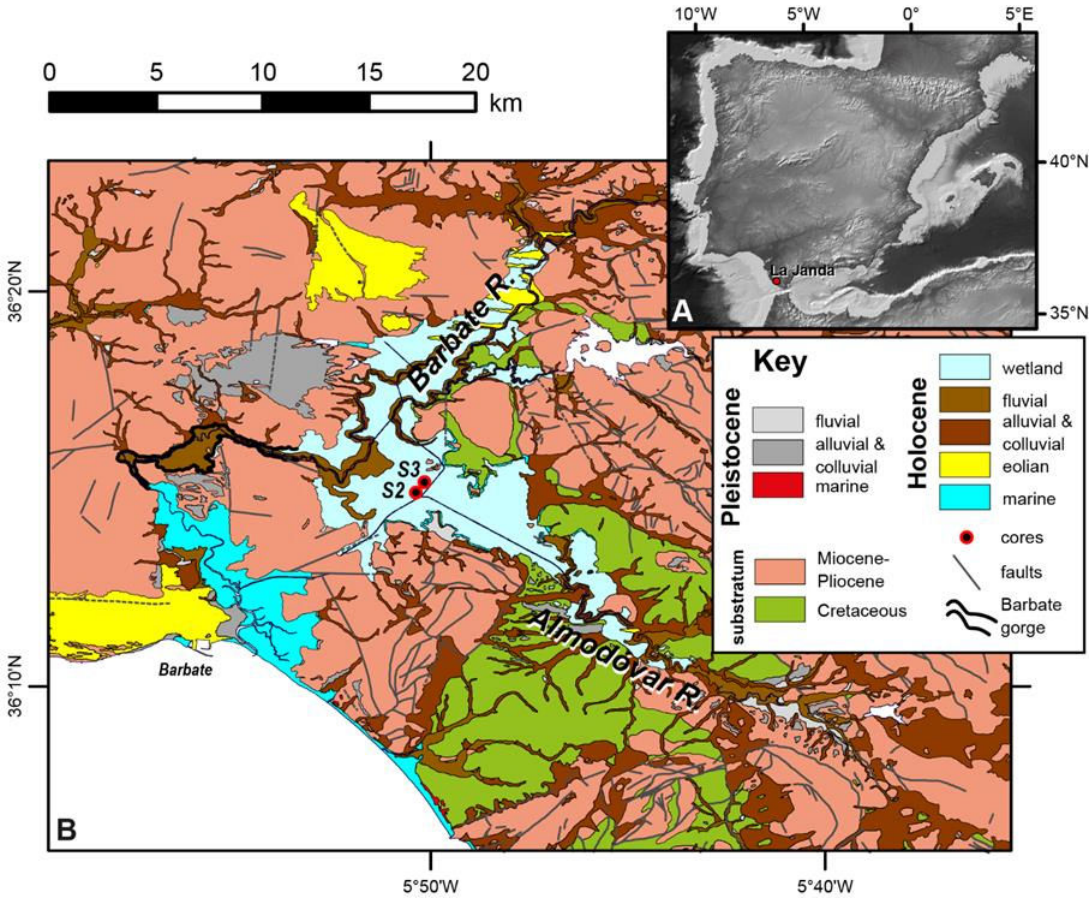

Figure 7.1. Location of the studied area in the Iberian Peninsula with cores S2 and S3 represented by green dots in the depression of La Janda. The zoomed area indicates the slopes of the terrain with their values in the legend.

The geology of the Gibraltar Arc in the studied area is composed by siliciclastic and carbonated pre- and synorogenic turbiditic deposits (Almarchal, Algeciras and Aljibe Series of the Gibraltar Flysch), spanning from Late Cretaceous to Middle Miocene times, affected by thrusts, backthrusts and dextral strike-slip faults (Hernaiz Huerta et al., 1991). Upper Miocene-Pliocene postorogenic sediments consist of breccias,

calcarenites and siliciclastic marine deposits filling subsiding troughs affected by Plio-Pleistocene compressive tectonics (García de Domingo et al., 1991; Goy et al., 1995). The distribution of Quaternary deposits is controlled by neotectonics, being preferential along the present coastline of the Gibraltar Strait (Rodríguez Vidal et al., 2004), fluvial valleys and La Janda basin (Fig. 7.1B). Luque et al. (1999) found estuarine siliciclastic deposits, dated as 3810 cal. BP, at −5 meters above sea level (m asl) revealing that the basin was below sea level. Later basin infill led to the isolation from the sea and the beginning of alluvial and, afterwards, lacustrine sedimentation (Luque et al., 1999, 2001; Dueñas López and Recio Espejo, 2000).

Following the Köppen–Geiger classification, this in an area with Mediterranean climate type Csa, defined by mild winters and hot and dry summers (Kottek et al., 2006). Mean annual temperature is 18.8ºC, with average minimum temperatures of 9.5ºC in January and average maximum temperatures of 28.2ºC in August (period 1991-2020; AEMET OpenData). Mean annual precipitation averages between 500-700 mm, concentrated in autumn and winter (period 1991-2020; AEMET OpenData). From a biogeographical point of view, La Janda depression is framed in the Gaditano-Onubense Littoral and the Aljibe sectors (Junta de Andalucía, 2004; Rivas-Martínez et al., 2014). The first is included within the humid to sub-humid thermomediterranean ombrotypes, and the second is categorized as thermomediterranean with dry to humid ombrotypes with a marked oceanic influence due to the proximity of the Gibraltar Strait (Rivas-Martínez et al., 2014).

The depression of La Janda is nowadays composed of different land units such as wetlands, farmlands and the mountains surrounding the area. One of the largest surfaces is dedicated to livestock and agricultural activities, with irrigated crops in flat areas, dry grasses on gentle slopes, and pastures on lands that are less suitable for agricultural purposes (Junta de Andalucía, 2014a, 2014b). Adding more complexity to the landscape, there are hills and patches of scrub and forest vegetation dominated by *Olea europaea* var. *sylvestris*, as well as *dehesas* or oak parklands of *Quercus suber* where extensive livestock use remains (Junta de Andalucía, 2014b).

Typical vegetation of lagoons, coastal wetlands, and marshes are present in the natural parks of La Breña y Marismas del Barbate and El Estrecho. Some of these vegetal communities are still identifiable in certain zones of La Janda during its periodic floodings. Temporary pools and ponds are usually flooded during the winter and spring. Plant communities vary according to the substrate and the drying cycle, but some of the most representative are macrophyte groups of *Myriophyllum* sp., *Ranunculus* sp., *Potamogeton* sp., *Callitriche* sp. and *Isoetes* sp. (Domínguez et al., 1993; Cirujano et al., 2014). Water channels within the marshes are usually covered by Cyperaceae (*Scirpus maritimus*, *S. lacustris*) and annual pioneer plants, mainly Chenopodiaceae (*Salicornia* sp., *Sarcocornia* sp., *Frankenia* sp., etc.), that dominate in temporary pools of

brackish or saline water, the edges of lagoons, the open spaces of coastal marshes, and areas affected by tides (Domínguez et al., 1993; Latorre et al., 1996; Galán de Mera et al., 1997; Rivas-Martinez et al., 1997).

At the slopes of the mountains or in depressions with groundwater permanence, hygrophilous shrubby heaths (*Erica ciliaris*, *Calluna vulgaris*, *Ulex minor*, etc.) develop in humid areas (Espírito-Santo et al., 2017). However, heathlands may also thrive in zones under natural or anthropogenic disturbance (Loidi et al., 2007). In low mountainous areas, sclerophyllous grooves of *Quercus ilex* and thermophilous forest of *Olea europaea* grow accompanied by thickets such as *Q. coccifera, Pistacia lentiscus, Phillyrea angustifolia, Myrtus communis, Rhamnus oleoides, Asparagus albus* and *Chamaerops humilis* (Domínguez et al., 1993; Gutiérrez et al., 1996; Latorre et al., 1996; Rivas-Martinez et al., 1997). In higher altitudes, oak forests are the characteristic formations, with special prominence of *Quercus suber* that expands over the Natural Park of Los Alcornocales (Latorre et al., 1993; Gutiérrez et al., 1996). Other oaks, such as *Quercus faginea, Q. canariensis* or *Q. rotundifolia* may be accompanied by other trees such as *Sorbus torminalis* or *Acer monspessulanum*, with an understorey consisting of *Arbutus unedo*, *Smilax aspera* and *Rosa sempervirens*, among others (Domínguez et al., 1993; Latorre et al., 1996; Rivas-Martinez et al., 1997; Latorre and Cabezudo, 2003). The multiple streams that cross and surround the depression of La Janda are associated to riparian elements such as *Fraxinus angustifolia* and different species of *Salix* and *Alnus* (Domínguez et al., 1993; Latorre et al., 1996).

7.2.2.- Archaeological context

The area of La Janda basin and its surroundings account for a long record of human occupations throughout Prehistory (Fig. 7.2). During the Upper Palaeolithic, open-air settlements of hunter-gatherer groups with Solutreogravettian and Solutrean technology were identified (Giles Pacheco et al., 1994; Gutiérrez et al., 1994; Ramos Muñoz et al., 1995a, 2006a, 2010a; Castañeda et al., 2020). In addition, other sites were found in the caves and rock-shelters of the area (Fig. 7.8), some of which yield artistic manifestations that offer valuable information to study the social and economic structures of these human groups (e.g., Mas, 2000; Collado et al., 2018a, 2018b, 2019; Fernández Sánchez et al., 2018, 2019a, 2019b, 2021; Hoffmann et al., 2018; Fernández Sánchez and Gómez-Sánchez, 2022; Barcia-García et al., 2023).

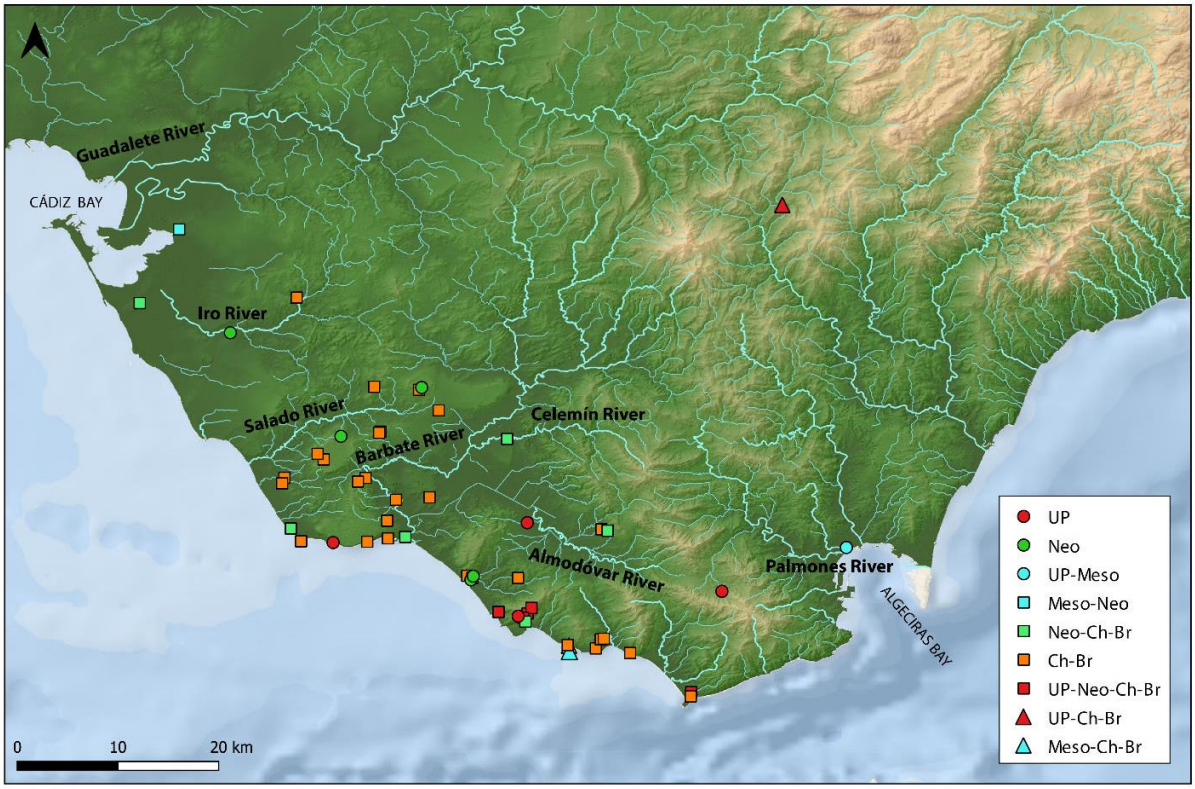

Figure 7.2.- Map of the study area indicating some of the archaeological sites included in this research and/or mentioned in the text. Some settlements record human occupations over different periods, so that the correspondence between cultural periods and symbols is explained in the legend: UP (Upper Palaeolithic), Neo (Neolithic), Meso (Mesolithic) and Ch-Br (Chalcolithic-Bronze Age).

The number of Mesolithic sites decreased dramatically in the study area (Fig. 7.2), and most of the information about this period is provided by the Embarcadero del Río Palmones, in the Bay of Algeciras, (Ramos Muñoz, 2004a) and El Retamar sites, in the Bay of Cádiz (Ramos Muñoz and Lazarich, 2002) (Fig. 7.9). The interdisciplinary studies of both enclaves provided information on marine (Soriguer et al., 2008) and terrestrial fauna (Cáceres, 2003), archaeobotany (Uzquiano and Arnanz, 2002; Rodríguez Ariza, 2005), lithic technology (Ramos Muñoz and Lazarich, 2002; Ramos Muñoz and Castañeda, 2005), as well as archaeometric data (Domínguez-Bella et al., 2002, 2004). These investigations allow inferring that these last hunter-gatherer-fisher groups mastered the exploitation of coastal and vegetal resources while maintaining hunting activities (Clemente Conte and Pijoan, 2005).

Archaeological surveys undertaken between the Algeciras and Cádiz bays, show a higher number of (preserved) sites during the Neolithic (Ramos Muñoz, 2008) (Fig. 7.2). Some of the best studied are Campo de Hockey (Vijande Vila, 2009; Vijande Vila et al., 2015, 2022), La Esparragosa (Vijande Vila et al., 2018, 2019; Ramos Muñoz et al., 2022) and SET Parralejos (Villalpando and Montañés, 2016; Cantillo Duarte et al., 2017) (Fig. 7.10). This last two, evidenced villages and settlements with specific spaces for

the production of lithic tools, as well as habitation and storage areas attributed to the 6th millennium BP (Ramos Muñoz et al., 1999). Animal husbandry practices were documented in the terrestrial record, as animal resources were mainly derived from domesticated fauna (75.14%) with a significant weight of ovicaprid herds (Riquelme, 2019). Moreover, the exploitation of marine resources is also significant during this period (Cantillo-Duarte et al, 2010; Cantillo-Duarte and Vijande Vila, 2014; Ramos Muñoz et al., 2022), as documented at El Retamar (Ramos Muñoz and Lazarich, 2002) and La Esparragosa (Cantillo-Duarte and Soriguer-Escofet, 2019).

This same area witnessed a concentration of the population in specific zones during the Chalcolithic (Fig. 7.2), with important settlement clusters in the area of Medina Sidonia (Montañés et al., 1999; Ramos Muñoz, 2008), El Berrueco (Escacena and Berriatúa, 1985; Escacena and De Frutos, 1985) y La Mesa (Ramos Muñoz et al., 1999), as well as in Conil de la Frontera (Ramos Muñoz, 2008; Ramos Muñoz et al., 2016b) (Fig. 7.11). In La Janda basin, the most important site is Los Charcones, located on a raised platform near the Celemín and Barbate rivers (Ramos Muñoz et al., 1995b). Its geological location results in a great potential for agricultural activities (A.A.V.V., 1963) and the collection of raw materials, such as the flint from the outcrops near Cerro de la Venta, Realillo and El Almarchal, and the sandstone from the immediate mountains of the Aljibe sector (Pérez Rodríguez, 1998; Domínguez-Bella et al., 2011). Most of these settlements are located in strategic sites with good communication and visibility, where they occupied prominent spaces. Although ceramics are those typical from the 5th millennium BP, the transition to the 4th millennium BP is identified by the presence of bell-shaped beakers as exotic products, which occurrence is mainly documented in megalithic areas such as in the dolmens of Aciscar (Mergelina, 1924; Montañés and García, 1999), Los Charcones (Ramos Muñoz et al., 1995) or Paraje Monte Bajo (Lazarich, 2007).

Those sites that have been important centres during the 5th millennium BP would witness a population continuity during the first quarter of the 4th millennium BP (Fig. 7.2): Medina Sidonia (Montañés et al., 1999; Ramos Muñoz et al., 2008), La Mesa (Ramos Muñoz et al., 1999), Cerro El Berrueco (Escacena and De Frutos, 1985) and Los Charcones (Ramos Muñoz et al., 1995b) (Fig. 7.11). The record of exotic elements (bell beakers, palmela points, etc.) increased during this period, which provide information about the existence of networks that reach the nuclear settlements (Lazarich, 2004, 2005; Domínguez-Bella et al., 2008; Ramos Muñoz, 2008). During this period, the funerary record is characterized by the existence of necropolis in artificial caves and tumular structures with chamber and small corridors, such as in Los Algarbes (Posac, 1975; Castañeda Fernández et al., 2022), Vejer de la Frontera (Negueruela, 1981-1982) or Trafalgar (Vijande Vila et al., 2022). In them, some elements could be interpreted as a reflect of social differences within these societies (Arteaga, 1992, 2002).

7.3.- Methods

7.3.1.- Coring

Cores S2 and S3 were recovered in 2016 and 2017 by triple barrel system (Mediavilla et al., 2023), they were encased in PVC pipes and stored at the Geological and Mining Institute of Spain (IGME, CSIC) (Spain) facilities at 4ºC. Both cores S2 and S3 were divided in two halves that were photographed, described, and sampled. Core S2 (36º14'53.88" N, 5º50'21.45" W) is 27.50 m depth and was drilled at 4.88 m asl, while core S3 (36º15'09.68" N, 5º50'08.52" W) is 26.78 m depth and was drilled at 5.59 m asl (Fig. 7.1).

7.3.2.- Dating and age-depth model

A total of 18 samples were collected from cores S2 and S3 (see Mediavilla et al., 2023 for more information) and were 14C-dated at Beta Analytic Inc. (USA) and Keck Carbon Cycle AMS Facility at UC Irvine (USA) (Table 1). Calibration was performed with CALIB 8.2 (Stuiver et al., 2021) using the IntCal20 and Marine20 calibration datasets (Heaton et al., 2020; Reimer et al., 2020) and different reservoir effect values (Soares and Dias, 2006; Soares and Martins, 2010; Martins and Soares, 2013). These values have been recalculated using the web application of Reimer and Reimer (2017) following Soulet (2015). Several calibration sets were developed to check which samples and reservoir effect value valid (if applied) and a simple lineal interpolation was used to build the age-depth model (Mediavilla et al., 2023) (Fig. 7.3).

Table 7.1. Radiocarbon data and calibration results from cores S2 and S3 (JAN-S2 and JAN-S3 in the Sample column); m bs: meters below surface. Most organic matter samples correspond to charcoal or leave remains.

Lab code	Number in figures	Sample	Depth in core (m bs)	^{14}C	error	$\delta^{13}C$	ΔR	error	Cal. BP 2σ median [range]	Material	Curve
UCIAMS-236153	**rejected**	JAN-S2-AMS new	0.46	1100	15		-	-	997 [957, 1007]	Charcoal	IntCal20
Beta-618143	**1**	JAN-S2-1	2.78	1440	30	-20.9	-	-	1331 [1297, 1373]	Organic matter	IntCal20
Beta-459036	**2**	JAN-S2-2	5.16	2480	30	-9.9	-315	220	2353 [1775, 2889]	Shell	Marine 20
Beta-459037	**3**	JAN-S2-4	11.55	6660	30	-2.6	301	201	6618 [6178, 7115]	Shell	Marine 20
Beta 459038	**4**	JAN-S2-5	14.60	7680	30	2	301	201	7670 [7260, 8093]	Shell	Marine 20
Beta-459039	**5**	JAN-S2-6	20.44	8220	40	-27.7	-	-	9185 [9024, 9302]	Charcoal	IntCal20
Beta-557793	**6**	JAN-S2-16	23.46	10440	30	-25.0	-	-	12.341 [12537, 12607]	Charcoal	IntCal20
Beta-635181	**7**	JANS2-17	26.67	16340	60	-25.0	-	-	19.723 [19552, 19882]	Organic matter	IntCal20

Lab code	Number in figures	Sample	Depth in core (m bs)	^{14}C	error	$\delta^{13}C$	ΔR	error	Cal. BP 2σ median [range]	Material	Curve
Beta-526017	**8**	JAN-S3-2	1.46	400	30	-25.8	-	-	471 [428,512]	Charcoal	IntCal20
Beta-618144	**9**	JAN-S3-3	4.04	1620	30	-23.2	-	-	1481 [1409, 1544]	Organic matter	IntCal20
Beta-618145	**rejected**	JAN-S3-4	5.75	2880	30	-26.1	-	-	3008 [2921, 3078]	Organic matter	IntCal20
Beta-526108	**10**	JAN-S3-5	6.33	2810	30	-25.9	-	-	2912 [2846, 2998]	Charcoal	IntCal20
UCIAMS-259331	**11**	JAN-S3-6	7.81	4115	15	-5.5	200	426	3744 [2702, 4833]	Shell	Marine 20
Beta-526109	**12**	JAN-S3-7	8.94	4570	30	-1.6	50	152	4516 [4076, 4925]	Shell	Marine 20
Beta-526110	**13**	JAN-S3-8	11.23	6760	30	-22.9	-	-	7615 [7574, 7668]	Organic matter	IntCal20
UCIAMS-259332	**14**	JAN-S3-9	15.51	8040	20	-2.1	17	183	8327 [7911, 8816]	Shell	Marine 20
Beta-526111	**15**	JAN-S3-10	18.30	7890	30	-26.4	-	-	8668 [8593, 8779]	Vegetal remain	IntCal20
Beta-540083	**16**	JAN-S3-11	22.64	22400	90	-26.5	-	-	26.728 [26405, 27006]	Organic matter	IntCal20

7.3.3.- Physical properties, mineralogical and geochemical composition of the sediments

Non-destructive analyses were run on the cores at the laboratories of the Geological and Mining Institute of Spain (IGME, CSIC), including:

- Core colour scan (high resolution images with a down core resolution of 50 μm) with a Geoscan IV coupled to the MSCL GEOTEK. Some of them are presented in Mediavilla et al. (2023).

- Colour (RGB) analyses were performed with 1 mm down core resolution using a Konica Minolta 700-d spectrophotometer integrated in the GEOTEK XRF core scanner. Each channel had values ranging from 0 up to 255. A R/(G+B) colour index was used to represent the dominant tones (red/brownish against green/greyish) and a (R+G+B)/3 index represents the grey scale range.

- Geophysical properties (P-wave velocity, gamma density, non-contact resistivity and magnetic susceptibility) were analysed with 1 cm down core resolution with a GEOTEK Multi-Sensor Core Logger (MSCL-GEOTEK).

- XRF scanning with a GEOTEK XRF core scanner in a He purged atmosphere with an illumination window of 15 mm (cross-core slit width) x 10 mm (down-core resolution). Two runs, with 30 seconds count time exposure, were performed for 10 kV and 40 kV (detecting from Mg

to U). XRF spectra were processed with bAxil. Element intensities are represented in counts per second (cps).

Destructive analyses were carried out in cores S2 and S3 to characterize the sedimentary facies at the IGME laboratories:

- Mineralogical analysis by X-ray diffractometry (PTE-RX-04) for bulk sample and <2μm fraction. These analyses were used to check the sources of the chemical elements obtained from geochemical analyses.

- Geochemical analysis of major oxides and trace elements by X-ray fluorescence and atomic absorption spectroscopy (XRF and AAS). The results were used to check the validity of the non-destructive high-resolution XRF scanning.

- Carbon (C), organic (TOC), inorganic (TIC) and total (TC), and sulphur (S) by elemental analyser (ELTRA). S data was used to check the results of XRF core scanning. TOC values gave an estimate of organic matter and carbonate content, and they can be compared to other results from non-destructive techniques (XRF core scanning and colour).

7.3.4.- Palynological analysis

Cores S2 and S3 were selected for being the longest, most continuous and for covering a longer period of time. Sampling for palynological analyses was undertaken at the sedimentological laboratory of the IGME, CSIC in different phases of the project. 52 test-samples were collected from core S2 at different intervals and 160 samples were collected from core S3 maintaining a regular interval of 10 cm. Sediment samples, of about 10gr each, were kept in plastic bags and stored in a fridge at 4ºC until analyses.

All samples were processed at the Institute of Neotectonics and Natural Hazards – RWTH Aachen University (Germany). They were chemically treated with HCl (10%) to remove carbonates, KOH (10%) to remove humic acids, and Sodium Polytungstate (SPT: $3Na_2WO_4 \cdot 9WO_3 \cdot H_2O$) at 2.0-2.1 gr/cm^3 for densimetric separation. The final residue was mounted on slides with the use of glycerol. Pollen concentrations (grains/gr of dry sediment) were estimated by adding two *Lycopodium clavatum* tablets to each sample (Stockmarr, 1971). Palynomorphs were counted using an optical microscope at 400x and 1000x up to a minimum pollen sum of 300 terrestrial pollen grains. Palynomorphs were identified using published keys (Moore et al., 1991; Reille, 1992, 1995; Van Geel, 1978, 2001; Van Geel et al., 1980, 1986, 1989, 2003).

In order to correlate the evolution of the natural deposit and the anthropogenic impact on the landscape, some specific taxa were chosen and categorized in seven ecological palynomorph-based groups. These are: Anthropozoogenous herbs (*Malva sylvestris* type*, Polygonum persicaria* type*, Rumex acetosa* type*, Rumex*

acetosella type, *Rumex obtusifolia* type, *Centaurea*, Boraginaceae, *Plantago lanceolata* type, *Plantago media/major* type, *Urtica dioica* type); Coprophilous fungi (*Coniochaeta* (HdV-172), *Podospora* (HdV-368), *Sporormiella* (HdV-113), Sordariaceae undiff., *Chaetomium* (HdV-7), *Cercophora* (HdV-112), *Gelasinospora* (HdV-2), *Trichodelitschia* (HdV-546)); Erosive processes (*Pseudoschizaea circula*, *Glomus* (HdV-207)); Cerealia; Freshwater vegetation (*Typha latifolia* type, *Typha angustifolia* type, Cyperaceae, *Isoetes*, *Myriophyllum verticillatum* type, *Myriophyllum alternifolium* type, *Callitriche*, *Potamogeton*, Ranunculaceae, *Riccia*); Salt marsh vegetation (*Artemisia*, Chenopodiaceae, Apiaceae); and Marine influence palynomorphs (foraminiferal linings, dynocists). Moreover, sums of the arboreal (AP), shrubs and herbaceous taxa (NAP) were included.

Poaceae ≥45µm was considered as Cerealia type according to López-Sáez and López-Merino, (2005). Terrestrial pollen sum (TPS) excluded aquatic pollen types, which were included in the total sum (TS) together with Non-Pollen Palynomorphs. Palynological diagrams were plotted against age and depth using TiliaIT software (version 2.1.1, Illinois State Museum, Research and Collection Center, Springfield USA).

7.4.- Results

7.4.1.- Age-depth model

Two samples collected from the S2 and S3 cores were discarded as they presumably contain reworked material. Differences in sedimentation rates, variable among facies and over time, between cores prevented to combine the age-depth model of each core in a single one (Mediavilla et al., 2023).

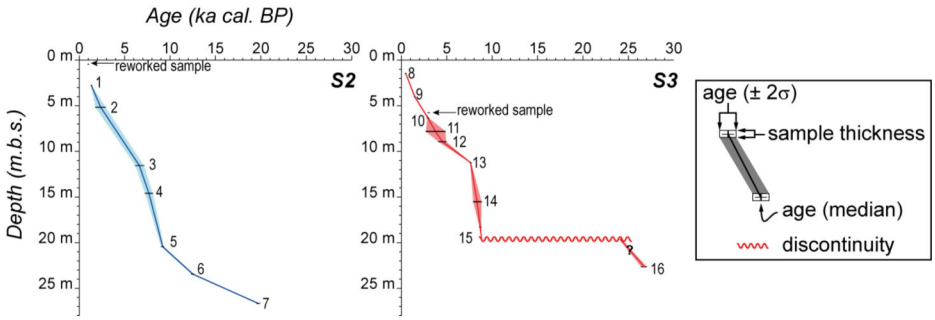

Figure 7.3. Age models for cores S2 and S3. Sample numbers correspond to those of Table 7.1.

Core S2 (ca. 20 ka cal BP) and core S3 (ca. 27 ka cal BP) begin with low sedimentation rates during the Late Pleistocene, which is interrupted by a discontinuity in core S3 and shows a continuous record in core S2 (Mediavilla et al., 2023). High sedimentation rates were identified in both cores until ca. 7 ka cal BP, when they decreased.

7.4.2.- Physical properties, mineralogical and geochemical composition of the sediments

Due to the homogeneity of the sediments, the more distinctive logs are those of colour that can be linked to their oxidation or reduction degree (Mediavilla et al., 2023).

The lowermost materials show higher values of the R/(G+B) and Grey indexes, indicative of warm pale tones. Similar R/(G+B) values can be observed at the top of the sections, but with darker tones (Grey scale). Between these levels, the R/(G+B) and Grey indexes fall except for some intercalations that show paler tones, and sometimes more ochre, coincidental with coarser siliciclastic levels.

The remaining parameters (gamma ray density, magnetic susceptibility and resistivity) are really homogeneous due to the dominance of clay minerals. They only change when coarser siliciclastic grains or mixed siliciclastic-bioclastic levels appear. However, the three parameters increase for coarser siliciclastic grains but not for bioclastic levels.

The studied sediments are composed by siliciclastics (mostly mud with some levels of sands and gravels) with contributions of carbonates (nodules and shells, sparse or in levels) and sparse organic matter, gypsum, pyrite, and halite (Fig. 7.4). Thus, the geochemical composition of these materials is controlled by this mineralogical composition (Mediavilla et al., 2023). The siliciclastic components (exogenous component) are best described by the content in Silicon (Si), Aluminum (Al), Zirconium (Zr), and Titanium Ti). The endogenous components are carbonates, gypsum, halite, and pyrite/haematite. Carbonates can be of either terrestrial or marine origin, while the remaining minerals are always of marine origin. Carbonates are recorded by TIC, Ca and CaO. They are present as two components: nodules and forming part of the matrix (edaphic) and shells (entire or broken, marine and transition). The content in S varies together with gypsum and pyrite content, but also with TOC. The upper and lower portions of the cores are S-poor and a sharp boundary can be traced with the S-rich levels. Cl and Br variations follow the Natrium (Na) and TOC changes, as well as the presence of halite. The lower part of cores S2 and S3 show low contents of Cl and Br, which increase somehow abruptly above the transition from the lowermost sands and gravels to the dark muds. This increment is also noticed in Na and TOC in cores S2 and S3. Upwards, they show an increasing trend that changes around the middle of both cores to a decreasing tendency in the uppermost part of the cores.

Geochemical data show no evidence of intensive human activity such as might result from metallurgy or an increase in agricultural activities, as possible proxy elements (metals or elements linked to organic matter) do not indicate any clear trend or distinct peaks above background trends, despite an increase of terrigenous input in the upper levels of the sections

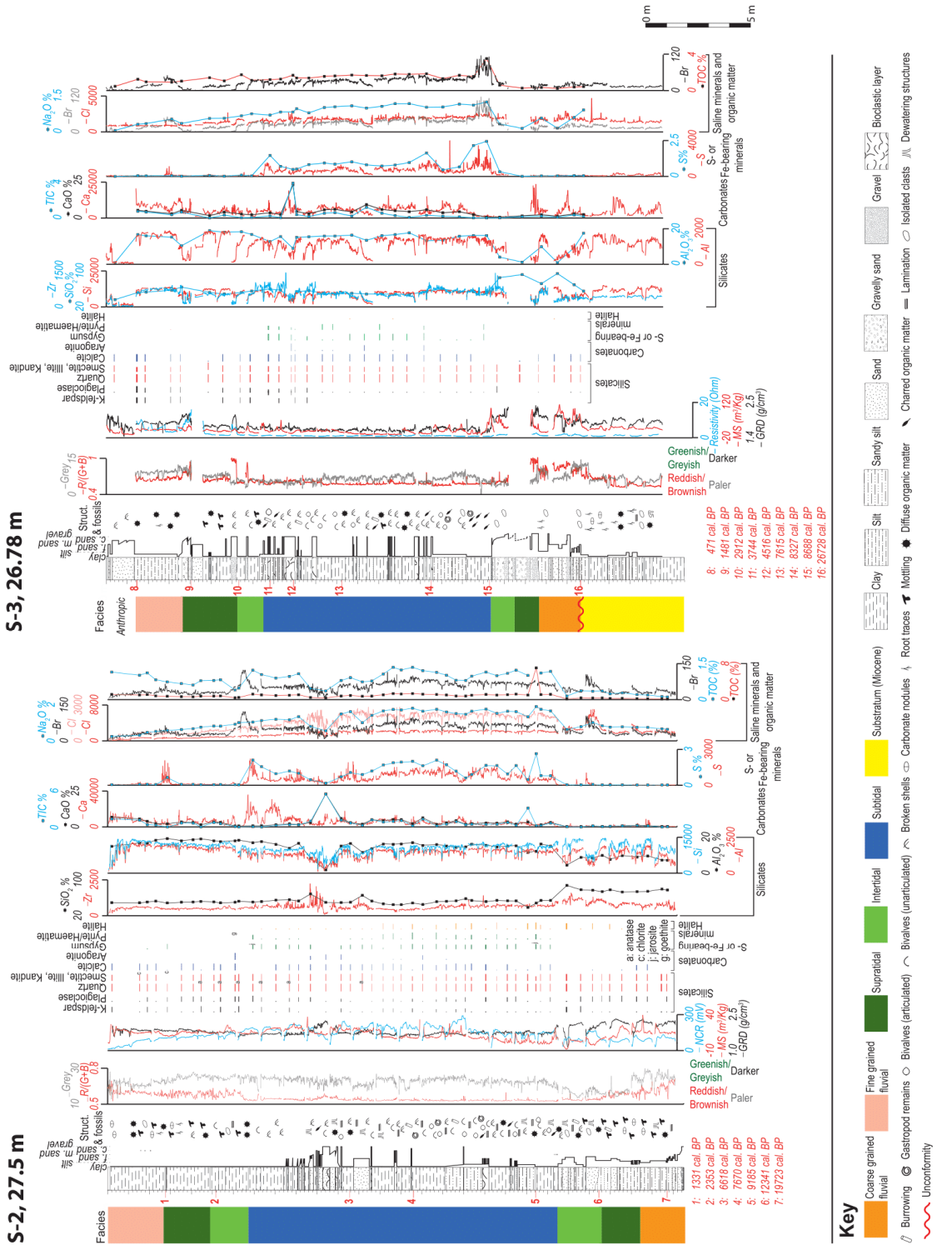

Figure 7.4.- Sections for cores S2 and S3 (modified from Mediavilla et al., 2023) showing selected parameters: facies, lithology, grain size, structures and fossil content, colour and geophysical logs (resistivity, magnetic susceptibility [MS], gamma ray density [GRD], non-contact resistivity [NCR]), mineralogy [relative abundance: width of the bars, thickness of the sample: height of the bars], selected oxides and inorganic (TIC) and organic (TOC) carbon (in percentage), and geochemical XRF scan (in counts per second).

7.4.3.- Facies and stratigraphy

Based on the visual description, geophysical, geochemical, and mineralogical analyses performed in cores S2 and S3, Mediavilla et al. (2023) identified different facies:

- Coarse grained fluvial facies: gravels, sands and muds, sometimes laminated, from ochre to orange, with grain-decreasing sequences. They show traces of roots, mottling and nodules indicative of edaphic processes.

- Fluvial wetland facies: brown to ochre muds with some sand layers. They show mottling, traces of roots, nodules and carbonaceous remains, as well as some scattered clasts. They contain freshwater ostracods and Characeae.

- Supratidal facies: brown to green muds with some levels of yellow sands and grey gravels forming grain-decreasing sequences. Traces of roots, hydromorphic features and flecks of organic matter are frequent. There are fragments of bivalves.

- Intertidal facies: green muds, sometimes laminated, with some levels of sands or gravels (siliciclastic or mixed with bioclasts). Broken or disarticulated bivalves are frequent, as well as mottled sediment due to iron oxides or organic matter. Bioturbation and fluid leakage may be present. These facies show a slight increase in Cl and Br content and evidence of halite.

- Subtidal facies: dark grey to black muds with bivalves in living position and disarticulated or broken shells. Sediments are laminated, bioturbated and have coarse-grained intercalations (mainly bioclastic). Gypsum-pyrite, hematite and halite are present. There are high contents of S, Cl, Br, and organic C. These facies contain marine foraminifera and marine ostracods.

These facies are arranged in four system tracts related to the sea level evolution (Mediavilla et al., 2023):

- The oldest deposits (27-20.6 ka cal BP) are only present in core S3. They are fluvial facies filling an erosive surface, carved on the Miocene substratum, during the end of the last glacial sea level fall and correspond to the falling stage systems tract (FSST).

- Upon them, in core S2, there are other fluvial deposits dated between 20.6 ka cal BP and 16.7 ka cal BP that are linked to the beginning of the last sea level rise and form the lowstand systems tract (LST).

- From 16.7 ka cal BP to 7 ka cal BP, the sea level rise rate was the greatest causing the progressive flooding of the basin and the upwards transition to supratidal (ca. 17-12 ka cal BP in core S2, ca. 11-10 ka cal BP at core S3), intertidal (ca. 12-10 ka cal BP in core S2, 10-8.7 ka cal BP in core S3) and subtidal

(ca. 10-7 ka cal BP in core S2, ca. 8.7-7 ka cal BP in core S3) deposits that represent the transgressive systems tract (TST).

- From 7 ka cal BP until present, the sea level rise rate falls dramatically causing a shallowing upwards sequence, from subtidal (7-3.2 ka cal BP in core S2, 7-3.5 ka cal BP in core S3) to intertidal (3.3-2.2 ka cal BP in core S2, 3.5- 2.5 ka cal BP in core S3), supratidal (2.2-1.3 ka cal BP in core S2, 2.6-1.3 ka cal BP in core S3) and fluvial facies, that records the closing of the basin during the highstand systems tract (HST).

7.4.4.- Palynology

Of the 52 samples collected from core S2, one was palynologically sterile. Of the 160 samples collected from core S3, those from 23 m to the bottom belonged to pre-Quaternary chronologies and thus were excluded from this research. Samples between 19 m and 23 m were found to be palynologically sterile, as well as two samples from the top. Therefore, a total of 51 samples from core S2 and 132 samples from core S3 are included in the present study.

Considering the selected ecological groups and sedimentary facies, the results are synthetized in Table 2 and illustrated in Figure 7.5.

Table 7.2.- Palynological synthesis for cores S2 and S3 according to the main vegetation trends, correlated with the different sedimentological facies, their depth (cm) and age ranges (cal BP).

JAN S2			
Sedimentary facies	**Depth range (cm)**	**Age range (cal BP)**	**Palynological synthesis**
Fluvial wetland	0-273.6	< 1310	High levels of shrubby and herbaceous taxa. Decrease of freshwater and salt marsh vegetation, with irregular values. Rise of coprophilous fungi and indicators of erosive processes.
Supratidal	273.6-489.5	1310-2239	Maximum values of shrubs and decrease of arboreal pollen. Increase of freshwater vegetation and irregular values of salt marsh taxa. Irregular values of anthropogenic indicators.
Intertidal	489.5-672.0	2239-3393	Rise of shrubs and decrease of arboreal pollen. Increase of freshwater vegetation and decrease of salt marsh taxa. Decrease of coprophilous fungi and indicators of erosive processes in the lowest samples. Presence of Cerealia.
Subtidal	672-2136.3	3393-10214	Increase of arboreal pollen, shrubs and freshwater taxa in the first half of the phase, with a posterior decrease. High values of salt marsh vegetation. Progressive increase of anthropogenic indicators and presence of Cerealia.
Intertidal	2136.3-2345	10214-12529	Dominance of herbaceous taxa. Variable values of freshwater and salt marsh vegetation. Marine indicators in the lowest sample.

Supratidal	2345-2542.7	12529-16957(¿)	Dominance of herbaceous taxa, increase of shrubs in some samples. Slight rise of salt marsh and fresh water vegetation with variable values. Marine indicators in the uppermost sample.
Coarse grained fluvial	>2542.7	>16957 (¿)	Dominance of herbaceous taxa, increase of shrubs in the uppermost sample.
JAN S3			
Sedimentary facies	**Depth range (cm)**	**Age range (cal BP)**	**Palynological synthesis**
Fluvial wetland	0-361.5	<1316	Decrease of shrubs, high values of herbaceous taxa and slight increase of arboreal pollen towards the end of the phase. Decrease of aquatic taxa. Increase of coprophilous fungi and indicators of erosive processes. Presence of Cerealia.
Supratidal	361.5-595.7	1316-2680	Peak of shrubs and freshwater vegetation, with irregular values. Progressive decrease of salt marsh taxa. Drop of anthropogenic indicators at the beginning of the phase with a posterior increase.
Intertidal	595.7-748.7	2680-3562	Rise of shrubs and freshwater taxa. Peak of salt marsh vegetation with posterior decrease. Drop of anthropogenic indicators at the beginning of the phase with a posterior increase.
Subtidal	748.7-1836.7	3562-8696	Increase of arboreal and freshwater taxa in the first half of the phase and posterior decrease. Progressive increase of shrubs towards the end of the phase. High values of salt marsh taxa vegetation and presence of marine indicators. High percentages of coprophilous fungi, progressive increase of anthropozoogenous herbs. Presence of Cerealia.
Intertidal	1836.7-1952.0	8696-8846	Lowest samples are sterile from a palynological point of view. Peak of herbaceous taxa in the uppermost sample.
Supratidal	1952-2067.4	8846-8995	Sterile samples from a palynological point of view.
Coarse grained fluvial	2067.4-2266.2	(hiatus)-26822	Sterile samples from a palynological point of view.

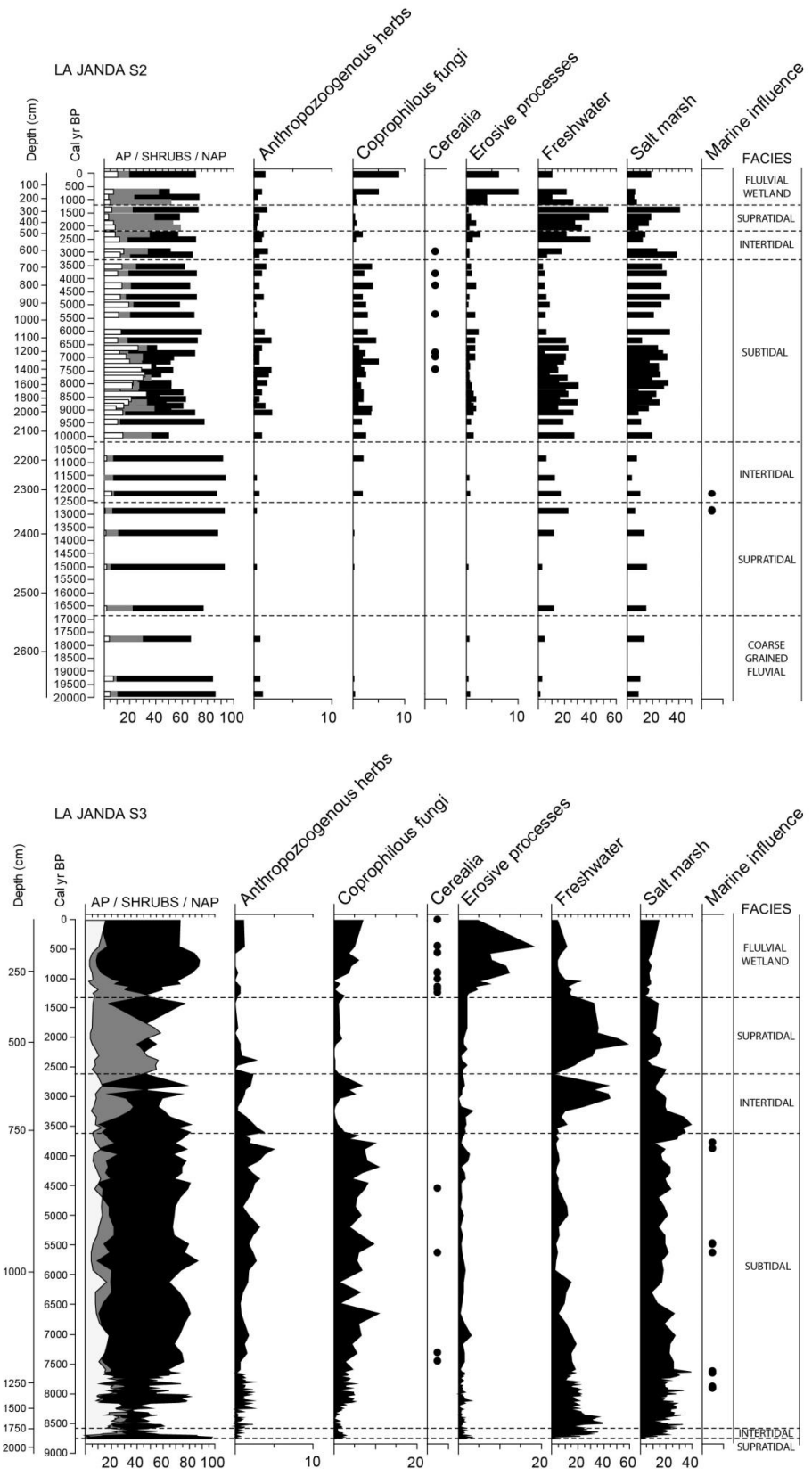
LA JANDA S2
Depth (cm)
Cal yr BP
AP / SHRUBS / NAP
Anthropozoogenous herbs
Coprophilous fungi
Cerealia
Erosive processes
Freshwater
Salt marsh
Marine influence
FACIES
FLULVIAL WETLAND
SUPRATIDAL
INTERTIDAL
SUBTIDAL
INTERTIDAL
SUPRATIDAL
COARSE GRAINED FLUVIAL
LA JANDA S3
Depth (cm)
Cal yr BP
AP / SHRUBS / NAP
Anthropozoogenous herbs
Coprophilous fungi
Cerealia
Erosive processes
Freshwater
Salt marsh
Marine influence
FACIES
FLULVIAL WETLAND
SUPRATIDAL
INTERTIDAL
SUBTIDAL
INTERTIDAL
SUPRATIDAL

Figure 7.5. Synthetic palynological diagrams of cores S2 (histogram) and S3 (curves) plotted against depth and age. They both show % of arboreal (AP), shrubby and non-arboreal (NAP) pollen, as well as the ecological groups listed above. Dots indicate values below 3%. Dashed lines represent the boundaries between sedimentary facies.

Although with variable values, both cores display high percentages of non-arboreal pollen through the sequences, which is in line with the important input of local herbaceous plants in a coastal deposit of these characteristics (Fig. 7.5). Arboreal taxa, with lower values, show an increase between ca. 10-7 ka cal BP and a progressive drop towards the top of both sequences. Shrubs show a similar trend but they also rise importantly between ca. 3-1 ka cal BP. Freshwater taxa show high percentages between ca. 10-7 ka cal BP and ca. 3-1 ka cal BP in core S2, and between ca. 8.7-7.5 ka cal BP and ca. 3-1.5 ka cal BP in core S3. By its turn, salt marsh vegetation, which shows a negative correlation with freshwater taxa in most cases, displays the highest values between ca. 9-3 ka cal BP. Indicators of marine influence appear at ca. 13.5-12.5 ka cal BP in core S2 and ca. 8, 5.5 and 4 ka cal BP in core S3. These three groups show a coherent correlation with the sedimentological results (Table 2).

Anthropozoogenous herbs slightly increase from ca. 9 ka cal BP onwards, with maximum values ca. 9-6 ka cal BP and ca. 3.5-2.5 ka cal BP in core S2, and ca. 6-2.5 ka cal BP in S3 (Fig. 7.5). However, it must be taken into account that these values are always below 6% and extremely irregular, especially in core S3, which has a higher resolution.

Coprophilous fungi also start to increase from ca. 9 ka cal BP onwards in both cores, showing percentages below 5% in all the samples from S2 core (except the uppermost) and higher values in core S3 (above 10% in some cases). Maximum percentages in core S2 appears ca. 9, 7.5, 6.5, 5.5-3.5 ka cal BP and the two uppermost samples. In core S3, they rise between ca. 7.5-4.3 ka cal BP and from 1 ka cal BP onwards. Indicators of erosive processes show values below 5%, except from ca. 1.5 ka cal BP onwards, when they rise in both cores. Cerealia appears for the first time ca. 7.4 ka cal BP in cores S2 and S3 and they will be present in isolated samples of both cores from this chronology to the top of both sequences (Fig. 7.5).

It must be noticed that, although the sampling resolution is different in both cores, there is a good correlation in the results once they are overlapped (Fig. 7.6), with a similar trend and a slight and constant mismatch. This is due to the characteristics of the deposit and the locations of the boreholes which, although quite close, show different rhythm in the evolution of the basin (especially in the lower half). Another important observation is the better preservation of palynomorphs in samples from core S2 for oldest chronologies, while samples from core S3 are palynologically sterile from ca. 8.7 ka cal BP to the bottom (Fig. 7.6).

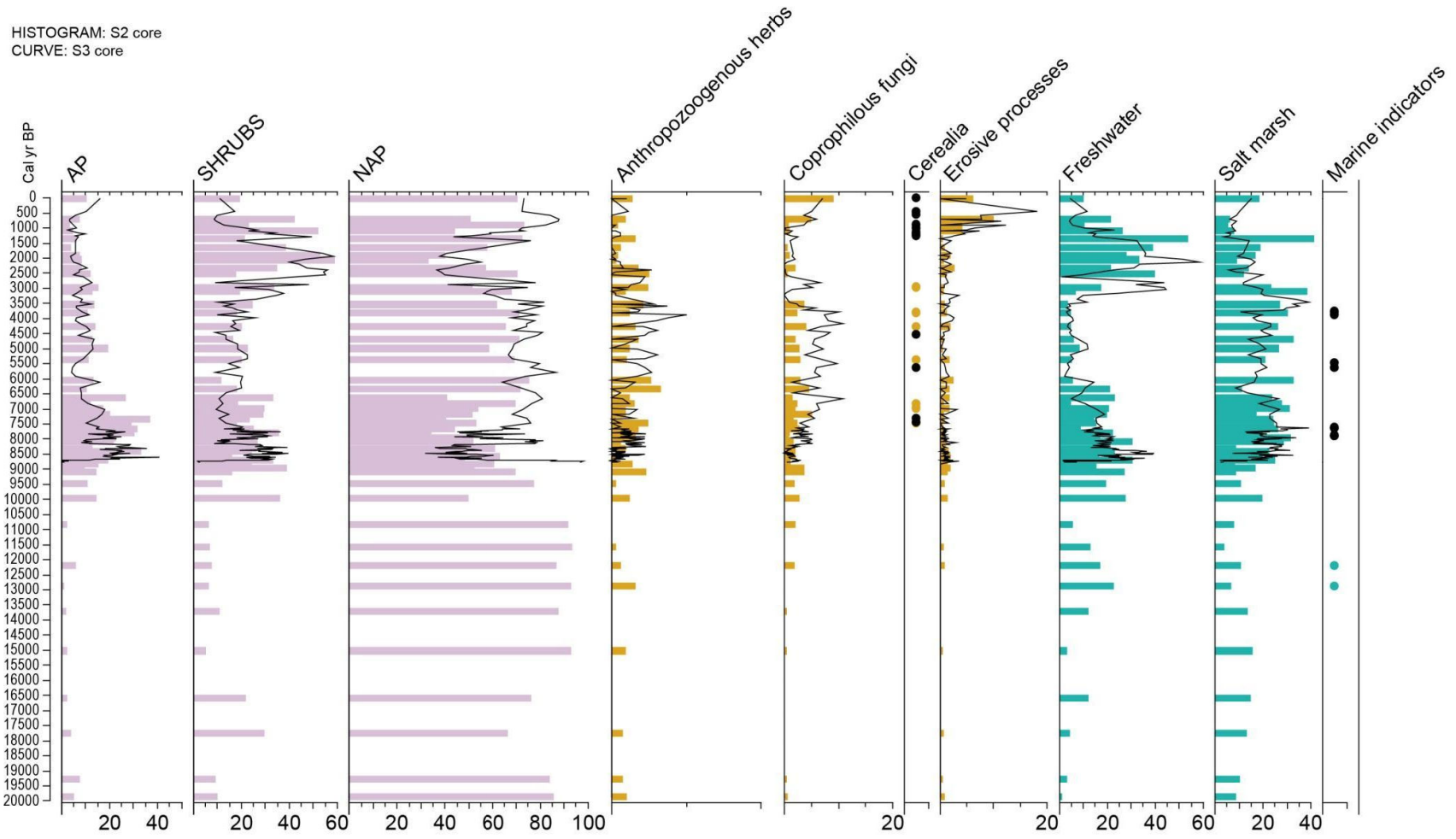

Figure 7.6. Palynological diagrams of cores S2 and S3 overlapped, plotted against age, and expressed in percentages with the selected categories. Histograms and coloured dots correspond to core S2 and black curves and dots to core S3. Dots represent values below 3%.

7.5.- Discussion: landscape evolution and prehistoric human occupation in La Janda basin

7.5.1. Late Pleistocene- Early Holocene: Upper Palaeolithic-Mesolithic (ca. 27-7.8 ka cal. BP)

This period coincides with the fall (FSST) and later rise (LST+TST) of sea level during which the basin transformed from a narrow fluvial valley (FSST+LST) to a progressively wider and less stepper estuarine basin (TST).

During the Late Pleistocene, the palaeovegetation cannot be reconstructed reliably and in detail due to the low resolution sampling from core S2 and the palynologically sterile samples in core S3, which mainly correspond to coarse grained fluvial facies. However, pollen samples from core S2 (corresponding to the beginning of the seal level rise and flattening of the landscape) indicate a predominance of herbaceous taxa, which could suggest an open landscape dominating the depression or could be the consequence of a bias affecting pollen preservation due to taphonomic alterations in fluvial deposits (Hunt, 1987; Carrión et al., 2009). La Janda would be progressively affected by the sea since ca. 17 ka cal BP (S2), enhancing the development of vegetal communities typical from temporary ponds, wetlands, and marshlands that are recorded in the transition from supratidal to intertidal facies. The presence of marine elements in the transition between supratidal to intertidal environments in core S2 corroborates the growing marine influence, coincidental with the increase in salinity recorded in the sediments. However, an important part of the floodplain would still be emerged at the marginal areas of the basin and, in some cases, subject to oxidation; this could be a factor to explain the differential preservation of palynomorphs between cores and the sterile samples in the S3 sequence (Fig. 7.7).

It should be highlighted the absence or punctual presence of anthropogenic indicators during this period, always in low percentages (Fig. 7.7). Some of the taxa included in the category of anthropozoogenous herbs can be found in the landscape without implying anthropogenic influence, especially when they are not correlated to other markers (López-Sáez et al., 2003; Deza-Araújo et al., 2020; Alba-Sánchez et al., 2021).

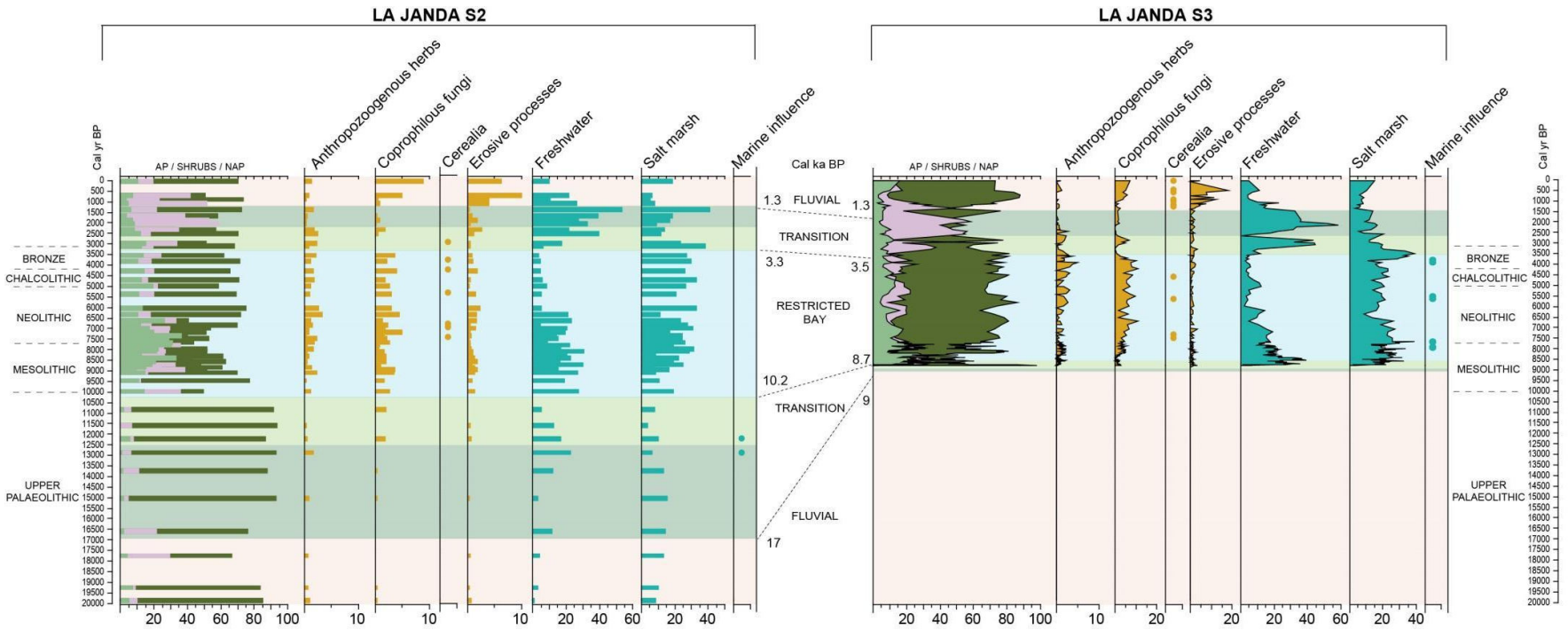

Figure 7.7. Cores S2 (left) and S3 (right) plotted against age (cal yr BP) showing the ecological palynomorph-based groups selected for this study (% values). The correlation between the environmental phases and their chronological boundaries (ca. cal ka BP) in both cores are described in the centre of the graphic. Cultural periods from the Upper Palaeolithic to the Bronze Age are displayed in both extremes of the plot.

Figure 7.8.- Map of the study area indicating the main rivers, the hydrographic basin of the Barbate River with black dashed lines and the Upper Palaeolithic sites considered in this research. Blue dots indicate the drilling location of the S2 and S3 cores. Red dots are used for sites located near La Janda basin and yellow dots for those located further away: 1 (Cueva de La Jara I), 2 (Cueva de Atlanterra), 3 (Cueva del Moro), 4 (Cueva Ranchiles), 5 (Cueva Helechar II), 6 (Cueva del Realillo I), 7 (Cueva de Las Palomas I), 8 (Caños de Meca), 9 (Cueva de Bailaoras II-Cueva del Ciervo), 10 (Embarcadero del Río Palmones). Light blue dotted areas indicate the potential supra/intertidal zones during the Late Pleistocene in La Janda basin.

The palaeoenvironmental reconstruction indicates that during the beginning of this period, the coastline was placed under present sea level and the basin was a fluvial plain, offering new land to settle (Fig. 7.8). The study of the open-air and cave sites ascribed to the Upper Palaeolithic supports the interpretation of a functional diversity of occupations, with residential camps, hunting camps and resource-gathering areas in different environments (Ramos Muñoz et al., 2006; Ramos Muñoz, 2008). In this regard, it should be also considered that the Iberian Peninsula has been recognised as a refuge for biodiversity in glacial periods and times of climatic instability (Carrión et al., 2010), which would have made it an attractive area for the establishment of hunter-gatherers.

During the Early Holocene (11.7-8.2 ka BP) the basin was progressively flooded by marine waters and transformed into a flat estuarine area surrounded by hills, while the terrestrial environments displaced upstream. Forests, accompanied by their understorey, progressively expanded through the region reaching maximum values (Fig. 7.5, 7.6 and 7.7). Saltmarsh vegetation gained more prominence together

with the important presence of freshwater communities, suggestive of the existence of a variety of transitional environments. By this time, anthropogenic indicators, although slightly higher than in the previous period, still display low values (Fig. 7.7).

The marine incursion caused changes in the landscape, resources, and the availability of settlement areas for human groups (Mediavilla et al., 2023). Numerous archaeological sites from earlier periods were submerged, which have conditioned the documentation of the archaeological record in lowlands and littoral areas, and resulted in explanations of a supposed population "decline" or occupational vacuum (Arteaga and Hoffmann 1999).

There is only one site of these chronologies preserved in the local study area (Fig. 7.9), while most of the information about the Mesolithic in the region is provided by the Embarcadero del Río Palmones (Ramos Muñoz, 2004a) and El Retamar settlements (Ramos Muñoz and Lazarich, 2002) (Fig. 7.9). Studies at both sites indicate that hunter-gatherer groups focused on the exploitation of marine resources, but they also carried out hunting activities and consumption practices at the sites.

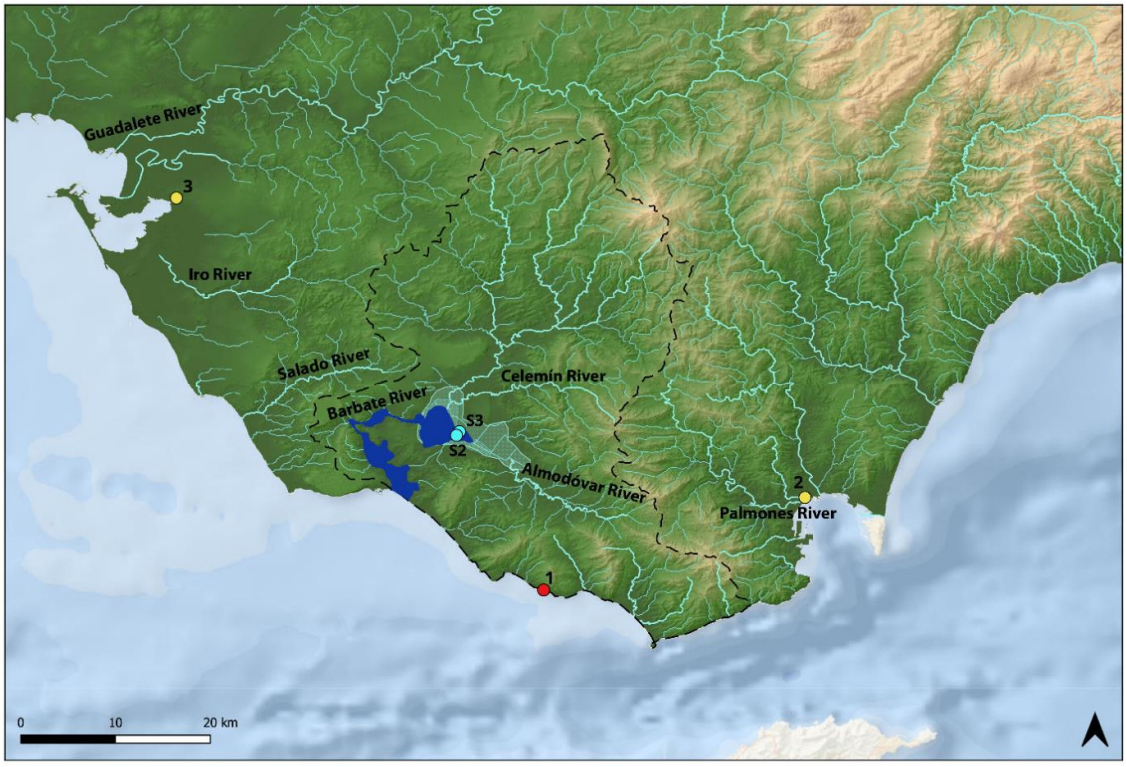

Figure 7.9.- Map of the study area indicating the main rivers, the hydrographic basin of the Barbate River with black dashed lines, and the Mesolithic sites considered in this research. Blue dots indicate the drilling location of the S2 and S3 cores. Red dots are used for sites located near La Janda basin and yellow dots for those located further away: 1 (Cala Picacho), 2 (Embarcadero del Río Palmones), and 3 (El Retamar). Light blue dotted areas

indicate the potential supra/intertidal zones and dark blue areas show the subtidal zones in La Janda basin between ca. 11-7 ka cal BP.

The progressive environmental changes during the Early Holocene led to the development of diverse ecosystems (marine, brackish, fluvial) with associated biotic diversity and productivity, which turned these areas favourable for activities such as fishing and shell gathering. Moreover, the expansion of forested areas may also have led to an increase in vegetal resources and the development of new areas frequented by animals, thus allowing for hunting activities.

7.5.2. Mid Holocene: Neolithic (ca. 7.8-5 ka cal BP)

Sediments for this period record the gradual decrease in the sea level rise rate that promoted the infill of the estuary and its progressive shallowing and expansion. Thus, the area was transformed in a wide and flat tidal plain but still with a noticeable influence of marine waters. A progressive decrease of the arboreal taxa can be placed from ca. 7.5 ka cal BP onwards, with a posterior and constant increase of shrubs (Fig. 7.5, 7.6 and 7.7). Freshwater communities gradually decline in favour of salt marsh vegetation and marine influence is also detectable in the punctual presence of marine indicators in core S3 at ca. 7.5 and 5.5 ka cal BP (Fig. 7.7), being coherent with salinity in geochemical proxies. Whether possible peaks of salinity were caused by marine pulses or aridity crises (Mediato et al., 2020) is something that should be further explored.

A visible increase of anthropogenic indicators is confirmed in both cores. Anthropozoogenous herbs and coprophilous fungi rise between ca. 7.5- 6 ka cal BP in core S2 and from 7 ka cal BP onwards in core S3 (Fig. 7.7). The ascospores of coprophilous fungi occur on the dung of wild herbivores as well as domestic livestock, being a good indicator of their presence (Van Geel et al., 2003; Cugny et al., 2010; Lee et al., 2022). This may point to the presence of wild herbivores congregating near the estuary, but this may also be indicative of livestock activities in nearby areas.

It should be highlighted the first presence of cereals ca. 7.4 ka cal BP in both cores, which also appear at ca. 6.9, 6.8, 5.3 ka cal BP in core S2 and at 7.3, 5.6, 4.5 ka cal BP in core S3 for this period (Fig. 7.7). However, only one grain of Cerealia was identified in each of these samples ca. 7.4 ka cal BP, suggesting a regional origin rather than local (López-Sáez and López-Merino, 2005). Although anthropozoogenous herbs and coprophilous fungi are present, there are not enough proves to confirm the practice of such activities, at least from a local point of view. Interestingly, there is an increase in the supply of clastic sediments to the coast, but there is no evidence of its relation to increasing erosion linked to agricultural practices or to the beginning of the retreat of the coastline (Mediavilla et al., 2023).

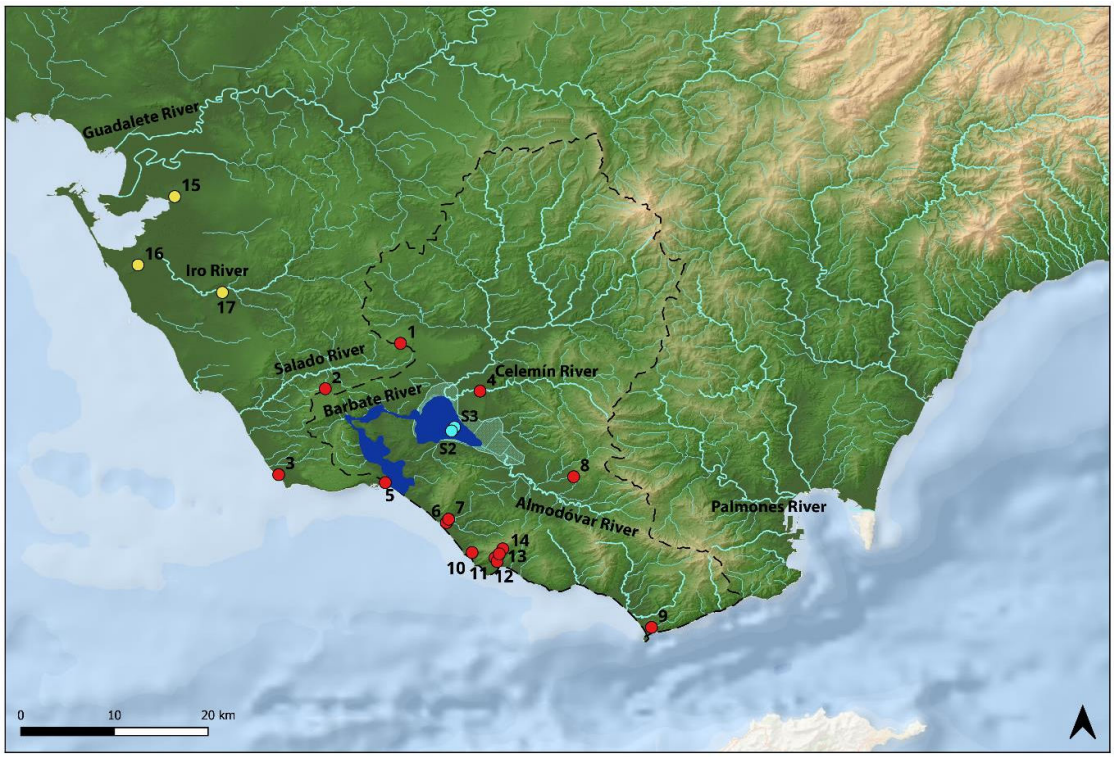

Figure 7.10.- Map of the study area indicating the main rivers, the hydrographic basin of the Barbate River with black dashed lines, and the Neolithic sites considered in this research. Blue dots indicate the drilling location of the S2 and S3 cores. Red dots are used for sites located near La Janda basin and yellow dots for those located further away: 1 (S.José Malcocinado), 2 (SET Parralejos), 3 (Zahora), 4 (Poblado Charcones), 5 (Barbate), 6 (Abrigo Fuentesanta), 7 (Abrigos Bullón y Peñón), 8 (Aciscar dolmens), 9 (Cueva de Las Palomas I), 10 (Cueva de Atlanterra), 11 (Cueva Ranchiles), 12 (Pico Camarinal-Arrollo Cañuelo), 13 (Cueva Helechar II), 14 (Cueva del Realillo I), 15 (El Retamar), 16 (Campo de Hockey), 17 (Esparragosa). Light blue dotted areas indicate the potential supra/intertidal zones and dark blue areas show the subtidal zones in La Janda basin ca. 7 ka cal BP.

The material culture at some Neolithic sites, such as La Esparragosa, SET Parralejos and Campo de Hockey (Fig. 7.10), indicates the practice of activities such as fish processing (Clemente Conte et al., 2010, Clemente Conte and Mazzuco, 2019), domestic work, and hunting (Ramos Muñoz et al., 2022), implying the existence of a diversified economy in the area (Arteaga and Roos, 2009; Pérez Rodríguez, 2003, 2005, 2008; Ramos Muñoz, 2004b). Agricultural practices were not consolidated until the 6th millennium BP (Pérez Rodríguez et al., 2005; Pineda and Toboso, 2010; Ramos Muñoz et al., 2008, 2022; Vijande Vila et al., 2019), moment from which the presence of seeds, the adoption of crop-storage and the increment of polished tools (mills, grinding wheels, etc.) confirm the relevance of agriculture within human groups. Nonetheless, although the archaeobotanical record can only confirm the existence of agricultural activities, in all probability, around 6 ka cal BP for the study area (López-Sáez et al., 2011), some authors suggest the existence of small human populations with a mixed cereal-livestock-based economy, according to new data for the Early Neolithic (ca. 7.5-7 ka cal BP) (García-Rivero et al., 2022).

The full development of a restricted estuary during the entire Neolithic reiterates the existence of a coastal ecosystem rich in resources. In addition to hunting, fishing and shell gathering activities, agricultural and livestock practices were well documented in the archaeological record, as well as in the palynological data from La Janda (Fig. 7.7). In line with these results, anthracological and palynological studies carried out at some sites indicate that scrublands were the dominant vegetal trend and the anthropogenic pressure resulted in the degradation of the forests (Uzquiano et al., 2021). This may be corroborated by the expansion of pastures and ruderal herbs, which together with the presence of nitrophilous taxa, Glomus, and coprophilous fungi, constitute a clear exponent of animal herding practises at some sites (Ruiz Zapata and Gil García, 2019; Uzquiano et al., 2021).

7.5.3. Mid-Late Holocene: Chalcolithic and Bronze Age (ca. 5-3 ka cal BP)

The palaeoenvironment of La Janda is still characterised by the existence of a restricted estuary connected to the Atlantic Ocean until ca. 3.5 and 3.2 ka cal BP in cores S3 and S2, respectively (Mediavilla et al., 2023). However, a gradual transition to a terrestrial environment is recorded during the last centuries of the 4th millennium BP with new emerged lands that are still under tidal influence (Fig. 7.7).

Vegetation remains similar to the previous period, with high values of local herbaceous taxa, a progressive increase of shrubs, and low percentages of arboreal vegetation (Fig. 7.5, 7.6 and 7.7). Freshwater communities display low values, while salt marsh vegetation reaches high percentages, and marine indicators appear, corroborating the influence of the ocean at this point of the sequence (Fig. 7.7). It should be noted that there is a peak of salt marsh taxa paralleled by the decrease of coprophilous fungi and, to a lesser extent, anthropozoogenous herbs between ca. 3.6-3.2 ka cal BP in both cores (Fig. 7.7). Anthropogenic markers show some of their highest values during this period, and their simultaneous decline during this time lapse may suggest a temporary cessation of anthropogenic impact, perhaps in relation to activities such as animal husbandry.

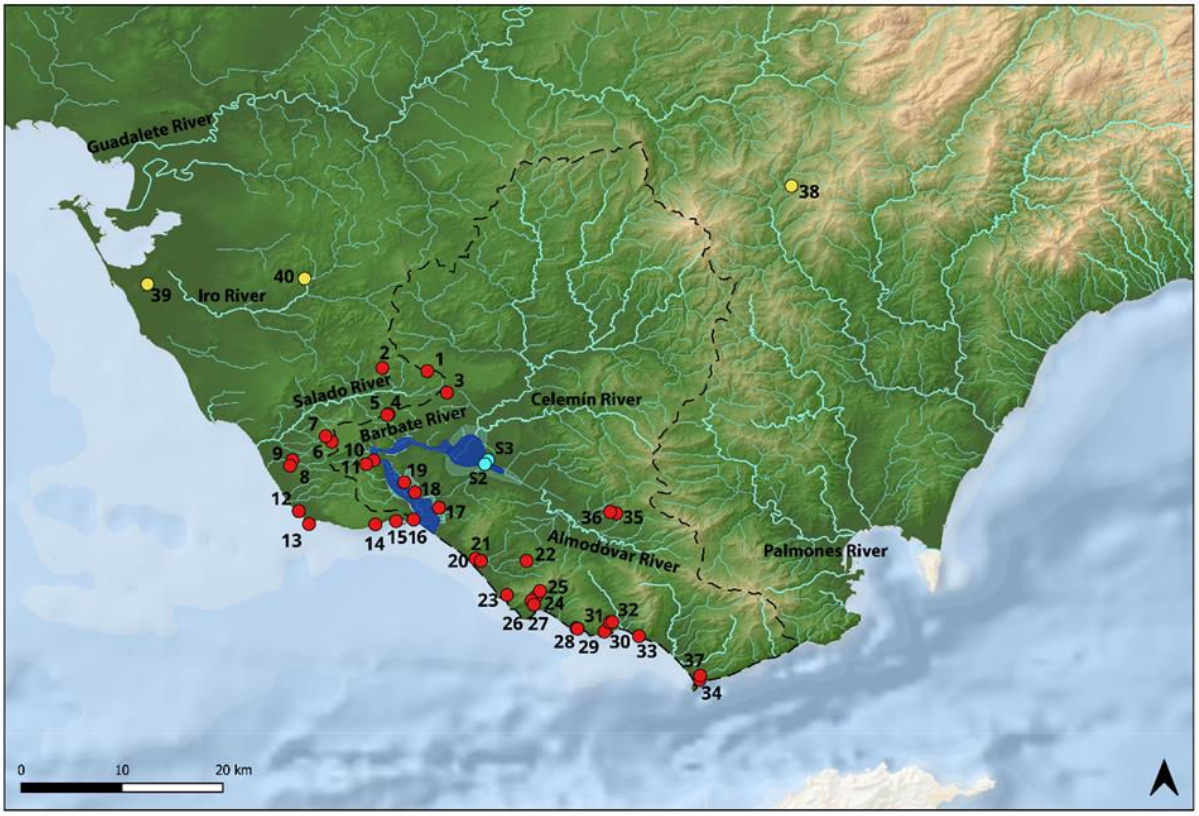

Figure 7.11.- Map of the study area indicating the main rivers, the hydrographic basin of the Barbate River with black dashed lines, and the Chalcolitic-Bronze Age sites considered in this research. Blue dots indicate the drilling location of the S2 and S3 cores. Red dots are used for sites located near La Janda basin and yellow dots for those located further away: 1 (Mesa Algar II), 2 (Cerro Cantabria), 3 (La Cruz), 4 (Nájara II), 5 (Nájara III), 6 (Carretera Muela), 7 (Arroyo Flamenquilla), 8 (Benitos del Lomo I), 9 (Benitos del Lomo II), 10 (Paseo Canalejas), 11 (Buenavista), 12 (Zahora), 13 (Trafalgar), 14 (Breña), 15 (Chorro-Yerbabuena), 16 (Barbate), 17 (Manzanete), 18 (Fuente del Viejo) , 19 (Medina Sidonia), 20 (Dólmenes Barranco Caño Arado), 21 (Peñas de Bullón), 22 (El Almarchal), 23 (Cueva de Atlanterra), 24 (Cueva del Realillo I), 25 (Cueva Helechar II), 26 (Cueva Ranchiles), 27 (Pico Camarinal y Arroyo Cañuelo), 28 (Baños Claudio), 29 (Cala Picacho), 30 (Punta Paloma), 31 (Los Algarbes), 32 (Los Algarbes necropolis), 33 (Torre Peña I), 34 (Tarifa), 35 (Aciscar dolmens), 36 (Purrenque-Larrázez dolmens), 37 (Cueva de las Palomas I)38 (Cueva de las Motillas), 39 (Campo de Hockey), 40 (Cerro Berrueco). Light blue dotted areas indicate the potential supra/intertidal zones and dark blue areas show the subtidal zones in La Janda basin between ca. 5- 3 ka cal BP.

A high number of archaeological sites are identified during the Chalcholithic and Bronze Age (Fig. 7.11), with settlement clusters located in strategic positions with good communication and visibility, some of them around important centres. Interestingly, some of the sites located in the littoral are dedicated to agricultural practices, while others show a preference for livestock activities, which corroborates the reasons for the increase of anthropogenic markers in the palynological record. At some sites, open landscapes dominated by Mediterranean and xeric taxa were documented together with maximum values of ruderal and nitrophilous herbs (Uzquiano et al., 2021). Although a compelling evidence of

anthropization is recorded in other natural deposits of the study area (López-Sáez et al., 2018), the geochemistry from La Janda does not show any evidence of intensive human activity such as might result from metallurgy or an intensification in agricultural practices. One explanation may be that soil salinity would have hampered the development of local agricultural activities, which would have been developed on more suitable soils in nearby areas. These practices would intensify in the basin with the establishment of a landscape composed of fluvial wetlands and ephemeral ponds in less saline soils.

7.6.- Conclusions

The multiproxy approach here presented has proven to be useful to identify different palaeoenvironmental phases in La Janda basin during the last ca. 20000 years, as well as to infer some anthropogenic processes in the landscape.

During the Late Pleistocene, the basin was occupied by different fluvial systems until the sea progressively flooded it. A transitional phase with increasing marine influence affecting the area is recorded in core S2 between ca. 17-10.2 ka cal BP. However, some parts of the basin would still be emerged as recorded in core S3, which is not affected by the sea until ca. 9 ka cal BP. During this time frame, more or less corresponding with the Upper Palaeolithic period, the presence of hunter-gatherer groups is recorded in the area. Most of the settlements are open-air sites identified as residential camps, hunting camps and resource-gathering areas. However, there are also a high number of caves with artistic manifestations that reflect part of the symbolic world of these human groups.

The first stages of a restricted estuary connected to the Atlantic Ocean through the Barbate River mouth are recorded ca. 10.2 and 8.7 ka cal BP in cores S2 and S3, respectively. During this period corresponding to the Mesolithic, seasonal camps of hunter-gatherer-fisher groups that mastered the exploitation of coastal and vegetal resources were documented. However, many archaeological sites from earlier periods may have been submerged as consequence of the sea level rise.

The first agricultural practices can be framed in a landscape defined by a restricted estuary already stablished during the Neolithic (ca. 7.8-5 ka cal BP). A higher number of sites are reported during this period and the human impact is visible in the record through the presence of anthropogenic markers related to agricultural and animal herding activities, especially from ca. 7 ka cal BP. In both S2 and S3 cores, single pollen grains of Cerealia were identified at ca. 7.4 ka cal BP. This, although attractive for the chronologies in which they are framed (Early Neolithic), must be taken with caution and should always be correlated with the archaeological record for a better interpretation. An increased anthropogenic impact is visible at some archaeological sites and other natural deposits such as Doñana during the Chalcolithic-Bronze Age (ca. 5-3 ka cal BP) (López-Sáez et al., 2018). During this period, La Janda basin is occupied by the restricted estuary that would progressively give way to intertidal areas ca. 3.5 and 3.2

ka cal BP (S3 and S2, respectively). Anthropogenic markers related to livestock and agricultural practices are present in both cores, indicating a significant human footprint on the landscape. However, this does not seem to be intensive enough to be recorded by the geochemistry record, which may be reflecting a local signal.

Finally, from ca. 1.3 ka cal BP onwards, the terrestrialization process affecting La Janda culminates with the development of emerged sediments and a fluvial landscape composed of wetlands and ephemeral ponds in different parts of the basin. Over the last centuries, the eminently fluvial and less saline landscape has been exploited for agricultural and livestock activities, which is reflected in the increase of coprophilous fungi and cereals. At the same time, the highest percentages of erosive process indicators (mostly *Glomus*) are recorded, probably as result of these farming activities or the development of new soils.

7.7.- Acknowledgements

This research was funded by the Deutsche Forschungsgemeinschaft-DFG (project no.57444011 – SFB 806); a "Severo Ochoa" extraordinary grant for excellence IGME, CSIC (AECEX2021); the Consejería de Cultura of the Junta de Andalucía (projects DGBC/IDBC3741 and 4766); the FEDER/MINECO-AGEINVES (HAR2017-8734P); and the Operational Programme and Department of Economy, Knowledge, Business and University of the Regional Government of Andalusia (FEDERUCA18-106917). The authors would also like to thank the direction and management of the "Las Lomas" farm for their assistance both in the precise positioning of the drilling points and during the drilling process.

8.- Environmental changes and cultural transitions in SW Iberia during the Early-Mid Holocene

This chapter is a slightly modified version of an article published in Applied Sciences:

Val-Peón, C., Santisteban, J.I., López-Sáez, J.A., Weniger, G.-C., Reicherter, K. (2021). Environmental changes and cultural transitions in SW Iberia. *Applied Sciences*, 11: 3580. https://doi.org/10.3390/app11083580

Abstract

The SW coast of the Iberian Peninsula experiences a lack of palaeoenvironmental and archaeological data. With the aim to fill this gap, we contribute with a new palynological and geochemical dataset obtained from a sediment core drilled in the continental shelf of the Algarve coast. Archaeological data have been correlated with our multi-proxy dataset to understand how human groups adapted to environmental changes during the Early-Mid Holocene, with special focus on the Mesolithic to Neolithic transition. Vegetation trends indicate warm conditions at the onset of the Holocene followed by increased moisture and forest development ca. 10–7 ka BP, after which woodlands are progressively replaced by heaths. Peaks of aridity were identified at 8.2 and 7. 5 ka BP. Compositional, textural, redox state, and weathering of source area geochemical proxies indicates abrupt palaeoceanographic modifications and gradual terrestrial changes at 8.2 ka BP, while the 7.5 ka BP event mirrors a decrease in land moisture availability. Mesolithic sites are mainly composed of seasonal camps with direct access to the coast for the exploitation of local resources. This pattern extends into the Early Neolithic, when these sites coexist with seasonal and permanent occupations located in inland areas near rivers. Changes in settlement patterns and dietary habits may be influenced by changes in coastal environments caused by the sea-level rise and the impact of the 8.2 and 7.5 ka BP climate events.

Keywords: Palaeoenvironment, Mesolithic, Neolithic, Palynology, Geochemistry, SW Iberian coast

8.1.- Introduction

The Early-Mid Holocene period is characterized by several environmental changes, such as the postglacial marine transgression, an increase of temperatures, and the existence of diverse episodes of ice-rafted debris in the North Atlantic Ocean. Littoral areas suffered a rapid transformation resulting from the inundation of the fluvial valleys and the progressive development of diverse coastal features. From a different perspective, the vegetation adapted to the new climatic-edaphic conditions and reacted to abrupt episodes, the so called Bond events, which are associated to dry conditions in the Mediterranean region (Bond et al., 2001). However, the Early-Mid Holocene was not only defined by unique environmental changes, but by important cultural transformations within hunter-gatherer groups and the adoption of new subsistence strategies.

The process of neolithization in Southwestern Iberia is controversially disputed and different theories attempt to explain its origin. Some authors interpret it as a maritime pioneer colonisation of depopulated regions by Neolithic groups from the Western Mediterranean (Zilhão, 2001), while others propose indigenous origins defined by the continuity of local Mesolithic groups in certain regions, suggesting that the beginnings of agriculture could have had an autochthonous nature (Massieu and Socas, 2013). Many authors consider that the area of Andalusia, the Algarve, and the Moroccan Atlantic fringe have shared similar traits during this process (Manen et al., 2004), which would explain the existence of Neolithic "enclaves" with specific regional features (Carvalho, 2010) or a southern neolithization route along the North African coast (Borja et al, 2010; Lindstäter et al., 2012). The inherently intricate interpretation of such a complex process is, in this case, weighed down by the lack of absolute datings in clear stratigraphic sequences, and the absence of information regarding the Mesolithic period at a regional scale (Martín-Socas et al., 2017).

Recent palaeogenetic studies have shed light on this complicated situation, confirming that Southern Iberian Neolithic humans share the same genetic composition as the Cardial Mediterranean culture that reached Iberia ca. 7.5 ka BP (Fregel et al., 2018). These early Neolithic Iberian groups present genetic differences with the early Neolithic central European farmers, pointing toward two different migrations and linking all Neolithic Iberians with the first migrants that arrived with the initial Mediterranean Neolithic wave of expansion (Valdiosera et al., 2018). It is evident that these Iberians mixed with local hunter-gatherers, maintaining and thus expanding their subsistence strategies. However, it is assumed that this process was not homogeneous and the introduction of new elements, such as food production techniques, can hardly be dissociated from the heterogenous geography, the environmental diversity, and the influence of local groups. Therefore, further research is needed to explain differences in both Mesolithic and Neolithic cultures at the regional scale, as well as to complete the complex environmental puzzle of this area.

Studies integrating archaeological and palaeoenvironmental data from a long-term perspective can provide a critical framework to examine the resilience of human groups to past and current global changes. Thus, this work focuses on the palaeoenvironmental reconstruction of the southwestern Iberian littoral area, with special focus on the occidental Algarve coast, in the course of the Mesolithic and Neolithic periods. We contribute with a new environmental dataset of palynological and geochemical data to discuss and define changes in the vegetation, reconstructing coastal landscapes, and understanding how human groups adapted to these transformations.

8.1.1.- Archaeological context

Two main clusters of Mesolithic and Neolithic sites are located in the southwestern Iberian coast, one in the westernmost extreme of the Algarve littoral, and the other one in the southeastern region of the Gulf of Cádiz towards the Strait of Gibraltar (Fig. 8.1; Supplementary data: Appendix 8.Sup1).

Most of all the Mesolithic sites are found in the Cape São Vicente region. They constitute shell-middens of different sizes (Castelejo, Barranco das Quebradas, Rocha das Gaivotas) and open air sites (Armação Nova, Vale Boi) interpreted as seasonal occupations based on the exploitation of coastal and/or lithic resources (Carvalho, 2007; Valente and Carvalho, 2009). Near the Straits of Gibraltar, the only site for this period is considered as a single occupation based on the exploitation of marine resources and hunting (Palmones), although there is some controversy about its chronology (Ramos-Muñoz, 2005; Uzquiano et al., 2020). The majority of these sites is located close to marine environments or in transitional areas between fluvial and marine influences.

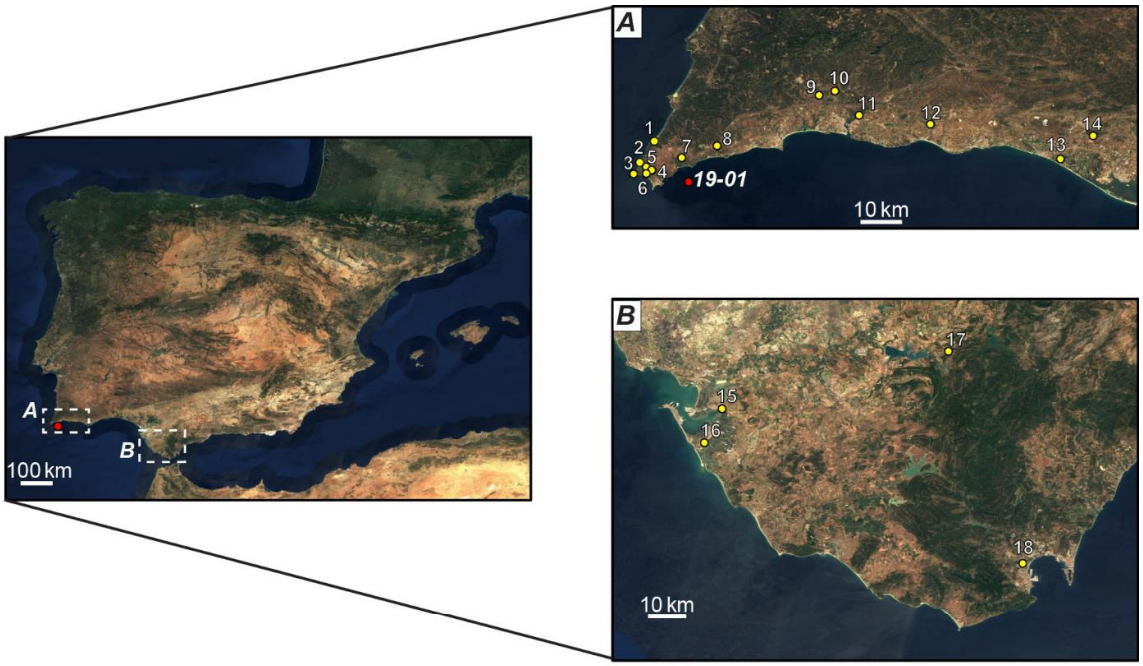

1	Castelejo	**7**	Padrão	**13**	Praia do Forte Novo
2	Barranco das Quebradas	**8**	Vale Boi	**14**	Algarão da Goldra
3	Rocha das Gaivotas	**9**	Alcalar 7	**15**	El Retamar
4	Armação Nova	**10**	Castelo Belinho	**16**	Campo de Hockey
5	Vale Santo I	**11**	Ibne-Ahmmar	**17**	La Dehesilla
6	Cabranosa	**12**	Ribeira de Alcantarilha	**18**	Palmones

1	Castelejo	**7**	Padrão	**13**	Praia do Forte Novo
2	Barranco das Quebradas	**8**	Vale Boi	**14**	Algarão da Goldra
3	Rocha das Gaivotas	**9**	Alcalar 7	**15**	El Retamar
4	Armação Nova	**10**	Castelo Belinho	**16**	Campo de Hockey
5	Vale Santo I	**11**	Ibne-Ahmmar	**17**	La Dehesilla
6	Cabranosa	**12**	Ribeira de Alcantarilha	**18**	Palmones

Figure 8.1. Map of the Iberian Peninsula indicating: the sediment core 19-01 (red dot), the distribution of archaeological sites in the region of the Algarve (A), and in the Southeast of the Gulf of Cádiz (B).

Several Neolithic sites have been discovered in both areas. In the Cape São Vicente region, shell-middens (Alcalar 7, Ribeira de Alcantarilha) and temporary open-air sites (Vale Santo I, Padrão) based on the seasonal exploitation of marine and lithic resources are still present (Carvalho, 2007). Moreover, some Mesolithic sites revealed later Neolithic layers (Castelejo, Barranco das Quebradas, Rocha das Gaivotas, Vale Boi) (Carvalho, 2007; Valente and Carvalho, 2009; Peyroteo-Sterna, 2020). Two necropolis caves (Ibn-Ahmmar, Algarão da Goldra) were also assigned to this period. There is one site considered a residential basecamp (Cabranosa), a settlement suggesting an obvious sedentary occupation with hut structures and grave burials (Castelo Belinho), and a possible long-term settlement in a beach environment (Praia do Forte Novo) which is considered a salt production site by some authors (Rocha,

2013). Many of these new Neolithic sites are located in fluvial environments some kilometres inland, if compared with those belonging to the Mesolithic (Alcalar 7, Ribeira de Alcantarilha, Castelo Belinho, Ibne-Ahmmar, Algarão da Goldra).

In the southeastern area of the Gulf of Cádiz it is possible to identify varying typologies of archaeological sites with Neolithic occupations: a single human occupation (El Retamar) based on the exploitation of marine resources, hunting, and animal domestication (Stipp and Timers, 2002; Ramos Muñoz et al., 2010), a permanent settlement (Campo de Hockey) with a large necropolis (Dabrio et al., 2000; Stipp and Timers, 2002; Vijande et al., 2015), and a necropolis cave (La Dehesilla) (García-Rivero et al., 2020). With the exception of the cave situated in a mountainous area, all other sites are located in the marine-fluvial environments of the Cádiz Bay.

8.1.2.- Regional settings

The study area comprises the southwestern coastal region of the Iberian Peninsula framed by the Atlantic Ocean and located north of the Africa-Iberia plate boundary. The westernmost part is a Meso-Cenozoic sedimentary basin overlying Carboniferous basement, which extends offshore as far as 100 km south (Ramos et al., 2016). However, most of the coast is dominated by Neogene basins defined by the presence of several estuaries conforming littoral lowlands. Some of them are sheltered by spits, with marshlands extending several kilometers inland (Dabrio et al., 2000; Hernández-Molina, 2006). These characteristics are mainly due to the morphology of the coast and the prevailing winds from SW that generate a littoral drift towards the East and SE of the Gulf of Cádiz, being responsible for the formation of beach and barrier systems that partially close some estuaries (Dabrio et al., 2000; Zazo et al., 2008).

The SW Iberian Peninsula has a Mediterranean climate with oceanic influence that can be defined by two climatic zones described by Köppen-Geiger (Kottek et al., 2006): a temperate climate with hot summers in oriental and inland areas (Csa), and a temperate climate with warm summers in occidental areas and the littoral (Csb). Considering both zones, the annual average minimum temperature oscillates between 12.5 °C and 15 °C, and the annual average maximum temperature ranges from 22.5 °C to 25 °C (AEMET, 2011). The average total annual precipitation fluctuates between 500 mm and

1000 mm, mostly concentrated during winter season (AEMET). The thermomediterranean belt of the coastal lowlands is defined by different ecosystems and vegetal ecological associations. Woodlands are mainly composed of evergreen (*Quercus suber, Q. rotundifolia*) and deciduous oaks (*Q. faginea, Q. estremadurensis*), together with some Mediterranean species, such *as Olea europaeae* subs. *sylvestris* or *Juniperus oxycedrus*, among others. Pre-forest scrubs are dominated by *Quercus coccifera, Phillyrea angustifolia, Pistacia lentiscus, Rhamnus* sp., and *Juniperus* sp, while riparian communities are formed by *Alnus glutinosa, Salix* sp., *Fraxinus angustifolia*, and *Tamarix* sp. (Rivas-Martínez, 1988; Rivas-Martínez et al., 1990; Rivas-Martínez et

al., 2001; Espírito-Santo et al., 2017). Heathlands are well represented by different genera of Ericaceae that grow on acidic low fertility soils, under high humidity levels and strong oceanic conditions (Loidi et al., 2007). In littoral areas and interdunal valleys the vegetation is mainly composed of *Pinus pinaster, P. pinea* and *P. halepensis*. The most representative herbaceous vegetation of the stable dunes are: *Polygonum maritimum, Artemisia crithmifolia, Eryngium maritimum, Cyperus capitatus, Anthemis maritima, Silene* sp., *Juniperus* sp. (Rivas-Martínez et al., 1980). Freshwater marshlands include species of Cyperaceae and *Isoetes* spp., *Typha* sp., *Hypericum tomentosum*, and *Phragmites australis*, while saltmarshes are dominated by species of Chenopodiaceae and some taxa such as Apium graveolens, Aster tripolium, Limonium, Juncus maritimus, and others (Rivas-Martínez et al., 1985; Espírito-Santo et al., 2017; Marcenò et al., 2018).

8.2.- Materials and methods

Twin sediment cores 19-01 and 19-02 (referenced as GeoB23519-01/-02 in the MARUM core repository in Bremen, Germany) were retrieved in the Algarve continental shelf (37° 00.656, 008° 52.247 and 37° 00.654, 008° 52.26, respectively) at ca. 65 m water depth and approximately 3 km from the coast using a vibracorer. The 3.64 m-long core 19-01 was sampled for palynological analysis and the neighboring core 19-02 (3.62 m-length) is added to increase data and resolution on sedimentation rates and chronology. In both cores, stratigraphic units were identified by visual description of the sediment. From bottom to top (Fig. 8.2), both cores are composed of greenish fine sands covered by muddy sediments and capped by coarse silt to silty sand (uppermost 1.5 m). Shells are common as well-preserved specimens and the clastic fraction is composed by bioclasts, siliciclastics, and lithic fragments.

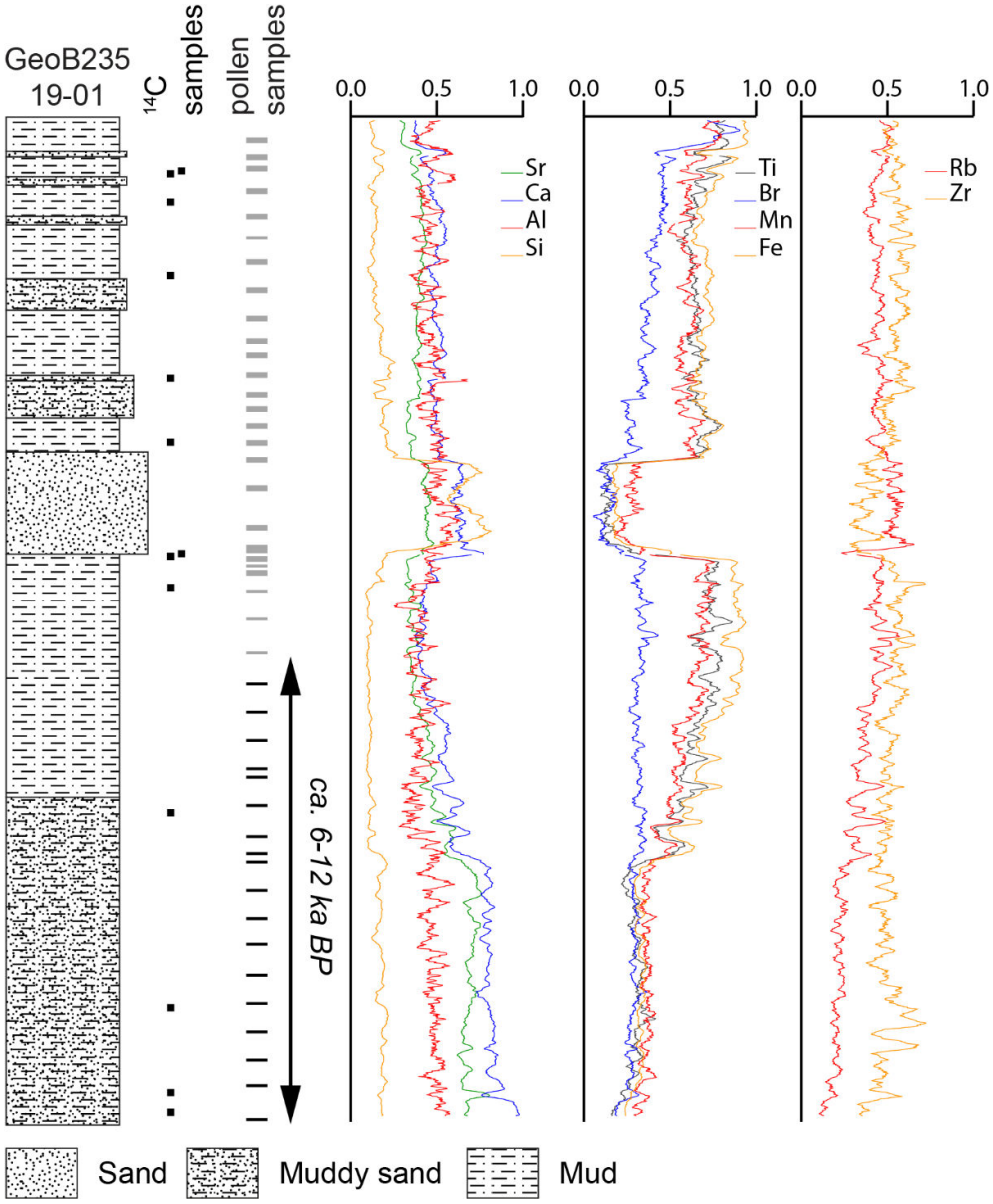

Figure 8.2. Lithological log, location of 14C and pollen samples (black: samples used in this study) and selected XRF parameters for core 19-01.

X-ray fluorescence scans (XRF) were measured using an ITRAX core scanner (resolution 2 mm, 20 s exposure time, 30 kV, 55 mA). Carbonate (Ca, Sr), siliciclastic (Si, Al, Ti, Zr, Rb), organic matter (Br, Mo incoherent and coherent scatter [Mo inc, Mo coh]), and redox geochemical (Mn, Fe) proxies were chosen (Fig. 8.2) and some useful ratios were analyzed (Ca/Si, Si/Al, Zr/Al, Zr/Rb, Mn/Fe, Mo inc/coh) (Calvert et al., 2007). Anomalous values were removed by comparison to the core photographs to minimize the effect of coarse grains, cracks, and surface irregularities. The remaining data were normalized by count per row to unit by column and smoothed with an arbitrary 11-point running mean filter to reduce the inherent data noise.

Seven articulated bivalves from core 19-01 and six more articulated valves from 19-02 were 14C-dated at the Beta Analytic Inc. and the University of California-Irvine (USA). Calibration was performed with CALIB 8.2 (Stuiver and Reimer, 1993) using the Marine20 calibration dataset (Heaton et al., 2020) and different ΔR calculated from the original datasets of (Soares, 1993; Soares and Dias, 2006; Soares and Martins, 2009, 2010; Martins and Soares, 2013) by using the online application of (Reimer and Reimer, 2017) (Table 8.1). After comparison of the sedimentological and geochemical logs, it was possible to correlate both cores by depth. The age model is based on a simple linear interpolation and sedimentation rates were calculated for each dated interval (Fig. 8.3).

Table 8.1. Radiocarbon samples and calibration parameters and results. * and italics: rejected sample due to possible reworking.

Core	Lab. code	Depth (m)	^{14}C age (yr BP)	error	DR	error	age cal. BP median	2s range (cal. BP)
GeoB23519-01	236164	0.21	650	15	-49	121	177	0-399
	Beta-526115	0.57	2610	30	-73	140	2212	1829-2622
	236165	0.93	3205	15	-36	152	2903	2505-3312
	236166	1.55	4245	15	50	152	4090	3660-4515
	236167	1.67	5390	20	407	165	5098	4673-5523
	236168	3.16	9230	20	740	225	8892	8354-9445
	236169	4.46	9530	20	-46	206	10292	9658-10910
GeoB23519-02	Beta-512669	0.2	600	30	-49	121	148	0-367
	Beta-512670	0.31	1570	30	-194	125	1155	864-1453
	*Beta-512668**	*1.16*	*4280*	*30*	*50*	*152*	*4136*	*3693-4564**
	Beta-512667	1.56	4330	30	50	152	4201	3759-4641
	Beta-512666	2.47	7910	30	301	201	7893	7488-8328
	Beta-512665	3.53	10360	30	-46	206	11458	10797-12104

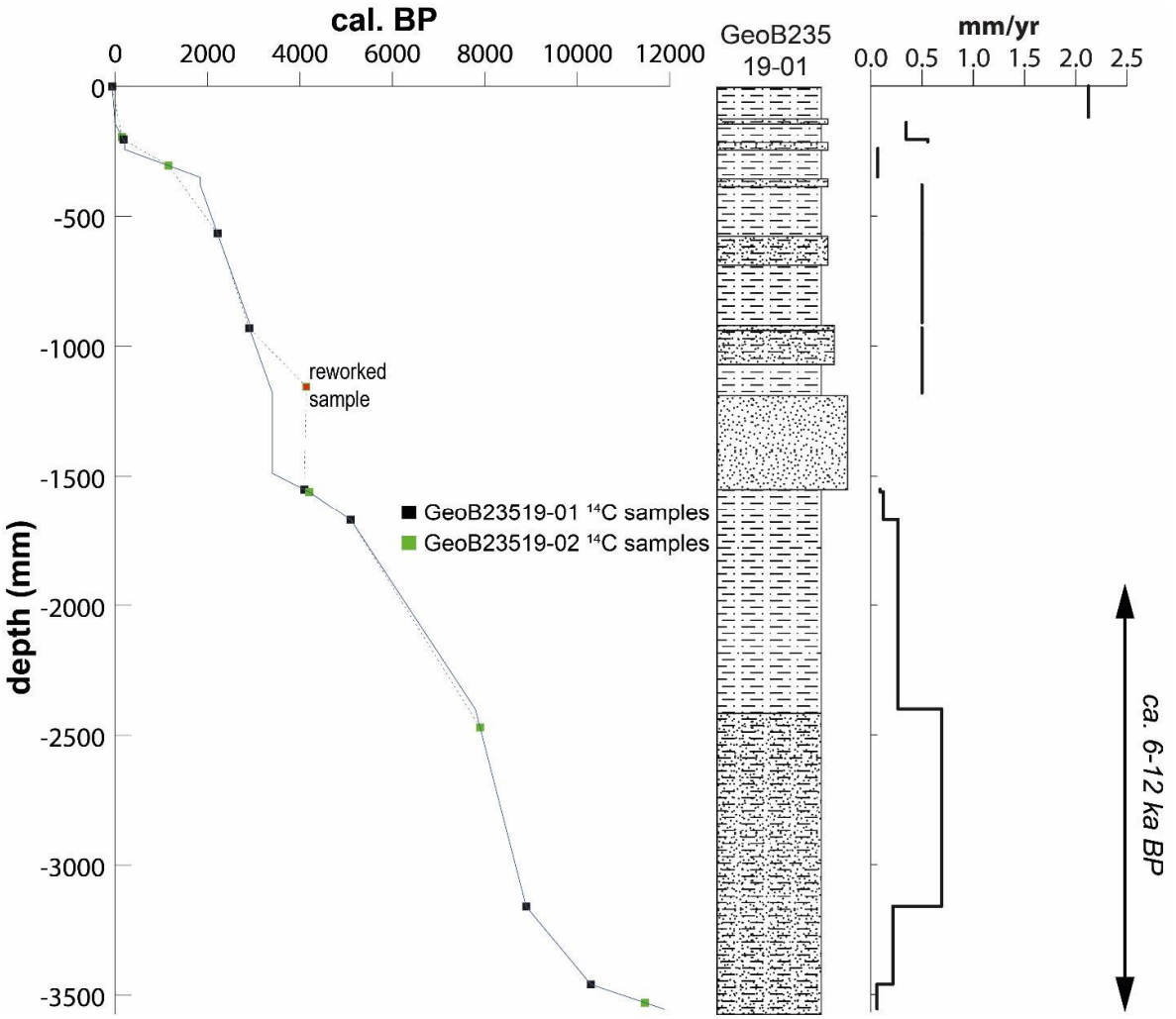

Figure 8.3. Age model, sedimentation rates and lithological log for core 19-01. Key for lithologies as Figure 8.2.

Palynological samples were collected from core 19-01 with an interval of 3–7 cm. All samples were chemically treated with HCl to remove carbonates, KOH to remove humic acids, and sodium polytungstate (SPT: 3Na2WO4·9WO3·H2O) at 2.0–2.1 cm3 for densimetric separation. The final residue obtained after the treatment was mounted on slides with the use of glycerol mixed with phenol. Palynomorphs were counted using an optical microscope at 400× and 1000× to a minimum pollen sum of 150 terrestrial pollen grains. Fossil pollen grains, spores, and non-pollen palynomorphs were identified using published keys (Van Geel, 1978, 2001; Pals et al., 1980; Moore et al., 1991; López-Sáez et al., 1999) and the modern pollen reference collection of the CSIC in Madrid (Spain). Microcharcoal particles >125 μm were counted alongside the identification of pollen grains and interpreted as indicators of regional fires (Whitlock et al., 2001). Pollen and microcharcoal concentrations (grains/gr and particles/gr of dry sediment, respectively) were estimated by adding one Lycopodium clavatum tablet to each sample [54]. Diagrams were plotted versus age using TiliaIT software (version 2.1.1, Illinois State Museum, Research and Collection Center. Springfield, IL, USA) (Figures 8.5 and 8.7). Palynological assemblage zones were

determined by Constrained Cluster Analysis Sum Squares (CONISS) based on a square root transformation (Edwards & Cavalli-Sforza chord distance).

In the synthetic diagram main categories are organized in the following way: High-mountain pines (*Pinus sylvestris-nigra* type), Mediterranean pines (*Pinus halepensis-pinea* type and *Pinus pinaster*), Mediterranean woodland (evergreen *Quercus, Olea europaea*), Mediterranean shrubland (*Phillyrea, Arbutus*), Riparian woodland (*Alnus, Fraxinus, Salix*), Mesophilous trees (deciduous *Quercus, Acer, Corylus, Betula*), Heathlands (*Erica* type, *Calluna*), Xerophytic taxa (*Juniperus, Ephedra fragilis* type, *Artemisia*), Asteraceae (Carduoideae, Asteroideae, Cichorioideae), Ferns & Mosses (see Figure 8.5), Hygro-hydrophytic herbs (*Typha*, Cyperaceae, *Callitriche, Potamogeton*), Coprophilous (Coniochaetae /HdV-172, *Sporomiella*/HdV-113, Sordariaceae, *Chaetomium*), and Erosive processes (*Glomus* sp., *Pseudoschizaeae circula*).

Pollen percentages for terrestrial taxa were calculated against the main sum of terrestrial grains, while percentages for aquatics, spores, and *Pinus* were calculated against the total sum of all pollen and spores. *Pinus* grains were excluded from the main sum because they are considered to be over-represented in marine sediment cores because of its extensive dispersal ability and buoyancy (Hopkins, 1950). However, morphometric analysis of their pollen grains was done using a measurement of the grain diameter, excluding sacci (Carrión, 2000; López-Sáez et al., 2010, 2020).

8.3. Results

8.3.1.- Age-depth model

According to the proposed age model, the period between 12 ka and 6 ka BP is placed in the lowermost 1.5 m of the core. From ca. 12 ka BP until ca. 8 ka BP, the sedimentation rate increases from 0.06 mm/yr to 0.69 mm/yr which corresponds to the maximum value for the Holocene in this core. From ca. 8 ka BP to 6 ka BP the depositional rate decreases to 0.27 mm/yr (Fig. 8.4a).

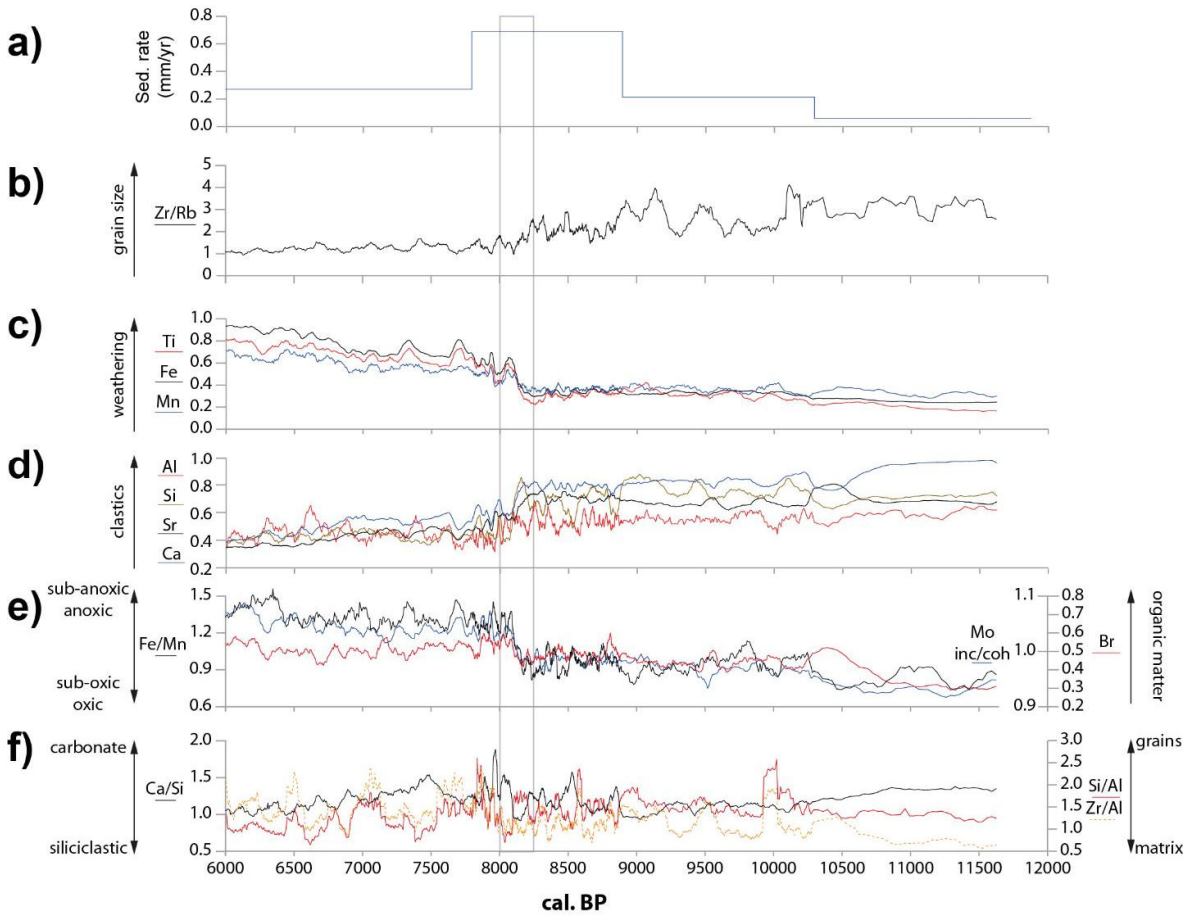

Figure 8.4. Age plot for the 12–6 ka BP period of the (a) sedimentation rate and (b–f) selected geochemical elements and ratios.

8.3.2.- Geochemistry

The selected elements can be grouped by similar behavior along time allowing the identification of some common periods and events despite the considered parameter.

Zr/Rb ratio has been linked to grain size changes (Schneider et al., 1997) and sediments older than ca. 8.1 ka BP show larger values and a clear decreasing trend than younger sediments (Fig. 8.4b).

Ti, Fe, and Mn run almost parallel during the studied period and they can be linked to weathering of siliciclastic rocks (Cornu et al., 1999). These elements show reverse trends and peaks as compared to Zr/Rb (Fig. 8.4c), showing large ratios and enhanced increase for the 8.2–6 ka BP period than for the Early Holocene.

Al, Si, Ca, and Sr can be correlated in the long term (Fig. 8.4d), while they show some differences for the shorter cycles. Al and Si are interpreted as representative of terrestrial input (Calvert et al., 2007). Comparable Ca and Sr trends represent carbonates (Calvert et al., 2007), and reflect high bioclastic

content. All elements are components of the dominant clastic fraction, while siliciclastics depend on the terrestrial supply, carbonate variability can be due to changes on marine productivity (in situ biogenic carbonate) and this could be responsible for the out-of-phase signal for the shorter cycles. All of them show higher values for the 8–12 ka BP period, with larger amplitudes for Si, Ca, and Sr compared to the 6–8 ka BP period, when Al shows wider amplitudes reflecting the clay-richer composition of the sediments (Fig. 8.2).

It is worth to mention the long- and short-term correlation of Br, Mo inc/coh, and Fe/Mn (Fig. 8.4e). Br and the Mo inc/coh ratio have been used as a proxy of organic matter in marine sediments (Thomson et al., 2006; Burnett et al., 2011; Chagué, 2020). The Fe vs Mn ratios can indicate changes in the redox state (Naeher et al., 2013; Demina et al., 2019), with Mn-displaced values indicating oxic conditions. All these values show a steady increase, broken by a sudden rise from 8.3 to 8 ka BP. However, they are lower for Br, mirroring the changes in clastic fraction (Al, Si, Ca, Sr).

Ca/Si ratio points to the carbonated vs. siliciclastic sources (Herrmann and Stroncik, 2013; Hoelzmann et al., 2017), while Si/Al and Zr/Al are used as textural proxies like sorting or grain size (Calvert, 2007; Santisteban et al., 2019) (Fig. 8.4f). These ratios show no clear trends, as those mentioned before, but they can be divided in three stages: from 12 until 8.8 ka BP, their record show low amplitude cycles that shorten their period in time, Ca/Si decreases while Zr/Al and Si/Al remain, showing a slowly increasing trend; from that time until ca. 7.8 ka BP, the amplitude increases while their period shortens, both Ca/Si and Si/Al increase but Zr/Al shows its average lowest values; from ca. 7.8 ka BP to 6 ka BP, the period of the cycles grows, while their amplitude slightly decreases without reaching values of the previous core section. Ca/Si and Al/Si values show a falling trend while Zr/Al remains nearly stable.

According to these observations, the 12–6 ka BP lapse can be split in three periods (Fig. 8.4):

12–8.4 ka BP. Low values in Ti, Mn, Fe reflect reduced weathering conditions and Fe/Mn, Br, and Mo inc/coh ratios imply low preservation potential of organic matter and point to oxic conditions. Si, Al, Ca, and Sr values are high and indicate dominance of clastic/tractive deposits; the Zr/Rb values correspond to coarser grain size. Si/Al, Zr/Al, and Ca/Si values show low amplitude and slow changes, implying an environment characterized by homogeneous conditions and only disturbed by some higher energy episodes—as evidenced by increases in Zr/Rb, Zr/Al, and Si/Al. The sedimentation rate increases to its highest values.

8.4–8 ka BP. Amplitude and frequency of changes started to increase shortly before it. The sedimentation rate was the highest. There are marked and sudden changes for a decrease in clastic input and an increase in organic components, while the decrease in grain size and increase in weathering proxies is fast but gradual.

8–6 ka BP. The sedimentation rate decreases from 0.69 to 0.27 mm/yr. Clastics and grain size fall to their minimum average values but amplitude of changes increases for sorting (grains vs. matrix) proxies. Organic matter preservation increases, coincidental to sub-oxic to anoxic conditions, as well as the weathering of source areas.

8.3.3.- Palynology

Four palynological zones were identified in this section of the GeoB235-19-01 core (Fig. 8.5; Table 8.2). Oakwoods dominate the landscape between ca. 10–7 ka BP (Z-1, Z-2, and Z-3), after which Erica type progressively increases (Z-4). Cichorioideae displays constant but irregular values (Z-1 and Z-4), and the presence of pinewoods, although scarce, is constant through time with a more noticeable presence ca. 11.7–10 ka BP (Z-1) and ca. 7.6–6.5 ka BP (transition Z3–Z4).

Table 8.2. Pollen zone description for marine core 19-01.

Zone	Depth range (cm)	Age range (cal yr BP)	Pollen signature
Z-1	354-323	11707-9242	Dominance of oakwoods (evergreen and deciduous *Quercus*: 17-20% and ~10-16% respectively) together with Cichorioideae (17-34%). *Olea* (~0-5%), *Phillyrea* (~4%), and Chenopodiaceae (~5-8%) slightly increase towards the end of the zone. *Juniperus* (~4-9%) Asteroideae (5-11%), and Poaceae (~5-9%) display discontinuous values. Pinewoods represent ~15% (*Pinus sylvestris-nigra* type, *Pinus halepensis-pinea* type, *Pinus pinaster:* ~5% each). Low % of *Isoetes* (~4-7%), and peaks of foraminiferal linings (~9-19%).
Z-2	323-263	9242-8132	Increase of deciduous and evergreen *Quercus* (~15-20% and ~17-29%), together with *Olea* (3-6%) *Phillyrea* (3-10%), and *Juniperus* (~7-11%). Slight decrease of Chenopodiaceae (3-10%) towards the end of the zone. Reduction of Poaceae (~1-5%), Asteroideae (~4-7%), and Cichorioideae (7-24%), the latter with notable peaks. Slight decrease of pinewoods (below 5% each). Progressive increase of *Isoetes* (~4-13%) and important increment of foraminiferal linings (~21-33%).
Z-3	263-230	8132-7441	Dominance of oakwoods, with peaks (deciduous: ~16-22%; evergeen: ~17-26%). Visible increase of *Erica* type (~1-11%). Decrease of *Olea* (below 3%), *Phillyrea* (~1-8%), Chenopodiaceae (~4-8%), and Cichorioideae (~7-13%). *Juniperus* (~6-12%), Asteroideae (~4-6%), and Poaceae (~2-6%) display similar values. Slight increase of pinewoods (*Pinus sylvestris nigra* type ~2-6%; *Pinus halepensis-pinea* type ~2-9%; *Pinus pinaster* ~1-5%). Increase of *Isoetes* (~12-19%) and decrease of foraminiferal linings (~7-15%).
Z-4	230-189	7441-5928	Drop of both deciduous and evergreen *Quercus* (~7-16% and ~5-12%) towards the end of the zone. Decrease of *Olea* and *Phillyrea* (both below 5%), *Juniperus* (~6-10%), and Chenopodiaceae (~3-7%). Slight increase of Poaceae (~3-8%) and Asteroideae (~5-8%). *Erica* type (~7-10%) increases approaching the end of the zone. Rise of Cichorioideae (~17-33%). Decrease of *P. sylvestris-nigra* type and *Pinus pinaster* (both below 5%) and same values for *Pinus halepensis-pinea* type (~2-9%). Increase of *Isoetes* (~14-27%) and decrease of foraminiferal linings (~2-14%).

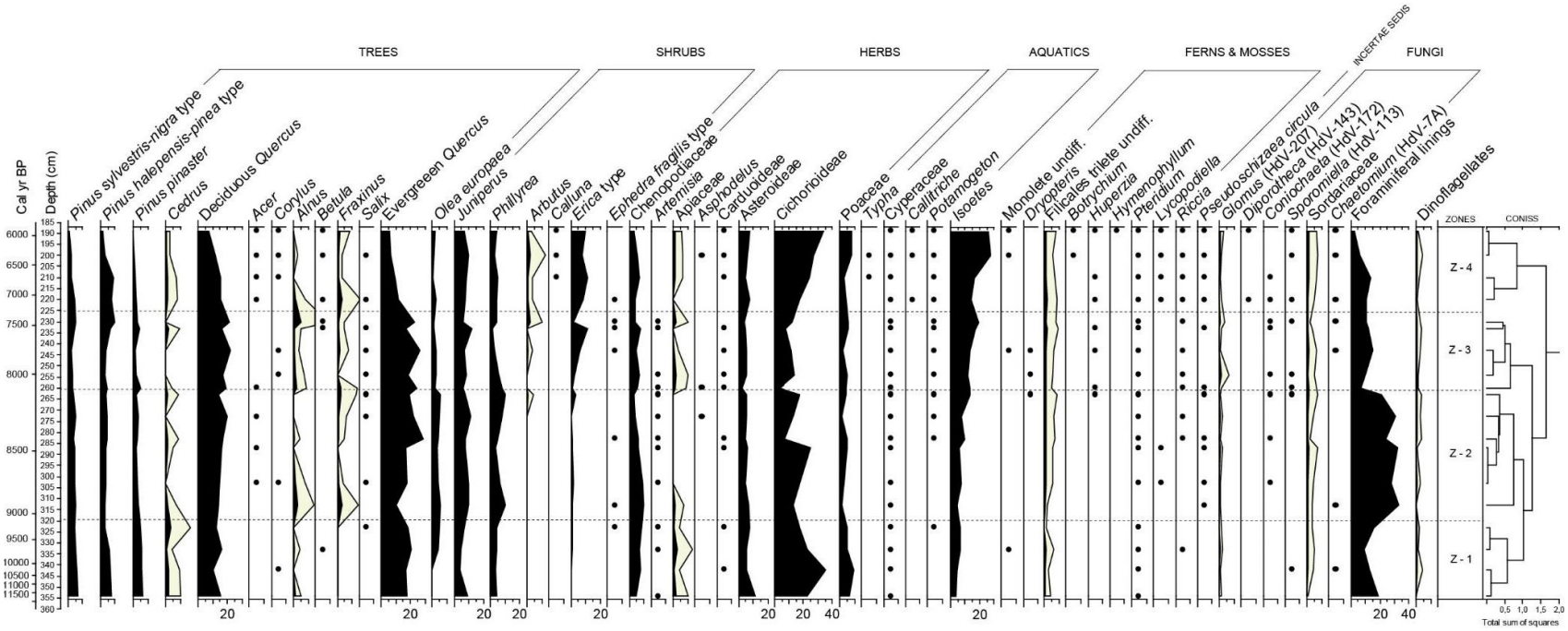

Figure 8.5. Pollen diagram for the core 19-01 showing trees, shrubs, herbs, aquatics, ferns and mosses, fungi, foraminiferal linings, and dinoflagellates with CONISS zonation vs. depth and age.

8.4.- Discussion

8.4.1.- Geochemical trends and events, sea level and palaeoceanographic changes

Comparison of the evolution of geochemical and sedimentary parameters against regional and global forcings (sea level, climate) (Fig. 8.6), allows us to correlate them and to identify links among the environment, these forcings, and human populations.

The ca. 10–6 ka BP period is known as the Holocene Thermal Maximum (HTM) (Kaufman et al., 2004; Marcott et al., 2013; Bova et al., 2021; Liu et al., 2021), a period of warm and humid climate as compared to previous and following periods and only interrupted by a short cooling period known as the 8 ka or the 8.2 ka BP event (Alley et al., 2005; Rohling and Pälike, 2005) (Fig. 8.6a).

Sea level rose from its previous minimum during the Last Glacial Maximum with maximum rates for the Algarve between 11–8 ka BP (from 9 to 7.4 mm/yr), that decreased between 8–7 ka BP (4.5 mm/yr), and another time from 7 to 6 ka BP (2.0 mm/yr) and fell to 0.7 mm/yr for the 6–5 ka BP period (García-Artola, 2018). Coeval to this change, sedimentary records of core 19-01 gradually decrease in grain size (Zr/Rb ratio, Fig. 8.6b) that can be interpreted as the result of deepening (drowning by flooding), increasing distance to the wave base, and the action of coastal currents and sedimentation rates changed accordingly (Fig. 8.6c).

Sea surface temperature decreased in the Gulf of Cádiz (Cacho et al., 2001) and Alborán Sea (Català et al., 2019), and this change correlates with the increase in the organic matter content of core 19-01 (Fig. 8.6d).

Weathering proxies are indicative of wet and warm conditions which prevail after 8.2 ka BP (Fig. 8.6e). These conditions are coherent with the alleged characteristics of the HTM and the African Humid Period (Adkins et al., 2006; Stumpf et al., 2011). Stumpf et al. (2011) showed a decrease in the illite/kaolinite ratio and interpreted this as related to a change in dust sources, but it is also coherent with an increase in weathering of the source areas.

The decrease in clastic fraction (Fig. 8.6f) can also be linked to the increase in weathering and the growing water depth. In addition, the continuity of terrestrial influx (Si/Al, Zr/Al, Fig. 8.6g) vs. the gradual increase in organic content and the abrupt and short increase in carbonates around 8.2 ka BP (Ca/Si, Fig. 8.6g) indicate a rise in marine productivity.

However, one of the main features of the geochemical record of core 19-01 is the abrupt change in marine productivity and clastic dynamics and gradual weathering of source areas along with waves/shallow currents. These changes relate to the 8.2 ka BP event.

Thornalley et al. (2009) interpret that there was an abrupt switch from a stratified upper ocean to well-mixed waters around 8.4 ka ago caused by changes in the relations between the subpolar and subtropical gyres. Bazzicalupo et al. (2020) showed from records of the Alborán Sea, that present oceanic gyres system developed around 8 ka ago. Also, model results indicate the changes in oceanic gyres around 8.2 ka BP as being responsible for the present day North Atlantic circulation (Born et al., 2010). Thus, it seems possible that the observed abrupt changes in the geochemical record of core 19-01 can be related to those palaeoceanographic changes, while the gradual ones are interpreted to link to terrestrial climate variations.

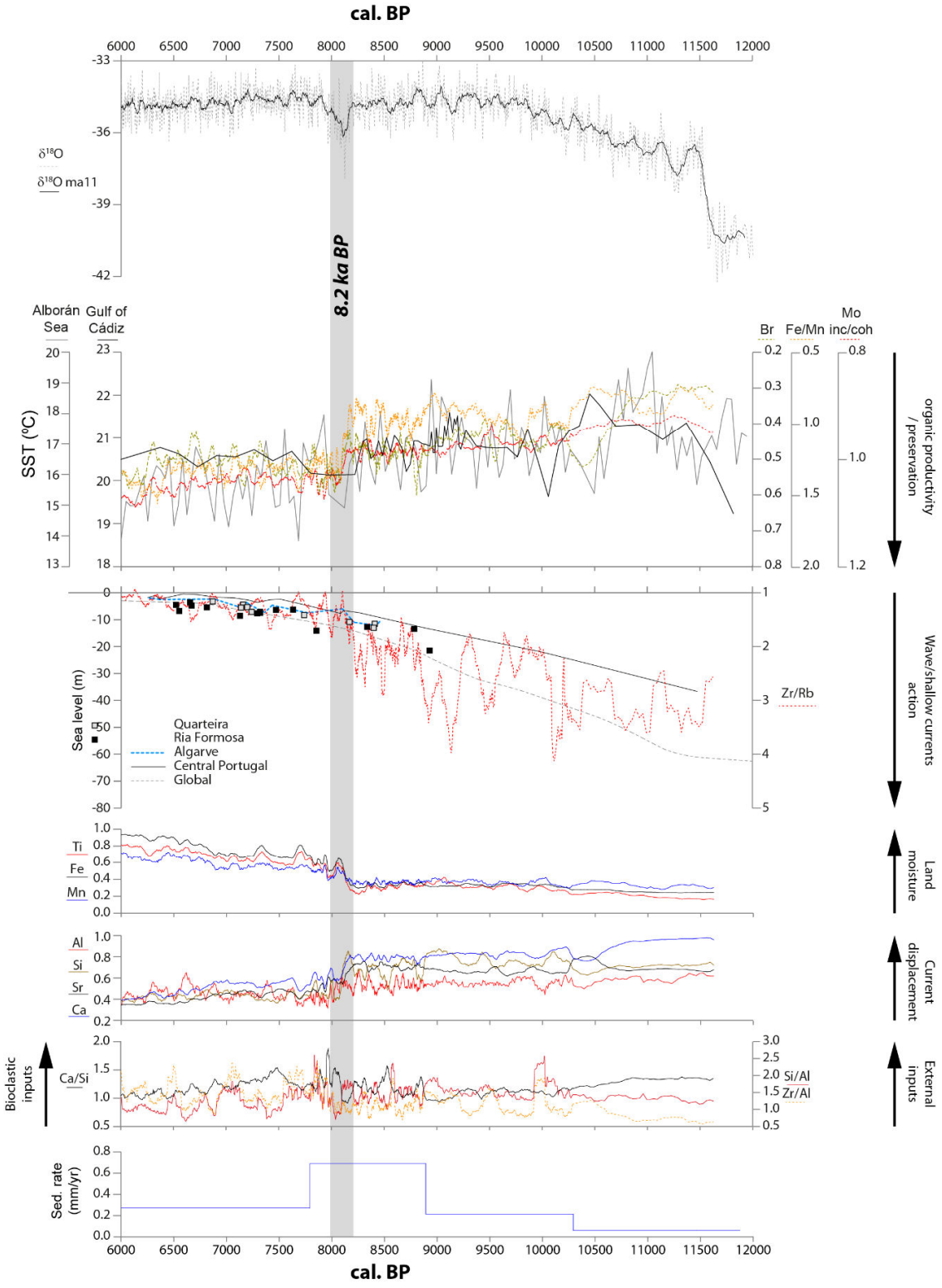

Figure 8.6. (a) Variations in δ18O in GRIP core (Johnsen et al., 1997); (b) sea level changes around SW Portugal (Quarteira (Teixeira et al., 2005); Ria Formosa (Sousa et al., 2019); Algarve and Central Portugal (García-Artola et al., 2018) and global (Lambeck et al., 2014) and Zr/Rb ratio (notice the reversed scale); (c) sea surface temperature (SST) reconstructions for the Gulf of Cádiz (alkenone Uk37 SST derived for core M39-008 (Cacho et al., 2001)

and Mg/Ca SST derived for the Alborán Sea (ALB2 (Català et al., 2019)); (d) Ti, Fe, and Mn, weathering proxies, as indicative of land moisture; (e) Al, Si, Sr and Ca, representative of clastic sedimentation, serve as proxies for activity of marine currents; (f) Ca/Si, carbonate vs. siliciclastics, and Zr/Al and Si/Al, proxies of siliciclastic grains vs. matrix, as indicative of land derived vs. bioclastic (marine) inputs; (g) sedimentation rate for core 19-01 for the 12–6 ka BP period.

8.4.2.- Vegetation trends and evolution of coastal environments

During the Early Holocene, the post-glacial marine transgression was progressively drowning the exposed continental shelf of the southwestern Iberian coast with a rapid sea level rise between ca. 13 ka BP and 7–6.5 ka BP, although with different responses depending on the geographic location and topography (Zazo et al., 2008). Initially, until ca. 10 ka BP, the first stages of the river valleys inundation resulted in pre-estuarine palaeovalleys and transitional areas of fluvial-saltmarsh deposits as the main coastal landscapes (Dabrio et al., 2000; Boski et al., 2008; Schneider et al., 2010; Delgado et al., 2012; Trog et al., 2013). For this period until ca. 9.2 ka BP, the core 19-01 indicates the existence of forests composed of mesophilous trees, and Mediterranean trees and shrubs which defined the onset of the Holocene as a warm phase. Mediterranean and high mountain pines were also present, although in low values, being that the latter (*Pinus sylvestris-nigra* type) may be a reminiscence of the continental climate of the previous glacial period, as reported in other deposits (Figueiral and Carcaillet et al., 2005). These conditions have been also inferred in continental deposits in the Guadiana Estuary and the Medina Lagoon, where the presence of open land indicators and high-mountain pines were recorded, respectively (Fletcher et al., 2007; Schröder et al., 2018). In this regard, it has been found that the hydrological response in some Western Mediterranean areas during the Early Holocene maintained prolonged arid conditions, with shallow lake levels followed by an increase of moisture ca. 10–9 ka BP (Morellón et al., 2018). This may have been linked to insolation and seasonality changes due to the orbital variability, the presence of the Laurentide and Fennoscandian ice sheets in the North Atlantic Hemisphere, and a series of ice rafted debris (IRD) provoking immediate ocean surface coolings associated with dry conditions in the Mediterranean region (Berger, 1978; Bond et al., 1997, 2001). Some of these events fall into this period (Fig. 8.7) and two of them appear to have triggered a reaction in the vegetation with a decrease of mesophilous trees and an increase of Asteraceae immediately after 10.3 ka BP, and a retraction of mesophilous and Mediterranean forests with a parallel rise of Mediterranean shrubland and xerophytic taxa after 9.4 ka BP. Diverse records from Greenland show anomalies in the mean δ18O curves ca. 9.95 and 9.3 ka BP interpreted as temperature irregularities, but also to changes in moisture sources and/or transport paths (Masson-Delmotte et al., 2005; Rasmussen et al., 2007). The slight delay in the vegetation reacting to these events indicates that changes in terrestrial landscapes were not immediate.

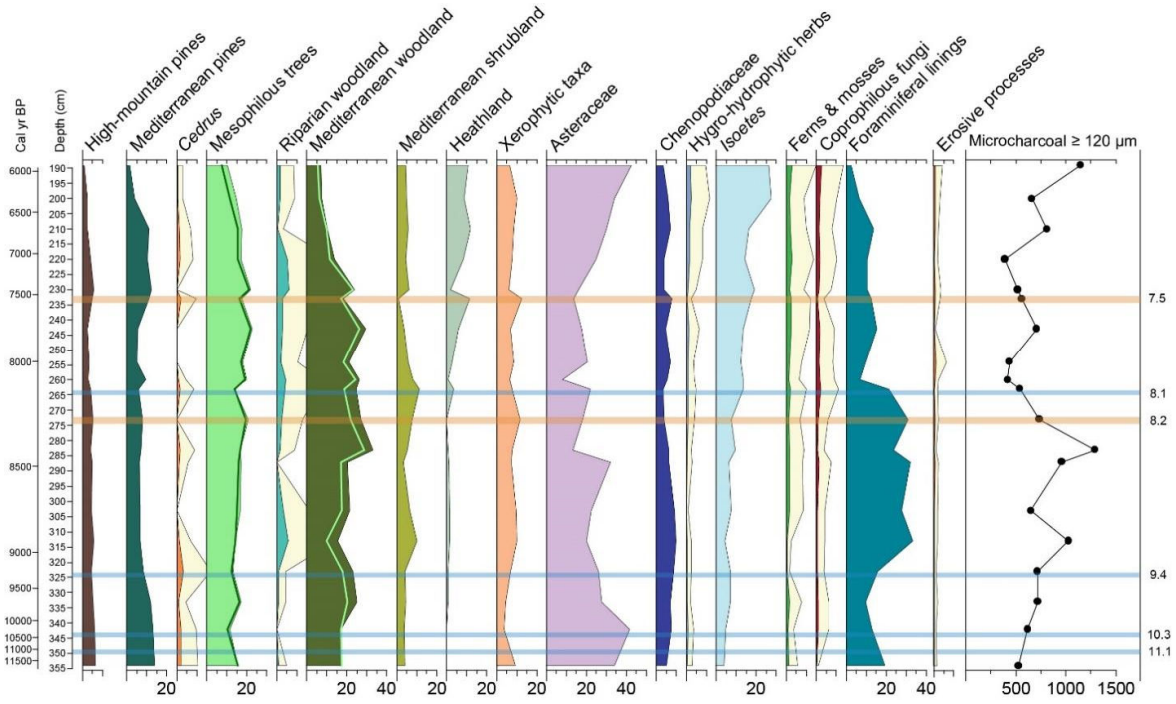

Figure 8.7. Synthetic diagram of the main ecological groups and taxa expressed in percentages. The dark green line plotted against the Mesophilous trees represents deciduous *Quercus* values, while the light green line plotted against the Mediterranean woodland shows evergreen *Quercus* values. Microcharcoals are expressed in concentrations (particles/gr of dry sediment). Blue lines correspond to the chronologies associated to some IRD events by Bond et al. (1997) with a more or less clear impact in the vegetation of the core 19-01, while orange lines highlight aridity crises.

Regarding the evolution of the coast, the period between ca. 10–7 ka BP is also coincident with a phase of intense marine influence due to the marine transgression into the river valleys of the SW Iberian margin, transformed in estuaries by drowning (Dabrio et al., 2000; Boski et al., 2008; Schneider et al., 2010; Delgado et al., 2012; Trog et al., 2013). As a result, salt marshes developed along the littoral of the Gulf of Cádiz and a landward shift of the boundary between marine and fresh waters took place, with a consequent increase of saline environments (Dabrio et al., 2000). High values of foraminiferal linings were recorded between ca. 9.5 to 8 ka BP, probably related to the development of estuaries. From ca. 8 ka BP onwards and abrupt drop on the foraminiferal linings gives way to a progressive increase of Isoetes, characteristic of seasonal fresh marshland environments (Pinto da Cruz, 1999; López-Sáez et al., 2018). The increase of wetland taxa seems to parallel the slight rise of riparian communities registered during this period, which may be a consequence of the influence of the river in the hinterland, as already recorded in other continental cores (Fletcher, 2005; Trog et al., 2013).

At ca. 10–9 ka BP an abrupt increase in moisture was identified in several lake records of the Western Mediterranean (Morellón et al., 2018), and the progressive expansion and maximum values of oakwoods

between ca. 10 to 7 ka BP seem to confirm this trend. Despite slight differences in the chronologies, this rise of temperate and Mediterranean forest taxa is also registered in other marine cores drilled in the Atlantic margin of southwestern Iberia (Chabaud et al., 2014; Oliveira et al., 2018; Gomes et al., 2020), as well as in some continental deposits of this area (Fletcher et al., 2007).

During this period, two peaks of microcharcoals were recorded and interpreted as episodes of increased regional wildfires at 8.8 and 8.4 ka BP (Fig. 8.7). Several forest contractions were also identified at different points and with diverse characteristics but it is noteworthy to highlight two episodes. At 8.2 ka BP there is an increase of xerophytic elements and afterwards an abrupt drop of the forest taxa took place, culminating with low values of mesophilous/Mediterranean trees and a rise of Asteraceae ca. 8.1 ka BP. Greenland ice cores reflect well-defined anomalies in the period between 8.4–8 ka BP with very low values of δ18O around 8.2 ka BP (Rasmussen et al., 2007). Although its origins remain unclear, the 8.2 ka BP event has been linked to a fresh water influx into the North Atlantic that would have provoked changes in temperatures and thermohaline circulation and thus, in moisture availability (Bond et al., 2001; Renssen et al., 2001). Indeed, the Medina Lagoon record shows a lake-level decrease for the period between ca. 8.5–7.8 ka BP, which has been related to global climatic instability centered on 8.2 ka BP, concluding in a desiccation phase (Reed et al., 2001). Events of forest decrease were also recorded in the SW Atlantic margin between ca. 8.6–8 ka BP, as well as in the Alborán Sea between ca. 8.3–8 ka BP (Fletcher et al., 2007; Combourieu Nebout et al., 2009; Chabaud et al., 2014; Oliveira et al., 2018; Gomes et al., 2020). In continental deposits, some forest setbacks and expansion of open-ground taxa were recorded in the Guadiana Valley and the Medina Lagoon at ca. 7.8 and 8.2 ka BP, respectively (Fletcher et al., 2007; Schröder et al., 2020); however, several sequences do not mirror any vegetal changes for this period (Manzano et al., 2018; Uzquiano et al., 2020).

Another important crisis was also identified in the GeoB235-19-01 core at ca. 7.5 ka BP, defined by a visible peak of xerophytes and an abrupt drop of mesophilous trees, riparian woodland, and Mediterranean woodland and shrubland, pointing to a rapid decrease of moisture availability (Figures 8.6e and 8.7). Diverse episodes of forest contractions were identified between 7.5 and 7 ka BP in different cores of the Atlantic Iberian Margin and the Alborán Sea, as well as in continental sequences (Fletcher et al., 2007; Combourieu Nebout et al., 2009; Chabaud et al., 2014; Manzano et al., 2018; Oliveira et al., 2018; Gomes et al., 2020). Diverse palaeorecords from SE Iberia suggest changes towards increased aridity between 7.8–7.3 ka BP (Cortés-Sánchez et al., 2012).

Regarding the coastal evolution, the core 19-01 recorded the maximum sea level rise rates for the Algarve between 11–7 ka BP, but in most of the estuaries located in this area (Alvor, Alcantarilha, Quarteira, Carcavai, Tinto & Odiel, Guadalete) the maximum flooding of the river valleys was registered at ca. 7–6 ka BP, resulting in the development of open estuaries, inundated channel banks, tidal flats, and even the

landward migration of estuarine barriers (Dabrio et al., 2000; Boski et al., 2008; Schneider et al., 2010; Delgado et al., 2012; Trog et al., 2013). The fluctuation between marine vs freshwater markers recorded in the core 19-01 seems to reflect the marine pulses and the diverse evolution of littoral features and edaphic conditions, depending on factors such as the accommodation space of the river valleys. During this millennium, mesophilous and Mediterranean woodland progressively decrease, while Mediterranean shrubland seem to stabilize at the same time that heaths start a stepwise expansion from this point onwards. An important increase of Cichorioideae occur ca. 6 ka BP, correlating the rise of *Isoetes* and hygro-hydrophytic herbs. The ambiguous significance of Cichorioideae makes it difficult to understand this episode, and its presence may suggest an important development of marsh/wetland communities, or either the development of a semi-open landscape paralleling the expansion of shrublands to the detriment of forests.

After ca. 6 ka BP, rates of sea level rise fell to 0.7 mm/yr in the Algarve (García-Artola et al., 2018), while in most of the estuaries of this area rates are of ca. 2.6 mm/yr and oscillations below 1 m defined the last 5000 years (Zazo et al., 2008; Lario et al., 2010; Costas et al., 2016). Some coastal elements like lagoons, spits, and barriers developed during this period (Dias et al., 2000).

8.4.3.- Human groups in dynamic littoral habitats

The rapid sea level rise occurring from ca. 13 to 7 ka BP was one of the main influential factors affecting the evolution of the coastal morphology and, therefore, human settlements. It is assumed that if the currently known Mesolithic sites were distributed along the coast, other hunter-gatherer occupations may have existed in the exposed continental shelf before its flooding due to marine transgression, which in that case may have been erased by the sea. The absence of any human settlement previous to ca. 9 ka BP in the studied area, with exception of one date in Barranco das Quebradas (Valente and Carvalho, 2005), is a clear example of the consequences of the sea level rise in this region.

From ca. 9 ka BP onwards, all the preserved Mesolithic sites are located at or above 50 m asl, except Castelejo and Palmones (supplementary material), and with direct access to the sea, considering the coastline at that time (Fig. 8.8). The lack of data in the littoral of the Gulf of Cádiz during this time span is critical, but it is especially dramatic in the central and eastern sector. The fact that most of the preserved sites are located in the cliffy area could be explained by a greater spatial impact of the sea level rise on the coastal plains at that time opened to the sea, since most of the spits and barriers developed after ca. 6 ka BP (Dias et al., 2000; Zazo et al., 2008; Lario et al., 2010; Costas et al., 2016).

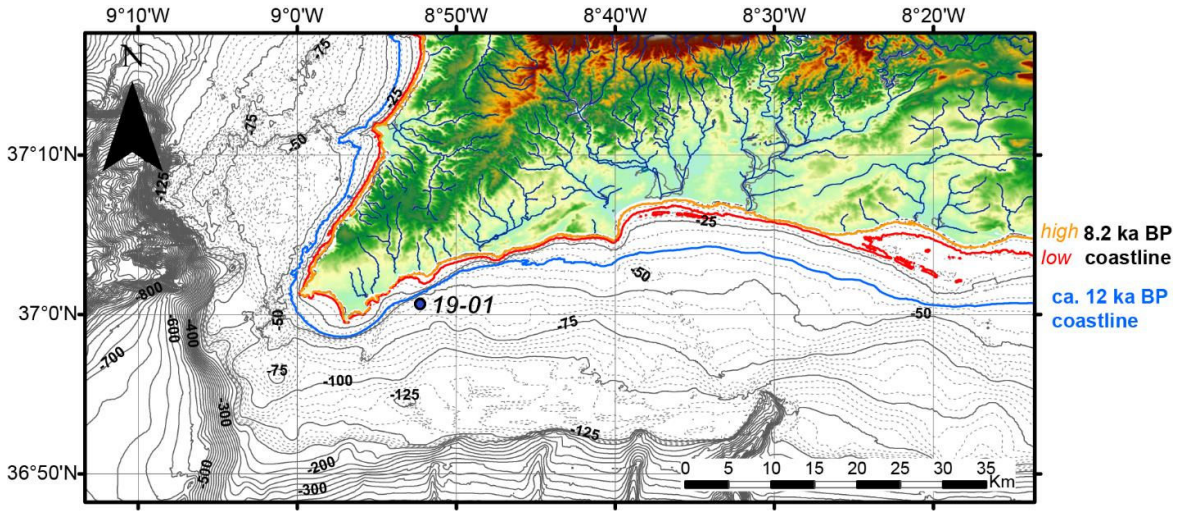

Figure 8.8. Digital terrain model map and bathymetry of the westernmost Algarve coast. Blue line indicates the coastline ca. 12 ka BP, red line shows the lowest possible coastline ca. 8. 2 ka BP, and yellow line situates the highest possible coastline ca. 8.2 ka BP. Blue dot represents the core 19-01. (Data source for bathymetry: EMODnet, https://www.emodnet-bathymetry.eu/ (accessed on 14/03/2021), for elevation: EU-DEM v.1.1, https://land.copernicus.eu/imagery-in-situ/eu-dem/eu-dem-v1.1 (accessed on 14/03/2021)).

For the period between ca. 9–7.5 ka BP, recent palaeodemographic studies propose a steady growth in population reflected in a concentration of archaeological sites in Central-South Portugal (Muge and Sado estuaries) and across the Algarve, although here in a more dispersed pattern (McLaughlin et al., 2020). Most of the sites concentrated in Western Algarve are shell-middens and with exemption of Vale Boi, where a human tooth dating of Mesolithic but without a funerary context was described [16], all the occupations in this region are seasonal camps focused on the collection of local resources, mainly marine food but also flint material (Valente and Carvalho, 2005). Some hypotheses correlate these sites with the existence of some (semi)permanent basecamps on which they would depend and that would have similar characteristics to those from the Sado and Tejo estuaries, with elaborated habitational structures, human burials, and broad-spectrum subsistence strategies (Bicho, 1994; Carvalho, 2007, 2010; Bicho et al., 2010). However, no (semi)permanent basecamps have been found in the Algarve region yet, and it seems to be a hard task considering the high level of human impact of this area during historic times. Regarding the eastern sector of the Gulf of Cádiz, environmental differences, and the specific cultural trajectories in the "Alborán territory" (Lindstädter et al., 2012), the nearest area where most of the pre-Neolithic sites are located, prevent us from establishing any comparison between archaeological sites of both zones.

Some authors consider that major changes in the social, technological, economic, and in settlement patterns of hunter-gatherer groups did not occur with the transition from the Late Pleistocene to the Holocene, but in relation to the 8.2 ka BP event. An example would be the development of the complex shell-midden basecamps located in inland areas following the course of the Tejo and Sado Rivers, as

opposed to the seasonal shell-middens located in the Algarve coast. This change of settlement patterns is explained as the result of a decline in the availability of the marine resources due to the joint action of a drop in the upwelling intensity together with an increased aridity ca. 8.2 ka BP (Bicho et al., 2010). This would have made the palaeoestuaries of these rivers stable resource-rich brackish environments, unlike the coastal unstable ecosystems adversely affected by this episode (Bicho et al., 2010). Likewise, results from the Pena d'Agua rock-shelter show important changes in the acquisition of raw material and technological features, which would be explained by modifications in mobility patterns from residential to logistic as an adaptive response to changing environments from 8.2 ka BP onwards (Pereira and Carvalho, 2016). Considering this hypothesis, these changes may have accelerated the confluence of human groups to settle in areas with stable and available resources, resulting in a (semi)sedentary pattern and social complexity (Bicho et al., 2010; Pereira and Carvalho, 2015; Pereira et al., 2016). However, there is no sign of the impact of the 8.2 ka BP event in the SW Atlantic Iberian margin in terms of settlement patterns. Notwithstanding, the bias caused by the lack of information needs more research in the study area to discern whether the seasonality of these sites reflect important regional differences, or if it is related to the existence of some (semi)permanent undiscovered basecamps.

Regarding the diet, not only shell-middens from Western Algarve display a specialization in the exploitation of marine resources, but also the seasonal occupation of Palmones revealed an intense gathering of shellfish (Uzquiano et al., 2020). Isotopic analysis of the Vale Boi teeth showed that, although marine resources were a prominent element, the diet of these Mesolithic groups was based on a mix of terrestrial and aquatic resources (Carvalho, 2007). However, there may have been important differences between sites, because isotopic data from the Sado shell-middens corroborated frequencies of marine diet ca. 25% (Stjerna, 2016), while in the Muge area the marine diet is above 50% (Bicho et al., 2017).

In the occidental area of the Algarve, topshells were the most abundant species consumed during the Early Mesolithic, while limpets and gooseneck barnacles were preferred during the Late Mesolithic and Early Neolithic (Valente, 2014). A reduction in the size of the shellfish collected was also identified in the transition from Mesolithic to Neolithic at Vale Boi, Rocha das Gaivotas, and Armação Nova, and it was considered a consequence of overexploitation (Carvalho, 2007) or a decrease in the foraging efficiency (Valente, 2014). However, in some Mediterranean areas such as the Pego palaeolagoon, a reduction of lagoon bivalve size during the Late Mesolithic has been observed, related to a decrease in resource productivity (Brisset et al., 2018). Despite this there was gently increase in ocean organic productivity linked to the slow overall cooling of the waters during the Mid Holocene, the warmer climate during the Holocene Thermal Maximum caused a weakening of the coastal upwelling, briefly interrupted during the short cooling episodes (Thornalley et al., 2009). This alteration in the coastal palaeoproductivity suggests that the modification in consumption patterns and the size decrease of

shellfish in SW Iberian sites may have been a consequence of these environmental alterations rather than being caused by cultural factors.

Commonly, the expansion of the Neolithic in both the western and eastern sectors of the Gulf of Cádiz is considered to have occurred around 7.5 ka BP (Carvalho, 2007; Martín-Socas et al., 2017). Corresponding to the period, different sequences reflect an aridity crisis affecting the vegetation of the SW Atlantic Iberian coast and the Alborán Sea (Fletcher et al., 2007; Fletcher and Goñi, 2008; Combourieu Nebout et al., 2009; Chabaud et al., 2014; Manzano et al., 2018; Oliveira et al., 2018; Gomes et al., 2020) and the geochemistry dataset reflects a decrease of land moisture (Fig. 8.6e). Some Mesolithic sites exhibit layers of Neolithic occupations (Castelejo, Barranco das Quebradas, Rocha das Gaivotas, Vale Boi, Palmones), although with hiatuses of several hundred years. The existence of several seasonal camps (Alcalar 7, Ribeira de Alcantarilha, Vale Santo I, Padrão, El Retamar) suggests the maintenance of previous subsistence strategies until this period. However, Neolithic times also involve new settlement patterns with sites located near rivers, shell deposits thinner than those in the Mesolithic, and caves. Only two sites suggest clear sedentary occupation (Castelo Belinho, Campo de Hockey) and the presence of seasonal camps reveals that the mobility was still key in the provisioning of different resources. Although the aim of this paper is not to discuss the origins of the Neolithic in the study area, the coexistence of previous (Mesolithic) and new (Neolithic) settlement patterns would be coherent with the idea of an integration of the two populations, rather than with the disappearance of the hunter-gatherer way of life (Bicho et al., 2017).

It is noteworthy to mention that except the pre-existing sites and some exceptions such as Praia do Forte Novo, El Retamar, and Campo de Hockey, all the Neolithic sites are located a few kilometres inland. Some changes in dietary habits regarding aquatic resources may be linked to this new settlement pattern, with the increased consumption of cockles and clams (Valente, 2014) typical from transitional brackish environments (rías), in contrast to the rocky-like shellfish preferred during the Mesolithic. Some ideas of what may lie behind this change in settlement patterns are:

Different populations would have a different perception of the same habitat, so they develop preferences for settling in distinct areas.

The maximum flooding of some river valleys would have forced human groups to settle in areas less close to the coastline. It should be also considered that archaeological sites located in the mouth of these rivers could have been buried or destroyed after this flooding episode and only those located in inland areas are preserved.

The weakening of the coastal upwelling during the Holocene Thermal Maximum may have caused a displacement toward areas with more stable resource availability, like what occurred in the Tejo and Sado

estuaries ca. 8.2–8 ka BP. Due to the bias in the preservation of Mesolithic sites in the study area, it is not possible to delineate to what extent this would have affected Mesolithic populations and to compare it to the Neolithic groups.

The aridity crisis reflected in the vegetation ca. 7.5 ka BP and recorded in other sequences ca. 7.5–7 ka BP may have led human groups to settle in areas more suitable for livestock and/or agriculture activities with available freshwater sources. One might speculate whether the aridity phase experienced during this period might have influenced the adoption of new subsistence strategies.

Regarding the resource exploitation and subsistence strategies, the introduction of a farming economic system resulted in a major dietary shift towards terrestrial food during this transitional period (Carvalho and Petchey, 2013). In relation to the agricultural practices, the first evidences were dated ca. 7.5–7 ka BP in Eastern Andalusia and Central-South Portugal, while there is not any direct evidence of their origins in the Occidental Andalusia and the Algarve area (López-Sáez et al., 2011). Livestock and grazing activities have direct testimony in zooarchaeological material. With respect to palynology, anthropogenic indicators are most likely to be identified in continental and especially archaeological deposits than in marine cores. However, the first manifestations of agricultural activities are only documented ca. 6 ka BP in areas with previous and important Mesolithic occupations (López-Sáez et al., 2011).

In relation to the preservation of human settlements, the lack of data in the central coast of the Gulf of Cádiz for both Mesolithic and Neolithic periods must be considered. Some archaeological sites and material identified in the surface are ascribed to the Early Neolithic, but the absence of systematic excavations and datings makes it presently impossible to shed light on the evolution of human groups during this time span. However, these settlements display a similar pattern compared with those of the Algarve, located close to the coast but some kilometers inland and near the Tinto, Odiel, Guadalquivir, and Guadalete rivers. An important issue to consider is related to the several high energy wave events that have been identified in this area during this period. In the Guadalquivir estuary, several high energy events were identified between 9.9–9.2 ka BP and 8.2–7.8 ka BP, some of them of unclear origin, some identified as storms, and one of them at 9.1 ka BP of tsunamigenic origins, while ca. 7–6.8 ka BP a palaeotsunami occurred (Manzano et al., 2018; Lario et al., 2011). The westernmost Algarve area was also hit by a high energy wave event, only identified in the Alvor estuary ca. 6.4 ka BP (Trog et al., 2013). Thus, not only the sea level rise but the hazardous nature of the coastal plain in this region, which seems to be constantly subject to these extreme events as well as affected by subsidence, may hamper the detection of potential archaeological sites.

8.5.- Conclusions

This paper presents a new palaeonvironmental dataset that contributes to a better understanding of the evolution of coastal landscapes in the littoral of the Gulf of Cádiz. The multi-proxy approach combining palynological, geochemical, and sedimentological data has provided a framework to better contextualize human occupations in SW Iberia during the Early-Mid Holocene (ca. 12–6 ka BP). A review of the state of the art regarding the archaeological research in this area was done considering the known archaeological sites with a reliable chronological control, which revealed an important lack of data. Some of our most important conclusions can be summed up as follows:

The onset of the Holocene is characterized by an increase in temperature, but weak continental conditions seem to remain until ca. 10 ka BP. Between ca. 10–7 ka BP there is an increase of forest values composed of mesophilous and Mediterranean taxa reflecting a rise of moisture, after which an important decrease in the forest cover occurred followed by a stepwise rise of heathlands ca. 7 ka BP.

Peaks of aridity indicators were identified at 8.2 and 7. 5 ka BP. The 8.2 ka BP event seems to affect vegetation with some delay, while the 7.5 ka BP event has an immediate impact in different taxa.

Changes detected in the geochemical record at ca. 8.2 ka BP seem to lead to abrupt palaeoceanographic modifications, but smooth gradual terrestrial changes. The first were responsible of modifications in the current system that could have affected the coastal productivity. The 7.5 ka BP event mirror a decrease in land moisture availability.

Holocene sea level rise shaped the coastal morphology and influenced the settlement patterns of human groups in both Mesolithic and Early Neolithic times, as well as the preservation of archaeological sites. High energy events and the subsidence to which certain areas are subjected have hampered the preservation of any potential remain.

Subsistence strategies based on the aquatic resource exploitation were common to hunter-gatherer groups during the Mesolithic, but also during the early stages of the Neolithic.

Only seasonal camps were identified among the Mesolithic sites in the study area, contrary to the (semi)permanent sites in South-Central Portugal. This may be tentatively interpreted as an effect of the lack of data due to the marine transgression or different regional patterns.

Mesolithic sites are located along the coastline with direct access to the sea. Although some of them persist during the Early Neolithic, in this period most of the sites are located near rivers some kilometers inland. Several hypotheses were presented to understand this change in settlement patterns.

Changes in dietary habits and the characteristics of some shellfish species during the Late Mesolithic/Early Neolithic seem to have been related to environmental changes rather than to cultural preferences or human overexploitation.

There are no clear evidences of the origins of agriculture in the studied area, which may be due to an archaeological bias or a consequence of a later adoption of this practice.

8.6.- Acknowledgements

This research was funded by the German Research Foundation (DFG)–project C1 within the CRC 806 "Our way to Europe" Deutsche Forschungsgemeinschaft (DFG, German Research Foundation) – Projektnummer 57444011, SFB 806 – and by the Fundação para a Ciência e Tecnologia (FCT) – Project OnOff, PTDC/CTAGEO/28941/2017. The authors are grateful to the research and technical crew under the command of Captain Hammacher from RV METEOR–M152 and to Prof. Dr. Melles (University of Cologne) who kindly facilitated access to an ITRAX core scanner for XRF analysis.

8.7.- Supplementary material

Site	Location	m asl	Lab Code	years BP	cal BC	mean cal BP	Cultures	Type of site	References
Castelejo	37° 5'59.40"N 8°56'38.89"W	20	ICEN-211			7970 ± 60	Mesolithic / Neolithic	Shell-midden	Araújo (2016)
			ICEN-213			7900 ± 40			Araújo (2016)
			ICEN-215			7880 ± 40			Araújo (2016)
			Beta-2908			7450 ± 40			Araújo (2016)
			BM-2276R	8.220 ± 120	7.050 - 6.450				Carvalho (2007)
			ICEN-743	7.530 ± 60	6.220 - 5.900				Carvalho (2007)
			ICEN-745	7.910 ± 60	6.510 - 6.230				Carvalho (2007)
			Beta-168461	6.830 ± 60	5.530 - 5.300				Carvalho (2007)
Barranco das Quebradas	37° 3'9.57"N 8°58'38.49"W	55	Wk-16428			9473 ± 54	Mesolithic / Neolithic	Shell-midden	Valente and Carvalho (2009)
			Wk-16427			8449 ± 51			Valente and Carvalho (2009)
			Wk-13693			8415 ± 74			Valente and Carvalho (2009)
			Wk-12134			8873 ± 57			Valente and Carvalho (2009)
			Wk-8951			8780 ± 60			Valente and Carvalho (2009)
			Wk-12133			8374 ± 54			Valente and Carvalho (2009)
			Wk-8940			8360 ± 80			Valente and Carvalho (2009)
			Wk-8950			9020 ± 70			Valente and Carvalho (2009)
			Wk-8939			8960 ± 70			Valente and Carvalho (2009)
Rocha das Gaivotas	37° 1'47.84"N 8°59'21.28"W	60	Wk-13691			8585 ± 60	Mesolithic / Neolithic	Shell-midden	Valente and Carvalho (2009)
			Wk-13690			8674 ± 52			Valente and Carvalho (2009)
			Wk-16425			8420 ± 60			Valente and Carvalho (2009)
			Wk-16426			8427 ± 51			Valente and Carvalho (2009)
			Wk-16424			8420 ± 60			Valente and Carvalho (2009)
			Wk-6075	7270 ± 70	5.980 - 5.640				Carvalho (2007)
			Wk-14794	7201 ± 39	5.810 - 5.620				Carvalho (2007)
			Wk-14793	7117 ± 38	5.730 - 5.550				Carvalho (2007)
			Wk-14797	6.862 ± 43	5.850 - 5.660				Carvalho (2007)
			Wk-14798	6.820 ± 51	5.810 - 5.620				Carvalho (2007)
			Wk-13692	7.092 ± 48	5.730 - 5.520				Carvalho (2007)
			Wk-17029	6.801 ± 39	5.480 - 5.310				Carvalho (2007)
Armação Nova	37° 1'48.00"N 8°57'44.69"W	60	ICEN-1228	8120 ± 60	6.700 - 6.440		Mesolithic	Open-air site / lithic workshop	Carvalho (2007)
			ICEN-1230	7530 ± 60	6.210 - 5.890				Carvalho (2007)
			ICEN-1229	7500 ± 60	6.210 - 5.840				Carvalho (2007)
			ICEN-1227	7350 ± 80	6.020 - 5.700				Carvalho (2007)
Cabranosa	37° 2'5.61"N 8°57'12.81"W	55	Sac-1321	6.930 ± 65	5.630 - 5.370		Neolithic	Base camp / settlement	Carvalho (2007)
Vale Santo I	37° 2'23.34"N 8°57'33.48"W	50	Wk-6673	6340 ± 120	5.550 - 5.000		Neolithic	Open-air site / lithic workshop	Carvalho (2007)
			Wk-12139	6.625 ± 51	5.350 - 5.030				Carvalho (2007)
Padrão	37° 3'47.80"N 8°53'7.01"W	76	ICEN-873	6560 ± 70	5.640 - 5.370		Neolithic	Open-air site	Carvalho (2007)
			ICEN-645	6440 ± 60	5.510 - 5.300				Carvalho (2007)

Vale Boi	37° 5'23.51"N 8°48'34.64"W	60	Wk-24761			8886 ± 30	Mesolithic / Neolithic	Open-air site	Cascalheira et al. (2012)
			AA-63305			8825 ± 57			Cascalheira et al. (2012)
			Wk-13685			8749 ± 58			Cascalheira et al. (2012)
			TO12197	7500 ± 90	6.530 - 6.100				Carvalho (2007)
			Wk17842	6095 ± 40	5.210 - 4.900				Carvalho (2007)
			OxA13445	6042 ± 34	5.040 - 4.840				Carvalho (2007)
			Wk17030	6036 ± 39	5.040 - 4.830				Carvalho (2007)
			Wk17843	6018 ± 34	5.010 - 4.800				Carvalho (2007)
Alcalar 7	37°11'56.73"N 8°35'16.90"W	60	Sac-1794	5640 ± 100	4.720 - 4.320		Neolithic	Shell-midden	Carvalho (2007)
			Beta-180978	5810 ± 40	4.780 - 4.540				Carvalho (2007)
			Sac-1608	6200 ± 70	5.320 - 4.980				Carvalho (2007)
			Sac-1601	6190 ± 80	5.320 - 4.930				Carvalho (2007)
			Sac-1602	6140 ± 70	5.300 - 4.900				Carvalho (2007)
			Sac-1594	6070 ± 70	5.210 - 4.800				Carvalho (2007)
			Beta-180181	5.690 ± 40	4.690 - 4.440				Carvalho (2007)
Castelo Belinho	37°12'23.62"N 8°33'16.21"W	80	Sac-2031	6260 ± 45	4772-4311		Neolithic	Base camp / settlement	Gomes (2013)
			Wk-28002	5436 ± 32	4345-4240				Carvalho and Petchey (2013)
			Sac-2030	5880 ± 55	4904–4598				Gomes (2013)
			Beta-199913	5720 ± 40	4685–4462				Carvalho (2007)
			Wk-28000	5662 ± 32	4582–4374				Carvalho (2007)
Ibne-Ahmmar	37° 9'21.97"N 8°30'0.27"W	10	Wk-17028	5150 ± 50	4000-3780		Neolithic	Necropolis cave	Boaventura et al. (2015)
Ribeira de Alcantarilha	37° 8'13.20"N 8°20'45.35"W	15	Wk-6672	6120 ± 70	5207–4859		Neolithic	Shell-midden	Bicho et al. (2003)
			Wk-6851	6160 ± 60	5227–4999				Bicho et al. (2003)
Praia do Forte Novo	37° 3'40.00"N 8° 3'54.08"W	5	SAC-1580	6090 ± 60	5211-5164		Neolithic	Settlement / salt production site	Leonor Rocha in Soares (2013)
			SAC-1639	6270 ± 100	5430-5393				Leonor Rocha in Soares (2013)
Algarão da Goldra	37° 6'40.89"N 7°59'34.44"W	300	Wk-31386	5336 ± 55	4330-4000		Neolithic	Settlement / Necropolis cave	Carvalho and Petchey (2013)
			Wk-31388	5642 ± 34	4545-4365				Carvalho and Petchey (2013)
Palmones	36° 09' 41"N 5°27' 26"W	9	-	<7500 / 8000 estimated			Mesolithic	Open-air site	Ramos-Muñoz and Castañeda (2005)
El Retamar	36° 31' 35"N 6° 09' 60"W	18	-			8211 ± 113	Neolithic	Open-air site	Ramos Muñoz (2008)
			-			7639 ± 59			Stipp and Timers (2002)
Campo de Hockey	36° 26' 44"N 6° 12' 36"W	14	-			6456 ± 53	Neolithic	Settlement / Necropolis	Vijande (2009); Vijande et al. (2015); Sánchez-Barba et al. (2019)
			-			6273 ± 32			
La Dehesilla	36° 39'40.0"N 5°38'45.0"W	284	GaK8954	7120 ± 200			Neolithic	Necropolis cave	Balsera et al. (2015) /supp material
			GaK8955	7040 ± 170					Balsera et al. (2015) /supp material
			UGRA259	6260 ± 100					Balsera et al. (2015) /supp material
			CNA4494	5900±30	4840–4713				García-Rivero et al. (2020)
			CNA4900	5870±30	4804–4683				García-Rivero et al. (2020)
			CNA4485	5790±30	4713–4551				García-Rivero et al. (2020)

Appendix 8.Sup1. Archaeological site framed between 10-6 ka cal BP in SW Iberia, with their coordinates, m asl and information about their chronologies, their cultural periods adscribed and references.

9.- Discussion

The palynological analysis of three different sequences, two continental cores from La Janda basin and one marine core from the Algarve continental shelf, allowed to reconstruct the palaeoenvironmental evolution of SW Iberia from a local and regional perspective. Through the correlation of the present data with the other palynological sequences from the study area, it was possible to define regional patterns in the vegetation dynamics and thus, infer the action of different climatic, edaphic and anthropogenic elements affecting them. It is important to mention that, although the results presented in chapter 5 include the Late Pleistocene, the palynological results do not allow to reconstruct the vegetation for this period (chapter 6 and 7): some pollen samples resulted sterile from a palynological point of view, and other samples were collected with a large interval that do not permit to infer detailed vegetal changes from a diachronic perspective. Thus, this discussion is focused on the Holocene.

In addition, thanks to the study of 49 modern pollen samples from SW Iberia, it was also possible to better understand which environmental variables and taphonomic elements affected the distribution of the vegetation and its representativeness in pollen samples. Because of this, some reasoning derived from the modern pollen-vegetation relationships can be extrapolated to the fossil pollen records, assisting in their interpretation. A discussion integrating all these data is presented in this section.

9.1.- Modern *vs* fossil pollen samples: taphonomic issues

Although a survey to collect and analyse modern pollen samples from the coring site and surroundings would be an ideal first step, especially to understand the local pollen signature, this is sometimes not possible for many reasons. In this thesis, publicly available data from the Eurasian Modern Pollen Database and surface samples from the cores drilled in La Janda basin were used to achieve these objectives. In this regard, it should be highlighted the role of open databases, as they allow research to be carried out using publicly available data in a transparent manner that ensures possible replication and can serve to establish new collaborative networks.

The floristic composition of the different contexts from which modern pollen samples were collected is well defined by the identified vegetal associations that are representative of these habitats. Some of them are perfectly reflected in the fossil pollen record of La Janda: subhumid forests, Mediterranean mixed oakwoods, Mediterranean shrubs, heathlands, riparian woodlands, salt marsh vegetation and freshwater communities, among others.

The role that some environmental variables have in the distribution of present plant communities revealed that: some taxa are highly dependent on precipitation and altitude, mostly those conforming forests in high-medium mountain areas, such as *Abies* and deciduous *Quercus*; precipitation seasonality

relates to samples from seasonal and semi-permanent lakes, as they are subjected to periods of seasonal droughts, and to Mediterranean taxa, as they can adapt to periods of water stress; some taxa are dependent on the characteristics of the soils, such is the case of Chenopodiaceae; and there is an heterogeneous group of taxa, mostly composed of herbs, that display a wide range of adaptability. Fossil pollen record show that, in some cases, the dominance or decrease of some vegetation groups that are dependent on high levels of humidity or are adapted to water stress, are related to climate variations: this scenario is generally defined by rise/drops of mesophilous trees (humidity), and depending on the period, increased/decreased values of grasslands or Mediterranean taxa (arid conditions). This corroborates the importance of precipitation as an environmental variable affecting vegetation. On the other hand, soil conditions are also determinant in the dynamics of freshwater/saltmarsh vegetation, as well as heathland communities in some parts of the core. Finally, human impact is reflected in La Janda through the presence of some anthropogenic indicators, but also through the peak of *Pinus* in the upper part of the core. Considering the low values of pines along the sequence, this seems to indicate the presence of modern monocultures, a feature that was also identified in some modern pollen samples.

Interestingly, modern moss samples reflect the dominant arboreal vegetation, while soil samples are mainly composed of herbaceous taxa. Although the habitat and its vegetal composition is determinant in this sense, sample type seems to reflect a certain bias in the pollen representation. The fact that samples of different type from the same context reflect the vegetation in a distinct way suggests variances at some point: during dispersal/transport, deposition and/or preservation, the latter being the most plausible. This is interesting because fossil pollen samples are in most cases sediment samples, although they may have plant macrofossils intercalated in the sedimentary matrix or consist of moss in peat bogs (which does not occur in any of the studied cores).

Transport is also a key element in the representativeness of pollen taxa. Modern lake samples (with river inputs) reflect floristic assemblages of both regional and local origins. However, aquatic environments affected by strong fluctuations in the water level are subjected to processes related with the oxidation, evaporation, repeated wetting and drying cycles, secondary transport and re-sedimentation, which affect pollen preservation and may result in the under/over-representation of some taxa. Although the input of local herbs is predominant in fossil samples from La Janda, the regional pollen signature is well reflected during the phase corresponding to subtidal facies, because a relatively stable water level existed, with river inputs transporting taxa from a wider catchment area. In contrasts, intertidal and supratidal deposits are clearly affected by taphonomic issues related to fluctuation in the water level and oxidation processes (Fig. 9.1). This resulted in a bad pollen preservation, as stated by the corrosion identified in many grains (ongoing research), leading to the over-representation of local taxa such as Asteraceae (in the lowest part of the studied sequence) and Asteraceae and Erica in the upper sections (Fig. 9.1).

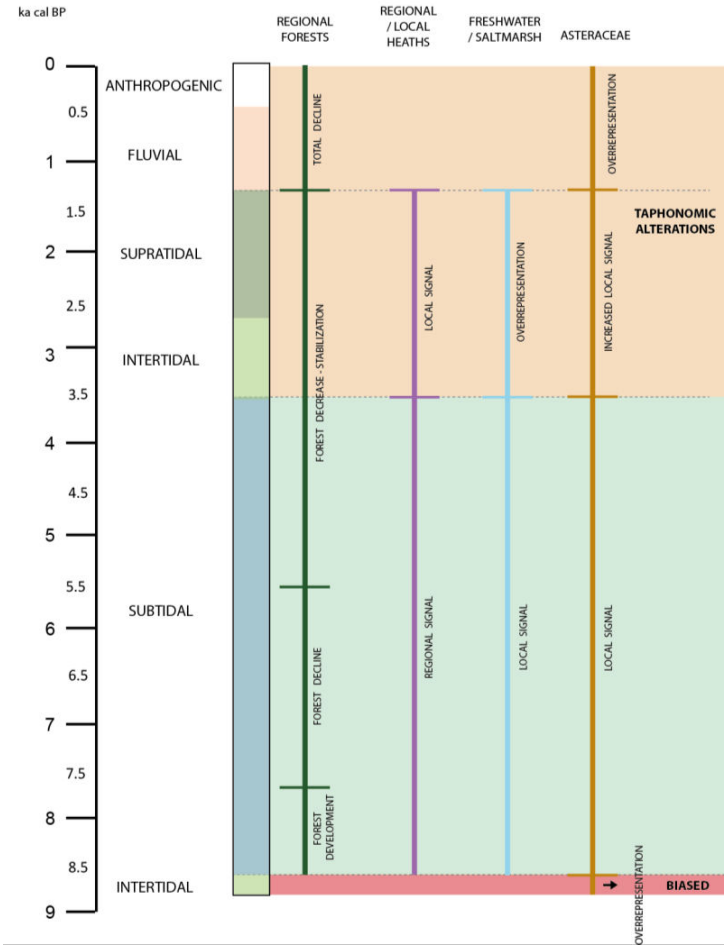

Fig. 9.1. Synthesis of the S3 core (La Janda) plotted against chronology with the facies that define the different environments through the sequence. Coloured lines represent the evolution of regional forests (green) and the character of the pollen signal (regional *vs* regional) referring to diverse groups of taxa (violet, blue and orange). The overrepresentation of some local taxa mask regional trends at some points of the sequence: the lower part of the core is completely biased preventing any reconstruction of the vegetation; the upper section (from ca. 3.5 ka cal BP) is affected by taphonomic factors that, once identified, allow to infer the local and regional scenario.

Regarding the fossil pollen record from the Algarve continental shelf, marine sequences reflect a regional-extraregional pollen signature due to their wider catchment areas, which provides an image of the regional vegetation colonising the adjacent continent. On the contrary, the interpretation of the local pollen signature results more confusing as it is not easy to infer their sources and define local patterns. Considering all the studied sequences, both continental and marine, some ideas can be proposed based on the study of modern-pollen samples. Pines were not an important element in La Janda basin until recent times (monocultures) as their values are rather low through the sequence. However, pine values in the GeoB23519-01 core were higher. *Pinus* grains are considered to be overrepresented in marine cores as they can travel over long distances by wind and their high values seaward also reflects certain hydrodynamic efficiency (Heusser and Balsam, 1977); therefore, they are usually excluded from the main pollen sum (Naughton et al., 2007; Gomes et al., 2020). In this sense it seems that pinewoods were not

abundant in the forests surrounding La Janda basin, but some authors also consider that the role of dominant winds coming from the North/Northwest may favour the transport of pine grains into the ocean (Sánchez-Goñi et al., 2018). The inherent characteristics of bisaccate grains and the role of wind direction may also explain the higher values of *Cedrus* in some points of the GeoB23519-01 core, while low percentages are identified in La Janda basin. High values of deciduous *Quercus* and *Quercus suber* during the maximum forest expansion in both marine and continental cores, suggest that their presence was considerable and they formed dense forests. Finally, the absence of *Abies* does not mean that fir forests were inexistent, but it seems more plausible to link this to the low dispersion of their grains (Arista and Talavera, 1994).

9.2.- Palaeoclimate variability in SW Iberia

As already stated at the beginning of this work, the Holocene is a period characterized by multiple palaeoecological changes defined by the complex interplay of different elements acting simultaneously at global, regional and local scales. Understanding factors of diverse nature and their interaction require proxies of diverse nature too. Thus, the combination of several proxies has proven to be key to fulfil the objective of identifying, defining and understanding the different phases and aspects implied in the palaeoenvironmental evolution of the study area from a climatic perspective.

Sedimentological analyses based on their visual inspection, and the study of their physical, mineralogical and geochemical properties were the main basis to reconstruct the diverse facies that allowed to decipher the paleogeographic evolution of La Janda basin (Mediavilla et al., 2023). The robust age-depth model based on 21 dating samples permitted to attribute precise chronologies and contextualise the various long and short-term processes described. Sedimentological analyses based on their visual inspection and the study of their geochemical properties were performed on the GeoB23519-01 core, which interpretation was supported by an age-depth model based on 13 dating samples.

The period corresponding to the Late Pleistocene is only present in La Janda sequences. Between ca. 20-16 ka cal BP, la Janda basin was characterized by the existence of an incised fluvial valley, which would be gradually flooded due to the sea level rise until reaching the maximum marine flooding ca. 7 ka cal BP. Sedimentological analyses allowed to reconstruct the evolution of the basin during this period, but the low sampling resolution in core S2 and the palynologically sterile samples in core S3 do not permit to draw the scenario from a palynological perspective to infer certain climatic factors. Because of this, the focus of the present discussion is centred on the Holocene.

The onset of the Holocene is defined by an increase of temperatures and moisture, but indicators of continental conditions have been identified in some marine (Carrión et al., 2000; Combourieu-Nebout et al., 2009; Lèzine and Denèfle, 1997; Val-Peón et al., 2021) and continental sequences (Fletcher et al.,

2007; Schröder et al., 2018, 2020) (Fig. 9.2). It has been found that the hydrological response in some Western Mediterranean areas during the Early Holocene maintained prolonged arid conditions, with shallow lake levels followed by an increase of moisture ca. 10-9 ka BP (Morellón et al., 2018). Some authors propose that this may have been linked to the presence of the Laurentide and Fennoscandian ice sheets in the North Atlantic Hemisphere, which may have had a strong impact on the atmospheric circulation by sustaining the North Atlantic storm track in a position that would not reach the Mediterranean region (Desprat et al., 2013; Gomes et al., 2020). After that, the maximum expansion of temperate and Mediterranean forests is recorded between ca. 10-7 ca kal BP in continental and marine sequences from SW Iberia, although with regional differences, as this period extends until ca. 5.5 ca kal BP in some cores (Fletcher et al., 2007; Fletcher and Sánchez-Goñi, 2008; Schröder et al., 2018, 2020; Val-Peón et al., 2021) (Fig. 9.2). The reason behind this expansion has been related to orbital-scale forces: high summer insolation would be translated in high temperatures and precipitation in the Western Mediterranean, defining the Holocene climate optimum (Dormoy et al., 2009; Anderson et al., 2011; Ramos-Román, 2018). Although summer insolation maxima may have favoured land-sea temperature contrast, this may have enhanced winter precipitation and maximum values of humidity (Meijer and Tuenter, 2007; Ramos-Román et al., 2018). However, some authors attributed regional differences in the maximum forest expansion timing to the diverse effect that high seasonality provoked in precipitation depending on the altitude, with higher evaporation rates during summer in lower areas (Anderson et al., 2011).

Palynological analysis in La Janda basin and the Algarve continental shelf record a progressive decrease of regional forest values, not abrupt but gradual, between ca. 7.5- 5.5 ka cal BP (chapters 6 and 7), being concomitant with the development of heaths in diverse continental and marine sequences (Fletcher and Sánchez-Goñi, 2008; Gomes et al., 2020; Val-Peón et al., 2021) (Fig. 9.2). Some authors consider this time frame as a transitional phase during which the present atmosphere circulation in the Northern Hemisphere was installed and the decrease in summer insolation led to a reduced thermal seasonality (Jalut et al., 2009; Walczak et al., 2015). Interestingly, it was during this period that regional climate models described a climatic transition towards drier and cooler conditions ca. 6 ka cal BP (Huntley and Prentice, 1988; Cheddadi et al., 1997), suggesting the establishment of the current NAO-like system that would support the interpretation of recurrent dry atmospheric conditions (Fletcher et al., 2013). This would be explained by the northward deviation of the North Atlantic westerlies with consequent reduced penetration of winter storm tracks into the Mediterranean region and reduced winter precipitation (Fletcher et al., 2013). In contrast, intervals of weakened westerly flow resulted in the southward displacement of Atlantic storm tracks, with increased winter precipitation in the western Mediterranean; this contrasting atmospheric pattern is reminiscent of the dipole pattern associated with the NAO (Fletcher et al., 2013).

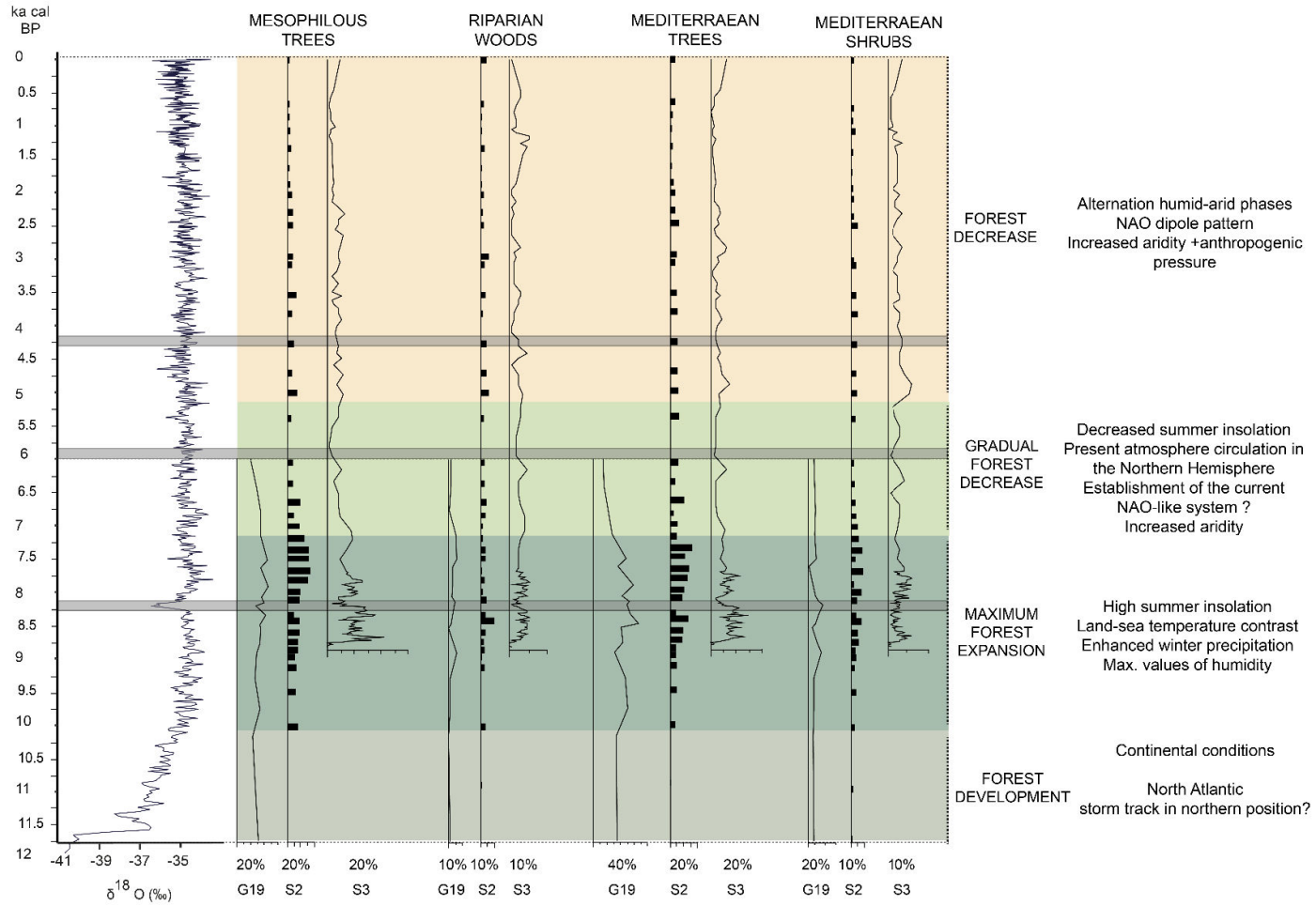

Fig. 9.2. Composite figure summarizing the main vegetation trends identified in the GeoB23519-01 (G19) and La Janda cores (S2 and S3), and their potential climatic drivers over the Holocene. From left to right: GISP2 oxygen isotope curve for the Holocene based on Grootes et al. (1999); percentage values of mesophilous trees, riparian taxa, Mediterranean trees and Mediterranean shrubs in the three studied cores; vegetation trends with a colour associated to each period; synthesis of the hypotheses presented in the text explaining how diverse climatic factors may have affected the evolution of the vegetation. Light grey lines correspond to those ice-rafted debris (IRD) events in the North Atlantic Ocean (Bond et al., 1997, 2001) that had an impact on the vegetation of the GeoB23519-01 (G19) and La Janda cores (S2 and S3).

An alternation of dry and humid phases was identified during the Late Holocene in different sequences from Southern Iberia (Fig. 9.2). Drier conditions were recorded ca. 3 ka cal BP and 1.3-0.6 ka cal BP (Mediaeval Climate Anomaly), and were correlated with the evolution of northern African climate (Martín-Puertas et al., 2008; Abel-Schaad et al., 2018; Schröder et al., 2020). Periods of higher moisture were identified between ca. 2.6-1.6 ka cal BP (Iberian Roman Humid Period), 0.8 ka cal BP, 0.6 ka cal BP and 0.4 ka cal BP (Little Ice Age), associated to negative NAO phases (Martín-Puertas et al., 2008; Fletcher et al., 2013). Although some of these trends are visible in La Janda record, such as the one related to the Medieval Climate Anomaly, others were not clearly identified. In this case, the prominence of the local vegetation and the impact of some taphonomic agents on the preservation of pollen grains in the upper part of the sequence could mask certain regional/global trends (Figs. 9.1 and 9.2).

There are a number of abrupt climatic events superimposed on these long-term trends occurring approximately at 11.1 ka, 10.4 ka, 9.3 ka, 8.2 ka, 5.9 ka, 4.2 ka, 2.8 ka, 1.4 ka, and 0.4 ka, according to Bond et al. (1997). Some authors describe them as aridification phases in the Western Mediterranean ca. 10.9-9.7, 8.4-7.6, 5.3-4.2, 4.3-3.4, 2.8-1.7 and 1.3-0.75 and correlate them with North Atlantic records, ^{14}C anomalies, glacial advances and palaeohydrological changes, suggesting that they are regional responses to global changes (Jalut et al., 2009). Although the causes behind some of these episodes are not totally clear, in some cases they had a strong impact on the vegetation. One of the most evident in the Algarve and La Janda sequences is the 8.2 ka cal BP event, for which the geochemical record of the GeoB23519-01 reveals abrupt palaeoceanographic modifications related with changes in the current system that could have affected the coastal productivity (Fig. 9.2). On the other hand, the vegetation points to abrupt cool and dry conditions. Another period of increased aridity is detected ca. 7.6-7.5 ka cal BP in these sequences, characterized by a decrease in land moisture availability according to the geochemical record (Val-Peón et al., 2021). Some other events with a visible impact on the vegetation were identified in La Janda basin at ca. 5.9 and 4.2 ka BP, probably associated to decreased precipitation (Fig. 9.2). The first is coincident with a lake level decrease in Laguna de Medina but is not clearly mirrored in other sequences (Reed et al., 2001). The 4.2 ka cal BP event id recorded in several cores from SW Iberia and the Western Mediterranean, although regional evidence is controversial and contradictory (Bini et al., 2019). Despite chronological problems and regional heterogeneity, recent studies interpret this episode as a cooling period with dry winters and summers (Bini et al., 2019).

Some authors, such as Zielhofer et al. (2019), associate these events during the Early Holocene with Atlantic coolings related with meltwater discharges and weakening of the Atlantic Meridonal overturning circulation, which would be in line with the interpretations for the GeoB23519-01 core and other records (Kilhavn et al., 2022). From ca. 5 ka cal BP, they correlate these episodes to humid winters and negative NAO conditions, evidencing a change in the ocean-atmospheric system as response to external forcing

(Ramos-Román et al., 2018; Schirrmacher et al., 2019; Zielhofer et al., 2019). However, other authors consider that the North Atlantic Oscillation-like pattern is not satisfactory to interpret some data regarding these episodes (Bini et al., 2019).

9.3.- Human-environment relationships during Prehistory

Whether as an expression of expansion into new territories or the exploitation of new ecosystems, among many other aspects, human behaviours and adaptive strategies may be reflected in material culture. But patterns of cultural change cannot be dissociated from the interaction between human groups and the environment, since behavioural responses to external environmental forces can be acquired, transmitted, and modified within the lifetimes of individuals (Henry, 1995). Therefore, by integrating data from both ecological and archaeological records, it is possible to contextualize various dimensions such as technical practices or spatial patterns in their landscape, which can lead to a better understanding of human behaviours in front of a changing environment.

During the Early Holocene, records do not show an impact on the landscape that could be associated to hunter-gatherer activities (Fig. 9.3). Only a few Mesolithic sites are recorded in this area, representing seasonal occupations of hunter-gatherer-fisher groups. A higher concentration of settlements is recorded in Southern Algarve, especially in the area of Cape São Vicente, and they are composed of shell-middens of different sizes and open air sites interpreted as seasonal occupations.

The main problem of this period is the lack of data in the study area, which is more dramatic in the Central-Eastern part of the Gulf of Cádiz. The marine transgression may have buried or eroded several archaeological sites located in the (at that time) exposed continental shelf, and this area was more exposed if compared to the Western rocky coast of the Algarve. Sea-level rise may have also affected Palaeolithic hunter-gatherer settlements, but the archaeological record for this period in the study area is more abundant, in part because an important number of Palaeolithic sites are located in rock-shelters and caves. Thus, it is worth asking whether there may be some cultural factors influencing settlement patterns of Mesolithic groups in SW Iberia, showing a preference for marine environments rather than mountainous areas. However, this idea cannot be extrapolated to other Mesolithic groups in the Western Mediterranean, as there are marked differences in technology, symbolism and preferences in settlement patterns from area to area. Behind this idea lie much deeper issues that are beyond the scope of this work, but it is interesting to highlight the importance of integrating ecological and archaeological data during this period in order to understand the role of the environment in the cultural and adaptive strategies of hunter-gatherer groups.

Without addressing the controversies regarding the neolithization process in SW Iberia, already summarised in chapter 3, there is an increase in archaeological sites during the Neolithic. Although several

settlements are situated near the coast, an important number are located inland. A gradual increment of human impact on the landscape is reflected in the presence of anthropozoogenous herbs and coprophilous fungi suggesting grazing and/or livestock activities with a progressive rise from ca. 7.3 ka cal BP on (Fig. 9.3). A punctual presence of Cerealia type was recorded ca 7.4 ka cal BP in La Janda basin (Fig. 9.3), but agricultural activities are only confirmed in the archaeological record ca. 6 ka cal BP (for now). From this time on, the presence of seeds, the adoption for crop-storage and the increment of polished tools (mills, grinding wheels, etc.) in the archaeological record confirm the relevance of agricultural practices within human groups. The local character of these anthropogenic markers complicates their interpretation in marine sequences, such as in the GeoB23519-01 core, with low values or absence of these elements.

A high number of archaeological sites are identified during the Chalcholithic and Bronze Age in the Eastern section of the Gulf of Cádiz, with settlement clusters located in strategic positions with good communication and visibility, some of them around important centres. Interestingly, the characteristics of the landscape is reflected in the main activities of some sites: those located in the littoral *campiña* show an inclination to agricultural practices, while those located in the area dominated by sandstones seem to be dedicated to livestock activities.

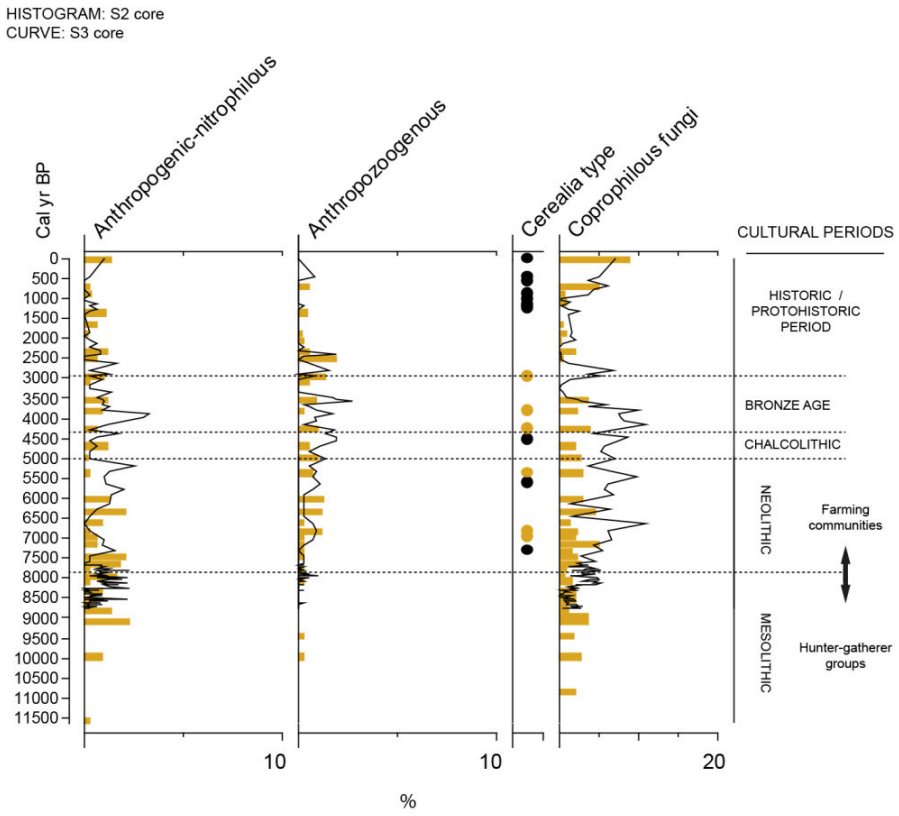

Fig. 9.3. La Janda diagrams overlapped and plotted against age indicating percentages of anthropogenic markers: anthropogenic-nitrophilous and anthropozoogenous herbs, grains of Cerealia type and coprophilous fungi. Prehistoric cultural periods are divided by dashed lines.

The palynological record show a slight but continuous increase of anthropogenic markers during the Chalcolithic and Bronze Age (Fig. 9.3). As already explained in chapter 7, an abrupt drop of coprophilous fungi is observable for the first time ca. 3.5-3.2 ka cal BP, fitting with the absence of anthopozoogenous markers in other sequences (López-Sáez et al., 2018) and suggesting the cessation of anthropogenic impact on the landscape, maybe related to an episode of a larger scale impact, perhaps culturally rooted. This phase (between ca. 3.6-3.2 ka cal BP) overlap and follow a period with maximum values of saltmarsh taxa, that may have growth in saline soils on the shores of the bay. Is it possible that an increase in salinity made the basin less attractive to herbivores as a drinking spot? Two other periods with low coprophilous fungi values are recorded during the Late Holocene between ca. 2.6-2.2 ka cal BP and ca. 1.2-1 ka cal BP, but their causes remain unclear. There is no evidence of the cessation of anthropogenic activity in other continental sequences for these same chronologies in the study area. However, a detailed interpretation of these last millennia of the sequence at a century resolution is complicated because two dating samples composed of reworked material had to be excluded from the age-depth model in both cores S2 and S3.

The sections of the core corresponding to historic times indicate an anthropogenic landscape in which agricultural activities are clearly represented in the palynological record, probably because crops are located on the new emerged soils of the basin. This may reinforce the idea that Cerealia pollen grains do not disperse long distances and their signature is only clear when it has a local origin (Fig. 9.3). When transported from other areas (regional origin), only a few grains would punctually appear, such may have been the case of the Cerealia presence in cores S2 and S3 at ca. 7.4, and later in punctual moments ca. 6.9, 6.8, 5.6 and 4.5 ka cal BP. This may also be coherent because the basin was flooded during these millennia. The lack of Cerealia type in intertidal and supratidal soils may be tentatively explained by the presence of saline soils that would not be the most suitable for cultivation. However, over the last millennia, the suitability of the new land in an eminently fluvial and less saline landscape has been exploited for agricultural and livestock activities, which is reflected in the increase of coprophilous fungi and cereals. At the same time, the highest percentages of erosive process indicators (mostly *Glomus*) are recorded, probably as result of these farming activities or the development of new soils.

In summary, La Janda may have acted as biodiversity hotspot congregating human groups and animals around as a resource-gathering area while it was a restricted bay connected to the sea. That status would have been maintained during the transitional period, with diverse ecosystems (marine, brackish, fluvial) acting as poles of attraction. However, soil salinity would have hampered the development of local agricultural activities, which would have been developed on more suitable soils in nearby areas. These practices would intensify in the basin with the establishment of a landscape composed of fluvial wetlands and ephemeral ponds in less saline soils.

10.- Conclusion and outlook

Based on the results presented and discussed in this work, some ideas for improving future research arise.

The most immediate improvement to be made is to further correlate the S3 core from La Janda basin with specific geochemical elements in order to identify any trends that might be related to vegetation dynamics, as it was done for the GeoB23519-01 core.

In addition to this ongoing task, probably the most obvious idea to improve the results of any palaeoecological research is to increase the resolution of palynological sampling (in this case) and dating. Apart from external factors such as funding, time, objectives of the project etc., which may limit our expectations, the possibility to carry out high-resolution research also depends on the sequences themselves: sedimentation rates may limit the resolution of palynological sampling, as this requires a minimum of sediment; and the existence of well-preserved and datable material is also not in our hands. But it is precisely through a multidisciplinary approach that certain gaps can be filled. Sedimentological, geochemical and palynological proxies are commonly used in palaeoecological research on natural and archaeological deposits. However, in recent years, advances in other proxies have shown to improve the ability to provide a detailed picture into past environmental changes.

One example is the study of compound-specific isotope analyses of sedimentary organic compounds, particularly hydrocarbons derived from fossil leaf waxes (n-alkanes) that have emerged as a powerful palaeoclimate proxy for reconstructing palaeohydrological (hydrogen isotope) and palaeoecological (carbon isotope) conditions at a high spatial and temporal resolution (Connolly, 2021). The combination of microscopic (e.g., pollen, micromorphology) and molecular approaches may offer the opportunity to improve the study of the natural palaeoenvironment, but also to reconstruct conditions in archaeological contexts where post-depositional disturbance or poor preservation may be a problem (Connolly et al., 2019).

Another example is the recent and successful study of sedimentary ancient DNA (sedaDNA) in sediment samples from different environments (Garcés-Pastor et al., 2022). With the development of new sequencing technologies such as polymerase chain reaction (PCR) and high-throughput sequencing (HTS), it is now possible to identify many organisms, including plant taxa, to a higher taxonomic level (Higuchi et al. 1984). Therefore, combining palynological and sedaDNA analyses in sediments from the same samples, from natural and/or archaeological deposits, may allow exploring the recent evolutionary history of specific plant communities, the ecology of paleoenvironments, and understanding population relationships, migration, and domestication processes (Ter Schure et al., 2022).

Finally, the use of recently developed statistical software, such as for example ChronoCurve (Lanos and Dufresne, 2019), may allow to calibrate and plot different dates into a Bayesian age-depth model that may help to test the contemporaneity (or not) of specific climate episodes and human occupations in a certain area (Lanos and Philippe, 2017).

References

A.A.V.V. (1963). Estudio agrobiológico de la provincia de Cádiz. Excma. Diputación Provincial. Cádiz.

Abel-Schaad D, Iriarte E, López-Sáez JA et al. (2018) Are Cedrus Atlantica forests in the Rif mountains Fof Morocco heading towards local extinction? The Holocene 28: 1023–1037.

Adkins, J., de Menocal, P., Eshel, G. (2006). The "African Humid Period" and the Record of Marine Upwelling from Excess 230Th in Ocean Drilling Program Hole 658C. Paleoceanography, 21, doi:10.1029/2005PA001200.

Agencia Estatal de Meteorología (AEMET) (2011) Atlas Climático Ibérico—Iberian Climate Atlas. Madrid, Spain, ISBN 978-84-7837-079-5.

Alba-Sánchez, F., López-Sáez, J.A., Pando, B.B. de, Linares, J.C., Nieto-Lugilde, D., López-Merino, L., (2010). Past and present potential distribution of the Iberian *Abies* species: A phytogeographic approach using fossil pollen data and species distribution models. Diversity and Distributions 16, 214–228. https://doi.org/10.1111/j.1472-4642.2010.00636.x

Allard, J., Chaumillon, E., Bertin, X., Poirier, C., Ganthy, F. (2010). Sedimentary record of environmental changes and human interferences in a macrotidal bay for the last millenaries: the Marennes-Oléron Bay (SW France). Bulletin de la Société Géologique de France, 181, 151-169. https://doi.org/10.2113/gssgfbull.181.2.151

Allen, G.P., Posamentier, H.W. (1994). Transgressive facies and sequence architecture in mixed tide-and wave-dominated incised valleys: example from the Gironde estuary, France. *In*: Dalrymple RW, Boyd R, Zaitlin BA (eds.), Incised-valleys systems: origin and sedimentary sequences. SEPM Special Publication, 51, 225-240. https://doi.org/10.2110/pec.94.12.0225

Alley, R.B. Ágústsdóttir, A.M. (2005). The 8k Event: Cause and Consequences of a Major Holocene Abrupt Climate Change. Quaternary Science Reviews, 24, 1123–1149, https://doi:10.1016/j.quascirev.2004.12.004

Anderson, R. S., Homola, R. L., Davis, R. B., Jacobson Jr., G. L. (1984). Fossil remains of the mycorrhizal fungal *Glomus fasciculatum* complex in postglacial lake sediments from Maine. Canadian Journal of Botany, 62, 235-2328. https://doi.org/10.1139/b84-316

Anderson, R.S., Jiménez-Moreno, G., Carrión, J.S., Pérez-Martínez, C. (2011). Postglacial history of alpine vegetation, fire, and climate from Laguna de Río Seco, Sierra Nevada, southern Spain. Quaternary Science Revies 30, 1615–1629. http://dx.doi.org/10.1016/j.quascirev.2011.03.005

Araújo, J., (2012). Pollen–vegetation relationships in SW Iberia: preliminary results and implications for Quaternary research. Quaternary International, XVIII INQUA Congress, 21st–27th July, 2011, Bern, Switzerland 279–280, 23. https://doi.org/10.1016/j.quaint.2012.07.098

Arista, M., Talavera, S., (1994). Pollen dispersal capacity and pollen viability of *Abies pinsapo* Boiss. Silvae Genetica 43, 2–3.

Arista Palmero, M., Herrera Maliani, F.J., Talavera Lozano, S., (1997). *Abies pinsapo* Boiss.: a protected species in a protected area. Bocconea 7, 427-436.

Arteaga, O., Hoffmann, G. (1999). Dialéctica del proceso natural y sociohistórico en las costas mediterráneas de Andalucía. Revista Atlántica-Mediterránea de Prehistoria y Arqueología Social II: 13-121.

Arteaga, O. (1992). Tribalización, jerarquización y estado en el territorio de El Argar, Spal 1, pp. 179-208.

Arteaga, O. (2002). Las teorías explicativas de los 'cambios culturales' durante la Prehistoria en Andalucía: Nuevas alternativas de investigación. In AA.VV., Actas del III Congreso de Historia de Andalucía, Córdoba, Publicaciones del Monte de Piedad y Caja de Ahorros de Córdoba, pp. 247-311.

Arteaga, O., Roos, A. M. (2009). Comentarios acerca del Neolítico Antiguo en Andalucía. In Cruz-Auñón, R., Ferrer, E., coords.: Estudios de Prehistoria y Arqueología en Homenaje a Pilar Acosta Martínez. Secretariado de Publicaciones. Universidad de Sevilla, pp. 37-73.

Azañón, J.M., Galindo-Zaldívar, J., García-Dueñas, V., Jabaloy, A. (2002). Alpine tectonics II: Betic Cordillera and Balearic Islands. *In*: Gibbons, W., Moreno, T. (eds.), The Geology of Spain. Geological Society of London, Geology of Series, pp. 401-416. https://doi.org/10.1144/GOSPP.16

Baena, J., Zazo, C., Goy, J.L., Dabrio, C., Leyva, F., Ruiz, P. (1987). Memoria y mapa geológico de Paterna de Rivera. Hoja 1.062. IGME, 54 pp., Madrid.

Balnayá, J.C., García Dueñas, V. (1988). Les directions structurales dans le Domaine d'Alborán de part et d'autre du Détroit de Gibraltar. Comptes rendus de l'Académie des sciences. Série 2, Mécanique, Physique, Chimie, Sciences de l'univers, Sciences de la Terre, 304, 929-932.

Barboni, D., Harrison, S.P., Bartlein, P.J., Jalut, G., New, M., Prentice, I.C., Sanchez-Goñi, M.F., Spessa, A., Davis, B. and Stevenson, A.C. (2004). Relationships between plant traits and climate in the Mediterranean region: A pollen data analysis. Journal of Vegetation Science, 15: 635-646. https://doi.org/10.1111/j.1654-1103.2004.tb02305.x

Barcia-García, C., Mas-Cornellá, M., Maximiano Castillejo, A.M., Jordá Pardo, J.F. (2023). Dots, circles and horses: New rock art evidence through image-based digital methods in Moro Cave (Tarifa, Spain). Journal of Archaeological Science: Reports 47, 103826. https://doi.org/10.1016/j.jasrep.2023.103826

Baringer, M.O., Price, J.F. (1999). A review of the physical oceanography of the Mediterranean outflow. Marine Geology, 155, 63-82

Barkley, F. A. (1934). The Statistical Theory of Pollen Analysis. Ecology, 15(3), 283–289. https://doi.org/10.2307/1932469

Basset, A., Sabetta, L., Fonnesu, A., Mouillot, D., Do Chi, T., Viaroli, P., Giordani, G., Reizopoulou, S., Abbiati, M., Carrada, G.C. (2006). Typology in Mediterranean transitional waters: new challenges and perspectives. Aquat. Conserv. Mar. Freshw. Ecosyst. 16, 441–455. https://doi.org/10.1002/aqc.767

Bazzicalupo, P., Maiorano, P., Girone, A., Marino, M., Combourieu-Nebout, N., Pelosi, N., Salgueiro, E., Incarbona, A. (2020). Holocene Climate Variability of the Western Mediterranean: Surface Water Dynamics Inferred from Calcareous Plankton Assemblages. Holocene 30, 691–708, https://doi:10.1177/0959683619895580

Beaulieu, J.-L.D., Miras, Y., Andrieu-Ponel, V., Guiter, F. (2005). Vegetation dynamics in north-western Mediterranean regions: Instability of the Mediterranean bioclimate. Plant Biosyst. - Int. J. Deal. Asp. Plant Biol. 139, 114–126. https://doi.org/10.1080/11263500500197858

Becerra, S., Cabello, L., Domínguez-Bella, S. (2019). Recursos líticos y distribución de productos arqueológicos en las dos orillas del estrecho de Gibraltar por las sociedades prehistóricas. In Ramos Muñoz, J., Otte, Vijande Vila (eds), Les Migrations entre Mëditerranée et terre promies. Vol. 1 Ocupaciones de la región geohistórica del estrecho de Gibraltar por sociedaes prehistóricas y de la antigüeda. Actas Historia y Arte. Editorial UCa. Universidad de Cádiz, Cádiz, pp. 27-48.

Belén, M., Anglada, R., Conlin, E., Gómez, T., Jiménez, A. (2000). Expresiones funerarias de la Prehistoriareciente de Carmona (Sevilla), Spal, 9, 385-403.

Benayas, R., José, M. and Scheiner, S.M. (2002), Plant diversity, biogeography and environment in Iberia: Patterns and possible causal factors. Journal of Vegetation Science, 13: 245-258. https://doi.org/10.1111/j.1654-1103.2002.tb02045.x

Benkhelil, J. (1976). Étude Tectonique de la Terminaison Occidentale des Cordillères Bétiques (Espagne). PhD Thesis. Univ. Nice, Nice (France).

Berger, A.L. (1978). Long-Term Variations of Caloric Insolation Resulting from the Earth's Orbital Elements. Quat. Res., 9, 139–167, https://doi:10.1016/0033-5894(78)90064-9

Beug, H.J. (2004). Leitfaden der Pollenbestimmung für Mitteleuropa und angrenzende Gebiete. Pfeil, München. 542 pp.

Bicho, N. (1994). The End of the Paleolithic and the Mesolithic in Portugal. Current Anthropology 35, 664–674.

Bicho, N., Umbelino, C., Detry, C., Pereira, T. (2010). The Emergence of Muge Mesolithic Shell Middens in Central Portugal and the 8200 Cal Yr BP Cold Event. Journal of Island and Coastal Archaeology5, 86–104, https://doi:10.1080/15564891003638184

Bicho, N., Cascalheira, J., Gonçalves, C., Umbelino, C., Rivero, D.G., André, L. (2017) Resilience, Replacement and Acculturation in the Mesolithic/Neolithic Transition: The Case of Muge, Central Portugal. Quaternary International, 446, 31–42, https://doi:10.1016/j.quaint.2016.09.049

Billeaud, I., Tessier, B., Lesueur, P. (2009). Impacts of late Holocene rapid climate changes as recorded in a macrotidal coastal setting (Mont-Saint-Michel Bay, France). Geology, 37, 1031-1034. https://doi.org/10.1130/G30310A.1

Bini, M., Zanchetta, G., Perşoiu, A., Cartier, R., Català, A., Cacho, I., Dean, J. R., Di Rita, F., Drysdale, R. N., Finnè, M., Isola, I., Jalali, B., Lirer, F., Magri, D., Masi, A., Marks, L., Mercuri, A. M., Peyron, O., Sadori, L., Sicre, M.-A., Welc, F., Zielhofer, C., Brisset, E. (2019). The 4.2 ka BP Event in the Mediterranean region: an overview. Climate of the Past, 15, 555–577. https://doi.org/10.5194/cp-15-555-2019

Birks, H.J.B, Birks, H.H. (1980). Quaternary Palaeoecology. University Park Press, Baltimore.

Blaauw M (2022). clam: Classical Age-Depth Modelling of Cores from Deposits. R package version 2.5.0, https://CRAN.R-project.org/package=clam

Blaauw M, Christen JA (2011). Flexible paleoclimate age-depth models using an autoregressive gamma process. Bayesian Analysis, 6(3), 457-474. https://doi.org/10.1214/11-BA618

Bond, G., Heinrich, H., Broecker, W., Labeyrie, L., McManus, J., Andrews, J., Huon, S., Jantschik, R., Clasen, S., Simet, C., Tedesco, K., Klas, M., Bonani, G., Ivy, S. (1992). Evidence for massive discharges of icebergs into the North Atlantic Ocean during the last glacial period. Nature 360, 245-249.

Bond, G., W. Showers, M. Cheseby, R. Lotti, P. Almasi, P. deMenocal, P. Priore, H. Cullen, I. Hajdas and G. Bonani, (1997). A pervasive millennial-scale cycle in North Atlantic Holocene and Glacial climates, Science 278, 1257-1266.

Bond, G., Kromer, B., Beer, J., Muscheler, R., Evans, M. N., Showers, W., Hoffmann, S., Lotti-Bond, R., Hajdas, I., Bonani, G. (2001). Persistent solar influence on North Atlantic climate during the Holocene. Science, 278, 1257-1266.

Bonny, A.P. (1976). Recruitment of pollen to the seston and sediment of some Lake District Lakes. Journal of Ecology 64 (3), 859. https://doi.org/10.2307/2258814

Bonny, A.P. (1978). The effect of pollen recruitment processes on pollen distribution over the sediment surface of a small Lake in Cumbria. Journal of Ecology 66 (2), 385. https://doi.org/10.2307/2259143.

Borrego, J., Morales, J.A., Pendón, J.G. (1993). Holocene filling of an estuarine lagoon along the mesotidal Coast of Huelva: the Piedras River mouth, southwestern Spain. Journal of Coastal Research, 8, 321-343.

Borja, P.G., Tortosa, J.E.A., Aubán, J.B., Pardo, J.F.J. (2010). Nuevas perspectivas sobre la neolitización en la cueva de Nerja (Málaga-España): La cerámica de la sala del vestíbulo. Zephyrus Revista de Prehistoria y Arqueología 66, 109–132, https://doi:10.14201

Born, A., Levermann, A. (2010). The 8.2 Ka Event: Abrupt Transition of the Subpolar Gyre toward a Modern North Atlantic Circulation. Geochemistry, Geophysics, Geosystems 11, https://doi:10.1029/2009GC003024

Borrego, J., Morales, J.A., Pendón, J.G. (1995). Holocene estuarine facies along the mesotidal coast of Huelva, south-western Spain. *In*: Flemming, B.W., Bartholomä, A. (eds.), Tidal Signatures in Modern and Ancient Sediments. International Association of Sedimentologists Special Publication, 24, 151–170. https://doi.org/10.1002/9781444304138.ch10

Borrego, J., Ruiz, F., González-Regalado, M.L., Pendón, J.G., Morales, J.A. (1999). The Holocene transgression into the estuarine basin of the Odiel River mouth (Cádiz Gulf, SW Spain): lithology and faunal assemblages. Quaternary Science Reviews, 18, 769-788. https://doi.org/10.1016/S0277-3791(97)00085-1

Borrego, J., López González, N., Carro, B., (2004). Geochemical signature as paleoenvironmental markers in Holocene sediments of the Tinto River estuary (Southwestern Spain). Estuarine, Coastal and Shelf Science, 61, 631-641. https://doi.org/10.1016/j.ecss.2004.07.004

Borzenkova, I.I., Zorita, E., Borisova, O., Kalniņa, L., Kisielienė, D., Koff, T., Kuznetsov, D., Lemdahl, G., Sapelko, T., Stančikaitė, M., Subetto, D.A. (2015). Climate Change During the Holocene (Past 12,000 Years). https://doi.org/10.1007/978-3-319-16006-1_2

Boski, T., Moura, D., Camacho, S., Duarte, R.D.N., Scott, D.B., Veiga Pires, C., Pedro, P., Santana, P. (2002). Postglacial sea level rise and sedimentary response in the Guadiana Estuary, Portugal/Spain border. Sedimentary Geology, 150, 103-121. https://doi.org/10.1016/S0037-0738(01)00270-6

Boski, T., Camacho, S., Moura, D., Fletcher, W., Wilamowski, A., Veiga-Pires, C., Correia, V., Loureiro, C., Santana, P. (2008). Chronology of the sedimentary processes during the postglacial sea level rise in two estuaries of the Algarve coast, Southern Portugal. Estuarine. Coastal and Shelf Science, 77, 230-244. https://doi.org/10.1016/j.ecss.2007.09.012

Bova, S., Rosenthal, Y., Liu, Z., Godad, S.P., Yan, M. (2021). Seasonal Origin of the Thermal Maxima at the Holocene and the Last Interglacial. Nature, 589, 548-553. https://doi.org/10.1038/s41586-020-03155-x

Boyd, R., Dalrymple, R.W., Zaitlin, B.A. (2006). Estuarine and incised-valley facies models. *In*: Posamentier, H.W., Walker, R.G. (eds.), Facies models revisited. SEPM Special Publication, 84, 171-235. https://doi.org/10.2110/pec.06.84.0171

Bradley, R.S. (1999). Paleoclimatology. Reconstructing Climates of the Quaternary, 2nd ed. International Geophysics Series, Volume 64. xv 613 pp. San Diego, London, Boston, New York, Sydney, Tokyo, Toronto: Academic Press. Price £44.95 (hard covers). ISBN 0 12 124010 X. Geological Magazine, 138(4), 499-508. https://doi:10.1017/S0016756801255599

Brisset, E., Burjachs, F., Ballesteros Navarro, B.J., Fernández-López de Pablo, J. (2018). Socio-Ecological Adaptation to Early-Holocene Sea-Level Rise in the Western Mediterranean. Global and Planetary Change 169, 156–167, https://doi:10.1016/j.gloplacha.2018.07.016

Brooks, J., Shaw, G. (1972). Geochemistry of sporopollenin. Chemical Geology 10, 69–87. https://doi.org/10.1016/0009-2541(72)90078-2

Brown, A.G., Carpenter, R.G., Walling, D.E. (2007). Monitoring fluvial pollen transport, its relationship to catchment vegetation and implications for palaeoenvironmental studies. Review of Palaeobotany and Palynology 147 (1-4), 60–76. https://doi.org/10.1016/j.revpalbo.2007.06.005

Burjachs, F. (1990). Palinologia dels dolmens de l'Alt Emporda i dels diposits quaternaris de la Cova de l'Arbreda (Serinya, Pla de l'Estany) i del Pla de l'Estany (Olot, Garrotxa): evolucio del paisatge vegetal i

del clima des fa mes de 140.000 anys al NE de la Peninsula Iberica. PhD Thesis, Univ. Autonoma de Barcelona, Barcelona (Spain).

Burjachs, F., López-Sáez, J.A., Iriarte, M.J. (2003). Metodología arqueopalinológica. In: Buxó, R., Piqué, R. (Eds.), La recogida de muestras en arqueobotànica: objetivos y propuestas metodológicas. Museu d'Arqueologia de Catalunya, Barcelona, pp. 11–18.

Burnett, A.P., Soreghan, M.J., Scholz, C.A., Brown, E.T. (2011). Tropical East African Climate Change and Its Relation to Global Climate: A Record from Lake Tanganyika, Tropical East Africa, over the Past 90+kyr. Palaeogeography, Palaeoclimatology, Palaeoecology 303, 155–167, https://doi:10.1016/j.palaeo.2010.02.011

Butzer, K. (1982). Archaeology as Human Ecology: Method and Theory for a Contextual Approach. Cambridge: Cambridge University Press. https://doi:10.1017/CBO9780511558245

Cáceres, I. (2003). La Transición de las sociedades cazadoras-recolectoras a pastoras-agricultoras en el Mediodía Peninsular a través de los restos óseos. BAR International Series 1194. Oxford.

Cacho, I., Grimalt, J.O., Canals, M., Sbaffi, L., Shackleton, N.J., Schönfeld, J., Zahn, R. (2001). Variability of the Western Mediterranean Sea Surface Temperature during the Last 25,000 Years and Its Connection with the Northern Hemisphere Climatic Changes. Paleoceanography, 16, 40–52, https://doi:10.1029/2000PA000502

Calvert, S.E., Pedersen, T.F. (2007). Chapter Fourteen Elemental Proxies for Palaeoclimatic and Palaeoceanographic Variability in Marine Sediments: Interpretation and Application. In Developments in Marine Geology; Hillaire–Marcel, C., De Vernal, A., Eds.; Proxies in Late Cenozoic Paleoceanography; Elsevier: Amsterdam, The Netherlands, Volume 1, pp. 567–644.

Campbell, I.D., Quaternary pollen taphonomy: examples of differential redeposition and differential preservation. Palaeogeography, Palaeoclimatology, Palaeoecology 149, 245–256. https://doi.org/10.1016/s0031-0182(98)00204-1

Campbell, I.D., Campbell, S., (1994). Pollen preservation: experimental wet–dry cycles in saline and desalinated sediments. Palynology 18, 5–10. https://doi.org/10.1080/01916122.1994.9989434

Camuera, J., Jiménez-Moreno, G., Ramos-Román, M.J., García-Alix, A., Toney, J.L., Anderson, R.S., Jiménez-Espejo, F., Bright, J., Webster, C., Yanes, Y., Carrión, J.S. (2019). Vegetation and climate changes during the last two glacial-interglacial cycles in the western Mediterranean: A new long pollen record from Padul (southern Iberian Peninsula). Quaternary Science Reviews 205, 86–105. https://doi.org/10.1016/j.quascirev.2018.12.013

Cantillo-Duarte, J.J., Ramos Muñoz, J., Soriguer-Escofet, M., Pérez Rodríguez, M., Vijande Vila, E., Bernal, D., Domínguez-Bella, S., Zabala, C., Hernando, J., Clemente Conte, I. (2010). La explotación de los recursos marinos por sociedades cazadoras-recolectoras-mariscadores y tribales comunitarias en la región histórica del Estrecho de Gibraltar. Férvedes 6, pp. 105-113.

Cantillo-Duarte, J.J., Vijande Vila, E. (2014). Análisis microespacial de la malacofauna marina en el asentamiento neolítico de Campo de Hockey (San Fernando, Cádiz). Nuevos datos sobre la función social del espacio. In J.J. Cantillo Duarte, D. Bernal, J. Ramos Muñoz (eds.): Moluscos y púrpura en contextos arqueológicos atlántico-mediterráneos. Nuevos datos y reflexiones en clave de proceso histórico. Servicio de Publicaciones de la Universidad de Cádiz. Cádiz, 51-58.

Cantillo-Duarte, J.J., Ramos Muñoz; J., Pérez Rodríguez, M., Vijande Vila, E., Domínguez-Bella, S., Montañés Caballero, M. (2017). I. Las sociedades prehistóricas en el término municipal de Vejer de la Frontera. In: Ferrer, E. y Cantillo Duarte, J.J. Arqueología en Vejer. De la Prehistoria al período andalusí. Editorial Universidad de Sevilla, Ayuntamiento de Vejer de la Frontera. Sevilla, 29-53.

Cantillo-Duarte, J.J., Soriguer-Escofet, M. (2019). Los moluscos marinos. In: Vijande Vila, E., Ramos Muñoz, J., Fernández Sánchez, D., Cantillo Duarte, J.J., Pérez Rodríguez, M. coords, 2019. La Esparragosa (Chiclana de La Frontera, Cádiz). Un campo de silos neolítico del IV milenio a.n.e. Arqueología Monografías. Junta de Andalucía, Sevilla, pp. 91-101.

Cañellas-Boltà, N., Rull, V., Vigo, J., Mercadé, A. (2009). Modern pollen–vegetation relationships along an altitudinal transect in the central Pyrenees (southwestern Europe). The Holocene 19, 1185–1200.

Carrasco, J.L., Reyes, G.D. (1986). El tránsito del Calcolítico al Bronce a través del "Monte Berrueco" de Medina Sidonia (Cádiz). Trabajos De Prehistoria, 43, 61-84.

Carrión, J.S. (1992). Late Quaternary pollen sequence from Carihuela Cave, southeastern Spain. Review of Palaeobotany and Palynology 71, 37–77.

Carrión, J.S., Van Geel, B. (1999). Fine-resolution Upper Weichselian and Holocene palynological record from Navarrés (Valencia, Spain) and a discussion about factors of Mediterranean forest succession. Review of Palaeobotany and Palynology, 106, 209– 236 https://doi.org/10.1006/jhev.1998.0276

Carrión, J.S., Parra, I., Navarro, C. and Munuera, M. (2000a). Past distribution and ecology of the cork oak (*Quercus suber*) in the Iberian Peninsula: a pollen-analytical approach. Diversity and Distributions, 6: 29-44. https://doi.org/10.1046/j.1472-4642.2000.00070.x

Carrión, J. S., Navarro, C., Navarro, J., Munuera, M. (2000b). The distribution of cluster pine (*Pinus pinaster*) in Spain as derived from palaeoecological data: relationships with phytosociological classification. The Holocene, 10(2), 243–252. https://doi.org/10.1191/095968300676937462

Carrión, J.S., Fernández, S., González-Sampériz, P., Leroy, S.A.G., López-Sáez, J.A., Burjachs, F., Gil-Romera, G., Rodríguez-Sánchez, E., García-Antón, M., Gil-García, M.J., Parra, I., Santos, L., López-García, P., Yll, E.I., Dupré, M. (2009). Sterility cases and causes in Quaternary pollen analysis in the Iberian Peninsula: the advantages of reporting bad luck. Internet Archaeology 25, 1–54. http://intarch.ac.uk/journal/issue25/5/toc.html

Carrión, J.S., Graciela Fernández, P.G.-R., Santiago González-Sampériz, Badal, E., Lourdes Carrión-Marco, Y.L.-M., López-Sáez, J.A., Fierro, E., Burjachs, F. (2010). Expected trends and surprises in the Lateglacial and Holocene vegetation history of the Iberian Peninsula and Balearic Islands. Review of Palaeobotany and Palynology 162, 458–475. https://doi.org/10.1016/j.revpalbo.2009.12.007

Carvalho, A.F. (2007). A Neolitização do Portugal Meridional: Os Exemplos do Maciço Calcário Estremenho e do Algarve Ocidental. PhD Thesis, Univ. Algarve, Faro (Portugal).

Carvalho, A.F. (2011). Le passage vers l'Atlantique : Le processus de néolithisation en Algarve (sud du Portugal). L'Anthropologie 2010, 114, 141–178, https://doi:10.1016/j.anthro.2010.03.008

Carvalho, A.F., Petchey, F. (2013). Stable Isotope Evidence of Neolithic Palaeodiets in the Coastal Regions of Southern Portugal. Journal of Island and Coastal Archaeology 8, 361–383, https://doi:10.1080/15564894.2013.811447

Castañeda Fernández, V., Pérez Ramos, L., Torres Abril, F., Costela Muñoz, Y. (2020). El sitio al aire libre con tecnología solutrense de la Fontanilla (Conil de la Frontera, Cádiz, España). Dataciones absolutas y estudio de los productos líticos a raíz de las últimas excavaciones. Lucentum 39: 31-51.

Castañeda Fernández, V., Costela Muñoz, Y., Fernández de la Gala, J.V., García-Jiménez, I., López Sáez, J.A. (2022). La cueva artificial 14 de la necrópolis de Los Algarbes (Tarifa, Cádiz). Muerte y ritual a mediados del III Milenio a.n.e. Saguntum 54: 43-64.

Castro Román, J.C., Núñez Granados, M.Á., Dueñas López, M.A., Recio Espejo, J.M., 2000. Génesis y funcionamiento de humedales en la depresión de La Janda: la zona palustre de Janda (Veger, Cádiz). Oxyura Revista Sobre Las Zonas Húmedas 10, 169–178.

Castro Román, J.C., Recio Espejo, J.M. (2007). La laguna de La Janda (Cádiz): 10 años después del inicio de los estudios básicos para su restauración ecológica. Almoraima Revista de Estudios Campogibraltareños 175–184.

Catuneanu, O. (2019). Model-independent sequence stratigraphy. Earth-Science Reviews, 188, 312-388. https://doi.org/10.1016/j.earscirev.2018.09.017

Català, A., Cacho, I., Frigola, J., Pena, L.D., Lirer, F. (2019). Holocene Hydrography Evolution in the Alboran Sea: A Multi-Record and Multi-Proxy Comparison. Climate of the Past, 15, 927–942, https://doi:10.5194/cp-15-927-2019

Catuneanu, O., Galloway, W.E., Kendall, C.G.St.C., Miall, A.D., Posamentier, H.W., Strasser, A., Tucker, M.E. (2011). Sequence Stratigraphy: Methodology and Nomenclature. Newsletters on Stratigraphy, 44, 173-245. https://doi.org/10.1127/0078-0421/2011/0011

Cearreta, A., Irabien, M.J., Pascual, A. (2004). Human activities along the Basque coast during the last two centuries: geological perspective of recent anthropogenic impact on the coast and its environmental consequences. In: Borja, A., Collins, M. (eds.), Oceanography and Marine Environment of the Basque Country, Elsevier Oceanography Series, 70, 27-50. https://doi.org/10.1016/S0422-9894(04)80040-0

Cearreta, A., García-Artola, A., Leorri, E., Irabien, M.J., Masque, P. (2013). Recent environmental evolution of regenerated salt marshes in the southern Bay of Biscay: anthropogenic evidences in their sedimentary record. Journal of Marine Systems, 109-110, S203-S212. https://doi.org/10.1016/j.jmarsys.2011.07.013

Chabaud, L., Sánchez Goñi, M. F., Desprat, S., Rossignol, L. (2014). Land–sea climatic variability in the eastern North Atlantic subtropical region over the last 14,200 years: Atmospheric and oceanic processes at different timescales. The Holocene, 24 (7), 787–797. https://doi.org/10.1177/0959683614530439

Chagué, C. (2020). Chapter 18—Applications of geochemical proxies in paleotsunami research. In Geological Records of Tsunamis and Other Extreme Waves; Engel, M., Pilarczyk, J., May, S.M., Brill, D., Garrett, E., Eds.; Elsevier: Amsterdam, The Netherlands, ISBN 978-0-12-815686-5.

Charlet, L., Tournassat, C. (2005). Fe(II)–Na(I)–Ca(II) Cation Exchange on Montmorillonite in Chloride Medium: Evidence for Preferential Clay Adsorption of Chloride – Metal Ion Pairs in Seawater. Aquatic Geochemistry, 11, 115-137. https://doi.org/10.1007/s10498-004-1166-5

Chaumillon, E., Proust, J.N., Menier, D., Weber, N. (2008). Incised-valley morphologies and sedimentary-fills within the inner shelf of the Bay of Biscay (France): a synthesis. Journal of Marine Systems, 72, 383-396. https://doi.org/10.1016/j.jmarsys.2007.05.014

Cheddadi, R., Yu, G., Guiot, J., Harrison, S.P., Prentice, I.C. (1997). The climate of Europe 6000 years ago. Climate Dynamics. 13, 1–9. http://dx.doi.org/10.1007/s003820050148

Cheng, Z., Weng, C., Steinke, S., Mohtadi, M., 2021. Marine pollen records provide perspective on coastal wetlands through Quaternary sea-level changes. Ecological Indicators 133, 108405. https://doi.org/10.1016/j.ecolind.2021.108405

Chéron, S., Etoubleau, J., Bayon, G., Garziglia, S., Boissier, A. (2016). Focus on sulfur count rates along marine sediment cores acquired by XRF Core Scanner. *X*-Ray Spectrometry, 45, 288-298. https://doi.org/10.1002/xrs.2704

Chevalier, M., Davis, B., Heiri, O., Seppä, H., Chase, B.M., Gajewski, K., Lacourse, T., Telford, R.J., Finsinger, W., Guiot, J., Kühl, N., Maezumi, S.Y., Tipton, J.R., Carter, V.A., Brussel, T.V., Phelps, L.N., Dawson, A., Zanon, M., Vallé, F., Nolan, C.J., Mauri, A., Vernal, A., Izumi, K., Holmström, L., Marsicek, J.P., Goring, S.J., Sommer, P.S., Chaput, M.A., Kupriyanov, D.A. (2020). Pollen-based climate reconstruction techniques for late Quaternary studies. Earth-Science Reviews.

Cirujano, S., Meco, A., Garcia Murillo, P. (2014). Flora acuática española. Hidrófitos vasculares. Real Jardín Botánico, Madrid.

Clemente Conte, I., Pijoan, J. (2005). Estudio funcional de los instrumentos de trabajo lítico en el "Embarcadero del río Palmones. In: Ramos Muñoz, Castañeda Fernández, V., eds.: Excavación en el asentamiento prehistórico del Embarcadero del río Palmones (Algeciras, Cádiz). Universidad de Cádiz y Ayuntamiento de Algeciras. Cádiz.

Clemente Conte I., García, V., Ramos Muñoz, J., Domínguez-Bella, S., Pérez Rodríguez, M., Vijande Vila, E., Cantillo Duarte, J.J., Soriguer-Escofet, M., Zabala, C., Hernando, J. (2010). The Lithic Tools of the La Esparragosa Site (Chiclana de la Frontera, Cádiz, Spain, fourth Millennium BC): A Methodological Contribution of the Study of Lithic Tools for the Consumption of Fish. In T. Bekker-Nielsen, D. Bernal Casasola (eds.) Ancient nets and fishing gear: proceedings of the International Workshop on Nets and Fishing Gear in Classical Antiquity: a first approach. Servicio de Publicaciones Aarhus University Press, Cádiz, pp. 275-286.

Clemente Conte, I., Mazzuco, N. (2019). Uso de los instrumentos líticos tallados: aportes para una interpretación socioeconómica a partir de los procesos productivos registrados. In: La Esparragosa (Chiclana de la Frontera, Cádiz). Un campo de silos neolítico del IV milenio A.N.E. (coords. Vijande Vija, E., Ramos Muñoz, J., Fernández-Sánchez, D.S., Cantillo Duarte, J.J., Pérrez-Rodríguez, M.) ISBN 9788499593456

Coles, G.M., Gilbertson, D.D., Hunt, C.O., Jenkinson, R.D.S. (1989). Taphonomy and the palynology of cave deposits. Cave Science 16, 83–89.

Collado Giraldo, H., Coord. (2018a). Handpas. Manos del pasado. Catálogo de representaciones de manos en el arte rupestre paleolítico de la península ibérica. Badajoz: Junta de Extremadura.

Collado Giraldo, H., García, J.J., Bea, M., Ramos, J., Cantalejo Duarte, P., Domínguez-Bella, S., Fernández Sánchez, D. (2018b). Cueva de las Estrellas. In Collado Giraldo, H. (ed.): Handpas. Manos del pasado. Catálogo de representaciones de manos en el arte rupestre paleolítico de la península ibérica. Badajoz: Junta de Extremadura.

Collado Giraldo, H., Bea, M., Ramos, J., Cantalejo Duarte, P., Domínguez-Bella, S., Ramón Bello, J., Angás, J., Miranda, J., Gracia, F.J., Fernández Sánchez, D., Aranda, A., Luque, A., García Arranz, J.J., Aguilar, J.C. (2019). Un nuevo grupo de manos paleolíticas en la provincia más meridional de Europa. La cueva de las Estrellas o Cueva Abejera 2 (Castellar de la Frontera, Cádiz, España). Zephyrus, LXXXIII, 15-38.

Combourieu Nebout, N., Peyron, O., Dormoy, I., Desprat, S., Beaudouin, C., Kotthoff, U., & Marret, F. (2009). Rapid climatic variability in the west Mediterranean during the last 25 000 years from high resolution pollen data. Climate of the Past, 5(3), 503–521. https://doi.org/10.5194/cp-5-503-2009

Connolly, R., Jambrina–Enríquez, M., Herrera–Herrera, A.V., Vidal-Matutano, P., Fagoaga, A., Marquina–Blasco, R., Marin–Monfort, M.D., Ruiz–Sánchez, F.J., Laplana, C., Bailon, S., Pérez, L., Leierer, L., Hernández, C.M., Galván, B., Mallol, C. (2019). A multiproxy record of palaeoenvironmental conditions at the Middle Palaeolithic site of Abric del Pastor (Eastern Iberia). Quaternary Science Reviews 225, 106023.

Connolly, R. (2021). Investigating microscopic and molecular organic matter to explore the role of climate in Neanderthal social and cultural evolution at a regional scale. PhD Thesis, Univ. La Laguna, La Laguna (Spain).

Cornu, S., Lucas, Y., Lebon, E., Ambrosi, J.P., Luizão, F., Rouiller, J., Bonnay, M., Neal, C. (1999). Evidence of Titanium Mobility in Soil Profiles, Manaus, Central Amazonia. Geoderma, 91, 281–295, https://doi:10.1016/S0016-7061(99)00007-5

Cortés-Sánchez, M., Jiménez-Espejo, F.J., Simón-Vallejo, M.D., Gibaja-Bao, J.F., Faustino Carvalho, A., Martínez-Ruiz, F., Rodrigo Gamiz, M., Flores, J.-A., Paytan, A., López-Sáez, J.A., et al. (2012). The Mesolithic—Neolithic Transition in Southern Iberia. Quaternary Research 77, 221–234, https://doi:10.1016/j.yqres.2011.12.003

Costas, S., Ferreira, Ó., Plomaritis, T.A., Leorri, E. (2016). Coastal Barrier Stratigraphy for Holocene High-Resolution Sea-Level Reconstruction. Scientific Reports, 6, 38726, https://doi:10.1038/srep38726

Crema, E.R. and Bevan, A. (2021). Inference from large sets of radiocarbon dates: software and methods. Radiocarbon, 63, 23-39. https://dx.doi.org/10.1017/RDC.2020.95

Cross, A.T., Thompson, G.G., Zaitzeff, J.B. (1966). Source and distribution of palynomorphs in bottom sediments, southern part of Gulf of California. Marine Geology 4 (6), 467–524. https://doi.org/10.1016/0025-3227(66)90012-0

Cour, P. (1974) Nouvelles techniques de détection des flux et des retombées polliniques. Pollen et Spores 16, 103–142.

Cugny, C., Mazier, F., Galop, D. (2010). Modern and fossil non-pollen palynomorphs from the Basque mountains (western Pyrenees, France): the use of coprophilous fungi to reconstruct pastoral activity. Vegetation History and Archaeobotany 19, 391–408. https://doi.org/10.1007/s00334-010-0242-6

Dansgaard, W., Johnsen, S.J., Clausen, H.B., Dahl-Jensen, D., Gundestrup, N.S., Hammer, C.U., Hvidberg, C.S., Steffensen, J.P., Sveinbjörnsdóttir, A.E., Jouzel, J., Bond, G.C. (1993). Evidence for general instability of past climate from a 250-kyr ice-core record. Nature, 364, 218-220.

Dabrio, C. J. (1982). Sedimentary structures generated on the foreshore by migrating ridge and runnel systems on microtidal and mesotidal coast on S. Spain. Sedimentary Geology, 32:141.151. https://doi.org/10.1016/0037-0738(82)90018-5

Dabrio, C.J., Zazo, C., Lario, J., Goy, J.L., Sierro, F.J., Borja, F., González, J.A., Flores, J.A. (1999). Sequence stratigraphy of Holocene incised-valley fills and coastal evolution in the Gulf of Cádiz southern Spain. Geologie en Mijnbouw 77, 263-281. https://doi.org/10.1023/A:1003643006015

Dabrio, C. J., Zazo, C., Goy, J. L., Sierro, F. J., Borja, F., Lario, J., González, J. A., Flores, J. A. (2000). Depositional history of estuarine infill during the last postglacial transgression (Gulf of Cádiz, southern Spain). Marine Geology, 162, 381-404. https://doi.org/10.1016/S0025-3227(99)00069-9

Dalrymple, R.W., Boyd, R., Zaitlin, B.A. (1994). History of research, types and internal organisation of incised valley systems: introduction to the volume. In: Dalrymple, R.W., Boyd, R., Zaitlin, B.A. (eds.), Incised-Valley Systems: Origin and Sedimentary Sequences, SEPM Special Publication, 51, 225-240. https://doi.org/10.2110/pec.94.12.0003

Dallmeyer, A., Claussen, M., Lorenz, S. J., Sigl, M., Toohey, M., Herzschuh, U. (2021). Holocene vegetation transitions and their climatic drivers in MPI-ESM1.2, Climate of the Past, 17, 2481–2513, https://doi.org/10.5194/cp-17-2481-2021

Davis, M.B. (1968). Pollen grains in lake sediments: redeposition caused by seasonal water circulation. Science 162 (3855), 796–799. https://doi.org/10.1126/science:162.3855.796

Davis, B.A.S., Chevalier, M., Sommer, P., Carter, V.A., Finsinger, W., Mauri, A., Phelps, L.N., Zanon, M., Abegglen, R., Åkesson, C.M., Alba-Sánchez, F., et al. (2020). The Eurasian Modern Pollen Database (EMPD), version 2. Earth System Science Data 12, 2423–2445. https://doi.org/10.5194/essd-12-2423-2020

DeBusk Jr, G.H. (1997). The distribution of pollen in the surface sediments of Lake Malawi, Africa, and the transport of pollen in large lakes. Review of Palaeobotany and Palynology 97, 123–153.

De Castro, S., Lobo, F.J. (2018). Sedimentary infilling of bedrock-controlled palaeo-embayments off Cape Trafalgar, Strait of Gibraltar (Gulf of Cádiz). Geo-Marine Letters, 38, 47-62. https://doi.org/10.1007/s00367-017-0508-4

De la Serna, B.V., Sánchez-Mata, D., Gavilán, R.G. (2016). Marcescent Quercus pyrenaica Forest on the Iberian Peninsula. In: Box, E. (eds) Vegetation Structure and Function at Multiple Spatial, Temporal and Conceptual Scales. Geobotany Studies. Springer https://doi.org/10.1007/978-3-319-21452-8_10

De Nascimento, L. de, Nogué, S., Fernández-Lugo, S., Méndez, J., Otto, R., Whittaker, R.J., Willis, K.J., Fernández-Palacios, J.M. (2015). Modern pollen rain in Canary Island ecosystems and its implications for the interpretation of fossil records. Review of Palaeobotany and Palynology 214, 27–39. https://doi.org/10.1016/j.revpalbo.2014.11.002

Delgado, J., Boski, T., Nieto, J.M., Pereira, L., Moura, D., Gomes, A., Sousa, C., García-tenorio, R. (2012). Sea-level rise and anthropogenic activities recorded in the late Pleistocene / Holocene sedimentary in fi ll of the Guadiana Estuary (SW Iberia). Quaternary Science Reviews 33, 121–141. https://doi.org/10.1016/j.quascirev.2011.12.002

Demina, L.L., Novichkova, E.A., Lisitzin, A.P., Kozina, N.V. (2019). Geochemical Signatures of Paleoclimate Changes in the Sediment Cores from the Gloria and Snorri Drifts (Northwest Atlantic) over the Holocene-Mid Pleistocene. Geosciences 9, 432, https://doi:10.3390/geosciences9100432

Desprat, S., Sanchez Goñi, M.F., Lourre, M.F. (2003). Revealing climate variability of the last three millennia in northwestern Iberia using pollen influx data. Earth and Planetary Science Letters 213, 63–78.

Desprat, S., Combourieu-Nebout, N., Essallami, L., Sicre, M.A., Dormoy, I., Peyron, O., Siani, G., Roumazeilles, V.B., Turon, J.L. (2013). Deglacial and Holocene vegetation and climatic changes in the southern Central Mediterranean from a direct land-sea correlation. Climate of the Past 9, 767–787. https://doi.org/10.5194/cp-9-767-2013

Desprat, S., Sánchez Goñi, M.F., Naughton, F., Turon, J.L., Duprat, J., Malaizé, B., Cortijo, E., Peypouquet, J.P. (2007) 25. Climate variability of the last five isotopic interglacials: direct land-sea-ice correlation from the multiproxy analysis of north-western Iberian margin deep-sea cores. In: Developments in Quaternary Sciences. 7. Elsevier, pp. 375–386. https://doi.org/10.1016/S1571-0866(07)80050-9

Dias, J.M.A., Boski, T., Rodrigues, A., Magalhães, F. (2000). Coast Line Evolution in Portugal since the Last Glacial Maximum until Present—A Synthesis. Marine Geology 170, 177–186.

Díaz Fernández, P.M., (1994). Relations between modern pollen rain and Mediterranean vegetation in Sierra Madrona (Spain). Review of Palaeobotany and Palynology 82, 113–125.

Dincauze, D.F. (2000). Environmental Archeology: Principles and practice. Univ. of Cambridge Press, Cambridge.

Djamali, M., Cilleros, K. (2020). Statistically significant minimum pollen count in quaternary pollen analysis; the case of pollen-rich lake sediments. Review of Palaeobotany and Palynology, 275, 104156. https://doi.org/10.1016/j.revpalbo.2019.104156

Domínguez, E., Blanca, G., Valdés, B., Cabezudo, B., Nieto, J.M., Silvestre, S. (1993). Introducción a la flora andaluza. Sevilla: Agencia del Medio Ambiente, 1993. ISBN: 84-87294-40-5

Domínguez-Bella, S., Pérez, M., Ramos Muñoz, J., Morata, D., Castañeda Fernández, V. (2002). Raw materials, source areas and technological relationships between minerals, rocks and prehistoric non-flint stone tools from the Atlantic zone, Cádiz province, SSW Spain. In: Jerem, E., Biró, K.T., eds.: Archaeometry 98. Archaeopress. BAR International Series 1043 II. Oxford.

Domínguez-Bella, S., Ramos Muñoz, J., Castañeda Fernández, V., Garcia, M.E., Sánchez, M., Jurado, G., Moncayo, F. (2004). Lithic products analysis, raw materials and technology in the prehistoric settlement of the river Palmones (Algeciras, Cádiz, Spain). BAR Internacional Series 1270. Oxford.

Domínguez-Bella, S., Ramos Muñoz, J., Pérez Rodríguez, M. (2008). Productos arqueológicos exóticos en los contextos de los yacimientos prehistóricos de la Banda Atlántica de Cádiz. Inferencias de su documentación. In Ramos Muño, J. (Coord.): La ocupación prehistórica de la campiña litoral y banda atlántica de Cádiz.

Domínguez-Bella, S., Ramos Muñoz, J., Martínez, J. (2011). Prehistoric Flint exploitation in Loma de Enmedio-Realillo (Tarifa coast, Cádiz, Spain). In Capote, M., Consuegra, S., Díaz-del-Río, P., Terradas, X. (eds.), Proceedings of the 2nd International Conference of the UISPP Commission on Flint Mining in Pre- and Protohistoric Times (Madrid, 14-17 October 2009). BAR International Series.

Domínguez-Bella, S. (2015). El estudio de las materias primas en la Prehistoria del ámbito gaditano. In: Bernal, D., Raissouni, B., Ramos Muñoz, J., Bouzouggar, Al (eds.). Actas del I Seminario Hispano-Marroquí de especialización en arqueología. Universidad de Cádiz, INSAP, Cádiz.

Domínguez-Bella, S., Ramos Muñoz, J., Vijande Vila, E. (2016). Materias primas silíceas en la prehistoria del occidente de Andalucía. Cuadernos de Prehistoria de Universidad de Granada. CPAG 26.

Dormoy, I., Peyron, O., Combourieu Nebout, N., Goring, S., Kotthoff, U., Magny, M., Pross, J. (2009). Terrestrial climate variability and seasonality changes in the Mediterranean region between 15 000 and 4000 years BP deduced from marine pollen records. Climate of the Past 5, 615–632. http://dx.doi.org/10.5194/cp-5-615-2009

Dueñas López, M.A., Recio Espejo, J.M. (2000). Bases ecológicas para la restauración de los humedales de La Janda (Cádiz, España). Universidad de Córdoba, Córdoba, Spain.

Dunlea, A. G., Murray, R. W., Tada, R., Alvarez-Zarikian, C. A., Anderson, C.H., Gilli, A., Giosan, L., Gorgas, T., Hennekam, R., Irino, T., Murayama, M., Peterson, L.C., Reichart, G.-J., Seki, A., Zheng, H., Ziegler, M. (2020). Intercomparison of XRF core scanning results from seven labs and approaches to practical calibration. Geochemistry, Geophysics, Geosystems, 21, e2020GC009248. https://doi.org/10.1029/2020GC009248

Efremov, I. A. (1940). Taphonomy: a new branch of paleontology. Pan-American Geology. 74: 81–93.

Elsik, W.C. (1971). Microbiological degradation of Sporopollenin. In: Brooks, J., Grant, P.R., Muir, M., van Gijzel, P., Shaw, G. (Eds.), Sporopollenin. Academic Press, London, pp. 480–509 https://doi.org/10.1016/B978-0-12-135750-4.50023-7

EMODNET (2020). EMODNET bathymetry (DTM) 2020. Accessed on 15/01/2023. https://emodnet.ec.europa.eu/en/bathymetry

Erdtman, G. (1932) Literature on Pollen-statistics and related topics published 1930 and 1931, Geologiska Föreningen i Stockholm Förhandlingar, 54:4, 395-418 https://doi.org/10.1080/11035893209448816

Escacena, J.L., Berriatúa, N. (1985). El Berrueco de Medina Sidonia (Cádiz). Testimonios de una probable expansión argárica hacia el Oeste. Cuadernos de Prehistoria y Arqueología de la Universidad de Granada Vol. 10: 225-242.

Escacena, J.L., De Frutos, G. (1985). Estratigrafía de la Edad del Bronce en el Monte Berrueco (Medina Sidonia-Cádiz). Noticiario Arqueológico Hispánico 24: 9-90.

Espírito-Santo, D., Capelo, J., Neto, C., Pinto-Gomes, C., Ribeiro, S., Canas, R.Q., Costa, J.C. (2017). Lusitania, in: Loidi, J. (Ed.), The Vegetation of the Iberian Peninsula. pp. 35–82. https://doi.org/10.1007/978-3-319-54784-8

Evans, G. (2008). Man's impact on the coastline. Journal of Iberian Geology, 34, 167-190.

Expósito, I. (2018). Aproximaciones metodológicas desde la Arqueopalinología a contextos antropogénicos de la Sierra de Atapuerca (Burgos) y a secuencias naturales del Litoral Mediterráneo. PhD Thesis, Univ. Rovira i Virgili, Tarragona (Spain).

Fægri, K., Iversen, J. (1951). Textbook of Pollen Analysis. John Wiley & Sons, Chichester.

Fang, Y., Bunting, M.J., Ma, C., Yang, X. (2022). Are modern pollen assemblages from soils and mosses the same? A comparison of natural pollen traps from subtropical China. CATENA 209, 105790. https://doi.org/10.1016/j.catena.2021.105790

Feist, L., Costa, P.J.M., Bellanova, P., Bosnic, I., Santisteban, J.I., Andrade, C., Brückner, H., Duarte, J.F., Kuhlmann, J., Schwarzbauer, J., et al (2023). Holocene offshore tsunami archive—Tsunami deposits on the Algarve shelf (Portugal). Sedimentary Geology, 448, 106369.

Fernández Sánchez, D., Ramos, J., Luque, A., Collado Giraldo, H., Domínguez-Bella, S., Bea, M., Cantalejo Duarte, P., Bello, J.R., Angás, J., Miranda, J., Gracia, F.J., García, M., García-Arranz, J.J., Aguilar, C., Vijande Vila, E., Almisas, S., Moreno, A., Aranda, A. (2018). El proyecto 'Abejeras': Estudio y documentación del arte rupestre prehistórico del Tajo de las Abejeras (Castellar de la Frontera, Cádiz, España). Contextualización de las manifestaciones gráficas prehistóricas de la región geohistórica del Estrecho de Gibraltar. X Encuentro de Arqueología del Suroeste peninsular. Zafra: Libro de Resúmenes.

Fernández Sánchez, D., Collado Giraldo, H., Ramos, J., Luque, A., Domínguez-Bella, S., Vijande Vila, E., Bea, M., Bello, J.R., Angás, J., Miranda, J., García, J.J., Aguilar, J.C, Mira, H., Escalona, S. (2019a).

Nuevos motivos de manos aerografiadas paleolíticas en Cueva de las Estrellas (Castellar de la Frontera, Cádiz) y Cueva de las Palomas IV (Tarifa, Cádiz): primeras evidencias de manos en negativo en la provincia de Cádiz. In: Garcia, G. y Barciela, V., coords., Sociedades prehistóricas y manifestaciones artísticas. Imágenes, nuevas propuestas e interpretaciones. Alicante: Instituto de investigación en Arqueología y Patrimonio Histórico (INAPH), Universidad de Alicante. Petracos 2, Alicante.

Fernández Sánchez, D., Ramos Muñoz, J., Collado Giraldo, H., Vijande Vila, E., Luque, A.J. (2019b). Tajo de las Abejeras y cueva de las Estrellas (Castellar de la Frontera, Cádiz). Arte rupestre de las sociedades cazadoras-recolectoras-pescadoras del campo de Gibraltar. ArdalesTur ediciones. Ardales, Málaga.

Fernández Sánchez, D., Collado Giraldo, H., Vijande Vila, E., Domínguez-Bella, S., Luque Rojas, A., Cantillo Duarte, J.J, Mira, H.A., Escalona, S., Ramos-Muñoz, J. (2021). A contribution to the debate about prehistoric rock art in southern Europe: New Palaeolithic motifs in Cueva de las Palomas IV, Facinas (Tarifa, Cádiz, Spain). Journal of Archaeological Science: Reports 38. https://doi.org/10.1016/J.JASREP.2021.103086

Fernández Sánchez, Goméz-Sánchez, L. (2022). Why is art disappearing? Problems with the preservation of prehistoric rock art on the north shore of the Strait of Gibraltar. Quaternary International. https://doi.org/10.1016/j.quaint.2023.01.009

Fick, S.E., Hijmans, R.J. (2017). WorldClim 2: New 1-km spatial resolution climate surfaces for global land areas. International Journal of Climatology 37, 4302–4315.

Figueiral, I., Carcaillet, C. (2005). A Review of Late Pleistocene and Holocene Biogeography of Highland Mediterranean Pines (Pinus Type Sylvestris) in Portugal, Based on Wood Charcoal. Quaternary Science Reviews 24, 2466–2476, https://doi.org/10.1016/j.quascirev.2005.02.004

Finlayson, C., Finlayson, G., Fa, D. (2000). Gibraltar during the Quaternary. The southernmost part of Europe in the last two million years. Monographs 1. Gibraltar.

Fischer, H. (1889). Beitrage zur vergleichenden Morphologie derPollenkorner. J.U. Kern's Verlag, Berlin.

Fletcher, W.J. (2005). Holocene Landscape History of Southern Portugal. PhD Thesis, Univ. Cambridge, Cambridge (UK).

Fletcher, W.J., Boski, T., Moura, D. (2007). Palynological evidence for environmental and climatic change in the lower Guadiana valley, Portugal, during the last 13 000 years. The Holocene 4, 481–494.

Fletcher, W. J., and Sánchez Goñi, M. F. (2008). Orbital- and sub-orbital-scale climate impacts on vegetation of the western Mediterranean basin over the last 48,000 yr. Quaternary Research 70, 451–464. https://10.1016/j.yqres.2008.07.002

Fletcher, W. J., Sánchez-Goñi, M. F. S., Peyron, O., Dormoy, I. (2010a). Abrupt climate changes of the last deglaciation detected in a Western Mediterranean forest record. Climate of the Past, 6(2), 245–264. https://doi.org/10.5194/cp-6-245-2010

Fletcher, W.J., Sánchez-Goñi, M.F.S., Allen, J.R.M., Cheddadi, R., Combourieu-Nebout, N., Huntley, B., Lawson, I., Londeix, L., Magri, D., Margari, V., Müller, U.C., Naughton, F., Novenko, E., Roucoux, K., Tzedakis, P.C., (2010b). Millennial-scale variability during the last glacial in vegetation records from Europe. Quaternary Science Reviews 29, 2839–2864. https://doi.org/10.1016/j.quascirev.2009.11.015

Fletcher, W.J., Debret, M., Sánchez-Goñi, M.F. (2013). Mid-Holocene emergence of a low-frequency millennial oscillation in western Mediterranean climate: implications for past dynamics of the North Atlantic atmospheric westerlies. The Holocene 23, 153–166. http://dx.doi.org/10.1177/0959683612460783

Fregel, R., Méndez, F.L., Bokbot, Y., Martín-Socas, D., Camalich-Massieu, M.D., Santana, J., Morales, J., Ávila-Arcos, M.C., Underhill, P.A., Shapiro, B.; et al. (2018). Ancient Genomes from North Africa Evidence Prehistoric Migrations to the Maghreb from Both the Levant and Europe. PNAS 115, 6774–6779, http://doi:10.1073/pnas.1811169115

Freitas, M.C., Andrade, C., Rocha, F., Tassinari, C., Munhá, J.M., Cruves, A. Vidinha, J., Marques da Silva, C. (2003). Lateglacial and Holocene environmental changes in Portuguese coastal lagoons 1: the sedimentological and geochemical records of the Santo André coastal area. The Holocene, 13, 433-446. https://doi.org/10.1191/0959683603hl636rp

Frigola, J., Moreno, A., Cacho, I., Canals, M., Sierro, F. J., Flores, J. A., Grimalt, J. O., Hodell, D. A., and Curtis, J. H. (2007), Holocene climate variability in the western Mediterranean region from a deepwater sediment record, Paleoceanography, 22, https://doi.org/10.1029/2006PA001307

Galán de Mera, A., Vicente Orellana, J., Sánchez, I., 1997. Coastal plant communities of the southwestern Iberian Peninsula, Spain and Portugal. Phytocoenologia 27, 313–352.

Garcés-Pastor, S., Coissac, E., Lavergne, S. *et al.* (2022). High resolution ancient sedimentary DNA shows that alpine plant diversity is associated with human land use and climate change. Nature Communications 13, 6559 https://doi.org/10.1038/s41467-022-34010-4

García-Artola, A., Stéphan, P., Cearreta, A., Kopp, R.E., Khan, N.S., Horton, B.P. (2018). Holocene Sea-Level Database from the Atlantic Coast of Europe. Quaternary Science Reviews, 196, 177–192, http://doi:10.1016/j.quascirev.2018.07.031

García de Domingo, A., González-Lastras, J., Hernaiz Huerta, P.P., Zazo Cerdeña, C., Goy Goy, J.L. (1991a). Cartografía geológica y memoria de la hoja 12–47/12-48 (Vejer de la Frontera). Mapa Geológico de España, Escala 1:50.000. Plan MAGNA, 2ª Serie. 43pp, IGME, Madrid, Spain.

Garcia de Domingo, A., González Lastra, J., Hernáiz, P.P., Zazo, C., Goy, J.L., Moreno, F. et al., (1991b). Memoria y Mapa Geológico de España, escala 1:50.000. Hoja 1069: Chiclana de la Frontera". Mapa Geológico de España. Hoja 1068. IGME. Madrid, 37 pp. + 1 mapa.

Garcia de Domingo, A., González Lastra, J., Hernáiz, P.P., Zazo, C., Goy, J.L. et al. (1991c). Memoria y Mapa Geológico de España, escala 1:50.000. Hoja 1073: Vejer de la Frontera". Mapa Geológico de España. Hoja 1073. IGME. Madrid, 43 pp. + 1 mapa

García-Moreiras, I., Sánchez, J.M., Sobrino, C.M. (2015). Modern pollen and non-pollen palynomorph assemblages of salt marsh and subtidal environments from the Ría de Vigo (NW Iberia). Review of Palaeobotany and Palynology 219, 157–171. https://doi.org/10.1016/j.revpalbo.2015.04.006

García-Rivero, D., Escacena-Carrasco, J. L. (2015). Del Calcolítico al Bronce antiguo en el Guadalquivir inferior. El Cerro de San Juan (Coria del Río, Sevilla) y el 'modelo de reemplazo'. Zephyrvs, 76, 15–38. https://doi.org/10.14201/zephyrus2015761538

García-Rivero, D., Taylor, R., Umbelino, C., Price, T.D., García-Viñas, E., Bernáldez-Sánchez, E., Pérez-Jordà, G., Peña-Chocarro, L., Barrera-Cruz, M., Gibaja-Bao, J.F., et al. (2020). The Exceptional Finding of Locus 2 at Dehesilla Cave and the Middle Neolithic Ritual Funerary Practices of the Iberian Peninsula. Plos One, 15 (8): e0236961, https://doi.org/10.1371/journal.pone.0236961

García-Rivero, D., García-Viñas, E., Pérez-Jordà, G., Taylor, R., Bernáldez-Sánchez, E., Peña-Chocarro, L. (2022). Human Ecology and the Southern Iberian Neolithic: An Approach from Archaeobotany and Archaeozoology. Journal of Field Archaeology, 47(8), 536–555. https://doi.org/10.1080/00934690.2022.2135248

Giles Pacheco, Sáez, A. (1978). Prehistoria de la Laguna de la Janda: nuevas aportaciones. Boletín del Museo de Cádiz I: 7-17.

Giles Pacheco, F., Santiago, A., Gutiérrez, J.M., Mata E., Aguilera, L. (1994). Nuevas aportaciones a la secuencia del Paleolítico Superior en Gibraltar y su enmarque en el contexto suroccidental de la Península Ibérica. In Gibraltar during the Quaternary, Sevilla.

Giles Pacheco, F., Finlayson, C., Santiago, A., Gutiérrez, J. M., Mata, E., Finlayson, G., Reinoso, C., Giles Guzmán, F., Allué, E. (2000). Investigaciones arqueológicas en Gorham's Cave. Gibraltar. Resultados preliminares de las campañas de 1997 a 1999. I Congreso Andaluz de Espeleología,. Ronda.

Goeury, C., de Beaulieu, J.L. (1979). À propos de la concentration du pollen à l'aide de la liqueur de Thoulet dans les sédiments minéraux. Pollen et Spores XXI (1–2), 239–251.

Gomes, S. D., Fletcher, W. J., Rodrigues, T., Stone, A., Abrantes, F., Naughton, F. (2020). Time-transgressive Holocene maximum of temperate and Mediterranean forest development across the Iberian Peninsula reflects orbital forcing. Palaeogeography, Palaeoclimatology, Palaeoecology, 550(4), 109739. https://doi.org/10.1016/j.palaeo.2020.109739

González-Castillo, L., Galindo-Zaldívar, J., Junge, A., Martínez-Moreno, F. J., Löwer, A., de Galdeano, C. S., Pedrera, A., López-Garrido, A. C., Ruiz-Constán, A., Ruano, P., Martínez-Martos, M. (2015). Evidence of a large deep conductive body within the basement of the Guadalquivir foreland Basin (Betic Cordillera, S-Spain) from tipper vector modelling: Tectonic implications. Tectonophysics, 663, 354-363. https://doi.org/10.1016/j.tecto.2015.08.013

González Porto, A.V., Díaz Losada, E.; Saa Otero, M.P., (1993). Aportación al conocimiento de la dinámica de la lluvia polínica en la sierra del Buyo (Lugo, N.O. de España). Nova Acta Científica Compostelana (Bioloxía), vol. 4. ISSN 1130-9717, pp. 41-48

González Porto, A.V., Díaz Losada, E., Saa Otero, M.P., (1997). Composición de la lluvia polínica de zonas de bosque y turbera en el NW de la Península Ibérica. Polen 8, 61-68.

Goy, J.L., Zazo, C., Silva, P.G., Lario, J., Bardají, T., Somoza, L. (1995). Evaluación geomorfológica del comportamiento neotectónico del Estrecho de Gibraltar (Zona Norte) durante el Cuaternario. *In*: Esteras, M. (ed.), El Enlace Fijo del Estrecho de Gibraltar, vol. 2. SECEGSA, Madrid, pp. 51-69.

Gracia, J. (2008). Geomorfología y estratigrafía del Pleistoceno y Holoceno en la banda atlántica de Cádiz. In: Ramos, J., coord., Memoria del proyecto de investigación: 'La ocupación prehistórica de la campiña litoral y banda atlántica de Cádiz. Arqueología Monografías, Junta de Andalucía, 53-68. Sevilla.

Gracia, F.J., Rodríguez-Vidal, J., Benavente, J., Cáceres, L., López-Aguayo, F. (1999). Tectónica Cuaternaria en la Bahía de Cádiz. *In*: Pallí, L., Roque, C. (eds.), Avances en el estudio del Cuaternario español, AEQUA-UdG, Girona, Spain. pp. 67–74.

Grootes, P.M., Stuiver, M., 1999. GISP2 Oxygen Isotope Data. PANGAEA, https://doi.org/10.1594/PANGAEA.56094

Gutiérrez, M.A., Diez, M.J., Nebot, M., (1996). Introducción al estudio polínico de sedimentos del parque natural de Los Alcornocales. Almoraima: revista de estudios campogibraltareños 87–92.

Gutiérrez, J.M., Santiago, A., Giles Pacheco, F., Gracia, J., Mata, E. (1994). Áreas de transformación de recursos líticos en glacis de la Depresión de Arcos de la Frontera (Cádiz). In Jordá Pardo, J.F., Ed.: Geoarqueología, pp. 305-316. Madrid.

Gutiérrez-Mas, J.M., Martín-Algarra, A., Domínguez-Bella, S., Moral Cardona, J. (1991). Introducción a la geología de la provincia de Cádiz. Servicio de Publicaciones, Universidad de Cádiz.

Guzmán Álvarez, J.R., de Azcárate, Giménez., Fernández, F., Aparicio Martínez, J., (2012). Guía de los paisajes del Pinsapar. Consejería de Agricultura, Pesca y Medio Ambiente, Junta de Andalucía, Sevilla.

Haasnoot, M., Winter, G., Brown, S., Dawson, R.J., Ward, P.J., Eilander, D. (2021). Long-term sea-level rise necessitates a commitment to adaptation: A first order assessment. Climate Risk Management, 34, 100355. https://doi.org/10.1016/j.crm.2021.100355

Haslett, J., Parnell, A.C. (2008). A simple monotone process with application to radiocarbon-dated depth chronologies. Journal of the Royal Statistical Society: Series C (Applied Statistics), 57, 399-418. https://doi.org/10.1111/j.1467-9876.2008.00623.x

Havinga, A.J. (1964). Investigation into the differential susceptibility of pollen and spores. Pollen et Spores 6, 621–635.

Havinga, A.J. (1967). Palynology and pollen preservation. Review of Palaeobotany and Palynology 2, 81–98.

Havinga, A.J. (1971). An experimental investigation into the decay of pollen and spores in various soil types. In: Brooks, J., Grant, P.R., Muir, M., van Gijzel, P., Shaw, G. (Eds.), Sporopollenin. Academic Press, London, pp. 446–479.

Heaton, T.J., Köhler, P., Butzin, M., Bard, E., Reimer, R.W., Austin, W.E.N., Bronk Ramsey, C., Grootes, P.M., Hughen, K.A., Kromer, B., Reimer, P.J., Adkins, J., Burke, A., Cook, M.S., Olsen, J., Skinner, L.C. (2020). Marine20 - The Marine Radiocarbon Age Calibration Curve (0-55,000 cal BP). Radiocarbon, 62, 779-820. https://doi.org/10.1017/RDC.2020.68

Henry, O.D. (1995). Prehistoric Cultural Ecology and Evolution: Insights from Southern Jordan. Plenum.Publishing Corporation, New York.

Hernaiz Huerta, P.P., García de Domingo, A., González-Lastras, J., Zazo Cerdeña, C., Goy Goy, J.L. (1991). Cartografía geológica y memoria de la hoja 13–47 (Tahivilla). Mapa Geológico de España, Escala 1:50.000. Plan MAGNA, 2ª Serie. 45pp, IGME, Madrid, Spain.

Hernández-Molina, F.J., Somoza, L., Rey, J., Pomar, L. (1994). Late Pleistocene-Holocene sediments on the Spanish continental shelves: model for very high-resolution sequence stratigraphy. Marine Geology, 120, 129-174. https://doi.org/10.1016/0025-3227(94)90057-4

Hernández-Molina, F.J., Llave, E., Stow, D.A.V., Garcia, M., Somoza, L., Vazquez, J.T., Lobo, F.J., Maestro, A., del Rio, V.D., Leon, R., Medialdea, T., Gardner, J. (2006). The contourite depositional system of the Gulf of Cádiz: a sedimentary model related to the bottom current activity of the Mediterranean outflow water and its interaction with the continental margin. Deep-Sea Research Part II 53 (11–13), 1420–1463.

Hernández-Molina, F.J., Maldonado, A., Stow, D.A.V. (2008). Abyssal Plain Contourites, in: Rebesco, M., Camerlenghi, A. (Eds.), Contourites. Elsevier, Amsterdam, Developments in Sedimentology 60, pp.345-378.

Hernández-Molina, F.J., Paterlini, M., Violante, R., Marshall, P., de Isasi, M., Somoza, L., Rebesco, M., (2009). Contourite depositional system on the Argentine slope: An exceptional record of the influence of Antarctic water masses. Geology 37, 507-510.

Hernández-Molina, F.J., Paterlini, M., Somoza, L., Violante, R., Arecco, M.A., de Isasi, M., Rebesco, M., Uenzelmann-Neben, G., Neben, S., Marshall, P., (2010). Giant mounded drifts in the Argentine Continental Margin: Origins, and global implications for the history of thermohaline circulation. Marine and Petroleum Geology 27, 1508-1530.

Hernández-Pacheco, E., Cabré, J. (1913). La Depresión del Barbate y sus estaciones prehistóricas. Boletín de la Real Sociedad Española de Historia Natural, 13, 349-359.

Herrmann, S., Stroncik, N. (2013). Data Report: Si, Al, Fe, Ca, and K Systematics of Volcaniclastic Sediments from Selected Cores of Hole U1347A, IODP Expedition 324. Proc. IODP, 324, https://doi.org/10.2204/iodp.proc.324.204.2013

Higuchi, R., Bowman, B., Freiberger, M., Ryder, O.A., Wilson, A.C. (1984). DNA sequences from the quagga, an extinct member of the horse family. Nature 312, 282–284. https://doi.org/10.1038/312282a0

Hindson, R., Andrade, C., Parish, R. (1998). A microfaunal and sedimentary record of environmental change within the late Holocene sediments of Boca do Rio (Algarve, Portugal). Geologie en Mijnbouw, 77, 311-321. https://doi.org/10.1023/A:1003651308741

Hoelzmann, P.; Klein, T.; Kutz, F.; Schütt, B. (2017). A New Device to Mount Portable Energy-Dispersive X-Ray Fluorescence Spectrometers (p-ED-XRF) for Semi-Continuous Analyses of Split (Sediment) Cores and Solid Samples. Geosci. Instrum. Methods Data Syst. 6, 93–101, https://doi.org/10.5194/gi-6-93-2017

Hoffmann, D.L., Standisch, C.D., García, M., Pettitt, P.B., Milton, J.A., Zilhao, J., Alcolea, J., Cantalejo Duarte, P., Collado Giraldo, H., Balbín, R., Lorblanchet, M., Ramos Muñoz, J., Weniger, G.C., Pike, A. (2018). U-Th dating of carbonate crusts reveals Neandertal origin of Iberian cave art. Science 359, 912-915.

Hooghiemstra, H., Stalling, H., Agwu, C. O. C., Dupont, L. M. (1992). Vegetational and climatic changes at the northern fringe ofthe Sahara 250.000–5.000 years BP: Evidence from 4 marinepollen records located between Portugal and the Canary Islands.Review of Palaeobotany and Palynology, 74, 1–53

Holloway, R.G., (1989). Experimental mechanical pollen degradation and its application to Quaternary age deposits. Texas Journal of Science 41, 131–145.

Hunt, C. O. (1987). Comment: The Palynology of Fluvial Sediments: With Special Reference to Alluvium of Historic Age from the Upper Axe Valley, Mendip Hills, Somerset. Transactions of the Institute of British Geographers, 12(3), 364–367. https://doi.org/10.2307/622414

Hunt, C.O., Fiacconi, M. (2018). Pollen taphonomy of cave sediments: what does the pollen record in caves tell us about external environments and how do we assess its reliability? Quarternary International 485, 68–75. https://doi.org/10.1016/j.quaint.2017.05.016

Huntley, B., Prentice, I.C. (1988). July temperatures in Europe from pollen data, 6000 years before present. Science 241, 687–690. http://dx.doi.org/10.1126/science.241.4866.687

Hurrell, J.W. (1995). Decadal trends in the North Atlantic oscillation: regional temperatures and precipitation. Science 269, 676. http://dx.doi.org/10.1126/science.269.5224.676

Iglesias, V., Quintana, F., Nanavati, W., Whitlock, C. (2017). Interpreting modern and fossil pollen data along a steep environmental gradient in northern Patagonia. The Holocene 27, 1008–1018. https://doi.org/10.1177/0959683616678467

Imbrie, J., McIntyre, A., Mix, A. (1989). Oceanic Response to Orbital Forcing in the Late Quaternary: Observational and Experimental Strategies. In: Berger, A., Schneider, S., Duplessy, J.C. (Eds.) *Climate and Geo-Sciences*. NATO ASI Series, vol 285, pp.121-164. Springer, Dordrecht. https://doi.org/10.1007/978-94-009-2446-8_7

Instituto Hidrográfico de la Marina (2019). Anuario de Mareas 2020. Regional 4. De la desembocadura del río Guadiana al Estrecho de Gibraltar. Ministerio de Defensa de España, Madrid. 46 pp. https://publicaciones.defensa.gob.es/media/downloadable/files/links/a/n/anuario_mareas_regional_4_2020.pdf

Jalut, G., Dedoubat, J.J., Fontugne, M., Otto, T. (2009). Holocene circum-Mediterranean vegetation changes: Climate forcing and human impact. Quaternary International 200, 4–18. https://doi.org/10.1016/j.quaint.2008.03.012

Jiménez-Moreno, G., Rodríguez-Ramírez, A., Pérez-Asensio, J.N., Carrión, J.S., López-Sáez, J.A., Villarías-Robles, J.J.R., Celestino-Pérez, S., Cerrillo-Cuenca, E., León, Á., Contreras, C. (2015). Impact of late-Holocene aridification trend, climate variability and geodynamic control on the environment from a coastal area in SW Spain. Holocene 25, 607–617. https://doi.org/10.1177/0959683614565955

Kottek, M., Grieser, J., Beck, C., Rudolf, B., Rubel, F., 2006. World Map of the Köppen-Geiger Climate Classification Updated. Meteorologische Zeitschrift 15(3), 259 - 263.

Junta de Andalucía (2014a). Análisis y diagnóstico territorial del litoral de La Janda. Access: https://www.jandalitoral.org/proyectos/redes-y-cooperacion/13-proyectos/204-evolucion-y-analisis-del-medio-rural-litoral-de-la-janda-retos-de-futuro

Junta de Andalucía (2014b). Caracterización agraria del territorio de la Oficina Comarcal Agraria "La Janda", provincia de Cádiz. Access: https://www.juntadeandalucia.es/sites/default/files/2020-12/1102_OCA_Litoral.pdf

Johnsen, S.J., Clausen, H.B., Dansgaard, W., Gundestrup, N.S., Hammer, C.U., Andersen, U., Andersen, K.K., Hvidberg, C.S., Dahl-Jensen, D., Steffensen, J.P., et al. (1997). The Δ18O Record along the Greenland Ice Core Project Deep Ice Core and the Problem of Possible Eemian Climatic Instability. Journal of Geophysical Research: Oceans , 102, 26397–26410, https://doi:10.1029/97JC00167

Kaufman, D.S., Ager, T.A., Anderson, N.J., Anderson, P.M., Andrews, J.T., Bartlein, P.J., Brubaker, L.B., Coats, L.L., Cwynar, L.C., Duvall, M.L., et al. (2004). Holocene Thermal Maximum in the Western Arctic (0–180°W). Quaternary Science Reviews 23, 529–560, https://doi:10.1016/j.quascirev.2003.09.007

Kilhavn, H., Couchoud, I., Drysdale, R. N., Rossi, C., Hellstrom, J., Arnaud, F., Wong, H. (2022). The 8.2 ka event in northern Spain: timing, structure and climatic impact from a multi-proxy speleothem record, EGUsphere [preprint], https://doi.org/10.5194/egusphere-2022-386

Kottek, M., Grieser, J., Beck, C., Rudolf, B., & Rubel, F. (2006). World Map of the Köppen-Geiger climate classification updated. Meteorologische Zeitschrift, 259–263. https://doi.org/10.1127/0941-2948/2006/0130

Lanos, P., Philippe, A. (2017). Hierarchical Bayesian modeling for combining dates in archeological context. Journal de la société française de statistique 158 (2), 72-88.

Lanos, P., Dufresne P. (2019). Chronomodel version 2.0: Software for Chronological Modelling of Archaeological Data using Bayesian Statistics. Available from: http://www.chronomodel.com

Lambeck, K., Rouby, H., Purcell, A., Sun, Y., Sambridge, M. (2014). Sea level and global ice volumes from the Last Glacial Maximum to the Holocene. Proceedings of the National Academy of Sciences USA, 111, 15296-15303. https://doi.org/10.1073/pnas.1411762111

Lario, J., Zazo, C., Goy, J.L., Dabrio, C.J., Borja, F., Silva, P.G., Sierro, F., González, A., Soler, V., Yll, E. (2002). Changes in sedimentation trends in SW Iberia Holocene estuaries (Spain). Quaternary International, 93-94, 171-176. https://doi.org/10.1016/S1040-6182(02)00015-0

Lario, J., Luque, L., Zazo, C., Goy, J.L., Spencer, C., Cabero, A., Bardají, T., Borja, F., Dabrio, C.J., Civis, J., et al. (2010). Tsunami vs. Storm Surge Deposits: A Review of the Sedimentological and Geomorphological Records of Extreme Wave Events (EWE) during the Holocene in the Gulf of Cádiz, Spain. Zeitschrift für Geomorphologie Supplement Issues 54, 301–316, https://doi:10.1127/0372-8854/2010/0054S3-0029

Lario, J., Zazo, C., Goy, J.L., Silva, P.G., Bardaji, T., Cabero, A., Dabrio, C.J. (2011) Holocene Palaeotsunami Catalogue of SW Iberia. Quaternary International 242, 196–200, https://doi:10.1016/j.quaint.2011.01.036

Latorre, A.V.P., Cabezudo, B., (2003). Notas sobre la vegetación de Andalucía V. Acta Botanica Malacitana 28, 258–260. https://doi.org/10.24310/abm.v28i0.7300

Latorre, A.V.P., Mera, A.G. de, Dell, U., Cabezudo, B., 1996. Fitogeografía y vegetación del Sector Aljíbico (Cádiz-Málaga, España). Acta Botanica Malacitana 21, 241–267. https://doi.org/10.24310/abm.v21i0.8678

Lau, P., Bryant, V., Rangel, J. (2018) Determining the minimum number of pollen grains needed for accurate honey bee (Apis mellifera) colony pollen pellet analysis, Palynology, 42:1, 36-42, https://10.1080/01916122.2017.1306810

Lazarich, M. (2004). Balance actual de la investigación sobre el Campaniforme en Andalucía Occidental. In III Simposio de Prehistoria Cueva de Nerja, pp. 393-404. Málaga.

Lazarich, M. (2005). La producción metalúrgica del IIº milenio a.C. en la Baja Andalucía: Las puntas de tipo 'Palmela'. Almajar 2, pp. 29-38.

Lazarich, M. (2007). La necrópolis de Paraje de Monta Bajo (Acalá de los Gazules, Cádiz). Un acercamiento al conocimiento de las prácticas funerarias prehistóricas. Universidad de Cádiz. Cádiz.

Leblanc, D. (1990). Tectonic adaptation of the External Zones around the curved core of an orogen: the Gibraltar Arc. Journal of Structural Geology, 12, 1013-1018. https://doi.org/10.1016/0191-8141(90)90097-I

Lebreton, V., Messager, L., Marquer, L., Renault-Miskovsky, J. (2010). A neotaphonomic experiment in pollen oxidation and its implications for archaeopalynology. Review of Palaeobotany and Palynology 162, 29–38. https://doi.org/10.1016/j.revpalbo.2010.05.002

Lee, C.M., van Geel, B., Gosling, W.D., (2022). On the Use of Spores of Coprophilous Fungi Preserved in Sediments to Indicate Past Herbivore Presence. Quaternary 2022, 5, 30. https://doi.org/10.3390/quat5030030

Legendre, P., Birks, H.J.B. (2012). From Classical to Canonical Ordination, in: Birks, H.J.B., Lotter, A.F., Juggins, S., Smol, J.P. (Eds.), Tracking Environmental Change Using Lake Sediments: Data Handling and Numerical Techniques, Developments in Paleoenvironmental Research. Springer Netherlands, Dordrecht, pp. 201–248. https://doi.org/10.1007/978-94-007-2745-8_8

Lézine, A.M., Denèfle, M. (1997) Enhanced anticyclonic circulation in the Eastern North Atlantic during cold intervals of the last deglaciation inferred from deep-sea pollen records. Geology, 25 (2): 119–122. doi: https://doi.org/10.1130/0091-7613(1997)025<0119:EACITE>2.3.CO;2

Li, Y., Xu, Q., Zhao, Y., Yang, X., Xiao, J., Chen, H., Xinmiao, L., Li, Y., Xu, Q., Zhao, Y. (2005). Pollen indication to source plants in the eastern desert of China. Chinese Science Bulletin 50, 1632–1641.

Lionello, P., Malanotte-Rizzoli, P., Boscolo, R. (2006). Mediterranean climate variability. Elsevier.

Lionello, P., Abrantes, F., Congedi, L., Dulac, F., Gacic, M., Gomis, D., Goodess, C., Hoff, H., Kutiel, H., Luterbacher, J., Planton, S., Reale, M., Schröder, K., Struglia, M.V., Toreti, A., Tsimplis, M., Ulbrich, U., Xoplaki, E. (2012). Introduction: Mediterranean Climate—Background Information. In: Lionello P et al. (eds) The climate of the Mediterranean region: from the past to the future. Elsevier, pp xxxv–xc. https://doi:10.1016/B978-0-12-416042-2.00012-4

Lillios, K.T., Blanco-González, A., Lee Drake, B., López-Sáez, J.A. (2016). Mid-late Holocene climate, demography, and cultural dynamics in Iberia: a multi-proxy approach. Quaternary Science Reviews 135, 138–153. https://doi.org/10.1016/j.quascirev.2016.01.011

Linstädter, J., Medved, I., Solich, M., Weniger, G.-C. (2012). Neolithisation Process within the Alboran Territory: Models and Possible African Impact. Quaternary International 274, 219–232, https://doi:10.1016/j.quaint.2012.01.013

Lisiecki, L.E., Raymo, M.E. (2005). A Pliocene-Pleistocene stack of 57 globally distributed benthic $\delta^{18}O$ records. Paleoceanography, 20, PA1003. https://doi.org/10.1029/2004PA001071

Lisitsyna, O. V., Hicks, S., and Huusko, A. (2012). Do moss samples, pollen traps and modern lake sediments all collect pollen in the same way? A comparison from the forest limit area of northernmost Europe. Vegetation History and Archaeobotany 21, 187–199. https://doi/10.1007/s00334-011-0335-x

Liu, Z., Zhu, J., Rosenthal, Y., Zhang, X., Otto-Bliesner, B.L., Timmermann, A., Smith, R.S., Lohmann, G., Zheng, W., Timm, O.E. (2014). The Holocene Temperature Conundrum. PNAS, 111, E3501–E3505, https://doi:10.1073/pnas.1407229111

Lobo, F.J., Días, J.M.A., González, R., Hernández-Molina, F.J., Morales, J.A., Díaz del Río, V. (2003). High-Resolution Seismic Stratigraphy of a Narrow, Bedrock-Controlled Estuary: The Guadiana Estuarine System, SW Iberia. Journal of Sedimentary Research, 73, 973-986. https://doi.org/10.1306/032303730973

Loidi, J., Biurrun, I., Campos, J.A., García-Mijangos, I., Herrera, M., (2007). A survey of health vegetation of the Iberian Peninsula and Northern Morocco: A biogeographic and bioclimatic approach. Phytocoenologia 37, 341–370. https://doi.org/10.1127/0340-269X/2007/0037-0341

López-Sáez, J.A., Van Geel, B., Martín-Sánchez, M. (2000). Aplicación de los microfósiles no polínicos en Palinología Arqueológica. *In*: Oliveira Jorge, V. (coord.), Contributos das Ciências e das Technologias para a Arqueologia da Península Ibérica. Actas 3º Congresso de Arqueologia Peninsular, 9, 11-20.

López-Sáez, J.A., Geel, B., Sánchez, M. (2002). Aplicación de Los Microfósiles No Polínicos En Palinología Arqueológica, Contributos das ciencias e das tecnologias para a arqueologia da Península Ibérica, Proceedings of the. Contrib. Ciênc. E Technol. Para Arqueol. Península Ibérica 11–20.3° Congresso de Arqueología Peninsular, Vila Real, Portugal, 1999; Oliveira, V., Ed. UTAD: Vila Real, Portugal.

López-Sáez, J. A., López-Merino, L. (2005). Precisiones metodológicas acerca de los indicios paleopalinológicos de agricultura en la Prehistoria de la Península Ibérica. https://digital.csic.es/handle/10261/93814

López-Sáez, J.A., Alba-Sánchez, F., López-Merino, L., Pérez-Díaz, S., (2010a). Modern pollen analysis: a reliable tool for discriminating *Quercus rotundifolia* communities in Central Spain. Phytocoenologia 57–72. https://doi.org/10.1127/0340-269X/2010/0040-0430

López-Sáez, J.A., López-Merino, L., Alba-Sánchez, F., Pérez-Díaz, S., Abel-Schaad, D., Carrión, J.S., (2010b). Late Holocene ecological history of *Pinus pinaster* forests in the Sierra de Gredos of central Spain. Plant Ecology 206, 195–209.

López-Sáez, J. A., Pérez-Díaz, S., Alba, F. (2011). Antropización y agricultura en el Neolítico de Andalucía Occidental a partir de la Palinología. Menga, 2, 72–85.

López-Sáez, J.A., Sánchez-Mata, D., Alba-Sánchez, F., Abel-Schaad, D., Gavilán, R., Pérez-Díaz, S., (2013). Discrimination of Scots pine forests in the Iberian Central System (*Pinus sylvestris* var. *iberica*) by means of pollen analysis. Phytosociological considerations. Lazaroa 34, 191–208.

López-Sáez, J.A., Alba-Sánchez, F., Sánchez-Mata, D., Abel-Schaad, D., Gavilán, R.G., Pérez-Díaz, S., (2015). A palynological approach to the study of *Quercus pyrenaica* forest communities in the Spanish Central System. Phytocoenologia 45, 107–124.

López-Sáez, J.A., Abel-Schaad, D., Luelmo-Lautenschlaeger, R., Robles-López, S., Pérez-Díaz, S., Alba-Sánchez, F., Sánchez-Mata, D., Gavilán, R.G., (2018). Resilience, vulnerability and conservation strategies in high-mountain pine forests in the Gredos range, central Spain. Plant Ecology & Diversity 11, 97–110

López-Sáez, J.A., Pérez-Díaz, S., Rodríguez-Ramírez, A., Blanco-González, A., Villarías-Robles, J.J.R., Luelmo-Lautenschlaeger, R., Jiménez-Moreno, G., Celestino-Pérez, S., Cerrillo-Cuenca, E., Pérez-Asensio, J.N., León, Á., (2018). Mid-late Holocene environmental and cultural dynamics at the south-west tip of Europe (Doñana National Park, SW Iberia, Spain). Journal of Archaeological Science: Reports 22, 58–78. https://doi.org/10.1016/j.jasrep.2018.09.014

López-Sáez, J.A., Alba-Sánchez, F., Sánchez-Mata, D., Luengo-Nicolau, E., (2019). Los pinares de la Sierra de Gredos. Pasado, presente y futuro. Ávila, Institución Gran Duque de Alba.

López-Sáez, J.A., Camarero, J.J., Abel-Schaad, D., Luelmo-Lautenschlaeger, R., Pérez-Díaz, S., Alba-Sánchez, F., Carrión, J.S., (2020). Don't lose sight of the forest for the trees! Discerning Iberian pine

communities by means of pollen-vegetation relationships. Review of Palaeobotany and Palynology 281, 104285. https://doi.org/10.1016/j.revpalbo.2020.104285

López-Tirado, J., Hidalgo, P., (2014). A high resolution predictive model for relict trees in the Mediterranean-mountain forests (*Pinus sylvestris* L., *P. nigra* Arnold and *Abies pinsapo* Boiss.) from the south of Spain: A reliable management tool for reforestation. Forest Ecology and Management 330, 105–114. https://doi.org/10.1016/j.foreco.2014.07.009

Lovelock, C.E., Duarte, C.M. (2019). Dimensions of Blue Carbon and emerging perspectives. Biology Letters 15, 20180781. https://doi.org/10.1098/rsbl.2018.0781

Lull, V., Pérez, R.M., Herrada, C.R., Risch, R. (2010). Metal and Social Relations of Production in the 3rd and 2nd Millennia BCE in the Southeast of the Iberian Peninsula. Trabajos De Prehistoria, 67, 323-347.

Luque, L., Zazo, C., Recio, J.M., Dueñas, M.A., Goy, J.L., Lario, J., González-Hernández, F., Dabrio, C.J., González-Delgado, A. (1999). Evolución sedimentaria de la laguna de La Janda (Cádiz) durante el Holoceno. Cuaternario y Geomorfología, 13, 43-50.

Luque, L., Silva, P.G., Zazo, C., Recio, J.M., Carrasco, P., Goy, J.L., Dueñas, M.I., Lario, J., Dabrio, C.J., González-Hernández, F.M., Poza, L. (2001). Datos geofísicos y evolución sedimentaria de la Depresión de La Janda (Cádiz). Geogaceta, 29, 69-72.

Lyle, M. (1983). The brown-green color transition in marine sediments: A marker of the Fe(III)-Fe(II) redox boundary. Limnology and Oceanography, 28, 1026-1033. https://doi.org/10.4319/lo.1983.28.5.1026

Lytle, D.E., Wahl, E.R. (2005). Palaeoenvironmental reconstructions using the modern analogue technique: the effects of sample size and decision rules. The Holocene, 15, 554 - 566.

Manen, C., Marchand, G., Carvalho, A. (2004). Le Néolithique Ancien de La Péninsule Ibérique: Vers Une Nouvelle Évaluation Du Mirage Africain? Société Préhistorique Française: Avignon, France, 3, 133–151.

Manzano, S., Carrión, J.S., López-Merino, L., Ochando, J., Munuera, M., Fernández, S., González-Sampériz, P., (2018). Early to mid-Holocene spatiotemporal vegetation changes and tsunami impact in a paradigmatic coastal transitional system (Doñana National Park, southwestern Europe). Glob. Planet. Change 161, 66–81. https://doi.org/10.1016/j.gloplacha.2017.12.013

Marcenò, C., Guarino, R., Loidi, J., Herrera, M., Isermann, M., Knollová, I., Tichý, L., Tzonev, R.T., Acosta, A.T.R., FitzPatrick, Ú., Iakushenko, D., Janssen, J.A.M., Jiménez-Alfaro, B., Kącki, Z., Keizer-

Sedláková, I., Kolomiychuk, V., Rodwell, J.S., Schaminée, J.H.J., Šilc, U., Chytrý, M., (2018). Classification of European and Mediterranean coastal dune vegetation. Applied Vegetation Science 21, 533–559. https://doi.org/10.1111/avsc.12379

Marcott, S.A., Shakun, J.D., Clark, P.U., Mix, A.C. (2013). A Reconstruction of Regional and Global Temperature for the Past 11,300 Years. Science 339, 1198–1201.

Martín-Puertas, C., Valero-Garcés, B. L., Pilar Mata, M., González-Sampériz, P., Bao, R., Moreno, A., Stefanova, V. (2008). Arid and humid phases in southern Spain during the last 4000 years: the Zoñar Lake record, Córdoba. The Holocene, 18(6), 907–921. https://doi.org/10.1177/0959683608093533

Martín-Socas, D., Camalich Massieu, M.D., Herrero, J.L.C., Rodríguez-Santos, F.J. (2017). The Beginning of the Neolithic in Andalusia. Quaternary International 470, 451–471, https://doi:10.1016/j.quaint.2017.06.057

Martínez, S.R., Valdés, E., Costa, M., Castroviejo, S. (1980). Vegetación de Doñana (Huelva, España). Lazaroa, 2, 5–190.

Martins, J., Soares, A. (2013), Marine radiocarbon reservoir effect in Southern Atlantic Iberian Coast. Radiocarbon, 55, 1123-1134. https://doi.org/10.1017/S0033822200048037

Martrat, B., J. O. Grimalt, C. Lopez-Martinez, I. Cacho, F. J. Sierro, J. A. Flores, R. Zahn, M. Canals, J. H. Curtis, D. A. Hodell (2004), Abrupt temperature changes in the western Mediterranean over the past 250,000 years, Science, 306, 1762–1765.

Mas, M. (2000). Proyecto de investigación arqueológica Las manifestaciones rupestres prehistóricas de la zona gaditana. Arqueología Monografías. Sevilla: Junta de Andalucía.

Massieu, M., Socas, D. (2013). Los Inicios Del Neolítico En Andalucía. Entre La Tradición y La Innovación. MENGA Revista de Prehistoria de Andalucía, 4, 103–129.

Masson-Delmotte, V., Jouzel, J., Landais, A., Stievenard, M., Johnsen, S.J., White, J.W.C., Werner, M., Sveinbjornsdottir, A., Fuhrer, K. (2005). GRIP Deuterium Excess Reveals Rapid and Orbital-Scale Changes in Greenland Moisture Origin. Science, 309, 118–121, https://doi:10.1126/science.1108575.

Mateus, J. (1992). Holocene and Present-day Ecosystems of the Carvalhal Region, Southwest Portugal. PhD Thesis, Univ. Utrecht, Utrecht, (Netherlands).

Mayewski, P.A., Rohling, E.E., Stager, J.C., Karlén, W., Maasch, K.A., Meeker, L.D., Meyerson, E.A., Gasse, F., van Kreveld, S., Holmgren, K., Lee-Thorp, J., Rosqvist, G., Rack, F., Staubwasser, M.,

Schneider, R.R., Steig, E.J., (2004). Holocene climate variability. Quaternary Research 62, 243–255. http://dx.doi.org/10.1016/j.yqres.2004.07.001

McLaughlin, T.R., Gómez-Puche, M., Cascalheira, J., Bicho, N., Fernández-López de Pablo, J. (2020). Late Glacial and Early Holocene Human Demographic Responses to Climatic and Environmental Change in Atlantic Iberia. Philosophical Transactions of the Royal Society B., 376, 20190724, https://doi:10.1098/rstb.2019.0724

Mediato, J.F., Santisteban, J.I., del Moral, B., Mediavilla, R., Dabrio, C.J. (2020). Aridity events during the last 4000 years in Western Mediterranean marshes (Almenara and Benicasim marshes, E Spain). Quaternary International, Quaternary Research in Spain: Environmental Changes and Human Footprint 566–567, 303–314. https://doi.org/10.1016/j.quaint.2020.04.021

Mediavilla, R., Santisteban, J.I., Val-Peón, C., Galán, L., Mathes-Schmidt, M., López-Sáez, J.A., Gracia, F.J., Reicherter, K. (2023). 26,000 years of environmental evolution of an incised valley in a rocky coast (La Janda wetland, SW Iberia), Continental Shelf Research. https://doi.org/10.1016/j.csr.2023.105028

Meijer, P.T., Tuenter, E. (2007). The effect of precession-induced changes in the Mediterranean freshwater budget on circulation at shallow and intermediate depth. Journal of Marine Systems 68, 349–365. http://dx.doi.org/10.1016/j.jmarsys.2007.01.006

Mendes, I., Lobo, F.J., Hanebuth, T.J.J., López-Quirós, A., Schönfeld, J., Lebreiro, S., Reguera, M.I., Antón, L., Ferreira, O. (2020). Temporal variability of flooding events of Guadiana River (Iberian Peninsula) during the middle to late Holocene: Imprints in the shallow-marine sediment record. Palaeogeography, Palaeoclimatology, Palaeoecology, 556, 109900. https://doi.org/10.1016/j.palaeo.2020.109900

Menier, D., Tessier, B., Proust, J.-N., Baltzer, A., Sorrel, P., Traini, C. (2010). The Holocene transgression as recorded by incised-valley infilling in a rocky coast context with low sediment supply (southern Brittany, western France). Bulletin de la Société Géologique de France, 181, 115-128. https://doi.org/10.2113/gssgfbull.181.2.115

Miola, A. (2012). Tools for Non-Pollen Palynomorphs (NPPs) Analysis: A List of Quaternary NPP Types and Reference Literature in English Language (1972–2011). Review of Palaeobotany and Palynology 186, 142–161, https://doi.org/10.1016/j.revpalbo.2012.06.010

Montañés, M., García, M.E. (1999). El conjunto dolménico de la Laguna de la Janda. Entre una refrescante revisión historiográfica y ochenta años de sequía investigadora. Almoraima 21, pp. 39-45.

Montañés, M., Pérez Rodríguez, M., GarcíaA, M.E., Ramos Muñoz, J. (1999b). Las primeras sociedades campesinas. Las sociedades comunitarias y los comienzos de la jerarquización social. In J. Ramos Muñoz, M. Montañés, M. Pérez Rodríguez, V. Castañeda Fernández, N., Herrero, M.E. García, I. Cáceres (eds.), Excavaciones arqueológicas en La Mesa (Chiclana de la Frontera, Cádiz). Campaña de 1998. Aproximación al estudio del proceso histórico de su ocupación (Arqueología en Chiclana de la Frontera 1), Chiclana de la Frontera, pp. 111-134

Moore, P.D., Webb, J.A., Collinson, M.E. (1991). Pollen Analysis. Blackwell Scientific Publications, Oxford.

Morales, J. A., Delgado, I., Gutierrez-Mas, J.M. (2006). Sedimentary characterization of bed types along the Guadiana estuary (SW Europe) before the construction of the Alqueva dam. Estuarine, Coastal and Shelf Science, 70, 117-131. https://doi.org/10.1016/j.ecss.2006.05.049

Morales-Molino, C., Devaux, L., Georget, M., Hanquiez, V., Goñi, M.F.S. (2020). Modern pollen representation of the vegetation of the Tagus Basin (central Iberian Peninsula). Review of Palaeobotany and Palynology 276, 104193. https://doi.org/10.1016/j.revpalbo.2020.104193

Morata, D. (1993). Petrología y geoquímica de las ofitas de las Zonas Externas de las Cordilleras Béticas. PhD Thesis, Univ. Granada, Granada (Spain).

Morellón, M., Aranbarri, J., Moreno, A., González-Sampériz, P., Valero-Garcés, B.L. (2018). Early Holocene Humidity Patterns in the Iberian Peninsula Reconstructed from Lake, Pollen and Speleothem Records. Quaternary Science Reviews, 1–18, https://doi:10.1016/j.quascirev.2017.11.016

Morgado, A., Pelegrin, J. (2012). Origin and Development of Pressure Blade Production in the Southern Iberian Peninsula (6th–3rd Millennia B.C.). In: Desrosiers, P. (eds) The Emergence of Pressure Blade Making. Springer, Boston, MA. https://doi.org/10.1007/978-1-4614-2003-3_8

Naeher, S., Gilli, A., North, R.P., Hamann, Y., Schubert, C.J. (2013). Tracing Bottom Water Oxygenation with Sedimentary Mn/Fe Ratios in Lake Zurich, Switzerland. Chem. Geol., 352, 125–133, https://doi:10.1016/j.chemgeo.2013.06.006

Nagao, S., Nakashima, S. (1992). The factors controlling vertical color variations of North Atlantic Madeira Abyssal Plain sediments. *Marine Geology*, 109, 83-94. https://doi.org/10.1016/0025-3227(92)90222-4

Naughton, F., Sánchez Goñi, M. F., Desprat, S., Turon, J.-L., Duprat, J., Malaizé, B., et al. (2007). Present-day and past (last 25000 years) marine pollen signal off western Iberia. Mar. Micropaleontol. 62, 91–114. https://doi/10.1016/j.marmicro.2006.07.006

Negueruela, I. (1981-1982). La cueva artificial de Buenavista, Vejer de la Frontera. Cádiz. Boletín del Museo de Cádiz III, pp. 23-26.

Newton, A., Icely, J., Cristina, S., Brito, A., Cardoso, A.C., Colijn, F., Riva, S.D., Gertz, F., Hansen, J.W., Holmer, M., Ivanova, K., Leppäkoski, E., Canu, D.M., Mocenni, C., Mudge, S., Murray, N., Pejrup, M., Razinkovas, A., Reizopoulou, S., Pérez-Ruzafa, A., Schernewski, G., Schubert, H., Carr, L., Solidoro, C., PierluigiViaroli, Zaldívar, J.-M., (2014). An overview of ecological status, vulnerability and future perspectives of European large shallow, semi-enclosed coastal systems, lagoons and transitional waters. Estuarine, Coastal and Shelf Science, 140, 95–122. https://doi.org/10.1016/j.ecss.2013.05.023

Newton, A., Icely, J., Cristina, S., Perillo, G.M.E., Turner, R.E., Ashan, D., Cragg, S., Luo, Y., Tu, C., Li, Y., Zhang, H., Ramesh, R., Forbes, D.L., Solidoro, C., Béjaoui, B., Gao, S., Pastres, R., Kelsey, H., Taillie, D., Nhan, N., Brito, A.C., de Lima, R., Kuenzer, C. (2020). Anthropogenic, Direct Pressures on Coastal Wetlands. Frontiers in Ecology and Evolution, 8.

Nicholls, R.J., Hanson, S.E., Lowe, J.A., Slangen, A.B.A., Wahl, T., Hinkel, J., Long A.J. (2021). Integrating new sea-level scenarios into coastal risk and adaptation assessments: An ongoing process. WIREs Climate Change, 12, e706. https://doi.org/10.1002/wcc.706

Oksanen, J., Simpson, G., Blanchet, F., Kindt, R., Legendre, P., Minchin, P., O'Hara, R., Solymos, P., Stevens, M., Szoecs, E., Wagner, H., Barbour, M., Bedward, M., Bolker, B., Borcard, D., Carvalho, G., Chirico, M., De Caceres, M., Durand, S., Evangelista, H., FitzJohn, R., Friendly, M., Furneaux, B., Hannigan, G., Hill, M., Lahti, L., McGlinn, D., Ouellette, M., Ribeiro Cunha, E., Smith, T., Stier, A., Ter Braak, C., Weedon, J., (2022). _vegan: Community Ecology Package_. R package version 2.6-4, <https://CRAN.R-project.org/package=vegan>.

Oldfield, F., Dearing, J. (2003). The Role of Human Activities in Past Environmental Change. https://doi.org/10.1007/978-3-642-55828-3_7

Oliveira, D., Desprat, S., Yin, Q., Naughton, F., Trigo, R., Rodrigues, T., Abrantes, F., Goñi, M.F.S. (2018). Unraveling the forcings controlling the vegetation and climate of the best orbital analogues for the present interglacial in SW Europe. Climate Dynamics 51, 667–686. https://doi.org/10.1007/s00382-017-3948-7

Ozturk, M., Dogan, Y., Sakcali, M., Doulis, A., Karam, F. (2010). Ecophysiological responses of some maquis (Ceratonia siliqua L., *Olea Oleaster* Hoffm. & Link, Pistacia lentiscus and *Quercus coccifera* L.) plant species to drought in the east Mediterranean ecosystem. Journal of Environmental Biology 31, 233–45.

Pals, J.P., Van Geel, B., Delfos, A. (1980). Paleoecological Studies in the Klokkeweel Bog near Hoogkarspel (Prov. of Noord-Holland). Review of Palaeobotany and Palynology 30, 371–418, https://doi:10.1016/0034-6667(80)90020-2

Pardoe, H.S., Giesecke, T., van der Knaap, W.O., Svitavská-Svobodová, H., Kvavadze, E.V., Panajiotidis, S., Gerasimidis, A., Pidek, I.A., Zimny, M., Święta-Musznicka, J., Latałowa, M., Noryśkiewicz, A.M., Bozilova, E., Tonkov, S., Filipova-Marinova, M.V., van Leeuwen, J.F.N., Kalniņa, L. (2010). Comparing pollen spectra from modified Tauber traps and moss samples: examples from a selection of woodlands across Europe. Vegetation History and Archaeobotany 19, 271–283. https://doi.org/10.1007/s00334-010-0258-y

Parra, I. (1994) Quantification des précipitations à partir des spectres polliniques actuels et fossiles: du Tardiglaciaire à l'Holocène Supérieur de la cote méditerranéenne espagnole. PhD Thesis, Univ. Montpellier, Montpellier (France).

Past Interglacials Working Group of PAGES (2016), Interglacials of the last 800,000 years, Reviews of Geophysics, 54, 162–219, https://doi.org/10.1002/2015RG000482

Peck, R.M. (1973). Pollen budget studies in a small Yorkshire catchment. In Birks, H.J.B. and West, R.G., editors. Quaternary Plant Ecology. 43-60. Blackwells, Oxford.

Pereira, T., Carvalho, A.F. (2015). Abrupt technological change at the 8.2 ky cal BP climatic event in Central Portugal. The Epipalaeolithic of Pena d'Água Rock-shelter. Comptes Rendus Palevol, 14, 423-435. https://doi:10.1016/j.crpv.2015.04.003.

Pereira, T., Andrade, C., Costa, M., Farias, A., Mirão, J., Carvalho, A.F. (2016). Lithic Economy and Territory of Epipaleolithic Hunter–Gatherers in the Middle Tagus: The Case of Pena d'Água (Portugal). Quaternary International 412, 135–144, https://doi:10.1016/j.quaint.2015.08.081

Pérez-Díaz, S., Ruiz Fernández, J., López-Sáez, J. A., García-Hernández, C. (2017). Cambio climático y cultural en la Península Ibérica: Una perspectiva geohistórica y paleoambiental. Servicio de Publicaciones. Unviersidad de Oviedo.

Pérez-Obiol, R., Julià, R. (1994) Climatic change on the Iberian Peninsula recorded in a 30 000-yr pollen record from lake Banyoles. Quaternary Research, 41, 91– 98

Pérez Rodríguez, M. (1998). La producción de instrumentos líticos pulimentados en el territorio de la Banda atlántica de Cádiz". Revista Atlántica-Mediterránea de Prehistoria y Arqueología Social I, pp. 97-124.

Pérez Rodríguez, M. (2003). Primitivas comunidades aldeanas en Andalucía. Libro electrónico. ProQuest Information and Learning.

Pérez Rodríguez, M. (2005). Sociedades cazadoras-recolectoras-pescadoras y agricultoras en el Suroeste: una propuesta para un cambio social. Arqueología y Territorio 2, pp. 153-168.

Pérez Rodríguez, M., Ramos Muñoz, J., Vijande Vila, E., Castañeda Fernández, V. (2005). Informe preliminar de la excavación arqueológica de urgencia en el asentamiento prehistórico de La Esparragosa (Chiclana de la Frontera, Cádiz). Anuario Arqueológico de Andalucía 2002-III. Junta de Andalucía, pp. 93-103.

Pérez Rodríguez, M. (2008). Sociedades tribales y modo de reproducción. Cuestionamientos al registro arqueológico del suroeste". In Escoriza, T., López, M. J., Navarro, A., eds.: Mujeres y arqueología. Nuevas aportaciones desde el Materialismo Histórico. Consejería de Cultura. Junta de Andalucía. Sevilla, pp. 157-194.

Peyroteo-Stjerna, R. (2020). Chronology of the Burial Activity of the Last Hunter-Gatherers in the Southwestern Iberian Peninsula, Portugal. Radiocarbon, 1–35, https://doi:10.1017/rdc.2020.100

Pineda, P., Toboso, E. (2010). Nuevas aportaciones a la prehistoria de Chiclana de la Frontera, Cádiz. Campaña de excavaciones en el yacimiento de "El Carrascal-La Esparragosa". Año 2004. In: Mata Almonte, E. (ed.): Cuaternario y Arqueología. Homenaje a Francisco Giles Pacheco. ASPHA y Servicio de Publicaciones de la Diputación Provincial de Cádiz.

Pinto da Cruz, C.S.B.P.C. (1999). Temporary Ponds Vegetation and Dynamics: SW Portugal. In Vegetação e Dinâmica dos Charcos Temporários do Sudoeste Alentejano. PhD Thesis, Univ. Lisboa, Lisboa (Portugal).

Pittam, N.J., Mighall, T.M., Foster, I.D.L., (2006). The effect of sediment source changes on pollen records in lake sediments, in: Water, Air, and Soil Pollution: Focus. pp. 677–683. https://doi.org/10.1007/s11267-006-9053-2

Poirier, C., Tessier, B., Chaumillon, E. (2017). Climate control on late Holocene high-energy sedimentation along coasts of the northeastern Atlantic Ocean. Palaeogeography, Palaeoclimatology, Palaeoecology, 485, 784-797. https://doi.org/10.1016/j.palaeo.2017.07.037

Pons, A., Reille, M. (1986). Nouvelles recherches pollenanalytiques à Padul (Granada): La fin du dernier Glaciaire et l'Holocène. En: López-Vera, F. (Ed.). Quaternary Climate in Western Mediterranean. Universidad Autónoma de Madrid: 405-420. Madrid.

Pons, A., and Reille, M. (1988). The Holocene-and Upper Pleistocene pollen record from Padul (Granada, Spain): a new study. Palaeogeography, Palaeoclimatology, Palaeoecology 66, 243–263. http://dx.doi.org/10.1016/0031-0182(88)90202-7

Posac, C. (1975). Los Algarbes (Tarifa). Una necrópolis de la Edad del Bronce. Noticiario Arqueológico Hispánico. Prehistoria 4.

Posamentier, H.W., Vail, P.R. (1988). Eustatic control on clastic deposition: II Sequence and System Tract Models. *In*: Wilgus, C.K., Hastings, B.S., Kendall, C.G.St.C., Posamentier, H.W., Ross, C.A., Van Wagoner, J.C. (eds.), Sea Level Changes – An Integrated Approach, SEPM Special Publication, 42, pp. 125-154. https://doi.org/10.2110/pec.88.01.0125

Punt, W.J., Hoen, P.P., Blackmore, S., Nilsson, S., Thomas, A.L. (2007). Glossary of pollen and spore terminology. Review of Palaeobotany and Palynology, 143, 1-81.

Ramos, A., Fernández, O., Terrinha, P., Muñoz, J.A. (2016). Extension and Inversion Structures in the Tethys–Atlantic Linkage Zone, Algarve Basin, Portugal. International Journal of Earth Sciences 105, 1663–1679, https://doi:10.1007/s00531-015-1280-1

Ramos Muñoz, J. (2004a): "Las últimas comunidades cazadoras, recolectoras y pescadoras en el Suroeste peninsular. Problemas y perspectivas del 'tránsito Epipaleolítico-Neolítico' con relación a la definición del cambio histórico. Un análisis desde el modo de producción". En: Sociedades recolectoras y primeros productores. Actas de las Jornadas Temáticas Andaluzas de Arqueología. Junta de Andalucía. Sevilla, pp. 71-89.

Ramos Muñoz, J. (2004b): El poblamiento calcolítico en la Banda atlántica de Cádiz. Aproximación a la sociedad clasista inicial del IIIer. milenio a.n.e.. In Las primeras sociedades metalúrgicas en Andalucía. III Simposio de Prehistoria. Cueva de Nerja, pp. 352-360. Málaga.

Ramos Muñoz, J. (2006): "La transición de las sociedades cazadoras-recolectoras a las tribales comunitarias en el sur de la Península Ibérica. Tecnología y recursos". En Alday, A., coord.: El Mesolítico. Cuenca del Ebro. Litoral Mediterráneo. Memorias de Yacimientos Alaveses 11. Vitoria, pp. 17-61.

Ramos Muñoz, J. (2008). La ocupación prehistórica de la campiña litoral y Banda Atlántica de Cádiz. Aproximación al estudio de las sociedades cazadoras-recolectoras, tribales-comunitarias y clasistas iniciales. Arqueología Monografías. Junta de Andalucía. Sevilla.

Ramos Muñoz, J, Castañeda, V., Gracia, F. J. (1995a). El asentamiento al aire libre de La Fontanilla (Conil de la Frontera, Cádiz). Nuevas aportaciones para el estudio de las comunidades de cazadores-recolectores especializados en la Banda Atlántica de Cádiz. Zephyrus XLVIII, pp. 269-288.

Ramos Muñoz, J., Castañeda Fernández, V., Pérez Rodríguez, M., Lazarich, M., Martínez, C., Montañés, M., Lozano, J.M., Calderón, D. (1995b). Los Charcones. Un poblado agrícola del III y II milenios a.C. Su vinculación con el foco dolménico de la Laguna de la Janda. Almoraima 13, pp. 30-50.

Ramos Muñoz, J., Domínguez-Bella, S., Morata, D., Pérez, M., Montañés, M., Castañeda Fernández, V., Herrero, N., García, M.E. (1998): Aplicación de las técnicas geoarqueológicas en el estudio del proceso histórico entre el V y III milenios a.n.e. en la comarca de La Janda (Cádiz). Trabajos de Prehistoria 55, 2, pp. 163-176.

Ramos Muñoz, J., Montañés, M., Pérez Rodríguez, M., Castañeda Fernández, V., Herrero, N., García, M.E., Cáceres, I. (1999). Excavaciones arqueológicas en La Mesa (Chiclana de la Frontera, Cádiz). Campaña de 1998. Aproximación al estudio del proceso histórico de su ocupación. Ayuntamiento de Chiclana, Fundación Vipren y Universidad de Cádiz. Chiclana de la Frontera.

Ramos Muñoz, J., Lazarich, M. (2002): El asentamiento de 'El Retamar' (Puerto Real, Cádiz). Contribución al estudio de la formación social tribal y a los inicios de la economía de producción en la Bahía de Cádiz. Universidad de Cádiz y Ayuntamiento de Puerto Real.

Ramos Muñoz, J., Castañeda Fernández, V. (2005): Excavación en el asentamiento prehistórico del Embarcadero del río Palmones (Algeciras, Cádiz). Universidad de Cádiz y Ayuntamiento de Algeciras. Cádiz.

Ramos Muñoz, J, Domínguez-Bella, S., Castañeda, V. (2006). Siliceous materials of the hunter-gatherer settlements from the Atlantic Band of Cádiz (SW Spain) in the Upper Pleistocene. Der Anschnitt. 19: 531-544.

Ramos Muñoz, J., Pérez Rodríguez, M., Clemente Conte, I., García, V., Ruiz Zapata, M.B., Gil García, M.J., Vijande Vila, E., Soriguer-Escofet, M., Hernando, J., Zabala, C. (2008). La Esparragosa (Chiclana de la Frontera). Un asentamiento con campo de silos en la campiña de Cádiz, del IV milenio a. n. e.". In M. S. Hernández, J.A. Soler y J.A. López (Eds.): IV Congreso del Neolítico Peninsular II, pp. 385-392. Museo Arqueológico de Alicante, Diputación de Alicante.

Ramos Muñoz, J., Domínguez-Bella, S., Pérez Rodríguez, M., Vijande Vila, E. (2009). Producción, distribución y consumo de los productos líticos laminares vinculados a las sociedades tribales y clasistas

iniciales del ámbito atlántico andaluz. In: Les grans fulles de sílex. Europa al final de la Prehistòria. Actes. Monografies 13. Museu d'Arqueologia de Catalunya. Barcelona, pp. 25-33.

Ramos Muñoz, J, Domínguez-Bella, S., Pérez, M. (2010a). Registros arqueológicos y materias primas de yacimientos con tecnología de Modo 4 vinculados a sociedades cazadoras-recolectoras en el litoral atlántico del sur de Cádiz. In Mata, E. (coord.): Cuaternario y Arqueología. Homenaje a Francisco Giles Pacheco, Servicio de Publicaciones Excma. Diputación Provincial de Cádiz, pp. 111-124. Cádiz.

Ramos Muñoz, J., Domínguez-Bella, s., Pérez Rodríguez, M. (2010b). Conceptual framework and Archaeological data of the initial classist society in the Atlantic Band of Cádiz (SW Spain) in 3rd and 2nd Millennia BC. In Calado, D., Baldia, M., Boulanger, M. (eds.), Monumental Questions: Prehistoric Megaliths, Mounds, and Enclosures. BAR International Series 2123, Oxford, pp. 161-167.

Ramos Muñoz, J., Domínguez-Bella, S., Cantillo-Duarte, J.J., Soriguer, M., Pérez, M., Hernando, J., Vijande Vila, E., Zabala, C., Clemente, I., Bernal, D. (2011). Marine resources exploitation by Palaeolithic hunter-fisher-gatherers and Neolithic tribal societies in the historical region of the Strait of Gibraltar. Quaternary International 239, 104-113.

Ramos Muñoz, J., Pérez Rodríguez, M, Domínguez-Bella, S., Vijande Vila, E., Cantillo Duarte, J.J. (2016). Las evidencias arqueológicas de las sociedades clasistas iniciales en Conil de la Frontera en el contexto de la banda atlántica de Cádiz. In: J. Ramos Muñoz, J.J. Cantillo Duarte, E. Vijande Vila (coords). Las sociedades prehistóricas y la Arqueología de Conil en el contexto de la Banda Atlántica de Cádiz. Edicions Pinsapar. Málaga, pp. 135-165.

Ramos Muñoz, J., Vijande-Vila, E., Domínguez-Bella, S., Clemente Conte, I., Fernández-Sánchez, D., Almisas Cruz, S., García, V., Mazzucco, N., Becerra Martín, S., Pérez Rodríguez, M. (2022). La industria lítica tallada del yacimiento neolítico del IVº milenio a.n.e. de La Esparragosa (Chiclana de la Frontera, Cádiz): Análisis de materias primas, tecnología y uso. In: Jiménez Ávila, J., Bustamante Álvarez, M., Heras Mora, J., eds.: X Encuentro de Arqueología del Suroeste Peninsular, Ayuntamiento de Zafra, pp. 202.242.

Ramos-Román, M.J., Jiménez-Moreno, G., Camuera, J., García-Alix, A., Anderson, R.S., Jiménez-Espejo, F.J., Sachse, D., Toney, J.L., Carrión, J.S., Webster, C., Yanes, Y. (2018). Millennial-scale cyclical environment and climate variability during the Holocene in the western Mediterranean region deduced from a new multi-proxy analysis from the Padul record (Sierra Nevada, Spain). Global and Planetary Change 168, 35–53.

Rasmussen, S.O., Vinther, B.M., Clausen, H.B., Andersen, K.K. (2007). Early Holocene climate oscillations recorded in three Greenland ice cores. Quaternary Science Reviews 26, 1907-1914. https://doi:10.1016/j.quascirev.2007.06.015

Reed, J.M., Stevenson, A.C., Juggins, S. (2001). A multi-proxy record of Holocene climatic change in southwestern spain: The Laguna de Medina, Cádiz. The Holocene 11, 707–719. https://doi.org/10.1191/09596830195735

Reicherter, K.R., Peters, G. (2005). Neotectonic evolution of the Central Betic Cordilleras (southern Spain). Tectonophysics, 405, 191–212. https://doi.org/10.1016/j.tecto.2005.05.022

Reicherter, K., Costa, P., Bellanova, P., and the research crew of M152 (2019). The off-shore Lisbon 1755 tsunami sediments. EGU General Assembly 2019 - EGU2019-18827 - NH5.5/GM11.11/OS2.15/SSP3.15 (Conference Abstract).

Reille, M. (1990). Leçons de palynologie et d'analyse pollinique. Éditions du CNRS, pp.206.

Reille, M., (1992). Pollen et Spores d'Europe et d'Afrique du nord. Laboratoire de Botanique Historique et Palynologie, Marseille.

Reille, M., (1995). Pollen et Spores d'Europe et d'Afrique du Nord (Supplément 1). Laboratoire de Botanique Historique et Palynologie, Marseille.

Reimer, R.W., Reimer, P.J. (2017). An online application for ΔR calculation. Radiocarbon, 59, 1623-1627. http://calib.org/JS/JSdeltar20/. Accessed 2021-01-26.

Reimer, P.J., Austin, W.E.N., Bard, E., Bayliss, A., Blackwell, P.G., Bronk Ramsey, C., Butzin, M., Cheng, H., Edwards, R.L., Friedrich, M., Grootes, P.M., et al. (2020). The IntCal20 Northern Hemisphere Radiocarbon Age Calibration Curve (0–55 cal kBP). Radiocarbon, 62, 725-757. https://doi.org/10.1017/RDC.2020.41

Renssen, H., Goosse, H., Fichefet, T., Campin, J.-M. (2001). The 8.2 kyr BP event simulated by a global atmosphere–sea–ice–ocean model. Geophysical Research Letters 28, 1567–1570. http://doi:10.1029/2000GL012602

Revelles, J., Burjachs, F., van Geel, B. (2016). Pollen and non-pollen palynomorphs from the Early Neolithic settlement of La Draga (Girona, Spain). Review of Palaeobotany and Palynology 225: 1–20.

Riquelme, J.A. (2019). Fauna terrestre. In: Vijande Vila, E., Ramos Muñoz, J., Fernández Sánchez, D., Cantillo Duarte, J.J., Pérez Rodríguez, M. coords, 2019. La Esparragosa (Chiclana de La Frontera, Cádiz). Un campo de silos neolítico del IV milenio a.n.e. Arqueología Monografías. Junta de Andalucía, Sevilla, pp. 70-90.

Rivas-Martínez, S.R., Belmonte-López, M.D.B. (1985). Sobre el orden Agrostietalia castellanae. Lazaroa, 417–420.

Rivas-Martínez, S., (1988). Bioclimatología, biogeografía y series de vegetación en Andalucía Occidental. Lagascalia 15, 91–119.

Rivas-Martínez, S., Lousa, M., Día, T.E., Fernández-González, F., Costa, J.C., (1990). La vegetación del sur de portugal (Sado, Alemtejo y Algarve). Itinera Geobotanica 3, 5–126.

Rivas-Martinez, S., Asensi, A., Diez-Garretas, B., Molero, J., Valle, F., (1997). Biogeographical Synthesis of Andalusia (Southern Spain). Journal of Biogeography 24, 915–928. https://doi.org/10.1046/j.1365-2699.1997.00149.x

Rivas-Martínez, S., Fernández-González, F., Loidi, J., Lousa, M., Penas, A., (2001). Syntaxonomical checklist of the vascular plant communities of Spain and Portugal to association level. Itinera Geobotanica 14, 5–341.

Rivas-Martínez, S., Penas, A., Díaz, T., del Rio, S., Cantó, P., Cembranos, L., Gomes, C., Costa, J. (2014). Biogeography of Spain and Portugal. Preliminary typological synopsis. International Journal of Geobotanical Research, 4, 1–64. https://doi.org/10.5616/ijgr14001

Rivas-Martínez S, Penas Á, Díaz TE, Rivas-Sáenz S. (2017). Bioclimatology of theIberian Peninsula and the Balearic Islands. In: Loidi J, editor. Vegetation ofthe Iberian Peninsula, Vol. 1. Cham: Springer.

Rocha, L. (2013). A praia do Forte Novo. Um sítio de produção de sal na costa Algarvia? Pré-História Das Zonas Húmidas. Paisagens de Sal/Pehistory of Wetlands. Landscapes of Salt. In Proceedings of the Setúbal Arqueológica, Volume 14, pp. 225–232

Rohling, E.J., Pälike, H. (2005). Centennial-Scale Climate Cooling with a Sudden Cold Event around 8,200 Years Ago. Nature 2005, 434, 975–979, https://doi:10.1038/nature03421

Rodríguez Ariza, M. O. (2005). Análisis antracológico del asentamiento prehistórico del Embarcadero del río Palmones. In Ramos Muñoz, J., Castañeda Fernández, V., eds.: Excavación en el asentamiento prehistórico del Embarcadero del Río Palmones. Universidad de Cádiz y Ayuntamiento de Algeciras. Cádiz, pp. 299-322.

Rodríguez-Ramírez, A., Flores-Hurtado, E., Contreras, C., Villarías-Robles, J.J.R., Jiménez-Moreno, G., Pérez-Asensio, J.N., López-Sáez, J.A., Celestino-Pérez, S., Cerrillo-Cuenca, E., León, Á., (2014). The role of neo-tectonics in the sedimentary infilling and geomorphological evolution of the Guadalquivir estuary (Gulf of Cádiz, SW Spain) during the Holocene. Geomorphology 219, 126–140. https://doi.org/10.1016/j.geomorph.2014.05.004

Rodríguez-Vidal, J., Cáceres, L.M., Finlayson, J.C., Garcia, F.J., Martínez-Aguirre, A. (2004). Neotectonics and shoreline history of the Rock of Gibraltar, south Iberia. Quaternary Science Reviews, 23, 2017–2029. https://doi.org/10.1016/j.quascirev.2004.02.008

Roldán, F.J., Rodríguez-Fernández, J., Villalobos, M., Lastra, J., Díaz-Pinto, G., Pérez Rodríguez, A.B. (2021). Mapa Geológico Digital continuo E. 1:50.000, Zonas: Subbético, Cuenca del Guadalquivir y Campo de Gibraltar. In: *GEODE*. Mapa Geológico Digital continuo de España. [online]. [02/november/2021]. http://info.igme.es/cartografiadigital/geologica/geodezona.aspx?Id=Z2600

Ruiz, F., Rodríguez-Ramírez, A., Cáceres, L.M., Rodríguez-Vidal, J., Carretero, M.I., Clemente, L., Muñoz, J.M., Yáñez, C. (2004). Late Holocene evolution of the southwestern Doñana National Park (Guadalquivir Estuary, SW Spain): A multivariate approach. Palaeogeography, Palaeoclimatology, Palaeoecology, 204, 47-64. https://doi.org/10.1016/S0031-0182(03)00721-1

Ruiz Zapata, B., Gil García, M.J. (2019). Estudio palinológico. In: Vijande Vila, E., Ramos Muñoz, J., Fernández Sánchez, D., Cantillo Duarte, J.J., Pérez Rodríguez, M. coords, 2019. La Esparragosa (Chiclana de La Frontera, Cádiz). Un campo de silos neolítico del IV milenio a.n.e. Arqueología Monografías. Junta de Andalucía, Sevilla.

Sánchez Goñi, M. F. (1993). Criterios de base tafonómica para la interpretación de análisis palinológicos en cueva: el ejemplo de la región cantábrica. En: Fumanal, M. P. y Bernabeu, J. (Eds.). Estudios sobre el Cuaternario. Medios sedimentarios. Cambios ambientales. Hábitat humano. Universitat de València: 117-130. València.

Sánchez-Goñi, M.F. (2006). Interactions végétation-climat au cours des derniers 425.000 ans en Europe occidentale. Le message du pollen des archives marines. Quaternaire 17(1): 3-25

Sánchez-Goñi, M. F., Desprat, S., Fletcher, W. J., Morales-Molino, C., Naughton, F., Oliveira, D., Urrego, D. H., Zorzi, C. (2018). Pollen from the Deep-Sea: A Breakthrough in the Mystery of the Ice Ages. Frontiers in Plant Science, 9. https://doi.org/10.3389/fpls.2018.00038

Sangster, A.G., Dale, H.M. (1964). Pollen grain preservation of underrepresented species in fossil spectra. Canadian Journal of Botany 42, 437–449. https://doi.org/10.1139/b64-044

Santisteban, J.I., Mediavilla, R., de Frutos, L.G., Cilla, I.L. (2019). Holocene Floods in a Complex Fluvial Wetland in Central Spain: Environmental Variability, Climate and Time. Global and Planetary Change, 181, 102986, https://doi:10.1016/j.gloplacha.2019.102986

Sanz de Galdeano, C. (1990). Geologic evolution of the Betic Cordilleras in the Western Mediterranean, Miocene to the present. Tectonophysics, 172, 107-119. https://doi.org/10.1016/0040-1951(90)90062-D

Schirrmacher, J., Weinelt, M., Blanz, T., Andersen, N., Salgueiro, E., Schneider, R. R. (2019). Multi-decadal atmospheric and marine climate variability in southern Iberia during the mid- to late-Holocene, Climate of the Past, 15, 617–634, https://doi.org/10.5194/cp-15-617-2019

Schneider, R.R., Price, B., Müller, P.J., Kroon, D., Alexander, I. (1997). Monsoon Related Variations in Zaire (Congo) Sediment Load and Influence of Fluvial Silicate Supply on Marine Productivity in the East Equatorial Atlantic during the Last 200,000 Years. Paleoceanography, 12, 463–481, doi:10.1029/96PA03640.

Schneider, H., Höfer, D., Trog, C., Busch, S., Schneider, M., Baade, J., Daut, G., Mäusbacher, R. (2010). Holocene estuary development in the Algarve Region (Southern Portugal) - A reconstruction of sedimentological and ecological evolution. Quaternary International, 221, 141-158. https://doi.org/10.1016/j.quaint.2009.10.004

Schröder, T., Hoff, J. van 't, Ortiz, J.E., Pèrez-Hidalgo, T.J. de T., López-Sáez, J.A., Melles, M., Holzhausen, A., Wennrich, V., Viehberg, F., Reicherter, K., (2018). Shallow hypersaline lakes as paleoclimate archives: A case study from the Laguna Salada, Málaga province, southern Spain. Quaternary International 485, 76–88. https://doi.org/10.1016/j.quaint.2017.08.006

Schröder, T., López-Sáez, J.A., Hoff, J. van't, Reicherter, K., (2020). Unravelling the Holocene environmental history of south-western Iberia through a palynological study of Lake Medina sediments. Holocene 30, 13–22. https://doi.org/10.1177/0959683619865590

Serrano, O., Kelleway, J.J., Lovelock, C., Lavery, P.S. (2019). Chapter 28 - Conservation of Blue Carbon Ecosystems for Climate Change Mitigation and Adaptation, in: Perillo, G.M.E., Wolanski, E., Cahoon, D.R., Hopkinson, C.S. (Eds.), Coastal Wetlands (Second Edition). Elsevier, pp. 965–996. https://doi.org/10.1016/B978-0-444-63893-9.00028-9

Soares, A.M.M. (1993). The 14C Content of Marine Shells: Evidence for Variability in Coastal Upwelling off Portugal during the Holocene. In Isotope Techniques in the Study of Past and Current Environmental Changes in the Hydrosphere and the Atmosphere; International Atomic Energy Agency: Vienna, Austria.

Soares, A.M.M., Dias, J.M.A. (2006). Coastal Upwelling and Radiocarbon—Evidence for Temporal Fluctuations in Ocean Reservoir Effect off Portugal During the Holocene. Radiocarbon 48, 45–60, https://doi:10.1017/S0033822200035384

Soares, A.M.M., Martins, J.M.M. (2010). Radiocarbon dating of marine samples from Gulf of Cádiz: The reservoir effect. Quaternary International, 221, 9-12. https://doi.org/10.1016/j.quaint.2009.10.012

Soriguer, M. C., Zabala, C., Jiménez, D., Hernando, J. A. (2008). La explotación de los recursos naturales en el territorio de la banda atlántica de Cádiz y área del Estrecho de Gibraltar durante la Prehistoria: Ictiofauna y Malacofauna. In Ramos Muñoz, J., coord.: Memoria del proyecto de investigación: La ocupación prehistórica de la campiña litoral y banda atlántica de Cádiz. Arqueología Monografías. Junta de Andalucía. Sevilla, pp. 273-286.

Soulet, G. (2015). Methods and codes for reservoir-atmosphere 14C age offset calculations. Quaternary Geochronology, 29, 97-103. https://doi.org/10.1016/j.quageo.2015.05.023

Sousa, C., Boski, T., Pereira, L. (2019). Holocene Evolution of a Barrier Island System, Ria Formosa, South Portugal. Holocene, 29, 64–76, https://doi:10.1177/0959683618804639

Spieksma, F.Th.M., Nikkels, B.H., Bottema, S., (1994). Relationship between recent pollen deposition and airborne pollen concentration. Review of Palaeobotany and Palynology 82, 141–145. https://doi.org/10.1016/0034-6667(94)90025-6

Spratt, R.M., Lisiecki, L.E. (2016). A Late Pleistocene sea level stack. Climate of the Past, 12, 1079-1092. https://doi.org/10.5194/cp-12-1079-2016

Stevenson, A.C., (1985). Studies in the vegetational history of S.W. Spain. III. Palynological investigations at El Asperillo, Huelva. Journal of Biogeography 11, 527–551.

Stevenson, A.C., Moore, P.D. (1988). Studies in the vegetational history of S.W. Spain. IV. Palynological investigations of a valley mire at El Acebron, Huelva. Journal of Biogeography 15, 339–361.

Stipp, J.J., Timers, M.A. (2002). Datación radiométrica. In Proceedings of the El Asentamiento de El Retamar (Puerto Real, Cádiz): Contribución al Estudio de la Formación Social Tribal y a los Inicios de la Economía de Producción en la Bahía de Cádiz; Ramos, Lazarich, Eds.; Servicio de Publicaciones de la Universidad de Cádiz y Ayuntamiento de Algeciras: Cádiz, Spain, ISBN 84-7786-802-6

Stjerna, R.P. (2016). On Death in the Mesolithic: Or the Mortuary Practices of the Last Hunter-Gatherers of the South-Western Iberian Peninsula, 7th–6th Millennium BCE; Department of Archaeology and Ancient History, Uppsala University: Uppsala, Sweden.

Stockmarr, J. (1971). Tablets with spores used in absolute pollen analysis. Pollen et Spores, 13, 615-621.

Strauss, B.H., Kulp, S.A., Rasmussen, D.J., Levermann, A. (2021). Unprecedented threats to cities from multi-century sea level rise. Environmental Research Letters, 16, 114015. https://doi.org/10.1088/1748-9326/ac2e6b

Stuiver, M., Reimer, P.J., Reimer, R.W. (2021). CALIB 8.2 [WWW program] at http://calib.org accessed 2021-9-14.

Stumpf, R., Frank, M., Schönfeld, J., Haley, B.A. (2011). Climatically Driven Changes in Sediment Supply on the SW Iberian Shelf since the Last Glacial Maximum. Earth and Planetary Science, 312, 80–90, http://doi:10.1016/j.epsl.2011.10.002

Tauber, H. (1967). Investigations of the mode of pollen transfer in forested areas. Review of Palaeobotany and Palynology 3 (1–4), 277–286.

Tavares, C.N. (1959). Protection of the flora and plant communities in Portugal. Revue d'Ecologie Terre et Vie, 86-94.

Teixeira, S.B., Gaspar, P., Rosa, M. (2005). Holocene sea-level index points on the Quarteira coast (Algarve, Portugal). Conference: Iberian Coastal Holocene Paleoenvironmental Evolution - Coastal Hope, Lisbon (Portugal), pp. 125–127.

Ter Braak, C.J.F., Verdonschot, P.F.M., (1995). Canonical correspondence analysis and related multivariate methods in aquatic ecology. Aquatic Science 57, 255–289. https://doi.org/10.1007/BF00877430

Ter Schure, A.T.M., Wang, Y., Chagas, A.L.J., Epp, L.S. (2022) Chapter 8. aDNA from sediments. In: de Boer H, Rydmark MO, Verstraete B, Gravendeel B (Eds) Molecular identification of plants: from sequence to species. Advanced Books. https://doi.org/10.3897/ab.e98875

Thomas, J. (2009). Approaching Specialisation: Craft Production in Late Neolithic/Copper Age Iberia. Papers from the Institute of Archaeology 19, 67-84. https://doi.org/10.5334/pia.325

Thomson, J., Croudace, I.W., Rothwell, R.G. (2006). A Geochemical Application of the ITRAX Scanner to a Sediment Core Containing Eastern Mediterranean Sapropel Units. Geological Society, London, Special Publications Home, 267, 65–77, https://doi:10.1144/GSL.SP.2006.267.01.05

Thornalley, D.J.R., Elderfield, H., McCave, I.N. (2009). Holocene Oscillations in Temperature and Salinity of the Surface Subpolar North Atlantic. Nature, 457, 711–714, https://doi:10.1038/nature07717

Tian, F., Cao, X., Xu, Q., Li, Y., (2009). A laboratorial study on influence of alkaline and oxidative environment on preservation of *Pinus* tabulaeformis pollen. Frontiers of Earth Science in China 3 (2), 226–230. https://doi.org/10.1007/s11707-009-0003-y

Tjallingii, R., Röhl, U., Kölling, M., Bickert, T. (2007). Influence of the water content on X-ray fluorescence core-scanning measurements in soft marine sediments. Geochemistry, Geophysics, Geosystems, 8, Q02004. https://doi.org/10.1029/2006GC001393

Tomescu, A.M.F. (2005). Selective pollen destruction in archeological sediments at Grădiştea Coslogeni (Călăraşi County, Romania). Studii de Preistorie 2, 181–186.

Traverse, A. (2007). Paleopalynology. Springer, Doordrecht.

Trigo, R. M., Osborn, T. J., Corte-Real, J. M. (2002). The North Atlantic Oscillation influence on Europe: climate impacts and associated physical mechanisms. Climate Research, 20(1), 9–17.

Trigo, R.M., Trigo, I.F., DaCamara, C.C, Osborn, T.J. (2004). Climate impact of the European winter blocking episodes from the NCEP/NCAR Reanalyses. Climate Dynamics. 23: 17–28.

Trigo, I.F. (2006). Climatology and interannual variability of storm-tracks in the Euro-Atlantic sector: a comparison between ERA-40 and NCEP/NCAR reanalyses. Climate Dynamics. https://10.1007/s00382-005-0065-9

Trog, C., Höfer, D., Frenzel, P., Camacho, S., Schneider, H., Mäusbacher, R., (2013). A multi-proxy reconstruction and comparison of Holocene palaeoenvironmental changes in the Alvor and Alcantarilha estuaries (southern Portugal). Rev. Micropaleontol. 56, 131–158. https://doi.org/10.1016/j.revmic.2013.10.003

Tschudy, R.H. (1961). Palynomorphs as indicators of facies environments in Upper Cretaceous and Lower Tertiary strata, Colorado and Wyoming. Wyoming Geol. Assoc. Guidebook. Annu. Field Conference, 16, 53–59.

Turon, J.-L. (1984). Direct land/sea correlations in the last interglacial complex. Nature 309, 673–676. https://doi/10.1038/309673a0

Turon, J.-L., Lézine, A.-M., Denèfle, M. (2003). Land-sea correlations for the last glaciation inferred from a pollen and dinocyst record from the Portuguese margin. Quaternary Research 59, 88–96. https://doi/10.1016/S0033-5894(02)00018-2

Twiddle, C.L., Bunting, M.J. (2010). Experimental investigations into the preservation of pollen grains: a pilot study of four pollen types. Review of Palaeobotany and Palynology 162, 621–630. https://doi.org/10.1016/j.revpalbo.2010.08.003

Ulbrich, U., Christoph, M. (1999). A shift of the NAO and increasing storm track activity over Europe due to anthropogenic greenhouse gas forcing. Climate Dynamics, 15:551–559

Uzquiano, P., Arnanz, A. M. (2002). La evidencia arqueobotánica. Los macrorestos carbonizados del yacimiento de 'El Retamar'. In Ramos Muñoz, J., Lazarich González, M., eds.: El asentamiento de "El Retamar". Universidad de Cádiz y Ayuntamiento de Puerto Real. Cádiz, pp. 205-216.

Uzquiano, P., Ruiz Zapata, B., Gil-García, M.J., Vijande Vila, E., Ramos Muñoz, J., Cantillo Duarte, J.J., Lazarich, M., Bejarano, D., Montañés, M. (2020). Mid-Holocene palaeoenvironmental record from the Atlantic Band of Cádiz (SW Spain) based on pollen and charcoal data. Quaternary International 593-594, 144-159. https://doi.org/10.1016/j.quaint.2020.11.016

Vacchi, M. et al. (2016). Multiproxy assessment of Holocene relative sea-level changes in the western Mediterranean: sea-level variability and improvements in the definition of the isostatic signal. Earth-Science Reviews 155, 172–197

Vacchi, M., Joyse, K.M., Kopp, R.E. et al. (2021). Climate pacing of millennial sea-level change variability in the central and western Mediterranean. Nature Communications 12, 4013. https://doi.org/10.1038/s41467-021-24250-1

Val-Peón, C., Expósito, I., Soto, M., Burjachs, F. (2019). A taphonomic approach to the pollen assemblage from layer M of the Abric Romaní archaeological site (NE Iberian Peninsula). Review of Palaeobotany and Palynology 270, 19–39. https://doi.org/10.1016/j.revpalbo.2019.07.004

Val-Peón, C., Santisteban, J.I., López-Sáez, J.A., Weniger, G.-C., Reicherter, K. (2021). Environmental changes and cultural transitions in SW Iberia. Applied Sciences, 11: 3580. https://doi.org/10.3390/app11083580

Val-Peón, C., López-Sáez, J.A., Santisteban, J.I., Mediavilla, R., Becerra, S., Domínguez-Bella, S., Fernández-Sánchez, D.S., Ramos Muñoz, J., Vijande Vila, E., Cantillo Duarte, J.J., Reicherter, K. (2023). Natural and anthropogenic processes in the depression of La Janda (SW Iberia) from the Late Pleistocene to the Mid-Late Holocene. Continental Shelf Research 265, 105067 https://doi.org/10.1016/j.csr.2023.105067

Valente, M.J., Carvalho, A.F. (2009). Recent Developments in Early Holocene Hunter-Gatherer Subsistence and Settlement: A View from South-Western Iberia. In Proceedings of the Mesolithic Horizons, Proceedings of thes: Papers Presented at the Seventh International Conference on the Mesolithic in Europe; Belfast, Iereland, 20059; McCartan, S., Schulting, R., Warren, G., Woodman, P., Eds. Volume 1, Oxbow Books: Belfast, Ireland.

Valente, M.J. (2012). Mesolithic and Neolithic Shell Middens in Western Algarve: Issues in Ecology, Taphonomy and Economy. In Proceedings of the Proceedings of the First Zooarchaeology Conference in Portugal, University of Lisbon, Lisbon, Portugal. Detry, C., Dias, R., (eds.) University of Lisbon: Lisbon, Portugal.

Valdiosera, C., Günther, T., Vera-Rodríguez, J.C., Ureña, I., Iriarte, E., Rodríguez-Varela, R., Simões, L.G., Martínez-Sánchez, R.M., Svensson, E.M., Malmström, H., et al. (2018). Four Millennia of Iberian Biomolecular Prehistory Illustrate the Impact of Prehistoric Migrations at the Far End of Eurasia. PNAS, 115, 3428–3433, https://doi.org/10.1073/pnas.1717762115

Van Geel, B. (1978). A palaeoecological study of Holocene peat bog sections in Germany and The Netherlands, based on the analysis of pollen, spores and macro- and microscopic remains of fungi, algae, cormophytes and animals. Review of Palaeobotany and Palynology, 25, 1-120. https://doi.org/10.1016/0034-6667(78)90040-4

Van Geel, B. (2001). Non-Pollen Palynomorphs. In: J. P. Smol, H. J. B. Birks, W. M. Last, R. S. Bradley, K. Alverson (eds.), Tracking Environmental Change Using Lake Sediments: Terrestrial, Algal, and Siliceous Indicators. Springer Netherlands, pp. 99-119. https://doi.org/10.1007/0-306-47668-1_6

Van Geel, B., Bohncke, S. J. P., Dee, H. (1980). A palaeoecological study of an upper late glacial and holocene sequence from "de borchert", The Netherlands. Review of Palaeobotany and Palynology, 31, 367–448. https://doi.org/10.1016/0034-6667(80)90035-4

Van Geel, B., Klink, A. G., Pals, J. P., Wiegers, J. (1986). An Upper Eemian lake deposit from Twente, eastern Netherlands. Review of Palaeobotany and Palynology, 47, 31-61. https://doi.org/10.1016/0034-6667(86)90005-9

Van Geel, B., Coope, G. R., Van Der Hammen, T. (1989). Palaeoecology and stratigraphy of the late glacial type section at Usselo (the Netherlands). Review of Palaeobotany and Palynology, 60, 25-129. https://doi.org/10.1016/0034-6667(89)90072-9

Van Geel, B., Buurman, J., Brinkkemper, O., Schelvis, J., Aptroot, A., van Reenen, G., Hakbijl, T. (2003). Environmental reconstruction of a Roman Period settlement site in Uitgeest (The Netherlands), with special reference to coprophilous fungi. Journal of Archaeological Science, 30(7), 873–883. https://doi.org/10.1016/S0305-4403(02)00265-0

Van Wagoner, J.C., Posamentier, H.W., Mitchum, R.M., Vail, P.R., Sarg, J.F., Loutit, T.S., Hardenbol, J. (1988). An Overview of the Fundamentals of Sequence Stratigraphy and Key Definitions. In: Wilgus, C.K., Hastings, B.S., Kendall, C.G.St.C., Posamentier, H.W., Ross, C.A., Van Wagoner, J.C. (eds.), Sea Level Changes – An Integrated Approach, SEPM Special Publication, 42, pp. 39-45. https://doi.org/10.2110/pec.88.01.0039

Vergés, J., Fernández, M. (2012). Tethys-Atlantic interaction along the Iberia-Africa plate boundary: The Betic-Rif orogenic system. Tectonophysics, 579, 144-172. https://doi.org/10.1016/j.tecto.2012.08.032

Vijande Vila, E., (2009). El poblado de Campo de Hockey (San Fernando, Cádiz): resultados preliminares y líneas de investigación futuras para el conocimiento en las formaciones sociales tribales en la Bahía de Cádiz (tránsito V-IV milenios a.n.e.). Revista Atlántica-Mediterránea de Prehistoria y Arqueología Social 11, 265-284.

Vijande Vila, E., Domínguez-Bella, S., Cantillo Duarte, J.J., Martínez, J., Barrena, A., (2015). Social inequalities in the neolithic of southern europe: the grave goods of the campo de Hockey necropolis (San Fernando, Cádiz, Spain). Comptes Rendus Palevol 14, 147-161.

Vijande Vila, E., Ramos Muñoz, J., Pérez-Rodríguez, M., Moreno-Márquez, A., Cantillo Duarte, J.J., Domínguez-Bella, S., Almisas, S., Riquelme, J.A., Soriguer, M., Clemente Conte, I., García, V., Barrena, A., Ruiz-Zapata, B., Gil, M.J., Fernandez-Sánchez, D., (2018). Estudio interdisciplinar de la tumba AV del asentamiento neolítico de La Esparragosa (Chiclana de la Frontera, Cádiz, Espana). Arqueología Iberoamericana 37, 40-47.

Vijande Vila, E., Ramos Muñoz, J., Fernández Sánchez, D., Cantillo Duarte, J.J., Pérez Rodríguez, M. coords, (2019). La Esparragosa (Chiclana de La Frontera, Cádiz). Un campo de silos neolítico del IV milenio a.n.e. Arqueología Monografías. Junta de Andalucía, Sevilla.

Vijande Vila, E., Cantillo Duarte, J.J., Gómez, M. L., Fernández Sánchez, D., Becerra, S., Moreno, A., Muñoz, A., Carmona, M., Corona, J.M., Ramírez, J.L., Pavón, L., Ramos Muñoz, J. (2022). Una morada

eterna. La necrópolis megalítica de Trafalgar. In Bernal, D., Díaz, J.J., Vijande Vila, E., Expósito, J.A., Cantillo Duarte, J.J. (eds.). Arqueología Acul en Trafalgar. De la investigación al turismo sostenible. Junta de Andalucía, Editorial UCA. Universidad de Cádiz. Cádiz, pp. 124-135.

Villalpando, A., Montañés, M., (2016). El yacimiento de Set Parralejos, Vejer de la Frontera (Cádiz). Un núcleo de población de la prehistoria reciente en las estribaciones del río Salado de Conil de la Frontera. In: Ramos Muñoz, J., Cantillo Duarte, J.J., Vijande Vila, E. (Eds). Las sociedades prehistóricas y la Arqueología de Conil en el contexto de la Banda Atlántica de Cádiz. Ediciones Pinsapar, Cádiz, pp. 115-134.

Von Post, L. (1916). Om skogsträdpollen i sydsvenska torfmossclagerfölyder, Geol. Fören. Stockholm Förh. 38:384–390.

Walczak, I. W., Baldini, J. U. L., Baldini, L. M., Mcdermott, F., Marsden, S., Standish, C. D, Richards, D. A., Andreo, B., Slater, J., (2015). Reconstructing high-resolution climate using CT scanning of unsectioned stalagmites: A case study identifying the mid-Holocene onset of the Mediterranean climate in southern Iberia. Quaternary Science Reviews, 127, 117–128, 2015

Walker MJC, Berkelhammer M, Björck S et al. (2012) Formal subdivision of the Holocene series/epoch: A discussion paper by a working group of INTIMATE (Integration of ice-core, marine and terrestrial records) and the subcommission on Quaternary stratigraphy (International commission on stratigraphy). Journal of Quaternary Science 27(7): 649–659.

Weniger, G.C., Pike, A. (2018). U-Th dating of carbonate crusts reveals Neandertal origin of Iberian cave art. Science 359, 912-915.

Whitlock, C., Larsen, C. (2001). Charcoal as a Fire Proxy. In Tracking Environmental Change Using Lake Sediments: Terrestrial, Algal, and Siliceous Indicators; Smol, J.P., Birks, H.J.B., Last, W.M., Bradley, R.S., Alverson, K., Eds.; Developments in Paleoenvironmental Research; Springer: Dordrecht, The Netherlands, ISBN 978-0-306-47668-6

Wodehouse, R. P. (1935). Pollen grains. McGraw-Hill Book Company, New York.

Xu, Q., Zhang, S., Gaillard, M.-J., Li, M., Cao, X., Tian, F., Li, F., (2016). Studies of modern pollen assemblages for pollen dispersal- deposition- preservation process understanding and for pollen-based reconstructions of past vegetation, climate, and human impact: a review based on case studies in China. Quaternary Science Review 149, 151–166. https://doi.org/10.1016/j.quascirev.2016.07.017

Yapiyev, V., Sagintayev, Z., Inglezakis, V.J., Samarkhanov, K., Verhoef, A., (2017). Essentials of Endorheic Basins and Lakes: A Review in the Context of Current and Future Water Resource Management and Mitigation Activities in Central Asia. Water 9, 798. https://doi.org/10.3390/w9100798

Yll, R., Zazo, C., Goy, J.L., Pérez, R., Pantaleón, J., Civis, J., Dabrio, C., González, A., Borja, B., Soler, V., Lario, J., Luque, L., Sierro, F., González, F.M., Lezine, A.M., Denèfle, M., Roure, J.M., (2003). Quaternary palaeoenvironmental changes in South Spain. In: Ruiz-Zapata, B., Dorado, M., Valdeolmillos, A., Gil, M.J., Bardají, T., Bustamante, I., Martínez, I. (Eds.), Quaternary Climatic Changes and Environmental Crises in the Mediterranean Region. Universidad de Alcalá-INQUA, Alcalá de Henares, pp. 201–213.

Zaitlin, B.A., Dalrymple, R.W., Boyd, R. (1994). The stratigraphic organization of incised-valley systems associated with relative sea-level change. *In*: Dalrymple, R.W., Boyd, R., Zaitlin, B.A. (eds.), Incised-valley systems: origin and sedimentary sequences. SEPM Special Publication, 51, 45-60. https://doi.org/10.2110/pec.94.12.0045

Zazo, C., Silva, P.G., Goy, J.L., Hillaire-Marcel, C., Ghaleb, B., Lario, J., Bardají, T., González, A. (1999). Coastal uplift in continental collision plate boundaries: data from the Last Interglacial marine terraces of the Gibraltar Strait area (south Spain). Tectonophysics, 301, 95-109. https://doi.org/10.1016/S0040-1951(98)00217-0

Zazo, C., Dabrio, C.J., Goy, J.L., Lario, J., Cabero, A., Silva, P.G., Bardají, T., Mercier, N., Borja, F., Roquero, E., (2008). The coastal archives of the last 15 ka in the Atlantic-Mediterranean Spanish linkage area: Sea level and climate changes. Quaternary International 181, 72–87. https://doi.org/10.1016/j.quaint.2007.05.021

Zhao, Y., Miao, Y., Fang, Y., Li, Y., Lei, Y., Chen, X., Dong, W., An, C., (2021). Investigation of factors affecting surface pollen assemblages in the Balikun Basin, central Asia: Implications for palaeoenvironmental reconstructions. Ecological Indicators 123, 107332. https://doi.org/10.1016/j.ecolind.2020.107332

Ziegler, M., Jilbert, T., de Lange, G.J., Lourens, L.J., Reichart, G.J. (2008). Bromine counts from XRF scanning as an estimate of the marine organic carbon content of sediment cores. Geochemistry, Geophysics, Geosystems, 9, Q05009. https://doi.org/10.1029/2007GC001932

Zielhofer, C., Köhler, A., Mischke, S., Benkaddour, A., Mikdad, A., and Fletcher, W. J. (2019). Western Mediterranean hydro-climatic consequences of Holocene ice-rafted debris (Bond) events, Climate of the Past, 15, 463–475, https://doi.org/10.5194/cp-15-463-2019

Zilhão, J. (2001). Radiocarbon Evidence for Maritime Pioneer Colonization at the Origins of Farming in West Mediterranean Europe. Proc. Natl. Acad. Sci. USA 98, 14180–14185, https://doi:10.1073/pnas.241522898.